COUNTERACTING NITRIFICATION PROBLEMS IN BIO-TRICKLING FILTERS AT WTP LEKKERKERK THROUGH MODELLING

Luis Seminario Ruiz

For the degree of:
Master of Science in Civil Engineering

Date of submission: 9th October 2013
Date of defense: 29th October 2013

Committee:

Prof. dr. ir. L.C. Rietveld	Delft University of Technology Sanitary Engineering Section
Dr.ir. W.W.J.M. de Vet	OASEN N.V. Drinking water specialist
Ir.P. S. Ross	Delft University of Technology Sanitary Engineering Section and ARCADIS Nederland B.V.
Dr. ir. P.J. van Overloop	Delft University of Technology Water Resources Management Section

Sanitary Engineering Section, Department of Water Management
Faculty of Civil Engineering and Geosciences
Delft University of Technology, Delft

"Originally thought to remove matter only by filtering it was fairly soon realized that the major mechanism was biological degradation rather than screening. At least partly, this explains the slight misnomer since the biological unit itself neither filters nor trickles." (Wik, 2003)

"Do not conclude anything… yet!" (Weren)

"It only makes sense if you have fun." (Petra)

"We are looking for information that contradicts our model." (Luuk)

"Today is the most beautiful day of our lives, dear Sancho. The biggest obstacle, our own indecision; our strongest enemy, fear of the powerful and of ourselves; the easiest thing, being mistaken; the most destructive, lying and selfishness; the worst defeat, discouragement; the most dangerous defects, pride and resentment; our strongest virtues, a good conscience effort to be better than perfect, and above all, the willingness to do good and fight injustice wherever it is." (Don Quixote)

Abstract

The origin of this MSc Thesis lies in a persistent nitrification problem in some filters of the Water Treatment Plant Lekkerkerk operated by the Drinking Water Company OASEN. Nitrification is the microbial conversion of ammonia via nitrite to nitrate in two consecutive steps by slow growing autotrophic microorganisms. These autotrophic microorganisms stick to each other on the surface of the inert media (filter material grains), forming biofilms. The first step, the microbial oxidation of ammonia to nitrite, becomes incomplete over the course of the time due to unknown causes. Typically the relapse becomes visible three to six months after the start-up of the filter. These filters remove methane, iron and manganese as well since these compounds are also present in the anaerobic groundwater.

OASEN has three techniques to counteract nitrification problems but there are factors that limit their use. These techniques are: the application of subsurface aeration in the aquifer which is only used in one (Schuwacht) of the two aquifers (Schuwacht and Tiendweg) from where the water is abstracted; to wash externally the filter material; and, to replace the old filter material by new one. The last two procedures are labour-intensive activities with high economic costs. Consequently, OASEN is looking for alternative ways to either restore or maintain a sound nitrification. Unfortunately these techniques are still under research or there is lack of full confidence despite the promising observed results.

But in reality ammonium removal in these bio-filters is a dynamic problem: superposed to the problem of relapse in nitrification there is the problem that there are variations in the raw water quality which are propagated through the consecutive filtration steps. Furthermore production flow variations also influence the process performance.

A mathematical model that describes the biological oxidation of ammonia in each of these filters has been developed. The model has provided better insight into the factors that govern nitrification and has contributed to increase understanding on the sequence of events that ultimately result in non-compliance of the company guideline (0.10 mg NH_4^+/L in the final mixed filtrate from all filtration sets).

The model provides relatively good estimates if the filters are operated within the wide range of flows and influent concentrations they usually work at or near to (goodness of fitting R^2 between 0.61and 0.86). Nevertheless during calibration and validation, the measurement data taken from full-scale filters showed unexpected deviations from what was expected and from the process model. The model may not provide good results when filters work at different loading conditions than usual since fails in predicting the transient behaviour between consecutive steady states (R^2 = 0.30) and the fluctuations typically observed in the effluent of primary filters (R^2 = 0.44). This mismatch between process and model is caused probably by partial misunderstanding of the process and thus modelling errors.

(A) Site-specific measurements indicate that the nitrification problem may be caused by growth inhibition resulting in very low cell-specific nitrification rates. One of the most plausible hypotheses around the nitrification problem is that results from the interaction with the other removal processes as it is only observed in the primary filters. This might occur through uptake of essential nutrients by competing organism or clogging material (e.g. inorganic deposits). Since none of these two elements exist in secondary filters calibration efforts support this idea as the simulated effective growth rate in secondary filters is significantly higher than in primary filters with nitrification problems.

(B) Model results suggest that mass transfer limitation between bulk water and biofilm surface is not the cause of the failure of nitrification. The model is not able to provide any insight about what the situation is regarding the transport of substrates and nutrients within the biofilm since the model covers only the outer layer of the biofilm where the substrates and nutrients fully penetrate.

(C) The model has also suggested that primary filters may have slowly varying behaviour if they are operated on the long-term at different average load rates. This needs to be taken into account if the load regime is varied since may bring the filters into steady-states concerning their biomass content.

(D) Additionally the model insinuates that the rate of relapse in nitrification can be counteracted by operation the filters at lower loads. Furthermore, the results also insinuate that the trend may even be neutralized provided that the filter is operated in such a way that long periods of low loads are alternated with short periods of high loads.

(E) Finally, the model also advocates for reducing the frequency of backwashing in secondary filters in order to: (1) bring to biomass content to a new (and higher) steady state in order to increase the critical loading capacity of these filters; (2) reduce the number of ammonium

breakthrough events. Both the model and full-scale measurements indicate that backwash causes significant washout in these filters and that the growth rate at these filters is high.

The individual models representing each filter have been combined in order to create a model of the entire plant. With this integrated model operational strategies are evaluated. According to that model the performance of the system can be improved at general level by adapting the overall load applied on the Tiendweg system to its true capacity which, with the current operation regime, is strongly dependant on the number of primary filters with poor ammonium removal. The three general recommendations are:

(1) To modify the production shares of the two well fields during periods of high demand. This might not be feasible when considering the legal concession on the maximum yearly water volume that can be abstracted from Schuwacht.
(2) To limit the number of primary filters that simultaneously have poor effluent ammonium to not more than 0-1 depending on the seasonal demand. This would require either to increase the number of external washings or to incorporate one of the currently techniques under research to the standard operation programme (e.g. recirculation).
(3) Not to perform maintenance actions simultaneously in more than one filter and to limit the execution of such operations to the low-demand season.

As there are constraints for the application of at least two of the three options a new operational strategy has been tested. Primary filters do not have always their optimal nitrification capacity. Thus, there are differences between filters. Considering these differences will improve the performance of the entire system:

(4) By reducing the flow, when the first filter is ageing, the average load entering the second filter is lowered, resulting in an improved performance of the second filter, thus a better effluent concentration. The increased flow entering another filter set, will not have ideally a huge effect on its performance, since the age of the first filter is low enough being able to handle the fluctuations. Nevertheless, this issue requires further research.

By controlling the flow distribution between filtration sets the model that the system is less dependent on the number of primary filters that perform badly. Indeed, the limit on the number of primary filters that simultaneously have poor ammonium removal increases to 2. In addition to this the range of safe flows not resulting in ammonium breakthrough in the mixed final filtrate expands. This will result in less strict operation restrictions than those ones indicated before. For instance, by following the threshold values presented in this document the number of hours with breakthrough events occurred in 2012 could have been reduced by 89%. Thus, flow control in each filter individually is desirable and the installation of flow controlled valves that can help fulfil that purpose is recommended.

Whatever the flow distribution is (homogeneous or adapted to the specific situation of each filtration set) the following to actions around a better control of the influent conditions are recommended:

(5) Continuously control of the raw water quality.
(6) Quick variations of raw water quality need to be minimised.

Concerning future research steps, as it is not possible to neither deducing the causes of relapse in nitrification nor improving the model reliability only from regular sampling, new measurements of the internal characteristics of the filters together with some campaigns of continuous measurements are recommended. Several of them are aimed at confirming the model based findings A to E listed above. Ideally, direct measurements of internal parameters of the filters and regular sampling of the water quality can be used with the mathematical model to periodically assess the process state.

From this study it can be concluded that a dynamic mathematical model can be successfully used as a diagnostic tool to evaluate the performance and operation of full-scale bio-trickling filters for ammonium removal. The model can be used for operational decision support and, at a later stage, to help a targeted optimization strategy.

Preface

First, I would like to thank my supervisors. They have supported me actively throughout the demarcation of my research. From the beginning till the end they have provided me with key inputs at several crucial moments. We have had several discussions and their challenging comments and observations have always boosted my thoughts, making me re-think things from a different perspective. Moreover, during the realization of this project I have broaden my knowledge in two new areas I knew almost nothing about when I started. I am deeply grateful about all this!

Second, I would like to mention here as well the people from OASEN I have talked to most during this project: Nienke, Falco, Ruud, Timothy, Patrick, Jos, Menno, Harmen, Mariëlla… Thanks for your nice welcome and support!

Finally, if I look back the first thing that comes to my mind about my time here in The Netherlands is the people I have met. Some of them have already left, some others stay in the country. Needless to say that they all have made this experience better: Anthonie, Dianne, Paul, Kate, Jose, Jon, Zaki, Rajit, Berta, Sadie, Nuria, Fred, Iovannis, Victor, Anneke, Aaron, Frans, Marij, Dirk, David, Remko, Wouter, Marisa, Jan Herman, Raluca, Ioanna, Maria, George, Laura, Pradeep, Tom, Omar, Morganne, Sara, Addis, Rohan, Jimena, Vishnu, Hyo, Lobke, Richard, Ephrem, Faranak, Fang, Nikola, Tomasz, Waldemar, Martin… thanks and all the best!

Content

List of illustrations

List of tables

List of abbreviations

ANO	Ammonia-oxidizing organisms
NNO	Nitrite-oxidizing organisms
WTP	Water treatment plant
AOB	Ammonia-oxidizing bacteria
EW	External washing
BW	Backwashing
CSTR	Complete stirred tank reactor
MAP	Microbiologically available phosphate
AOA	Ammonia-oxidizing *archae*

1 Introduction

Groundwater treatment plants include specific treatment steps aimed at achieving the complete removal of several inorganic compounds typically present in groundwater (de Moel et al., 2006): typically iron, ammonium and manganese. In the treatment plant Lekkerkerk, in Krimpen a/d Lek, this is done in some biological trickling filters. This treatment plant is operated by OASEN, which is a drinking water company in the Dutch province of Zuid-Holland. The supply area covers an area of 1,115 km^2. The company produces drinking water for about 750,000 inhabitants and 7,500 businesses.

In the mentioned filters the removal of iron and manganese is robust but nitrification is often hampered (De Vet et al., 2010). Ammonium is considered to be a potential health risk (WHO, 2006) if present in drinking water: since ammonium is a nutrient for many microorganisms, incomplete ammonium removal in drinking water treatment plants may lead to re-growth in chlorine free distribution systems where nitrite could appear as product of the corresponding bacterial activity; moreover, at low concentrations nitrite is toxic and reduces the oxygen transport capacity of blood in humans.

Consequently, the treatment policy of drinking water companies towards the presence of ammonium in water is to oxidize all ammonium and nitrite into nitrate before it is distributed. According to Dutch drinking water standards , ammonium concentrations are not allowed to exceed 0.2 mg NH_4^+/L (VROM, 2001). OASEN has set its own limits of ammonium concentrations which should not exceed 0.1 mg NH_4^+/L (de Vet et al., 2009b).

This research focuses on the development of mathematical modelling for improving the operation and maintenance of these filters with the aim of ensuring ammonium concentrations below the guideline value in the plant effluent at all times. Ideally, the implementation of model based recommendations will result in lower ammonium concentrations in the produced water.

1.1 Problem definition

Nitrification relapses in many of the trickling filters at WTP Lekkerkerk (De Vet, 2011): typically, it starts up almost completely during the first half year after renewal or intensive washing of the filter sand; after this period, the nitrification activity typically starts relapsing (see Figure 1).

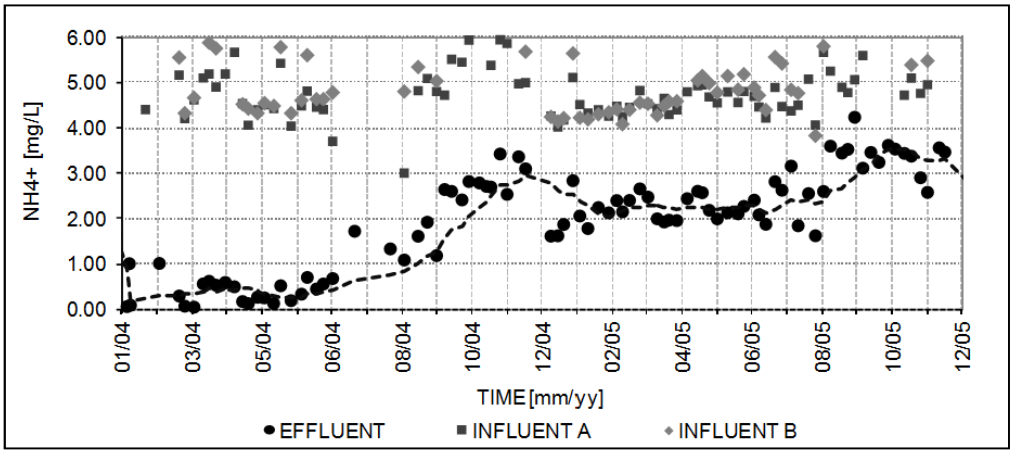

Figure 1 Typical fallback pattern for ammonium removal observed in primary filters at WTP Lekkerkerk

In general, nitrification performance of biological sand filtration in drinking water applications is habitually evaluated based on effluent concentrations with little attention to the actual nitrification mechanism occurring at the micro-level (Zhu et al., 2010). Accordingly, filters operation is mostly often on empirical rules (Lawler and Nason, 2006).

Plant operators and water technologists at OASEN have accumulated a lot of knowledge about the history of these filters through regular supervision and extensive research. Despite this, the causes for the decline in nitrification are still unknown and the filters need a lot of attention and maintenance. Up to four different methods are used by OASEN in order to overcome this problem, either by prevention or counteraction (de Vet et al., 2009b, de Vet et al., 2011a): underground aeration, external washing,

renewal of filter material and backwashing with expansion. The first method is limited to the filters fed by one of the well fields (Schuwacht). The other three methods are presented in Paragraph 2.3.2, where the typical operation regime of the bio-trickling filters is described. Furthermore, observations indicate that the occurrence of ammonium breakthrough depends on the filter position in the treatment line (each filtration set comprises two filters in series), the filter runtime, the age, the loading and the last maintenance activity applied (e.g.: external washing, filter material replacement or backwashing). In addition to these techniques, alternative remedial solutions have not attempted but either they have been not successful in terms of solving the problem or there is lack of full confidence on them.

When the problem is analyzed at a higher level than looking at each single individual filter, findings indicate that there are at least two factors hampering with the overall goal of having almost zero ammonium concentration in the plant mixed effluent at all times: first, the inexistence of continuous control of the abstracted water quality causing insufficient knowledge about the actual loading; and, second, the ability to operate bio-filters in a flexible way: nowadays the filters are operated in a fixed manner, which includes equal flow distribution among filters in parallel with a pre-set planning for maintenance activities and without considering the differences between them. The first issue is currently being faced with the development of soft-sensors in the plant influent according to already available measurements such as the wells in operations and the water quality in each well.

This MSc thesis deals with the construction of a mathematical model for nitrification in this plant. Such model should be able to predict the final effluent ammonium concentration under different operational conditions. Flexible operation of these filters and alternative control regimes could be evaluated with the help of this model. In conclusion, the research problem can be summarized as follows:

How should the bio-trickling filters at WTP Lekkerkerk be operated so full nitrification is achieved at all times (mixed filtrate of all sets always below the company guideline value)?

1.2 Objectives

The final goal is to make recommendations in order to achieve full and continuous ammonium removal at WTP Lekkerkerk. This result is planned to be achieved through: (1) defining a new operating strategy for the bio-trickling filters; and, (2) developing soft-sensors for continuous control and production of a more stable raw water quality. The second issue is currently under development and its study and implementation goes beyond the scope of this thesis. Therefore, the efforts focus on developing that help improve the operation of bio-trickling filters.

Although there are many operational constraints such as the existence of block hours for backwashing, the external washing operations being limited to summer periods, or the inexistence of devices to a real-time control of the flow distribution among filters, there is still room for improvement. Ideally, the operational regime of each filter could be adapted to the actual raw water quality and flow (both change continuously).

An important task in achieving this goal is the construction of a mathematical model of the system. The model is expected to provide very valuable information concerning the operation of the filters: first, the model is aimed at providing a stronger insight in nitrification kinetics that eventually can reveal potential process limitations; second, t can be used to identify the most important parameters influencing their performance; and, third, it may serve to identify threshold values below/above which the filter sets should (not) be operated. In short, the process of constructing the model should provide information about nitrification at each single filter that allow to answer the following questions:

- What are the causes for the observed incomplete nitrification?
- Can those causes be influenced by modifying the operational conditions?
- It possible to guarantee full nitrification through operating the filter in a different way than what is done nowadays?

In principle, optimal operation of the bio-trickling filters could be achieved in the nitrification activity of the filters is kept at its maximum all the time. The more frequently backwashing and external washing are applied, the better the water quality of the effluent results. But such solution would multiply both the operational and the environmental costs. Accordingly, the requirement is to improve the water quality without increasing the operational costs.

Since nowadays the relapse in nitrification occurs due to unknown causes, the optimisation criteria for the operation of the filters consist on seeing them not only as single treatment steps that need to be optimized individually but as a group so that the quality of the mixed effluent is optimized. The mathematical model should be able to predict the ammonium effluent concentration under different operational conditions such that ammonium breakthrough can be anticipated and, therefore, avoided.

According to model simulations, specific recommendations regarding a two folded strategy based on continuous process operation and a tailored maintenance strategy will be formulated. All the recommendations will be aimed at achieving ammonium concentrations levels in the mixed filtrate of all filters below the company guideline. Ideally, if that is achieved then the frequency of external washing could be reduced with the corresponding savings on exploitation costs. In short, the three following practical question about the operation of all filters have been defined:

- What is an optimal operation and maintenance regime for all filters to guarantee full nitrification (mixed filtrate of all sets always below OASEN standard of 0.1 mg/L NH_4^+)?
- How should they be optimally operated during periods of low and high demand?
- How should they be operated in case of instant loading increase due to maintenance?

1.3 Scope

The physical limits of the system to be studied are shown in Figure 2 that represents the process flow diagram of the treatment plant Lekkerkerk. The area object of study comprises all the bio-trickling filters that are supposed to remove completely ammonium. The boundaries of the area object of study are: upstream, the wells and the continuous flow measurement points; downstream, the sampling points downstream each filter and the continuous measurement point in the common pipe collecting all the filtrate. In Figure 2 the filters are highlighted with a dotted circle that surrounds them.

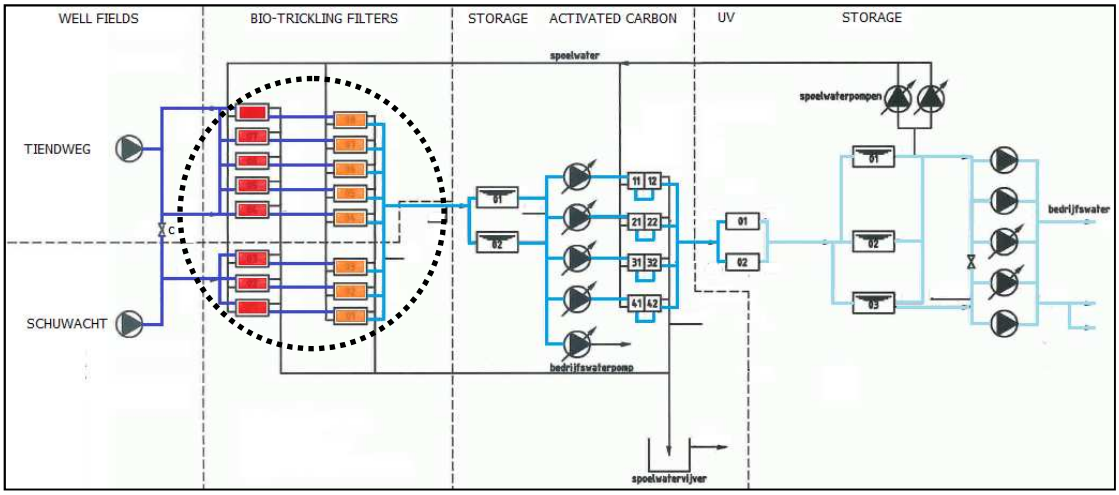

Figure 2 Process flow diagram of WTP Lekkerkerk and bio-trickling filters location

1.4 Outline

Chapter 1 consists on a general introduction into the topic. In Chapter 2 the problem and some general research questions are formulated and developed in combination with an overview of the plants, the filters and the description of the observed ammonium breakthrough problems. Data availability is stated as well, together with differences between filters and some specific cases that may be of interest. Chapter 3 deals exclusively with the model construction part of this research. The approach and the research questions and hypothesis are presented at the beginning. Special attention is paid to describe the model structure and parameters. Chapter 4 specifically deals with gathering of information specifically needed for model calibration and validation. Chapter 5 discusses possible operational improvements supported by mathematical model results. Specific recommendations concerning periods of low and high demand are presented. The issue of how to operate the system when one or two of the filters go out of production as a result of maintenance is addressed as well. A new control strategy based on distributing the flow according to nitrification capacity of each filtration set is analyzed and proposed. Finally, the general conclusions and recommendations are presented in Chapter 6.

2 Process description of WTP Lekkerkerk

2.1 Introduction

Groundwater is the most common water source in treatment plants operated in The Netherlands (de Moel et al., 2006). Often, the abstracted water is a mixture of river bank filtrate and local infiltrated water in near polders which makes it to contain a variety of compounds. The most common inorganic chemicals are methane, ammonium, iron, manganese, phosphate and sulphate.

Concerning ammonium, complete nitrification is required to prevent accumulation of toxic nitrite, to limit microbial growth in the distribution system, and to avoid the potential consumption of oxygen. Therefore, the presence of ammonium in drinking water is considered to be a potential health risk. More specifically, ammonium needs to be removed for different reasons. First, if ammonium is present in chlorine free water supply systems, as in The Netherlands, it may lead to the formation of nitrites as product of the corresponding bacterial activity. Nitrites have a serious potential impact on the oxygen transport capacity of blood in humans. Second, if chlorine is used for disinfection as it happens in other countries than in The Netherlands, it may react with the ammonium to produce produce chloramines, for which there is evidence of being carcinogenic. Third, the presence of ammonium in water may lead to oxygen depletion. Furthermore, nitrite can form carcinogenic compounds in the body. Nitrate is not a direct threaten for the health, but it may be reduced to nitrite in the human body.

Table 1 is a comparative of the standards for drinking water concerning ammonium, nitrite and nitrate from the World Health organization (WHO), the Environmental Protection Agency of the United States (US-EPA), The Netherlands and the OASEN. Although nitrate and nitrite are not present in anaerobic groundwater, the standards for these compounds are relevant for the treatment of ammonium since they are the intermediate and final product, respectively, of nitrification. As it can be seen, the standard of the company for ammonium and nitrite are twice stricter than the national standards.

Table 1 Guideline values for ammonium, nitrite and nitrate in drinking water

Compound Source	Ammonium [mg NH4+/L]	Nitrite [mg NO2- /L]	Nitrate [mg NO3- /L]
WHO	-	3.00 (*)	50
US-EPA (**)	-	3.2 (***)	44
THE NETHERLANDS	0.2	0.05	50
OASEN	0.1	0.025	50

A wide range of treatment technologies are available for groundwater treatment either physicochemical or biologically based. Although biological processes have been widely used in waste water treatment for a long time, a positive attitude towards them in drinking water treatment is more recent (De Vet, 2011). One of the advantages of biological treatment with respect to conventional physicochemical treatment is that there is no use of chemicals required and higher filtration rates can be applied (Tekerlekopoulou et al., 2013).

In this chapter an overview of the ammonium removal process occurring in the trickling filters at Lekkerkerk is provided. Their characteristics together with the way they are operated and the characteristics of the influent water are reviewed. Furthermore, a general overview of the state of the art around factors hampering nitrification in these filters is also covered.

2.2 Process description of WTP Lekkerkerk

OASEN's major efforts towards achieving continuous ammonium removal is currently focused on two different water treatment plants (WTP): WTP Lekkerkerk, in Krimpen a/d Lek, and WTP Reijerwaard, in Ridderkerk. In both cases, when the problem is analyzed at a general level, it becomes clear that there are two factors hampering with the overall goal of having almost zero ammonium concentration in the plant mixed effluent at all times: first, the lack of on-line measurements for continuous control of the groundwater quality; and, second the current way the filters are operated both individually and as a group. This document deals exclusively with the problem of nitrification in the Lekkerkerk filters. Eventually, similar solutions to those ones that will be proposed at the end of this document could be applicable to Reijerwaard.

In this section, the most important characteristics of the treatment process at WTP Lekkerkerk (see Figure 3) are shortly presented. The treatment process at Lekkerkerk starts even prior abstraction since bank filtration of the surface water from the river Lek works as a kind of natural pre-treatment step. There are 16 filters grouped in two different filtration steps: FF and FK, respectively. The effluent of each FF filter becomes the influent of the filter FK downstream.

The filters are grouped according to the well field they receive water from: Schuwacht and Tiendweg. The water derived from Tiendweg is treated by 10 filters (5+5) while the water derived from Schuwacht is treated by 6 filters (3+3). The Schuwacht filters are numbered from 1 to 3: FF01, FF02, FF03, FK01, FK02 and, FK03. The Tiendweg filters are numbered from 4 to 8: FF04, FF05, FF06, FF07, FF08, FK04, FK05, FK06, FK07 and FK08.

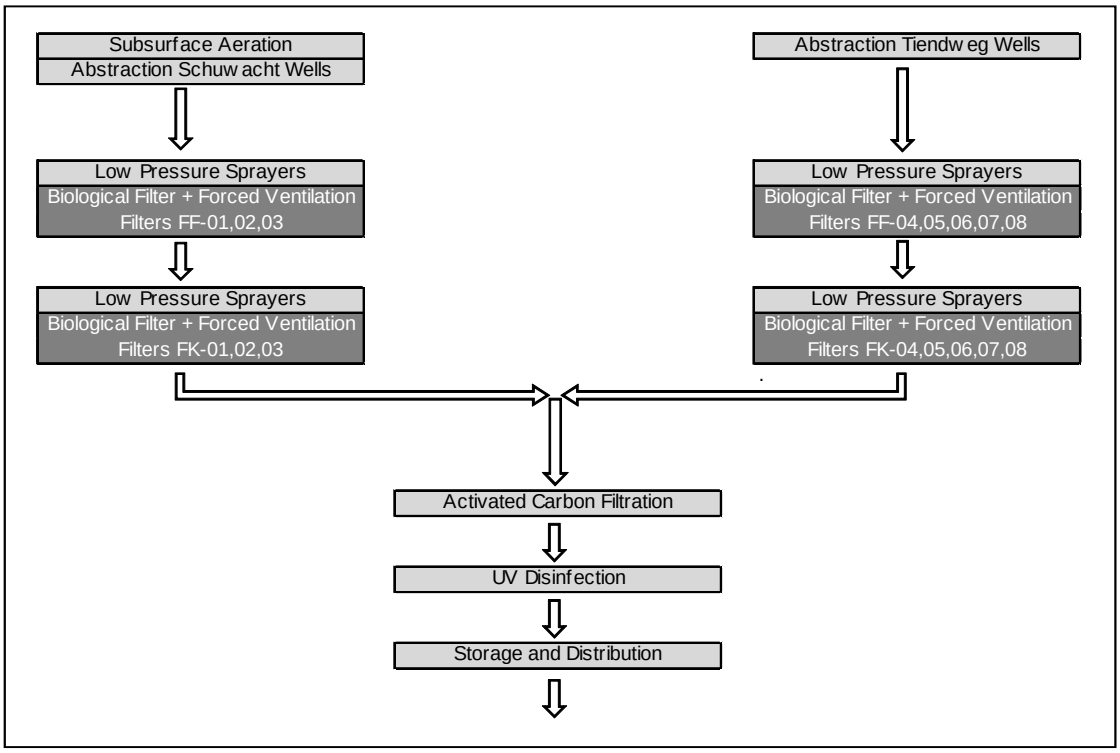

Figure 3 Process scheme of WTP Lekkerkerk

The use of several filtration steps (in this case, two) becomes almost unavoidable and very common when there exist high feed concentrations or there are several different compounds need to be removed (Tekerlekopoulou et al., 2013) as it is the case (see Section 2.4). The consecutive filtration steps are aimed at ensuring long enough contact surface and time so that all four compounds are removed in the two filtration steps. In practice, while in the first filtration step there is combined and simultaneous removal of the four mentioned compounds, the second filtration step is aimed at removing the carry over and the remaining ammonium.

Filtration is combined with aeration to remove methane, ammonium, iron and manganese. From groundwater, iron (II) and manganese need to be removed through oxidation. By adding oxygen, iron (II) is transformed into iron (III) and iron flocs are formed. The iron flocs are retained by the grains. Manganese is transformed to manganese oxide in the presence of previously deposited manganese oxide (catalytic process). Consequently, it can take several months before manganese removal in the filter bed is initialized. Ammonium is transformed into nitrate in two steps by biological oxidation. A group of nitrifiers take care of the transformation of ammonium into nitrite; another group of nitrifiers transform nitrite into nitrate. The decomposition of methane in the filter bed has to be avoided, because it results in an uninhibited growth of bacteria, which can lead to clogging and breakthrough. Methane, therefore, needs to be removed in early aeration. Spray aeration is also used to distribute the water over the surface of the filter. Forced ventilation accompanies the process of filtration as the oxidation of ammonia, iron and manganese requires large amounts of oxygen. Besides this, forced aeration is used for stripping of methane, hydrogen sulphide and carbon dioxide.

Schuwacht differs from Tiendweg since subsurface aeration is used to promote nitrification through pre-oxidation of iron present in water with long residence time (de Vet et al., 2009c). This is thought to be the cause of the excellent behaviour of the Schuwacht bio-trickling filters, compared to Tiendweg trickling filters. More about this issue is discussed later in this document.

The treated water coming out from the secondary filters is mixed before continuing the treatment. Activated carbon filters are used to remove organic micro pollutants. UV-disinfection is used as the final disinfection stage, to reduce specifically heterotrophic plate counts after start-up of activated carbon filtration after regeneration.

Regular sampling

Several samples are taken throughout the treatment train. OASEN has developed a special system for identification. This is explained in Table 2 since these names are used in this document. Each sampling point name consists of eight digits. The first digit indicates whether the sampling point corresponds to abstraction, treatment process or clean water. The second and third digits consider the possibility of having several production lines in parallel. The fourth and fifth digits correspond to the treatment step. The sixth and seventh digits indicate whether the sampling point relates to a specific treatment unit or the mixed stream. Finally, the last digit indicates if the measurement corresponds either to the influent or the effluent. For a better understanding, the process flow diagram can be found in Annex A.1, where each of these allocations is accompanied with the corresponding letters.

Table 2 Identification system for sampling points

DIGIT	1	2,3	4,5	6,7	8
MEANING	Stage	Stream	Step	Unit	Location
EXAMPLES	G: Groundwater	LT: Tiendweg	FF: First	02: Unit 02	Z: Effluent
	P: Product water	LS: Schuwacht	FK: Second	00: Mixed stream	A: Influent
				99: Mixed stream	B: Influent

Figure 4 identifies the sampling points of interest for this project:

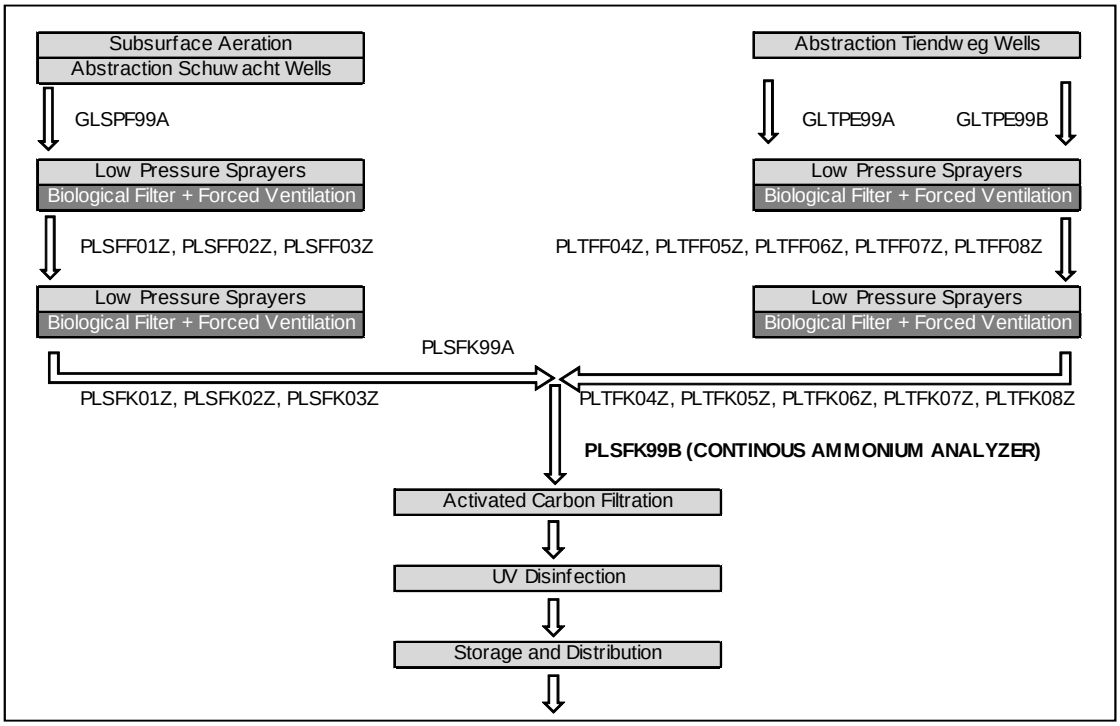

Figure 4 Existing sampling points and allocation of continuous ammonium analyzer at WTP Lekkerkerk

The specific sampling points for the effluent of each individual filter are indicated with the number of the filtration unit and the letter 'z', e.g.: PLTFF04Z stands for the effluent of the filter FF-04 while PLTFK04Z stands for effluent of the filter FK-04.

The general sampling points are:

- GLSPF99A: raw water quality for the Schuwacht filters.
- GLTPE99A: raw water quality for the Tiendweg filters at header A.
- GLTPE99B: raw water quality for the Tiendweg filters at header B.
- PLSFK99A: water quality of the mixed filtrate of all the Schuwacht filters.
- PLSFK99B: water quality of the mixed filtrate of all the Lekkerkerk filters.

Laboratory measurements are taken on a weekly-monthly basis in these sampling points. On a regular basis the water quality in the effluent of single filters is determined for parameters such as ammonium (NH_4^+), nitrite (NO_2^-), nitrate (NO_3^-), iron (Fe) and manganese (Mn), methane (CH_4), ortho-phosphate (PO_4^-), alkalinity (pH), oxygen (O_2), temperature and, bicarbonate (HCO_3^-) are controlled too. Continuous water quality measurements are available only in the final mixed filtrate (PLSFK99B).

2.3 Bio-trickling filters at WTP Lekkerkerk

2.3.1 Description

At WTP Lekkerkerk dry filters are used to remove ammonium. This means that in these filters there is no supernatant water level above the filter bed. The raw water is distributed through sprayers placed directly above them (see Figure 5). The water trickles down passing through the filter bed. Simultaneously, forced ventilation is used causing downward air flow. The water that passes the filter bed is drained through nozzles and collected below the filter bottom, where it flows by gravity to the collector. From the first filtration step, the water follows to the second filtration step. Figure 6 illustrates better the process the water goes through.

Figure 5 Bio-trickling filter in production

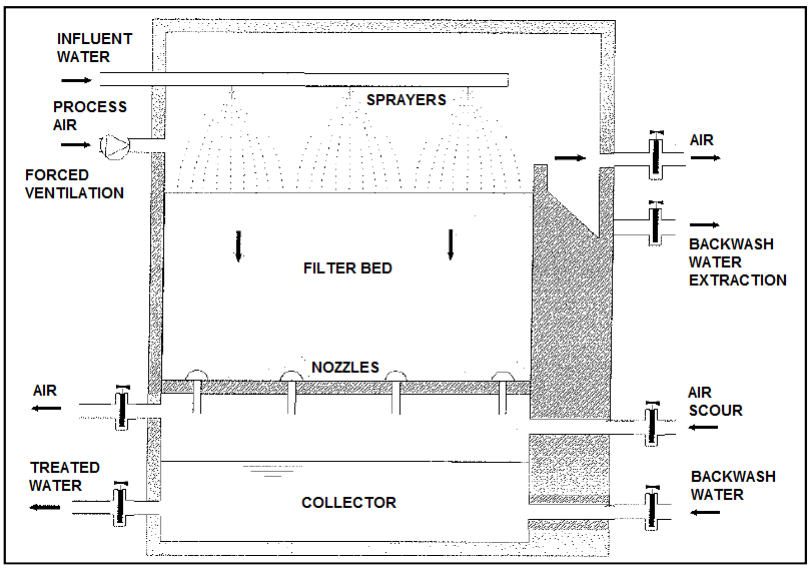

Figure 6 Simplified cross-section of bio-trickling filter at WTP Lekkerkerk

At WTP Lekkerkerk there are 8 filtration sets at WTP Lekkerkerk. Each set is formed by two filters in series: the primary filters are usually named with the letters FF while the secondary filters are referred with the letters FK. Concerning the filters fed by the Tiendweg well field (sets 04 to 08), all the

primary filters (FF) are dual media filters which means that they consist of a layer of anthracite on top of a layer of sand. Filters in the second filtration step (FK) are single media filters filled with sand. The two main advantages of the dual media filters is that the coarse material on top provides a large storage volume for iron flocs and other suspended material while it allows to have a more effective backwash in terms of the achievable bed expansion. This issue is further explained in Paragraph 2.3.2. Table 3 summarizes the main physical characteristics of the filters.

Table 3 Bio-trickling filters characteristics (Tiendweg)

Filter	Material	Density [kg/m^3]	Height [m]	Bed area [m^2]	Grains size [mm]
Primary	Anthracite	700	1	18	1.4-2.5
	Sand	1600	1		0.8-1.25
Secondary	Sand	1600	2	18	1.7-2.5

In reality dry filters at WTP Lekkerkerk, known as well as bio-trickling filters, are used to remove not only ammonium but also other compounds such as iron and manganese. Despite the fact that their lay-out is relatively simple the removal processes occurring inside are in fact a complex combination of biological, chemical and physical processes. Concerning biological oxidation, it is the result of the action of different micro-organisms which are naturally present in the filter. These microorganisms stick to each other on the surface of the inert media (filter material grains), forming biofilms. In the presence of appropriate electron donor substrates, they can sequentially make use of those substrates, generating spatially distributed 'terminal electron accepting process zones' (Upadhyaya et al., 2010). This results in spatial positioning of different groups of microorganisms with diverse metabolic capabilities along the flow direction (and the biofilm layers), which, in turn, facilitates the formation of a redox gradient across the reactor bed (and the biofilm depth). This further allows the removal of multiple contaminants in a single fixed-bed bioreactor system (Upadhyaya et al., 2012). This is the reason because the biological removal of ammonia, iron and manganese tends to concentrate at different bed positions (Tekerlekopoulou et al., 2013). At the top layer there would be mostly iron removal; after the iron has been removed, manganese and ammonia removal would occur more or less simultaneously in the intermediate and bottom layers.

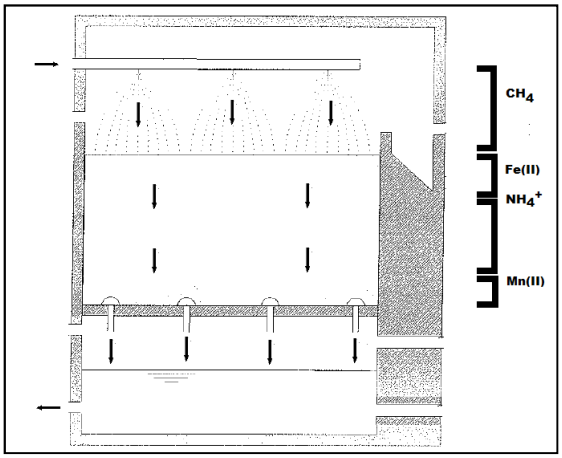

Figure 7 Simplified representation of simultaneous biological removal processes

Key factors in efficient biological removal are the environmental conditions (adequate presence of nutrients and substrates) and the size of the population of microorganisms. Efficient biological removal depends on having the adequate specific surface area, voiding and water retention times too (Tekerlekopoulou et al., 2013). The attachment of the microorganisms to the surface of the grains is important because this makes that the hydraulic retention time is decoupled from the solid retention time. Only in this way, the slowly growing specialized bacteria (e.g. nitrifiers) can develop enough (Boller et al., 1994).

At OASEN regular effluent sampling shows that bio-trickling filters only have problems to achieve complete ammonium removal, but achieve good results for iron and manganese. A quick review of the available literature shows that although considerable effort has been put into researching individual ammonium, iron and manganese removal separately, only a few of the published studies focus on combined and simultaneous biological removal (Tekerlekopoulou et al., 2013). Differences in the time filters need to reach maximum oxidation have been reported (Vayenas et al., 1997).

Nitrification

Nitrification is a two-step biological process. In nitrification, ammonia (NH3) is first oxidized into nitrite (NO2-) by several genera of autotrophic bacteria, being the most important Nitrosomonas. It has been proved that other bacterial species than generally accepted in textbooks are the dominant players of nitrification in groundwater filtration. Extensive characterization of the relevant microbial populations in both families, ammonia oxidizing organisms (ANOs) and ammonia-oxidizing archae (AOA) has been preformed. Those results have shown that ammonia-oxidizing archae are also present in these filters but they are not dominant (De Vet et al., 2009a). Subsequently, nitrite is oxidized into nitrate (NO3-) by several other genera of bacteria, the most important of which is Nitrosospira (De Vet, 2011). The oxidation of nitrites to nitrates is much faster than the oxidation of ammonium to nitrites. The following equations illustrate the chemical conversions occurring:

Equation 1

$$2\,NH_4^+ + 3\,O_2 \rightarrow 2\,NO_2^- + 4\,H^+ + 2\,H_2O$$

Equation 2

$$2\,NO_2^- + 2\,O_2 \rightarrow 2\,NO_3^-$$

These reactions require oxygen, produce hydrogen ions (lowering the pH) and produce nitrite as an intermediate product. The acid produced in the oxidation of ammonium is neutralized by reduction of the alkalinity. The nitrification process influences the carbon dioxide and the carbonate content as well. According to the reaction, the oxidation of 1 mol of ammonia produces 2 mol protons. The protons react with the carbonate present in water:

Equation 3

$$2\,H^+ + 2\,HCO_3^- \rightarrow 2\,CO_2 + 2\,H_2O$$

The complete nitrification equation looks as (USEPA, 1984):

Equation 4

$$NH_4^+ + 1.83\,O_2 + 1.98\,HCO_3^- \rightarrow 0.021\,C_5H_7O_2N_1 + 0.98\,NO_3^- + 1.041\,H_2O + 1.88\,H_2CO_3^-$$

This reaction can be used to estimate the cell biomass production and the oxygen and alkalinity requirements of nitrification. In the expression, the term $C_5H_7O_2N_1$ represents the bacterial cell of nitrifiers, both ammonia and nitrite oxidizing organisms (ANOs and NOOs respectively). For every gram of NH_4^+ and NH_3 converted to NO_3^--N, approximately 4.18 grams of oxygen and 7.07 grams of alkalinity ($CaCO_3$) are consumed and 0.17 grams of bacteria biomass are produced (Chen et al., 2006).

Moreover, since autotrophic microorganisms do not produce any carbon dioxide (as heterotrophs do) the only way of influencing the CO_2 content is through the carbonic acid equilibrium.

Other removal processes

Iron

It has been proved that iron oxidation in trickling filters under neutral and well aerated conditions is not predominantly chemical (de Vet et al., 2011c). Although there is a theoretical competition between chemical iron oxidation and the growth of the *Gallionella* spp., competition is in favour of the second one. Homogeneous iron oxidation seems to be marginal in trickling filtration of anaerobic groundwater because of a residence time of only seconds between spraying and filtration. Additionally, it has been demonstrated that iron oxidizing *Gallionella* bacteria can grow in a wider range of conditions that originally thought of neutral pH and oxygen saturation of the water. *Gallionella* spp. grows comparably well up to pH 7.7 and only significantly less at pH 8.25. In fact, in the normal non-subsurface aerated groundwater trickling filter with incomplete nitrification, it has been found that *Gallionella* spp. grows excessively (de Vet et al., 2012a).

Equation 5

$$4\,Fe^{2+} + 8\,HCO_3^- + O_2 + H_2O \rightarrow 4\,Fe(OH)_3 + 8\,CO_2$$

Manganese

For manganese, although it is above the permitted limit in raw water and it is unstable, the effluent concentrations are almost always below the limit, indicating that total manganese removal is achieved usually. The removal of manganese (Mn (II) is the dissolved form) is accomplished through oxidation, precipitation and sand filtration for the separation of the oxidized insoluble products (Katsoyiannis and Zouboulis, 2004). It is known that manganese chemical oxidation is very slow at pH below 8.5-9.0 (Stembal et al., 2005). Since the average pH value of the raw water before spray aeration is much lower (7.24, in average), the biological oxidation of manganese is considered predominant. Nevertheless, chemical oxidation should not be neglected because of the catalytic effect on Mn2+ oxidation of the oxidized manganese (MnO_2) precipitate coating the grains surface under certain conditions (De Vet, 2011).

Methane

Methane oxidation is a potential competing microbial process but, because of the fact that almost all methane is removed by stripping, this possibility is not plausible (De Vet, 2011).

Competition

In the specific case of the Tiendweg filters, competition of manganese with nitrification might occur: despite the fact that the order of standard potentials suggests that oxidation of manganese should occur after nitrification, full scale observations show full manganese removal combined with incomplete nitrification. Interestingly, the end of the start-up period of the manganese removal of three to six months coincided with the start of the nitrification problems but for the moment this has not been demonstrated. Concerning competition with simultaneous biological iron removal, nitrification strongly improved after the products of iron oxidations were more efficiently removed from the filter bed. Finally, with regard methane, it is removed either before the water enters into the filter bed or very soon after due to forced ventilation so that it is not seen as a likely competitor. More about the issue of competition and possible causes of poor performance is discussed in Paragraph 2.3.2. Therefore, although the different biological oxidation processes may affect each other the characteristics of such interference, if existing, are not yet known.

Aeration

In general, the control of several parameters such as dissolved oxygen, pH and redox is achieved through in an extra aeration step (e.g. cascade) prior filtration if the raw water quality fluctuates widely and frequently or if methane and other gasses need to be removed (as it is the case). At WTP Lekkerkerk, this is combined in the filtration vessel. The raw water is sprayed directly on top of the filter bed (see Figure 8) followed by forced co-current aeration.

Figure 8 Spraying on top of a trickling filter

Aeration is a process which function is to mainly assist with the removal processes occurring within the filter. These are two main reasons because aeration is needed prior filtration:

- The biological processes occurring in the bio-filters require oxygen: (1) conversion of 1 mg/l Fe_2^+ uses 0.14 mg/l O_2; (2) conversion of 1 mg/l Mn^{2+} uses 0.29 mg/l O_2; and (3) Conversion of 1 mg/l NH_4^+ uses 3.55 mg/l O_2. Nevertheless, regular sampling in the effluent shows that oxygen content of filtrated water is close to saturation values. Therefore, more oxygen than required is supplied.
- Methane, which is present in raw water, needs to be removed; otherwise, it could damage the filter bed but also interfere with other biological processes. Methane removal is essentially a physical process that takes place through stripping. Site-specific measurements have shown that methane is easily but not completely stripped by spray aeration (see Section 4.1). Therefore, some methane stripping takes places in the first layers of the filter bed, enhanced by forced

ventilation. Its impact is mainly through disturbing the flow rather than biological competition (De Vet, 2011).

The gas exchange also strips oversaturated gases like carbon dioxide from the groundwater. This increases the pH which, in turn, may stimulate the biological oxidation processes occurring in the filter bed. Moreover, the forced ventilation system could be having another function: by creating a turbulent air flow, it may be contributing to better mixing and turbulent conditions within the filter, which would have a positive effect both through enhancing the transport of substrates and by avoiding the formation of flow channelling.

This and the coming sections focus on analyzing nitrification in these filters under different operating conditions and circumstances in order to think about possible solutions to achieve full nitrification.

2.3.2 Operation

Bio-trickling filters are designed and operated often according to rules of thumb since many processes occur in biological filters and their interactions are not fully understood yet (Tatari et al., 2013). There is a knowledge gap between the way these filters are controlled and how these actions impact each of the processes that are necessary to achieve complete ammonium removal.

The most intuitive way of controlling the operation is through flow adjustment but there are no flow valves installed in the pipe feeding each filter that can be used for that purpose. Therefore, the load is exclusively dependant on the well scheme applied. Recirculation may slightly modify the load but this possibility is available only in a few sets and it is still under investigation. Concerning aeration, the forced aeration systems work continuously at its maximum capacity. Therefore, the various cleaning operations used on the filters are the truly means nowadays through which the filters can be influenced by active control.

This paragraph focuses on describing the behaviour of filters trying to identify relationships and patterns between the operating conditions and the performance of the filters.

Flow rates

In general, biological systems are intended to be operated at relatively constant loads. Since there are not individual flow meters installed in each filtration line, the flow through each filter needs to be estimated based on the total abstracted flow.

The analysis of the total abstracted flow from each well field shows that this premise is clearly not the case for the Schuwacht filters and only partially the case for the Tiendweg filters. The individual flow rate through each filter has been estimated based on the total flow rates presented in Figure 31 and Figure 32 in the next section and assuming that there is equal flow distribution between the filters and that they all are in operation. The results are shown in Figure 9 and Figure 10 and show the hourly variation of the flow over a 24 hours period for the days with maximum and minimum production. Moreover the annual hourly average value and the standard deviation are included to be able to compare the extreme and the average situations.

These results are not valid if some of the filters are out of service due to maintenance reasons. Under that circumstance, the flow through the filters that are still in operation may be significantly higher. Moreover, the specific case of filter FF-05 has been considered in order to determine the unitary flows through the Tiendweg filters as this affects the number of units the total flow needs to be divided into. As it will be explained later, this filter receives approximately half of the raw water that the other filters receive.

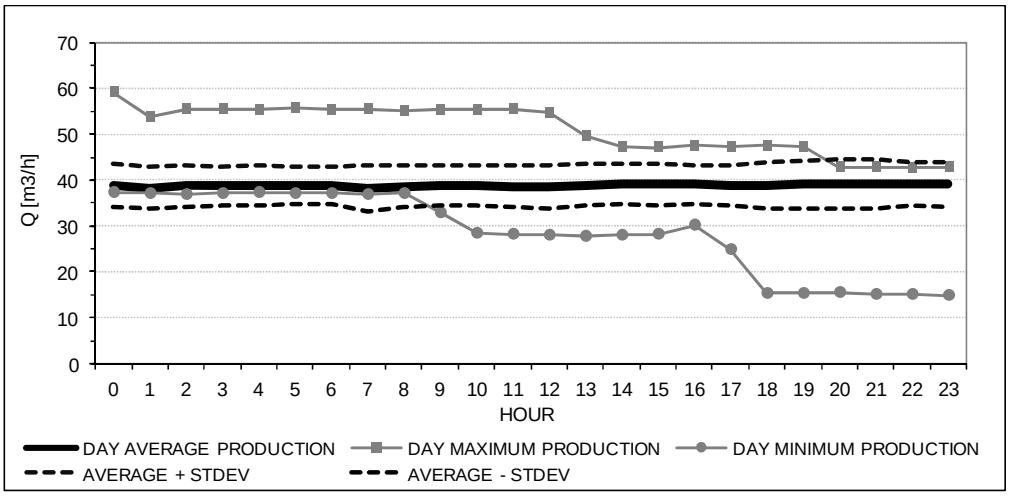

Figure 9 Estimated hourly unitary flows for Tiendweg filters (2012)

According to Figure 9, the Tiendweg filters receive mostly flows within the range 33-45 m^3/h. But these filters also operate sometimes at very high flow rates: e.g. up to 55-60 m^3/h during the day of maximum production.

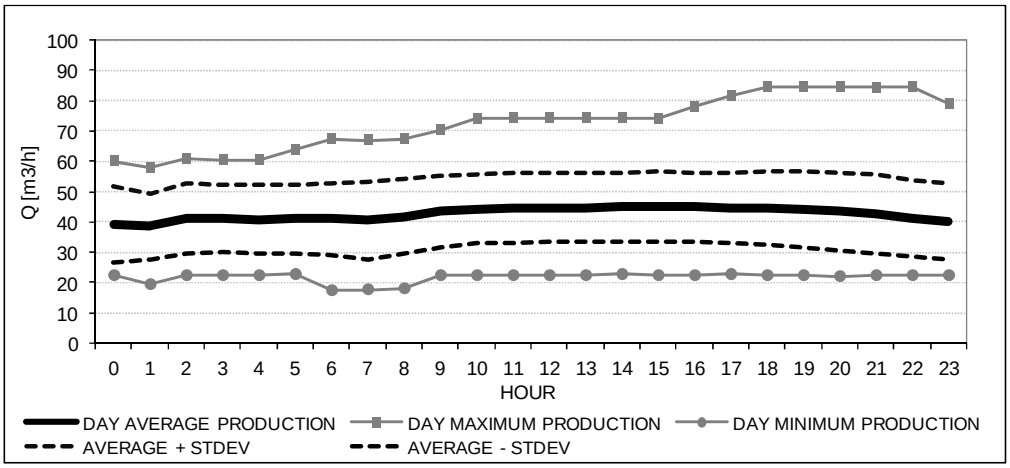

Figure 10 Estimated hourly unitary flows for Schuwacht filters (2012)

According to Figure 10 the unitary flow through Schuwacht varies much more, ranging mostly between 29 m^3/h and 58 m^3/h and with peak values of 83 m^3/h.

Effluent characteristics

Filters performance is often evaluated solely based on effluent concentrations. Bio-trickling filters are monitored weekly with laboratory analysis of the effluent. When comparing the effluent concentrations of ammonium, iron and manganese over the time two things become clear. First, the ammonium concentration in the effluent of filters 01, 02 and 03 at WTP Lekkerkerk is zero or almost zero (see Figure 11). These filters perform well, achieving total ammonium removal and for this reason, this project will focus exclusively on Tiendweg filters.

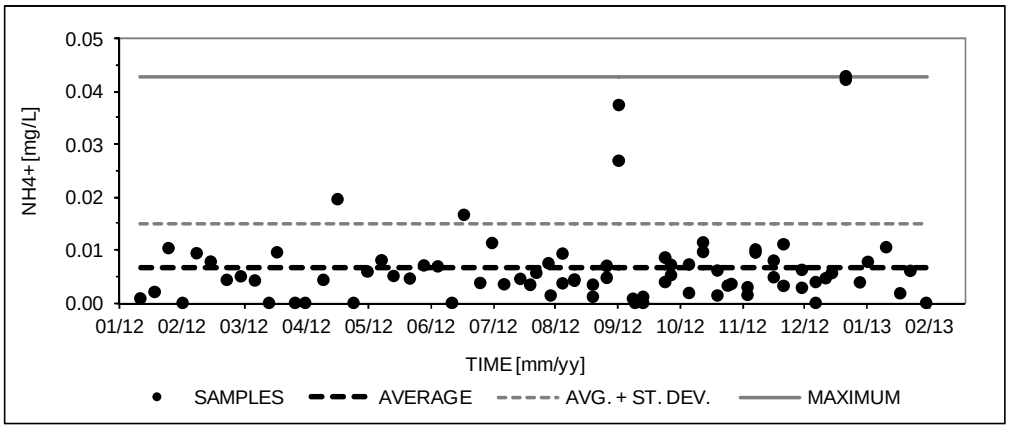

Figure 11 Ammonium concentrations in Schuwacht mixed filtrate (01/01/2012-01/02/2013)

Concerning the Tiendweg filters, it has known the different ability of the dry-bio-filters to remove iron and manganese on one side and ammonium in the other side (de Vet et al., 2009c). While the removal efficiencies for iron and manganese remain constant and high, the efficiency of ammonium removal shows significant variations. In addition to this, effluent measurements have proved that there is no nitrite accumulation. This implies that ammonium is completely oxidized to nitrate (NO3-) except for short periods during some filter startup periods. Full-scale measurements have proved that oxygen concentration in the effluent of the filters is close to saturation as well, which seems to exclude the occurrence of oxygen depletion at any loading condition. The pH increases slightly after aeration, due to the release of CO_2.

Figure 12 and Figure 13 are aimed at illustrating better how the performance of primary filters change with time and how that impacts the response of secondary filters. Figure 12 stands for filtration set FF-FK-07. Figure 13 stands for set FF-FK-08. On the x-axis the time is displayed (10 years period). On the vertical axis on the left there is the range for the measured ammonium concentrations. On the plotting space, there are four groups of dots, representing the observed ammonium content along the process. The dark and light small squares are the concentrations measured upstream the filters. The light grey dots stand for the ammonium concentration in the effluent of the first filtration step and, hence, indirectly represent the goodness of its performance. Finally, the black small dots correspond to the concentrations downstream the second filtration step.

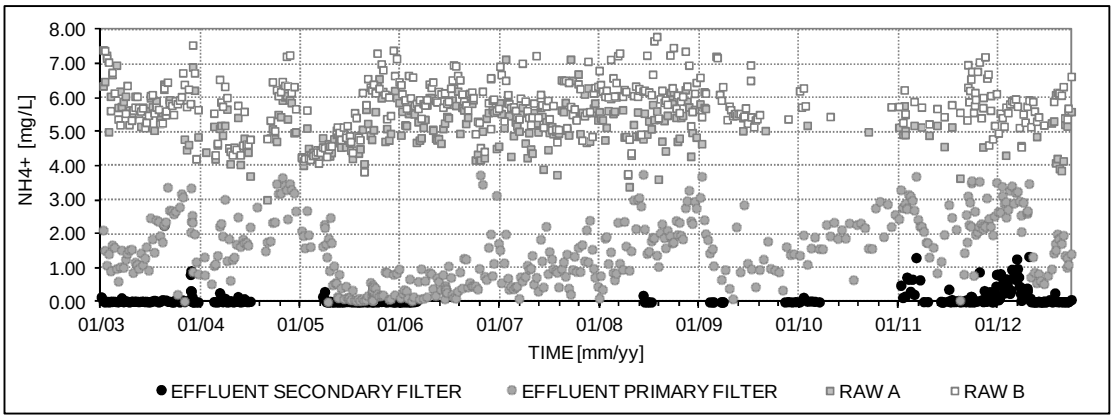

Figure 12 Influent and effluent ammonium concentrations in filter set FF-FK-07 (2003-2012)

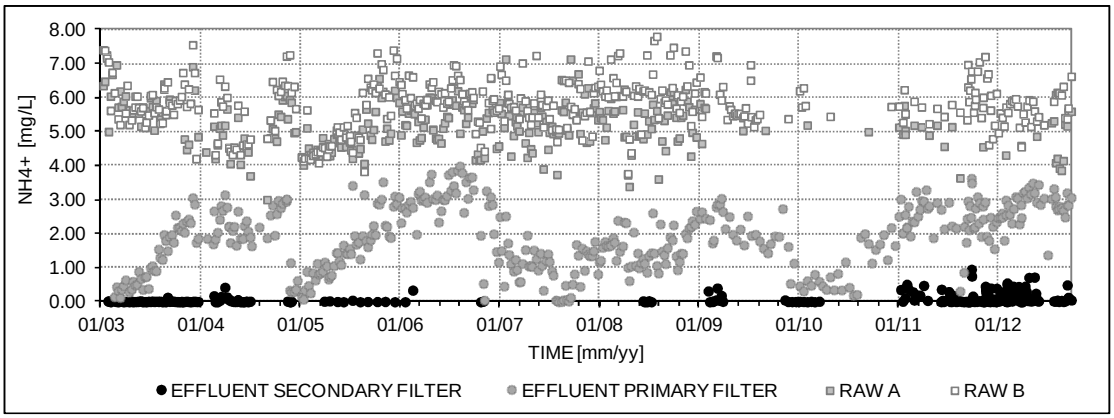

Figure 13 Influent and effluent ammonium concentrations in filter set FF-FK-08 (2003-2013)

Although these figures only show the big picture without paying attention to the small details, they portray the main facts that characterize nitrification in the Tiendweg bio-trickling filters:

- It can be clearly seen that filters operate under extreme dynamic conditions due to the fluctuation of the ammonium concentration in their feeds. Whether this affects the bacterial growth or not it will be studied later, with the help of the mathematical model (see Section 4.5).
- Primary filters show often incomplete nitrification (effluent much greater than 0-1 mg NH_4^+/L).
- There seems to be a kind of cyclic behaviour when it comes to defining such deterioration in the behaviour of first filters.
- Sudden changes in the effluent ammonium concentration of primary filters are not infrequent. They are thought to be linked to sudden increases in the loading that the filter is not able to cope with.

Therefore, the system response can be seen as the combination of a general trend with short-term response. In the following paragraphs, it will be shown how those patterns and the effluent of primary filters is related to the occurrence of two kinds of operations: external washing and renewal of the filter material. Similarly, it will be shown how the response of secondary filters is influenced through the application of backwashing.

Backwashing in primary and secondary filters

Both primary and secondary filters are routinely backwashed. Backwash is primarily performed in order to avoid clogging. Clogging implies the progressive obstruction of some parts of the filter, the appearance of flow channelling and the reduction of the specific surface area. Therefore clogging may come along with a modified gas and liquid flow behaviour (Iliuta and Larachi, 2006), which may affect the efficiency of aeration and/or the substrate transport process, resulting in ammonium breakthrough.

In primary filters, clogging is mainly caused by inorganic deposits that accumulate in the filter pores over the course of the time. These deposits mostly consist on iron oxyhydroxides deposits (De Vet, 2011). The limited growth of autotrophs (nitrifiers) seems to exclude potential clogging problems related exclusively to biomass accumulation. For secondary filters iron is not present and clogging, which is not always externally observed, is thought to be caused by biomass accumulation. In these filters backwashing is performed with the sole intention of preventing ammonium breakthrough from happening. This difference is important since it may help to explain the differences in the response of each filtration step to backwashing.

Backwash is performed every time the filter run time reaches a certain time of operation (3-4 days for filters in the first filtration step and 20 days for filters in the second step). This difference in the frequencies is related to the risk of clogging assigned to each filtration step. During backwash, the water flows in upward direction through the filter. The water scours the filter grains, erodes the accumulated solids from the filter material, expands the filter bed, and transports the solids towards the backwash collection hoods. Backwash can be performed with up-flow wash water alone or combined with air scour. Figure 14 and Table 4 show the characteristics of the backwash programme characteristics for primary filters at WTP Lekkerkerk.

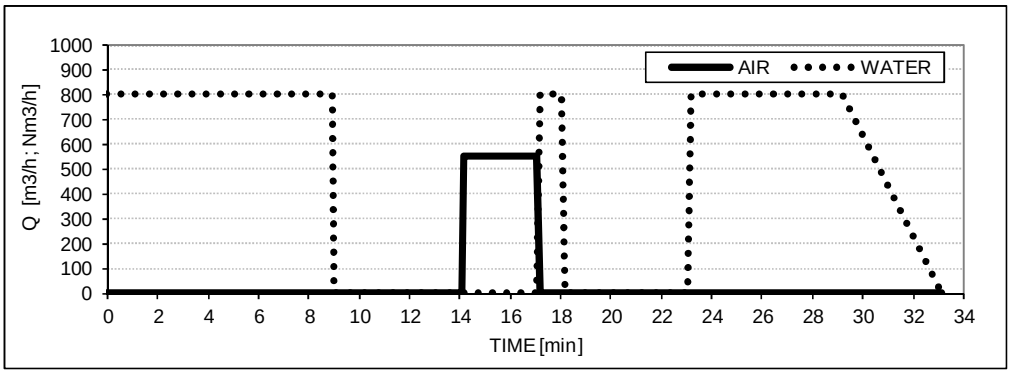

Figure 14 Air and water flows for backwashing of primary filters at Tiendweg

Table 4 Backwash programme characteristics for primary filters at Tiendweg

Runtime [h]:				96.00
Backwash programme Dual-media filters	Duration [min]	Air [Nm³/h]	Water [m³/h]	Water [m³]
Filling	9.00	0.00	800.00	120.00
Drain to FK	5.16	0.00	0.00	0.00
Air	3.00	550.00	0.00	0.00
Water	1.00	0.00	800.00	13.33
Drain to FK	5.00	0.00	0.00	0.00
Water	6.00	0.00	800.00	80.00
Water reduction to 0%	4.00	0.00	0.00	0.00
Total	33.16			213.33

Literature indicates that the effectiveness of the backwash is related to the flow velocity, the achieved filter expansion (de Moel et al., 2006) and the right combination of water and air. The higher the flow velocity is, the more efficient the backwash results. Nevertheless, the backwash rate is limited by different conditions: first, the size of the backwash pumps; second, the risk of causing overflow; and, third, filters should be washed gently so that the biological film on the grains is not completely removed. In that respect, vigorous backwashing might adversely impact the nitrification capacity of the filter through removing undesirably too many ammonia-oxidizing organisms.

There are indications that backwashing may significantly reduce the microbial abundance. The observed ammonium breakthrough episodes in secondary filters have a shape resembling the Monod growth curve which supports this idea (see Figure 15). After backwashing, second stage filters may respond in two different ways according to the available full-scale measurements. Sometimes, there is a 'ripening' period characterized by an initial breakthrough of the ammonium concentration in the effluent. In those cases, the filters needs certain time to return to full nitrification. In other cases, there is no breakthrough after backwashing.

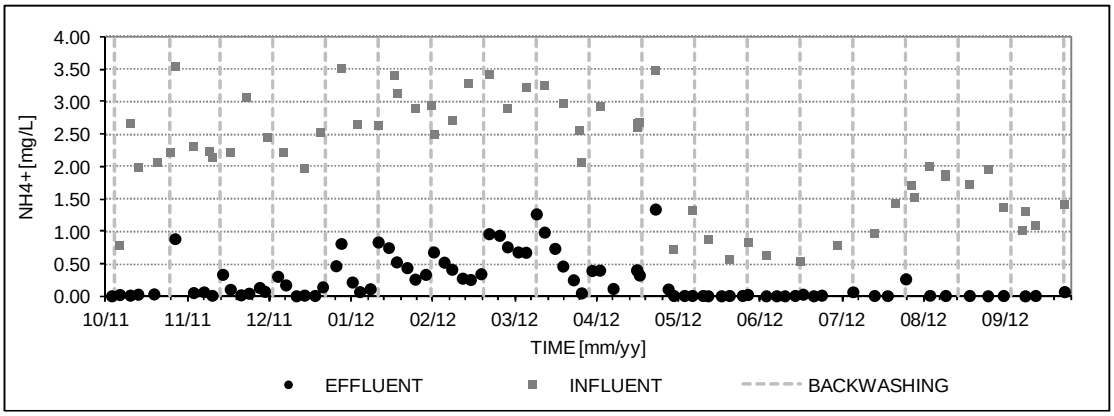

Figure 15 Influent and effluent ammonium concentrations in secondary filter FK-05 (10/2011-09/2012)

Continuous measurements in primary filters show peak levels of ammonium after backwashing sometimes but very similar values for the ammonium concentration in the effluent before and after backwashing some other times. Figure 16 and Figure 17 illustrate both cases.

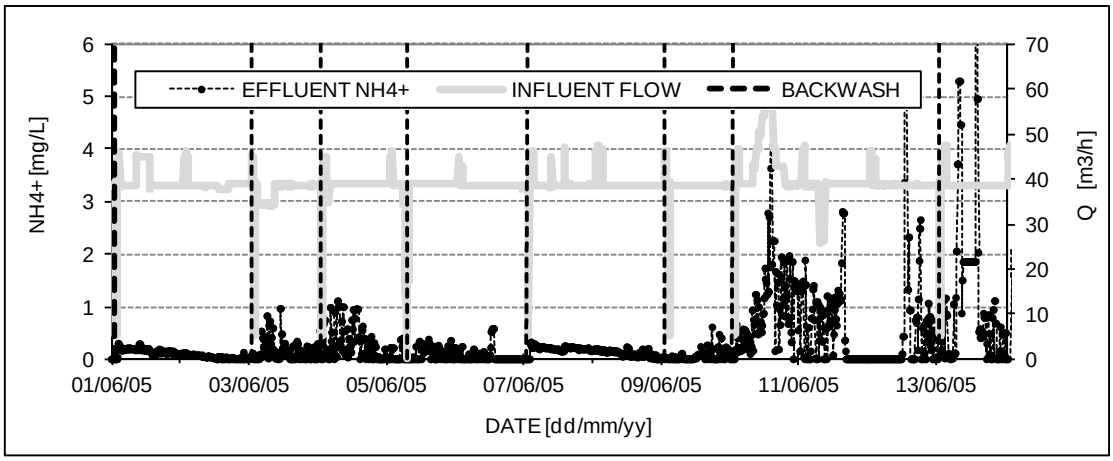

Figure 16 Continuous ammonium effluent concentration and flow in primary filter FF-07 (05/2005)

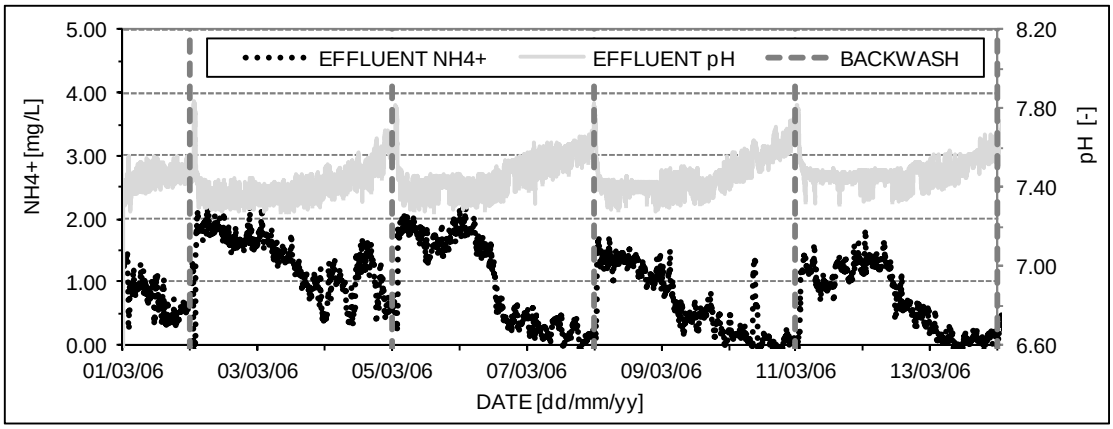

Figure 17 Continuous ammonium effluent concentration and pH in primary filter FF-05 (03/2006)

Some past research in the studied filters (De Vet, 2011) found that there is no excessive washout and detachment of ammonia-oxidizing organisms (ANOs) in primary trickling filters with poor nitrification rates. In addition to this, some authors (Upadhyaya et al., 2012) have claimed that backwashing may help establish desired microbial populations and prevent the apparition of preferential flow channels although that depends on the water quality, the filter bed material characteristics and the capacity of microorganisms to be retained in the system.

According to this information, there are no conclusive results about how backwashing affects the microbial community structure. These results suggest that there are differences in the effect of backwashing depending on the filter. They suggest for instance that if there are not elements other than biomass causing clogging, the effect of backwashing on the nitrification capacity may be just negative, e.g. filters in the second filtration step.

The reasons for the described differences are unknown but they could be linked to the amount of biomass present in the filter, the characteristics of the filter bed (dual or single media) and the existence of accumulated inorganic deposits since they all three are characteristics that change between the three cases considered: primary filters with high ammonium removal, primary filters with low ammonium removal and secondary filters. Hence, it might be interesting to asses the effect that filter coating and inorganic precipitates may have on the abundance of ANO cells and their structure**.**

Figure 17 also shows another interesting issue: it is seen that the pH increases at the same time that nitrification improves. This result, which suggests a better gas exchange at the end of each cycle, is further analyzed in Section 4.1.

Bed expansion

A major difference between primary and secondary filters is the achievement of expansion during backwashing. For an effective removal of the clogged material, at least about 10% expansion is necessary. Figure 18 shows the expansion curves for sand and anthracite where the flushing water speed is indicated in the figure with a dotted vertical line.

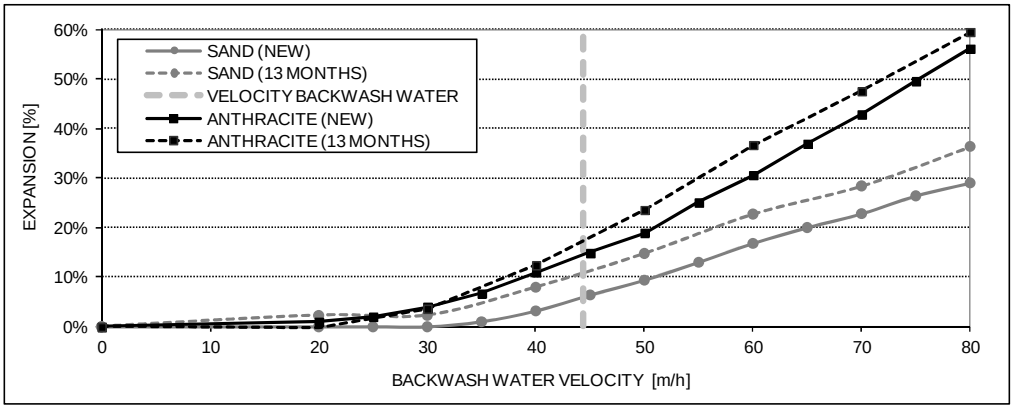

Figure 18 Filter bed expansion for anthracite and sand as a function of backwash velocity

Measurements show that around 13-17% of expansion of the anthracite layer is achieved. This is important because in dual media filters, most of the deposits are retained in the upper layer. This allows counteracting more effectively the accumulation of sludge. By contrast, the lower layer of the filter, which is conformed by sand, is not likely to achieve a minimum level of expansion. Something similar is likely to occur in secondary filters with are single-media sand filters.

Figure 18 also proves that the expansion does not decrease despite the growth of the grains over time. Indeed, with aged filter material the expansion is significantly higher: 5% for sand and 3% for anthracite. The hypothesis is that this might be due to the lower density of the material covering the sand grains and the reduction in the size of the anthracite grains.

Past experiments have demonstrated that the usage of dual media filters in combination with the application of backwashing with media expansion slowed down the relapse in nitrification (De Vet, 2011). Figure 19 illustrate this: nitrification remained better in the dual media filter for which partial expansion of the filter bed was achieved. Contrarily, the filter where expansion was hardly achieved showed a higher rate of relapse of nitrification. The specific reasons for such different are not fully known yet.

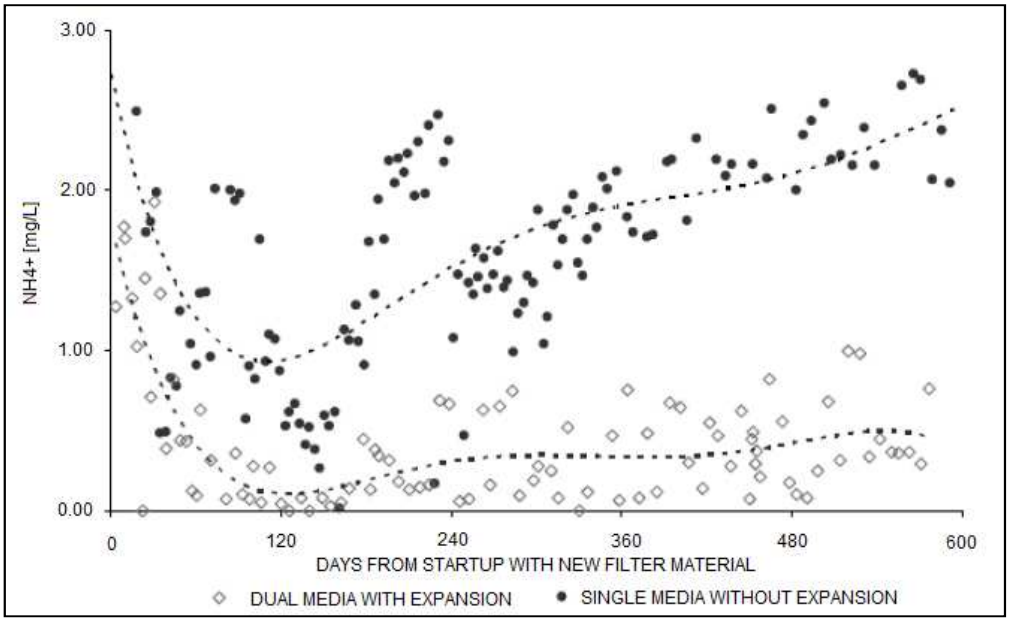

Figure 19 Ammonium in the effluent of a filter with backwashing without expansion and a filter with backwashing with bed expansion (De Vet, 2011)

External washing of primary filters

As shown in Figure 19, primary filters do not perform anymore as required after certain time, usually months. Whatever the causes for the observed decrease in nitrification are, the current backwashing programme is ineffective to restore nitrification in primary filters. External washing of the filter

material is the first measure that is used in primary filters in order to restore their nitrification capacity. Usually external washing takes place when the company guidelines of the quality parameter in the effluent are reached or when some operational parameters such as the filter bed height reach their threshold level. Filter material remains from 2 to 4 days out of the filter vessel. This procedure is a labour-intensive activity with high economic cost. As a result of external washing, accumulated deposits and biomass is removed.

Although the working mechanisms and relevant factors are not fully understood yet (De Vet, 2011), primary filters usually go through the same stages after external washing. Figure 20 clearly illustrates this point. The dots on the plotting space represent the ammonium concentrations upstream-downstream one primary filters at WTP Lekkerkerk over a 6 years period. The time is shown on the horizontal axis. The vertical dotted lines represent the times when external washing was performed.

The decrease in the ammonium removal capacity generally evolves fast. At first, when the filter material is placed back into the vessel and the filter returns in operation significant improvement in nitrification is observed after a very short start-up period: full-scale measurements show that external washing restores almost complete nitrification. Unfortunately, the effect on nitrification is temporary and nitrification starts to relapse after a few months: 4-6 months. The relapse in nitrification develops until a turning point in this process seems to be reached, which occurs after 8-10 months of operation. From that moment, the filter behaviour enters a different stage: primary filter seem to have lost its capacity to cope with fluctuations in the influent since the ammonium concentrations oscillate more and more accordingly to the change sin the influent.

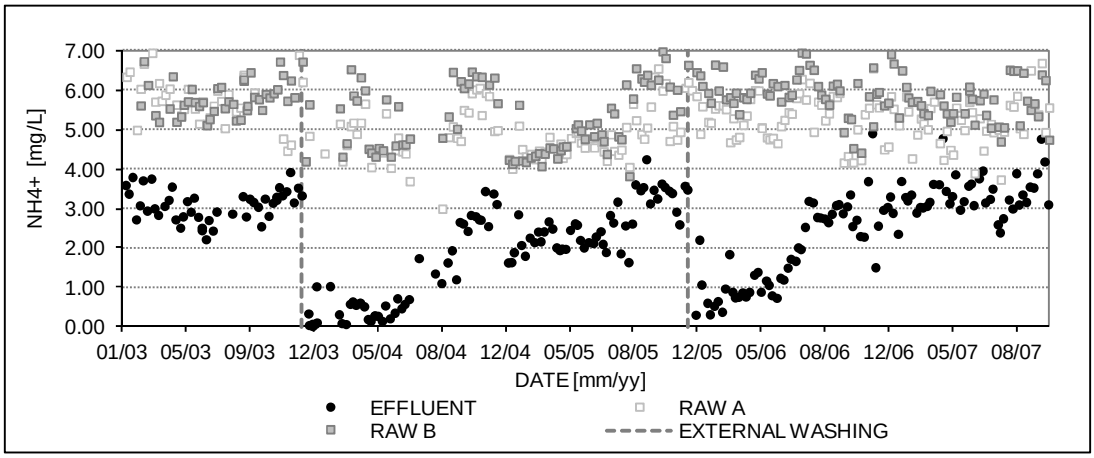

Figure 20 Typical fallback patter of ammonium removal in primary filters after external washing

The graph also suggests that there are differences between cycles of the same filter, which means that the precise time when nitrification starts to relapse varies and the rate of relapse too. Figure 21 proves that there are differences also between cycles.

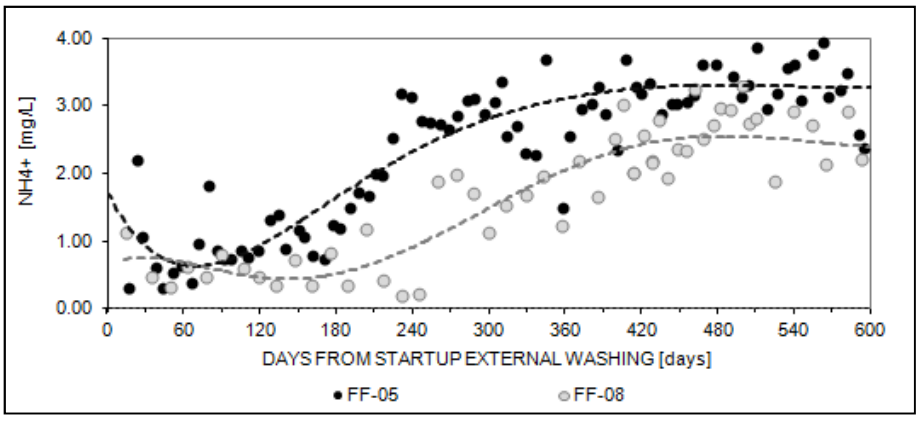

Figure 21 Comparison of fallback patterns of ammonium removal in two primary filters after external washing

Renewal of primary filters

Experience indicates that after a long time, usually years, external cleaning is not effective anymore as a way of restoring nitrification. When that happens, the filter material needs to be renewed. The frequency of maintenance and the number of times external cleaning (2 times external cleaning; third time new material) is determined pragmatically, with all filters of a purification step maintained the same way, regardless of process operation.

There are important differences between the way the filter behaves after external washing and material replacement. Figure 23 (filter FF-07) and Figure 22 (filter FF-08) illustrate the typical response after renewal.

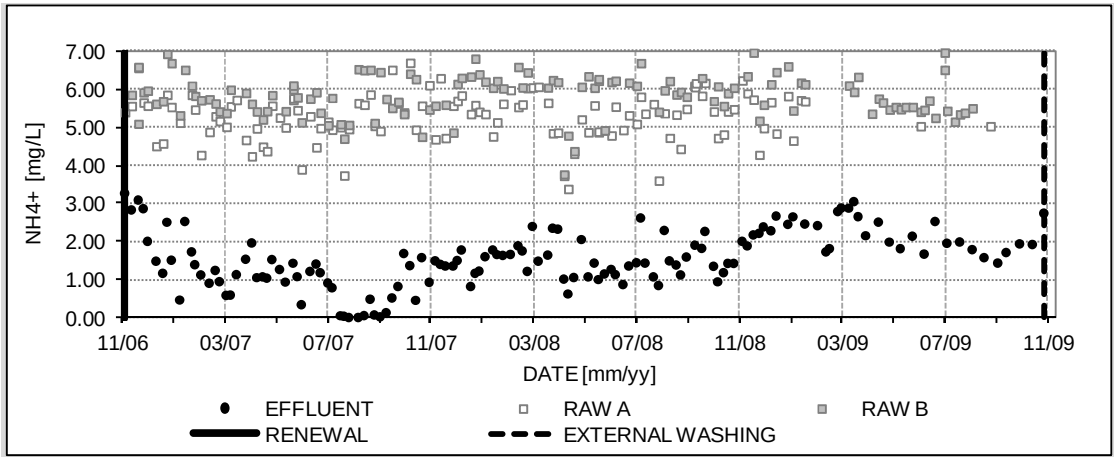

Figure 22 Influent and effluent ammonium concentrations after filter material renewal in filter FF-08

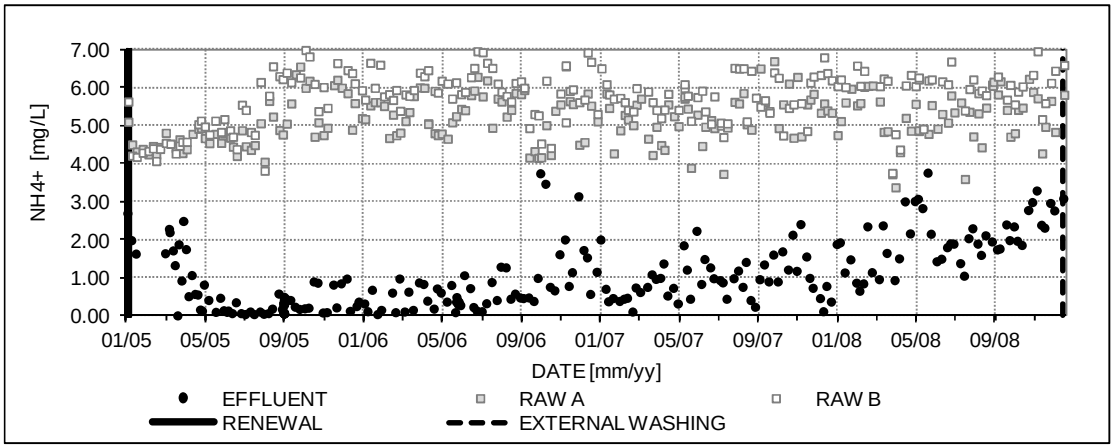

Figure 23 Influent and effluent ammonium concentrations after filter material renewal in filter FF-07

According to the above shown figures, the start-up takes considerably longer than after external washing. Several months may be necessary to reach complete ammonium removal. Such behaviour is thought to be linked to the process of growth of nitrifying bacteria. Some authors (Van Hulle et al., 2007) have reported that the limited amount of nitrifying organisms and, consequentially, a lower biofilm thickness limits the capability of the bio-filter to remove either to deal with the influent ammonium concentration or with sudden peaks in ammonium concentration that may occur. According to this idea, it is the rate at which population develops what determines the filter response during this start-up period.

Once complete ammonium removal is reached, the decline starts after a few months (around 4-6 months). Interestingly, the rate the rate of relapse in nitrification is lower after filter material renewal than after external washing if comparing the time scales of Figure 21, Figure 22 and Figure 23.

Other events

The previous described operations correspond to the set of actions that have been defined by OASEN as the standard operation regime for bio-trickling filters. They are regularly implemented and the

performance of the filter can only be explained the load and the history of these kind of actions are considered.

But, during the last years, some other actions have been performed on some of the filters as well. All these actions were aimed at investigating methods for nitrification enhancement. Such actions are under research and, therefore, must not be considered as part of the standard maintenance regime. All these events have been excluded from the statistical analysis presented in Section 4.1 in order to not undermine the validity and representativeness of such results. However, they may have strongly affected the filter response and, consequently, are listed here.

- **Phosphate dosage** has been tested in filter FF04, FK07 and FK08 in order to check if the relapse in nitrification is related to the lack of microbiologically available phosphate. It is believed that iron and manganese oxidizing organisms (IOOs and MOOs, respectively) have a higher affinity for phosphate than ammonia-oxidizing organisms (ANOs). With this in mind, it has been hypothesized that the precipitation of phosphate with biogenic oxyhydroxides and the competition for phosphate by Gallionella spp. are the causes of phosphate limitation for ammonia-oxidizing bacterial leading to low microbially available phosphate (de Vet et al., 2012b). There is not a clear picture since the results derived from full-scale filters, batch experiments and small scale column tests have not provided conclusive results.

- Since November 2004, the water from six wells follows a separate pre-treatment step: since that raw water contains high chloride concentrations is purified by a reverse osmosis (RO) step prior biological filtration. The resulting **RO permeate is mixed with the raw water** derived from other wells before going into the trickling filter **FF05**. A flow meter downstream the RO units register their contribution to the total flow. The usual mixing ratio is 1:1 (25 m^3/h each stream). As a results filter FF05 is half-loaded (ammonium load, not hydraulic load) if compared to the other filters in the first filtration step. Figure 24 shows this change.

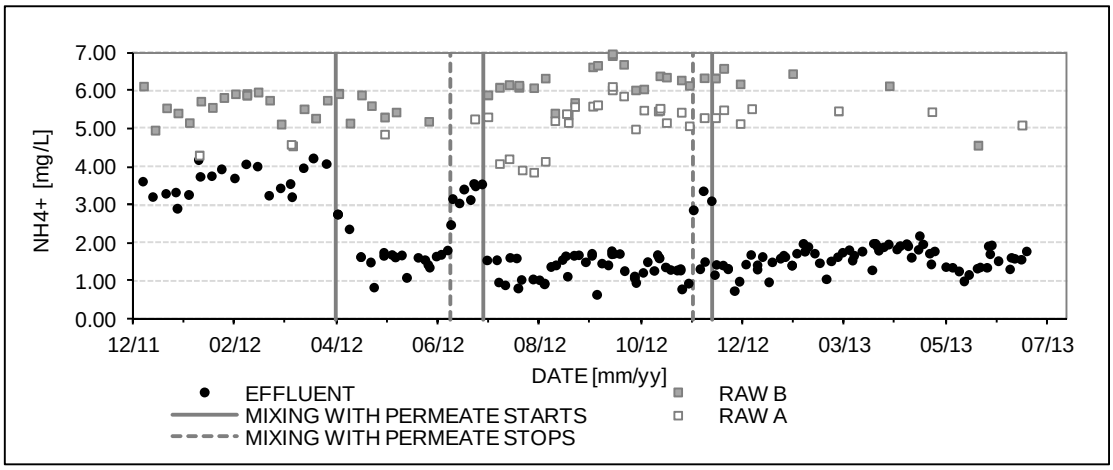

Figure 24 Influent and effluent ammonium concentrations during mixing of raw water with RO permeate in filter FF-05

- **Effluent recirculation** has been tested at different time periods in sets FF-FK-04, FF-FK-05, FF-FK-06 and FF-FK-07. A fraction of the effluent of a secondary filter is recirculated and mixed with the influent water of a primary filter. In general a positive effect has been observed although not always. Furthermore, the positive effect tends to disappear after certain time. The mechanisms by which recirculation stimulates nitrification are not clear and further research is needed (de Vet et al., 2012b). The mechanisms could be linked to the inoculation of active cells coming from the second filtration stage into the stream that feeds the primary filter. By doing that before the water enters into the filter, the interference with the same cause(s) that inhibits nitrification in the bed may be being avoided. If the inoculation of new microbial 'actors' is the case, that could mean that either (1) the washout of biomass is not negligible in filters with full nitrification (second stage filters) although this is the case in filters with poor nitrification; (2) the washout is negligible (low cell numbers are re-circulated) but what enhances nitrification in recirculation is having an optimal contact between the (active) biomass population (scarce, theoretically, in the effluent of any filter) and the substrate(s). Moreover, it is not known if the inoculated (re-circulated) nitrifying cells keep being active in the bioreactor or they become inactive, as it is known that this is what happened with the original cells present in the filter. Therefore, several hypotheses are possible: (1) the inoculation of (active) nitrifiers (ANOs); (2) the recirculation of basic nutrients; (3) the enhancement of chemical iron (and manganese) removal; and, (4) the suppression of the growth of iron oxidizing bacteria (IOB). An interesting (and alternative)

application could consist on applying it in order to accelerate the start-up period after renewal of the filter material.

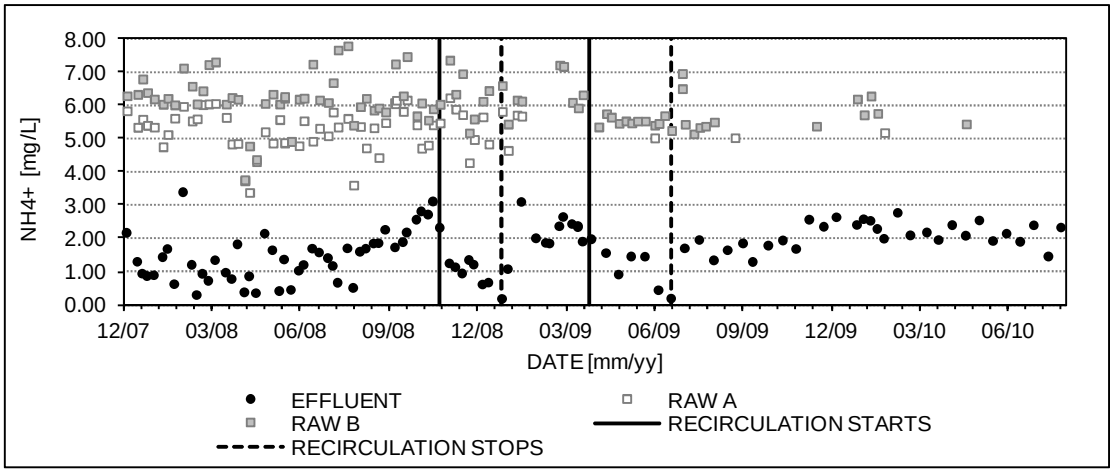

Figure 25 Influent and effluent ammonium concentrations during recirculation in filter FF-06

- In order to get better insight into whether simultaneous iron removal contributes to the decline of nitrification through phosphate limitation, an experiment where biological iron and ammonium oxidation are performed in different filtration units was planned. Iron has been removed from the influent of filter **FF04** between April 2011 and February 2012 by a pair of highly loaded dry filters (filtration velocities of 10-25 m/h) upstream where chemical iron oxidation took place. One of the hopes behind this experiment was that the **suppression of simultaneous biological iron removal** upstream would result on better nitrification in the trickling filter. Additionally, some other experiments were performed such as phosphate dosing and changes in the backwash programme. Unfortunately, results showed that although nitrification was stable at the beginning, relapse started after 6 to 12 months with similar pattern than in other Tiendweg filters. This suggests that either iron biological oxidation is not the cause or there are several causes, one of which is due to simultaneous iron-ammonium biological removal whose effects superpose to each other. Figure 26 illustrates the filter response during that time.

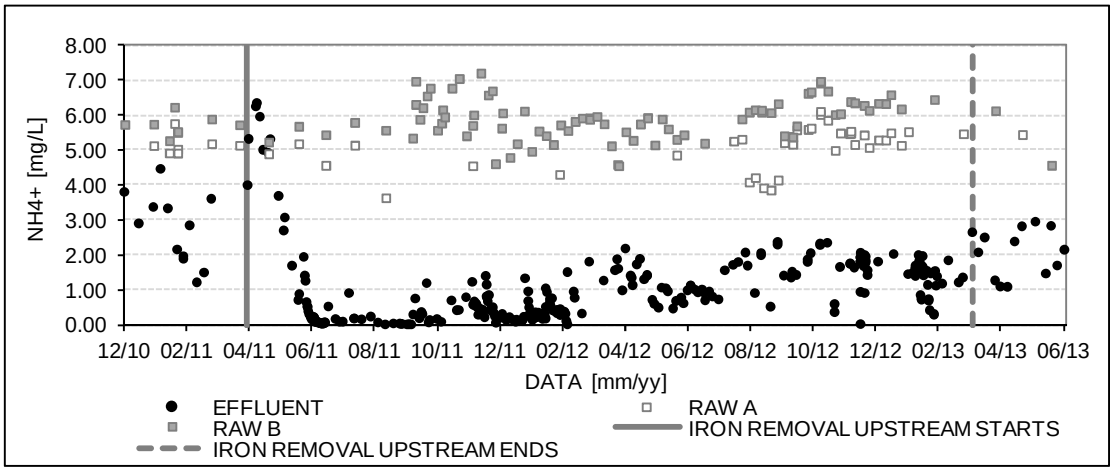

Figure 26 Influent and effluent ammonium concentrations during suppression of simultaneous biological iron removal in filter FF-04

2.4 Raw water at WTP Lekkerkerk

The operation of WTP Lekkerkerk is aimed at a constant flow for Tiendweg, possible fluctuations in demand are theoretically only covered by Schuwacht. The reason for that mode of operation has been discussed in Paragraph 2.3.2 but in short it is attributable to the fact that nitrification in Schuwacht filters is stable, even under variable loads, and almost complete. By contrast, the primary filters fed by the Tiendweg wells show efficient nitrification only from the start-up period till the first couple of months. After that time, the ammonium concentration in the filter effluent starts to rise as shown in Figure 1.

The abstracted **flow** is determined from the level in the clear water storage and the actual water consumption. Submerged pumps in the wells are operated at fixed velocity. The number and combination of wells, known as "well schemes", is decided beforehand in order to meet the demand and to distribute the working hours homogeneously among all the wells. Figure 27 provides an order of magnitude of the total flow abstracted daily throughout the year. In 2012 the total flow varied between a minimum of 196 m^3/h and a maximum of 434 m^3/h. The average abstracted flow was 302 m^3/h.

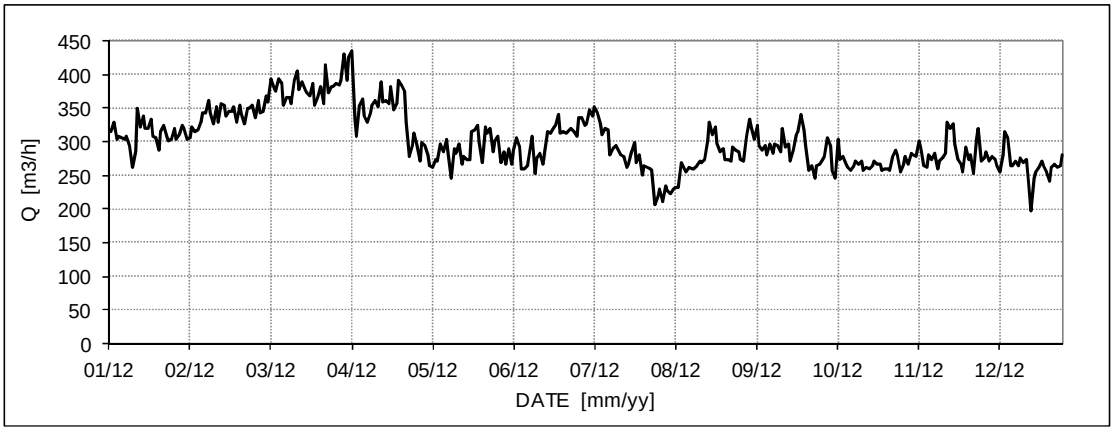

Figure 27 Flow daily values at WTP Lekkerkerk (2012)

Figure 28 illustrates the contribution of each well field to the total plant flow shown in the previous figure. It is seen that Tiendweg has a higher share than Schuwacht which seems logical taking into consideration the number of filters fed by each well field. Furthermore, although Tiendweg is theoretically aimed at operating at a fixed flow rate, the figure also proves that the flow throught the Tiendweg filters may vary significantly. According to the figure, the average daily flow was 197 m^3/h from January to March and 167 m^3/h in the period April-December. The minimum and maximum daily flows were 128 and 230 m^3/h respectively.

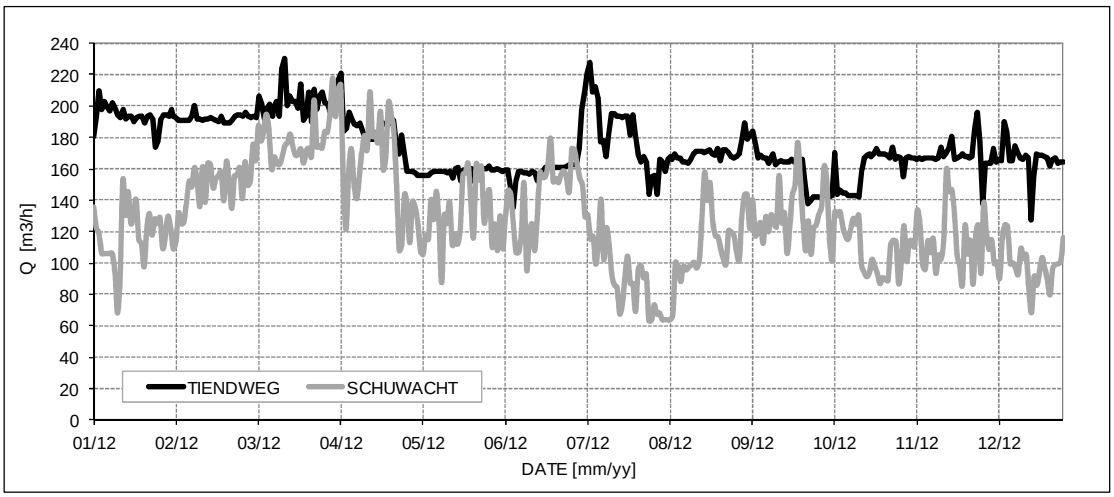

Figure 28 Schuwacht and Tiendweg flow daily values at WTP Lekkerkerk (2012)

These flows can be converted into percentages that indicate the importance of each well field over the year. In Figure 29 it can be seen that the contribution of Schuwacht was mostly between 36% and 47% (42% on average) in 2012, being the extreme values 26% and 54%. The share of Tiendweg was mostly between 53% and 64% (58% on average), with extreme values of 46% and 74%. This means that Schuwacht barely reaches 50% of the production and at all times contributes no less than 25%. This has consequences with regard the maximum admissible ammonium concentration in the mixed filtrate of all Tiendweg filters. This issue is further explained in Section 2.5 and a key aspect considered in the solutions presented in Sections 5.2 and 5.3.

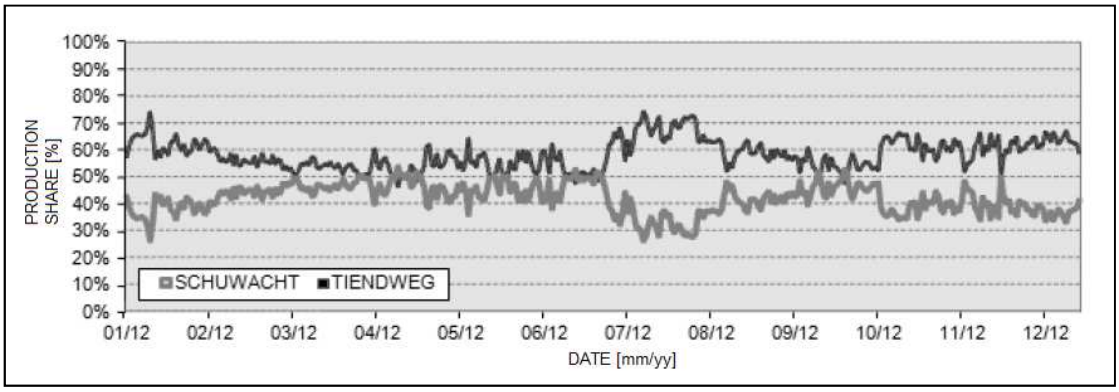

Figure 29 Schuwacht and Tiendweg production shares (2012)

Figure 30 shows the flow division between the two pipes that bring the raw water from the Tiendweg wells to the bio-trickling filters FF-04 to FF-08. This flow division is important since there are differences in the water quality measured in each stream. It can be seen that the preferential operation is to feed the water almost completely through one of the headers in order to ensure that all filters receive water with the same quality. The last shift took place in September 2012. From then the supply is given almost exclusively through the pipe A. The flow through pipe B is minimum and with the only purpose of avoiding the existence of dead zones in the pipe.

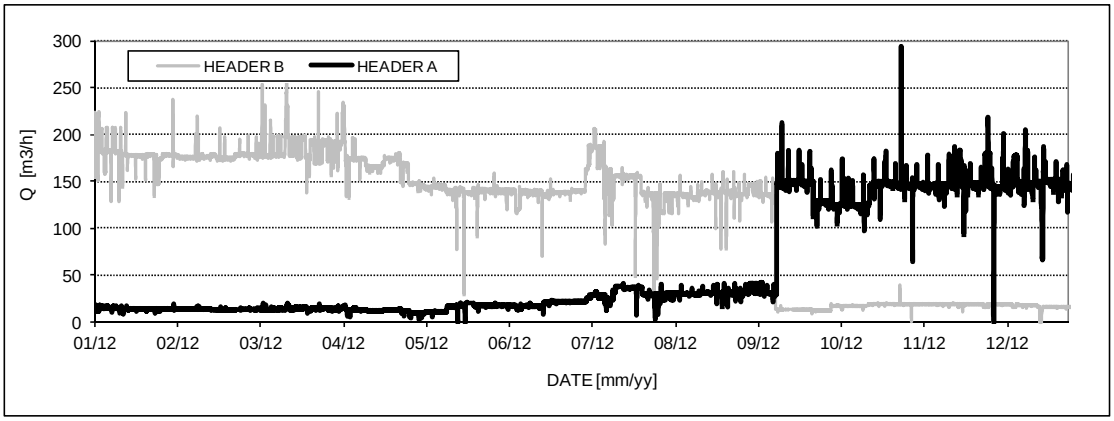

Figure 30 Flow rates to Tiendweg filters through headers A and B (2012)

The analysis of the registered hourly flow values shows that the flows can vary significantly sometimes. This is illustrated in Figure 31 and Figure 32 for Tiendweg and Schuwacht, respectively. These figures show the hourly variation of the flow over a 24 hours period for the days with maximum and minimum production. Moreover the annual hourly average value and the standard deviation are included to be able to compare the extreme and the average situations.

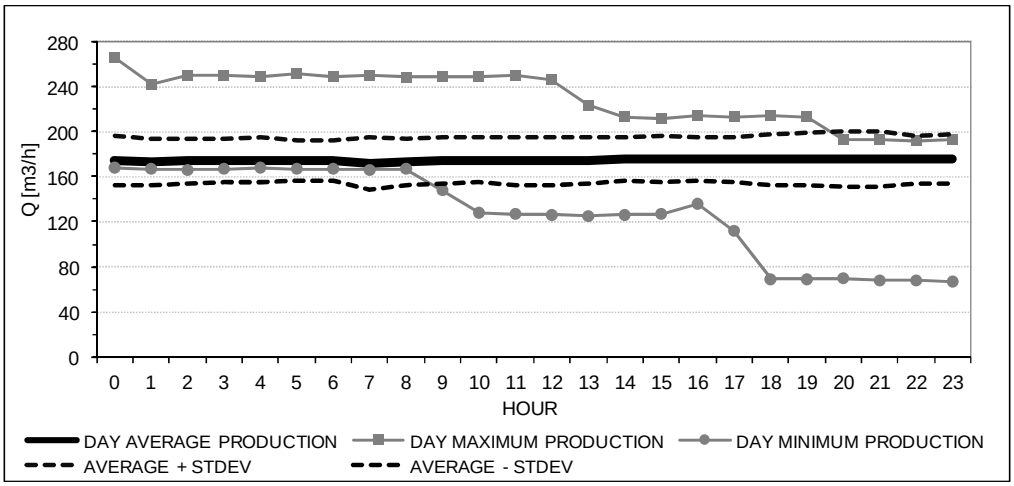

Figure 31 Tiendweg hourly flows the days with maximum, minimum and average production (2012)

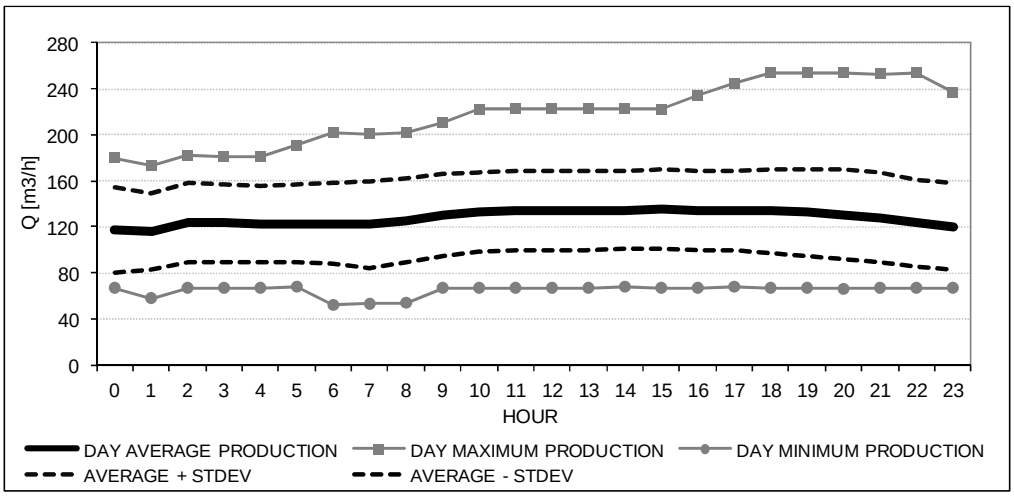

Figure 32 Schuwacht hourly flows the days with maximum, minimum and average production (2012)

In the above shown figures, the flow values between the dotted lines represent the most common flow rate values through each group of filters. They are between 150 and 195 m^3/h for Tiendweg and, between 80 and 170 m^3/h for Schuwacht. The range for Tiendweg is narrower (45 m^3/h), in accordance with the idea that those filters must operate at a fixed rate. The figures also shown that Tiendweg works with flows that are well above or well below the range mentioned: up to 270 m^3/h and 70 m^3/h, respectively.

In order to assess better how often Tiendweg works at extreme flow values, the distribution function has been calculated. Figure 33 shows the probability distribution curve of the Tiendweg flow. The last full year (2012) has been taken as reference for this study. The range of the registered rates is represented in the x-axis. The vertical axis on the left side shows the probability of having a flow rate equal or lower than the values in the x-axis. The probability has been calculated as the number of hours per year over a total of 8784 hours (366 days).

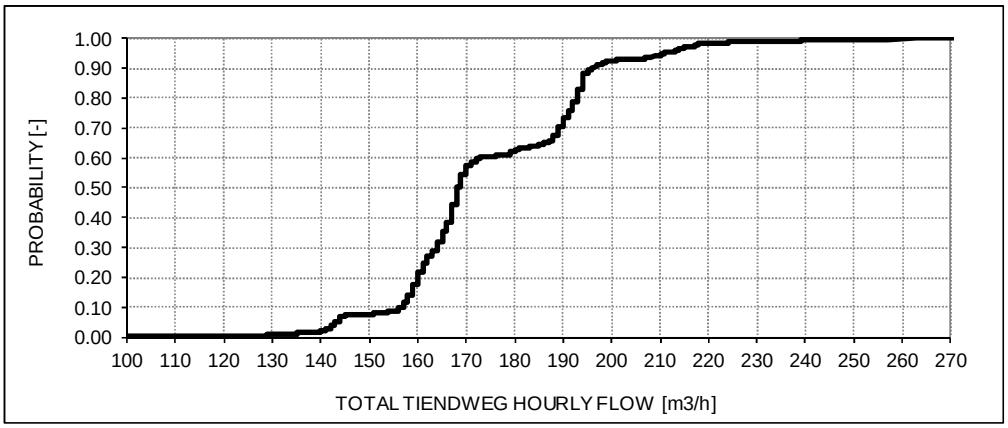

Figure 33 Probability distribution of Tiendweg hourly total flow (2012)

From the figure it can be deduced that the flow rates are mostly within the range 130-240 m^3/h. Within this range there are two sub-ranges where Tiendweg operates most and correspond to the steepest parts: 158-170 m^3/h and 188-198 m^3/h. By contrast, the more horizontal sections represent flow rates that are not so common: 145-155 m^3/h, 170-180 m^3/h and above. The identification of these areas can be useful to define the most common loading conditions. Besides this, some other values of interest can be deduced. For instance, the flow rate was greater than 170 m^3/h during 45% of the time and higher than 190 m^3/h during one third of the time in 2012. Only for a few hours (50) the flow was above the range 130-240 m^3/h.

The high flows values are, in principle, attributable to special production days. In that case, it is reasonable to think that such flows occur during a relatively long time period (days or weeks). These cases would correspond to the day of maximum demand presented in Figure 31 and Figure 32. But there is another possibility as well: although the well schemes are designed to maintain stable the number of Tiendweg wells in service, during peak hours it may happen that, if the water level stored at the end of the plant drops below a certain level, some additional wells become operational for one to two hours to restore and maintain the level in the drinking water reservoirs within the safety range. Analogously the Tiendweg wells may be switched off occasionally, when the drinking water storage is full. This could explain the existence of short and abrupt changes in the abstracted flow.

Finally, the extreme time periods have been identified. Table 5 shows the flows of the hour, day and week of minimum and maximum production in the last year (2012) together with the average hourly flow.

Table 5 Minimum, maximum and average production at Schuwacht and Tiendweg (2012)

Flow [m3/h] (2012)				
Demand situation		Schuwacht	Tiendweg	Lekkerkerk
Minimum	Hourly	50	180	230
	Daily	88	158	246
	Weekly	121	157	278
Average	Yearly	138	192	330
Maximum	Weekly	189	204	393
	Hourly	241	265	506

Concerning the **raw water quality**, samples are periodically taken from the headers connecting the well fields with the bio-trickling filters. As previously shown in Figure 4, there are two sampling points for Tiendweg (GLTPE99B and GLTPE99A) and one for Schuwacht (GLSPF99A). Raw water quality parameters are summarized in Table 6. The shown values correspond to the period 2004-2012.

Table 6 Raw water quality: averages and standard deviations at Schuwacht and Tiendweg (2004-2012)

Compound	Units	Tiendweg B			Tiendweg A			Schuwacht		
		Average	St. Dev.	%	Average	St. Dev.	%	Average	St. Dev.	%
Ammonium	[mg NH4+/L]	5.81	0.81	14%	5.18	0.80	15%	1.89	0.44	23%
Nitrite	[mg NO2-/L]	0.00	0.00	-	0.00	0.00	-	0.00	0.01	-
Iron	[mg Fe2+/L]	5.44	0.92	17%	5.17	0.89	17%	3.08	0.62	20%
Manganese	[mg Mn/L]	0.52	0.09	18%	0.57	0.11	20%	0.85	0.08	10%
Methane	[mg CH4/L]	-	-	-	-	-	-	-	-	-
Ortho-Phosphorus	[mg P/L]	1.27	0.76	60%	1.04	0.58	55%	0.89	0.49	54%
Conductivity	[mS/m]	71.15	3.51	5%	76.39	2.52	3%	69.34	2.01	3%
Bicarbonate	[mg HCO3-/L]	235.78	4.63	2%	226.88	4.92	2%	231.06	8.52	4%
Temperature	[oC]	11.76	1.27	11%	11.76	0.91	8%	12.82	1.07	8%
pH	[-]	7.22	0.06	1%	7.26	0.07	1%	7.35	0.06	1%
Oxygen	[mg O2/L]	0.58	0.23	39%	0.63	0.29	46%	0.81	0.71	87%

Based on the values given in Table 6 it can be concluded that:

- The general quality of the water in both well fields is highly comparable. Parameters such as conductivity, pH or temperature show very similar values.
- The largest differences between the well fields correspond to the content of ammonium, iron and manganese. The presence of manganese is higher in Schuwacht (0.85 mg Mn/L) than in Tiendweg (0.52 and 0.57 mg Mn/L). By contrast, Tiendweg shows higher ammonium (5.44 and 5.17 mg NH_4^+/L) and iron (5.44 and 5.17 mg Fe^{2+}/L) concentrations than Schuwacht (3.08 mg Fe^{2+}/L). Methane measurements were not available.
- The results also indicate that the variability of some parameters is significant. The standard deviation of ammonium concentration is around 14-15% of the average value in Tiendweg and 23% in Schuwacht. For iron it is 17% in Tiendweg and around 20% in Schuwacht.
- The analysis of the data shows that the iron and the ammonium concentration are typically higher in header B than in header A. The reasons for such differences are unknown. The most plausible hypothesis is the existence of preferential flows.

Since not all the wells have the same groundwater quality (De Vet et al., 2010) it is believed that the fluctuations may be caused by switching between abstraction wells. The wells are switched on and off in a set order of preference, based on the water demand. These plans, which are known as "well schemes", are designed to ensure a relatively fixed raw water quality for ammonium and that all the wells work a sufficient number of hours per year in order to maintain stable water quality and water levels in the aquifer.

Based on the idea that the fluctuations in the raw water quality are mainly caused by changes in the state of the wells, the ammonium concentration in the influent could be estimated based on the wells in operation. The water quality in each well is determined through laboratory analysis once a year. The individual well flows can be estimated based on some tests carried out in the past, when different wells have been switched on and off alternatively and the changes in total flow (measured by the existing flow meters) has been registered. In reality these unitary flows are approximations and are in principle valid under the conditions existing (pressures in the pipes) at the moment the test was performed. Figure 34 shows the results of that work. On the horizontal axis there is the time. The ammonium concentration values are shown along the y-axis. On the plotting space the measured and the estimated concentrations.

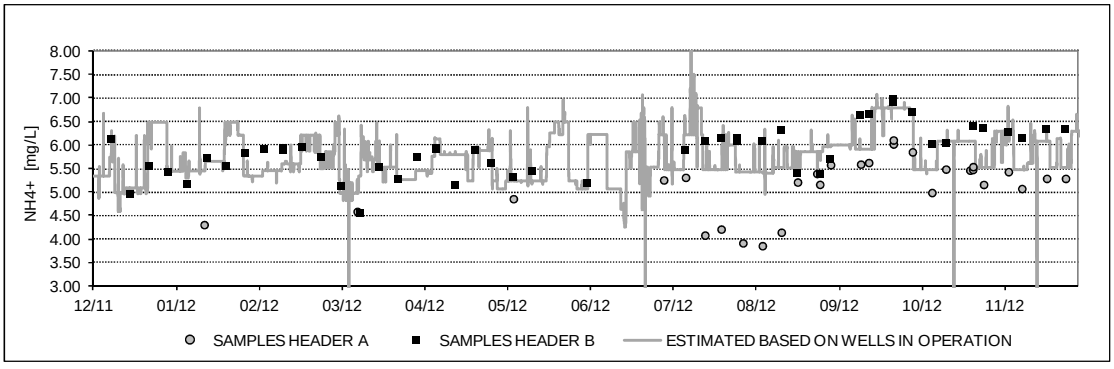

Figure 34 Measured and estimated ammonium concentration in raw water at Tiendweg (2012)

The results shown in Figure 34 suggest that the raw water quality may vary even more than what it is expected based on regular sampling results. It can be quickly deduced then that any improvement in the operation of the bio-trickling filters requires for a better monitoring of the ammonium concentration in the raw water.

In order to proper characterize the loading conditions applied on the filters, a better assessment of the ammonium concentrations in the raw water is desired. Table 7 compares the average and maximum values for the entire available data set (period 2004-2013) and a most recent time period (years 2010-2013).

Table 7 Average and maximum ammonium concentrations at Schuwacht and Tiendweg (2004-2013)

Ammonium NH4+	Tiendweg B		Tiendweg A		Schuwacht	
[mg/L]	2004-2013	2010-2013	2004-2013	2010-2013	2004-2013	2010-2013
Average	5.81	5.80	5.18	5.11	1.89	1.80
St. Dev.	0.81	0.89	0.80	0.53	0.44	0.40
Average + St. Dev.	6.62	6.69	5.98	5.64	2.32	2.20
Maximum	7.80	7.21	7.26	6.11	5.58	3.14

The values show that while the average and the standard deviation values remain almost the same the highest recorded value varies. The origin of these differences may be due either to the sampling frequency (insufficient to adequately characterize variations in the ammonium content of the raw water) or to changes in the well schemes. Whatever the cause is and based on the approach described before, it is believed that by having a look on the well schemes, the highest raw ammonium concentration associated to each of them could be determined beforehand.

Conclusion

These results demonstrate the existence of wide ranges of flow rates and raw water qualities. This has implications on the ammonium loads being applied on the bio-trickling filters. The loading rate (g NH_4^+/H), which is defined as the influent ammonium concentration times the flow through the filter, is difficult to assess since only the flow is continuously measured (every 5 minutes) while the raw concentration is measured only weekly and may fluctuate significantly due to well-scheme related issues. Since there are indications that both parameters significantly fluctuate it can be concluded that filters are work in a regime such that could be defined as a succession of transient states. Considering that bio-trickling filters are biological system that require certain time until adapting to new loading conditions that may have negative consequences with regard the achievement of complete ammonium removal at all times.

2.5 Mixed filtrate quality at WTP Lekkerkerk

As previously explained, the reduction in the nitrification capacity of one filter is related to its age. It is through the application of remediation actions, which are either external cleaning or filter material renewal, that the number of filters with incomplete nitrification is controlled. It has been also explained that the decline in nitrification in primary filters impacts on the performance of secondary filters and, consequently, on the final mixed effluent water quality. In this section this aspect is more clearly illustrated.

Table 8 shows in a simplified manner the recent history of the set of primary filters. In the upper three rows of the table, the time is displayed ranging from January 2012 to March 2013. On the left side, in the first two columns, the names of the filters are indicated. Next to the name of each filter there are the cells (one per month) that represent how its performance was, which is strongly conditioned by its age, which is further explained in Section 4.1. The criteria used for deciding the colour assigned to each filter is:

- Green colour corresponds to primary filters with good behaviour (stage 0), which means that the effluent does not compromise the effluent of the filtration step downstream. This depends both on the concentration and the flow but for simplicity purposes only the effluent has been considered this time.
- Red colour has been assigned to those primary filters with poor effluent quality (stage 2).
- Orange has been assigned to those filters in between the two previous stages (stage 1).

In addition to this information, some cells in Table 8 contain letters that indicate the type of operation applied at that time: 'EW' means that external washing was applied at that time; 'R' for recirculation; and 'RO' indicates that the raw water is mixed with clean water from the nearby reverse osmosis installation (this is only for set 5).

Table 8 Recent performance of primary filters at Tiendweg (01/2012-03/2013)

	Year	2012												2013		
	Month	01	02	03	04	05	06	07	08	09	10	11	12	01	02	03
Primary Filter	FF-04															
	FF-05				RO	RO	RO	RO	RO	RO	RO	RO	RO	RO	RO	RO
	FF-06			R	R	R	R	R	R	R	EW					
	FF-07				EW										R	R
	FF-08												EW			
Notation: R: Recirculation; EW: External washing; RO: feed mixed with RO permeate;																

Colour	Meaning
GREEN	Effluent NH_4^+ < 2 mg/L
YELLOW	2 mg/L < Effluent NH_4^+ < 3 mg/L
RED	Effluent NH_4^+ > 3 mg/L

Table 8 clearly illustrates how filters with different ages (at different life cycle stages) work simultaneously. Over the time, the system goes through different combinations depending on the remedial actions that are performed. According to Table 8, the situation during the first quarter of 2012 was by far the most unfavourable, with 4 filters out of 5 with poor ammonium removal. A year later, in the first quarter of 2013, the situation was the most favourable one, with only 0-1 primary filter in operation with poor effluent quality. In between (second, third and fourth quarter of 2012), the situation varied between these two extremes.

This information is important because it can help understanding why company standards are exceeded and how the nitrification capacity of the system, the individual state of each filter and the overall loading conditions relate to each other. Figure 35 shows the measured ammonium concentration in the mixed filtrate of all sets (Tiendweg and Schuwacht) over 2012. The concentration is measured every 5 minutes. The original data set has been converted into hourly values by identifying and selecting the highest concentration within each hour. The results are shown in Figure 35, where it can be also seen that there were not measurements available for some weeks in February-2012.

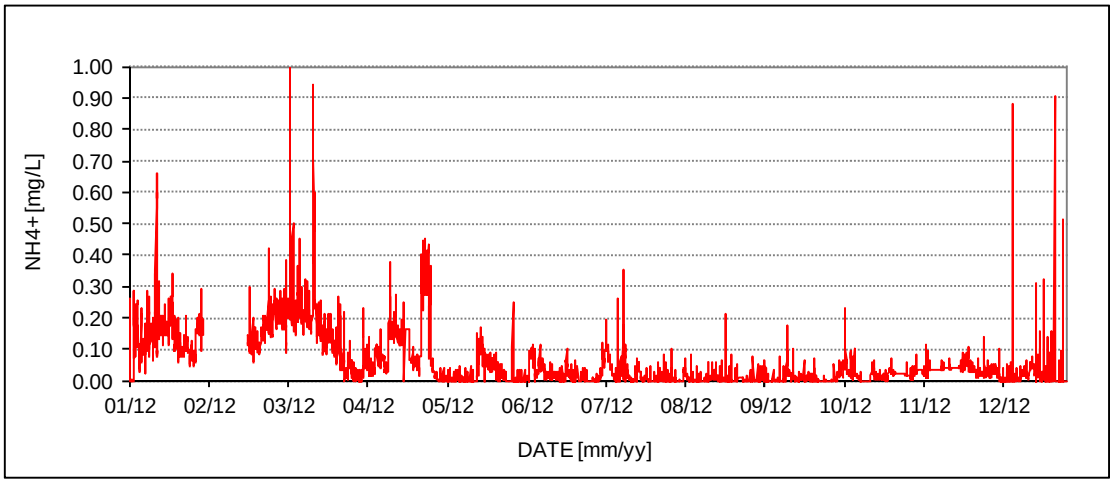

Figure 35 Continuous ammonium concentration in Schuwacht and Tiendweg mixed filtrate (2012)

When Figure 35 and Table 8 are analyzed together, the relation between the state of the filters and the final quality of the effluent becomes clearer. The company guideline (0.10 mg/L) was exceeded often during the first 3-4 months of the year. These results agree with the general state of the family of filters described shown in Table 8. Later, ammonium breakthrough episodes occurred much less frequently, accordingly to the reduction of the number of filters with bad performance from 4 to 2 filters. At the end of the year the results worsen again despite the fact that the number of filters with poor nitrification does not increase.

Figure 36 provides a better impression on how often the company guideline was exceeded. The bars in the figure account for the number of hours per month when the company guideline was exceeded at least once.

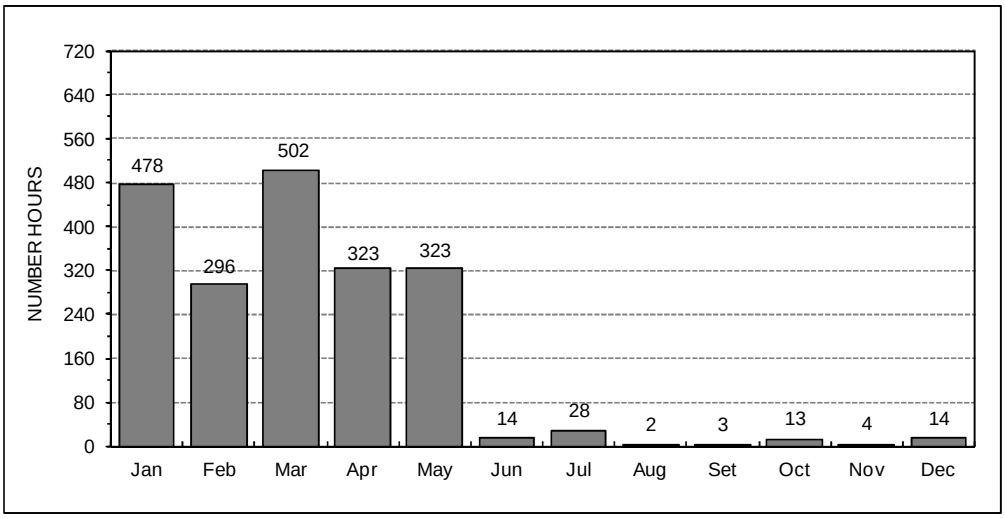

Figure 36 Number of hours per month in which the guideline value for ammonium was exceeded at least once (2012)

By looking at these bars, three different situations can be defined:

- January-March: the guideline was exceeded most of the time (at least one breakthrough event was detected during 65% of the hours of the month).
- April-May: the situation improves slightly. The number of hours is still high but this situation is not longer the majority (45%).
- June-December: the situation improves significantly. The number of hours is between 0.3-4%.

These results are can be better interpreted when analyzing the loading conditions represented by the flows shown in Figure 37, which are monthly averages. Therefore, it is necessary to take into account that the daily flows values may significantly deviate from the monthly average value.

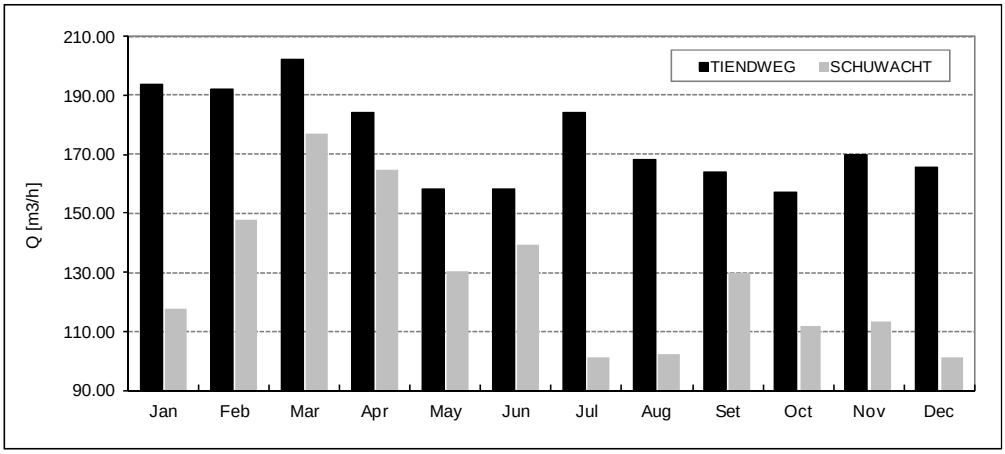

Figure 37 Tiendweg and Schuwacht monthly average flows (2012)

If these flow values are compared to the bars in Figure 36 and the state of the system given in Table 8 it becomes clear that the occurrence of ammonium breakthrough is linked to the flow through the system but also to its situation. January, February and March combine the highest flows with the higher number of filters with poor nitrification being in operation simultaneously. April is a kind of transition month, when the state of the system improves and the flow is reduced. From May to December the situation improves but it is difficult to say which factor contributed most: if reducing the number of filters with problems from 4 to 2 or the reduction of the flow. According to these the worsening in July (28 hours in Figure 36) is attributed to flow increase. However, this is not exactly the case for December, when the number of episodes increased (compared to the month before) while the flow decreased.

Until this moment the role played by Schuwacht has not been included in this analysis. In order to better illustrate this aspect, the ammonium concentration in the mixed filtrate of all Tiendweg filters can be estimated based on the measured ammonium concentration in the mixed Schuwacht-Tiendweg (Figure 35) and the flows of each stream (Figure 28) together with the quality of the mixed filtrate of

all Schuwacht filters (Figure 11). The results are shown in Figure 38, where the quality in both streams can be compared.

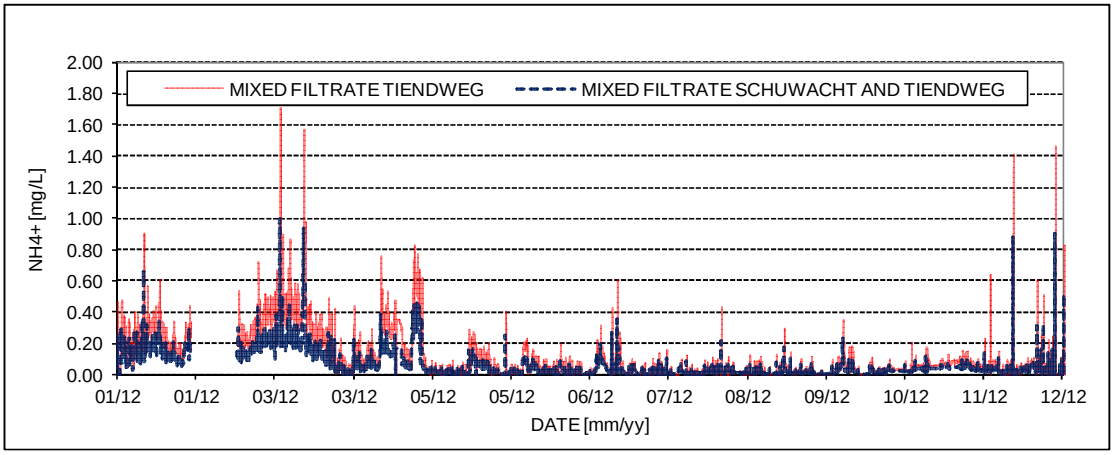

Figure 38 Ammonium concentrations in Tiendweg and Lekkerkerk mixed filtrates (2012)

The results look very similar to the values in Figure 35. In order to make these results easier to compare and analyze, they have been converted into number of hours when the concentration was at least once above 0.20 mg/L or between 0.10 and 0.20. The results are plotted in Figure 39.

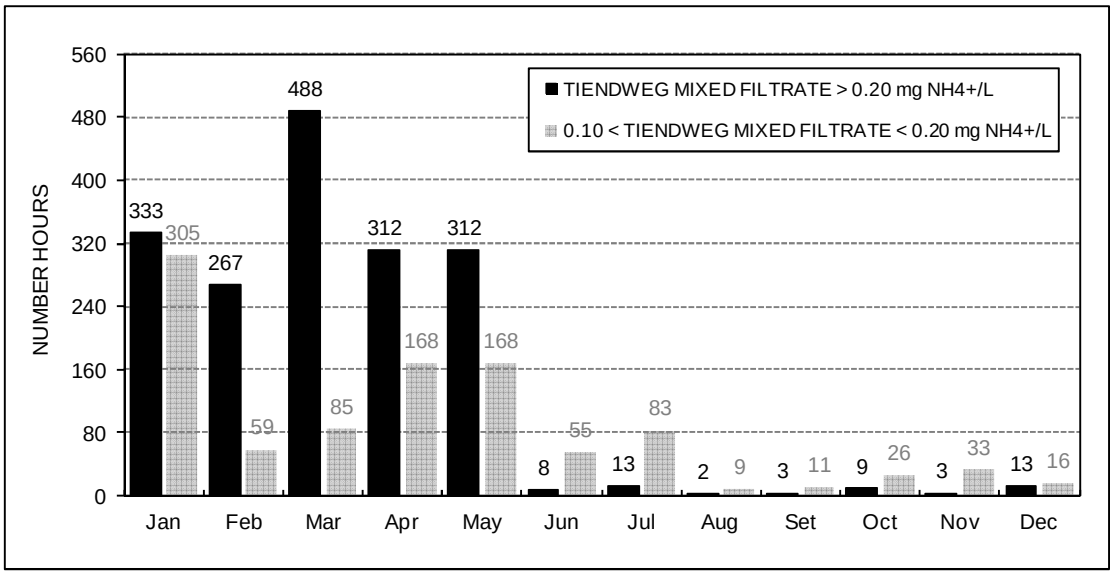

Figure 39 Number of hours per month in which ammonium concentration in Tiendweg mixed filtrate was at least once between 0.1-0.2 mg NH_4^+/L or above 0.2 mg NH_4^+/L (2012)

The reason for such classification is because of the meaning of each of these values:

- If the mixed filtrate of all Tiendweg filters is above 0.20 mg/L, it is almost certain that the company guideline will be exceeded in the mixed final effluent since the flow through Schuwacht barely goes beyond 50% of the total flow, as shown in Figure 29.
- Values between 0.10-0.2 will result in non compliance of the company guideline depending on the flow through Schuwacht.

Therefore, the flow through Schuwacht is what decides if the cases in light red colour in Figure 39 become ammonium breakthrough episodes or not. This factor was especially important between June and December.

3 Modelling nitrification in bio-trickling filters

3.1 Introduction

In the previous section, information about the bio-trickling filters at WTP Lekkerkerk, the conditions under which they operate and their performance has been summarized. The measurements indicate that the filters operate at changing flow rates. Moreover, the raw water quality is far from being constant. Therefore, ammonium removal in these bio-filters is a dynamic problem. Measurements have also shown the influence that the actions that can be considered as part of the standard operation regime have on the ammonium removal capacity of these filters. These actions are backwashing, external washing and filter material renewal. To be able to understand what should be done best a model can be useful. This chapter deals with the development of a mathematical model for nitrification in these dry filters. The model has been elaborated within the modelling environment Stimela, which is programmed in Matlab/Simulink™.

3.2 Approach

In modelling, one of the most important questions is what the purpose of the model is since that strongly determines its characteristics and capabilities. The model must be able to predict the effluent quality. If the model it is able to predict the behaviour of the system under different conditions (e.g. raw water quality and flow) then it will become a reliable tool for operation improvement.

In reality, the accomplishment of the final goal comprises the achievement of smaller goals each of which can be linked to one stage of the model construction process. First, the model can be used to encapsulate historic data about the operation of the filters and to extend previous hypothesis about the existence of behavioural patterns. Then, mathematical models can be very useful tools to obtain valuable insights, to identify bottlenecks in the process and to diagnose the state of the system (Sin et al., 2011). Second, the model can be used to validate some past findings that suggest potential ways of improving the operation: for instance, adapting the load to the filter conditions (age and removal capacity) or proposing changes to enhance transportation within the filter bed. Indeed, the models can be seen as a reflection of the existing knowledge about the system: they are fed by data but also by (new) hypotheses (Rietveld, 2005). Therefore, the process of constructing the model also provides information for selecting and managing better the best factors to optimize the performance of the trickling filters.

Steps

The model construction process requires to go through different stages: (1) understanding the physical mechanisms occurring in bio-trickling filters; (2) understanding of the biological mechanisms occurring in the biofilm; (3) characterizing mathematically the key processes; (4) simulating the current situation (model calibration and validation); and, (5) identifying which of those mechanisms affect the performance most, identifying if possible the rate-limiting steps. Only once the model has been calibrated and validated, it is possible to use it in order to simulate the response for various alternative operational scenarios, so that the most promising one can be identified (Van Schagen, 2009).

Cases

As explained in Paragraph 2.3.1, there are two possible cases to be modelled: (1) a dual-media filter where up to four different compounds are removed: iron, ammonium and manganese. This case corresponds to primary filters; and, (2) a single-media filter where only ammonium is removed. This case corresponds to the filters in the second filtration step. Whatever the case is, the same model structure is intended to be able to mimic both situations.

Processes

Biological ammonium removal is performed by the ammonia-oxidizing organisms (ANOs) that are attached to the filter media grains. These colonies of microorganisms are known as biofilms. Biofilms are adaptive systems that result from environmental conditions and respond to them. It has been

widely proven (van Loosdrecht et al., 1995, Van Loosdrecht et al., 2002) that it is the balance between opposing processes what ultimately governs the biofilm formation and decides its structural properties. This idea is illustrated by Figure 40.

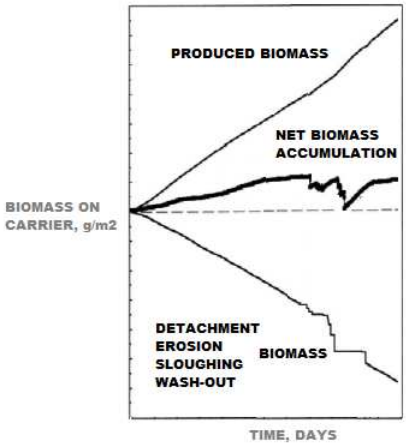

Figure 40 Schematic of the evolution in time of newly grown, detached and accumulated biomass (Picioreanu et al., 2001)

Some of these processes can be intuitively understood but various others can be really complex (Van Loosdrecht et al., 2002) and need to be hugely simplified in the model when modelling. The processes controlling the development of biofilms can be classified as "positive" and "negative" (Picioreanu et al., 2000b): while the former ones contribute to the development of the biofilm (e.g., cell attachment, cell growth), the latter ones lead to biofilm shrinking (e.g., cell death, cell detachment).

In reality, the mentioned processes can be grouped in two categories: processes related to biological aspects of the microorganisms (e.g. kinetic aspects and microbial transformations); and, processes related to the physical characteristics of the biofilm. Each category contains both positive and negative processes. In the first group there are processes such as cell growth, decay, inactivation and, endogenous respiration (maintenance). The second group includes cell attachment and different types of detachment (e.g. abrasion, erosion, sloughing…). Although the processes in both categories are influenced by environmental conditions, this differentiation may become important in order to better understand the mechanisms involved in nitrification in trickling filters and, eventually, the causes behind the observed relapse in nitrification. Another aspect of interest is to know whether these processes can be influenced through operating the filters in a different way. They are schematized in Figure 41.

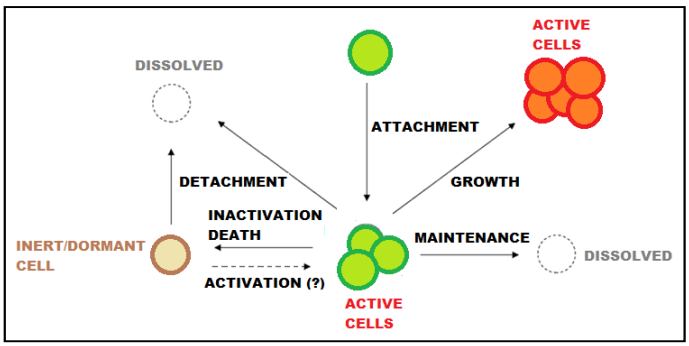

Figure 41 Schematic of cell processes

The model considers three phases: the gas phase (the air passing through the filter bed), the bulk liquid (the water trickling down) and, the solid phase (represented by the biofilm attached to the sand/anthracite grains). With respect to the channels and pores in the biofilm, which are filled with liquid, they have been considered part of the solid phase as well. The processes occurring in these phases to be modelled are: (1) the hydraulics within the filter; (2) the mass transfer from the gas phase to the water phase in the interstitial areas between the pores; (3) the substrate mass transport processes within the liquid phase; (4) the mass transfer from the bulk into the surface of the biofilm and vice-versa (transport within the solid phase is neglected accordingly to the simplification presented before); (5) the microbial conversion processes on the surface of the filter grains; and, (4) the net growth of biomass. Figure 42 is an illustration of the mentioned mass transfer and biological processes that somehow illustrates the complexity of the system. Before describing the role of each process and how they are going to be modelled, the issue of simplification is addressed.

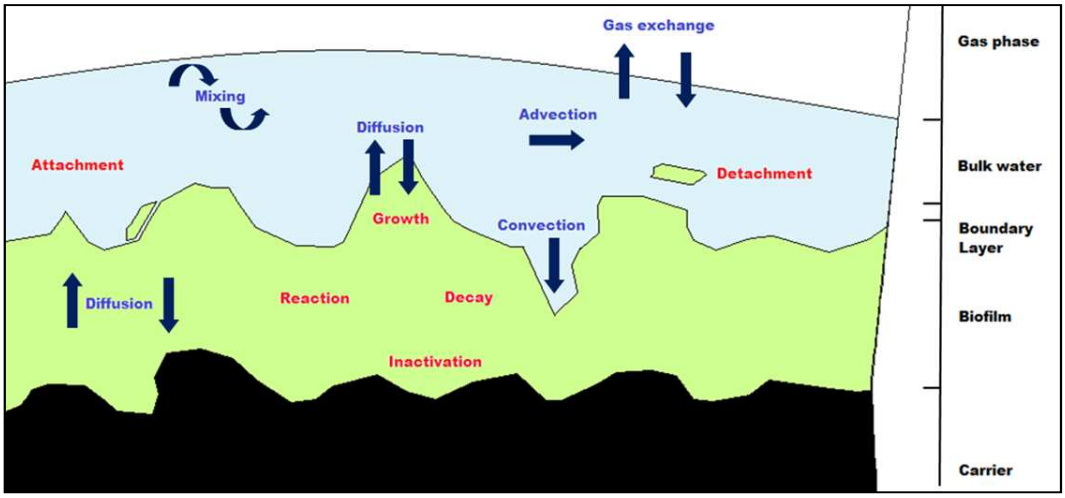

Figure 42 Biofilm processes and transport mechanisms

Simplifications

Modelling is always the result of the observation and interpretation of the studied system, based on the fact that what is observed is the overall result of many individual events (Savenije, 2009). Although the development of mathematical models is often based on conceptual understanding of the processes, mathematical models must include simplifications as well. Even the more sophisticated models representing natural processes are a simplification of reality. Typically, key processes can be represented either through statistical or mathematical relationships that, ideally, cover the most important aspects. Simplifications should not be seen as a drawback but as an advantage: too detailed models may require the knowledge of different parameters which are difficult to measure in practice. For instance, in biofilm systems diffusion coefficients within the biofilm, biofilm thickness and detachment are often unknown and difficult to measure.

One of the key model simplifications has consisted on assuming that all the ammonia conversion into nitrite happens on the outer layer of the biofilm. Despite authors have indicated that a failure to properly simplify the complexity of the biofilm may result in erroneous model results (Boltz et al., 2011), this simplification was thought to be justified even before the model was ready due to several reasons:

1. This assumption is the same as assuming that the active biomass is located only on the external layers of the biofilm, while inactive biomass is constrained to the deeper layers as some authors have reported (Queinnec et al., 2006). This means that only nitrifiers in the outer layers of the biofilm, which have better access to substrates in the bulk phase, contribute significantly to the overall substrate removal.
2. This hypothesis is equivalent with assuming that the model covers only the part (layers) of the biofilm where the substrates and nutrients penetrate, excluding the parts that are beyond. Around this idea, some authors (Wik, 2003) have indicated that greater wetting efficiencies together with high shear stress result in thinner biofilms. With sprayers distributing the water over the upper layer of the filter bed and the filters being operated at high flow rates (compared to what literature states for trickling filters in (tertiary) wastewater treatment: 0.08-1.7 m/h (Henze, 2008)), that seems to be the situation in this case. Moreover, the hypothesis of full-penetration seems to be more plausible for slow-growing microbial systems (autotrophs have lower growth rates than heterotrophs) and, consequently, uniform biofilm properties are more probable.
3. It simplifies the model enormously: only the concentrations on the surface of the biofilm have been considered; moreover, all the microbial activity develops at the same pH (existing on the biofilm surface), neglecting the pH gradient that according to literature (Zhang and Bishop, 1996) may exist over the layers of the biofilm.
4. It is difficult to characterize the processes occurring within the biofilm (e.g. the parameter values for the correct description of transport into the biofilm are unknown and there are not site-specific measurements that can be used to infer them). This means that although they could have been modelled their calibration would have resulted very complex.
5. Although the biofilm itself is not modelled, the biomass content is. In this respect it was believed that the overall behaviour observed in the filters could be simulated with proper calibration without going into so much detail.

Hydrodynamic regime

Modelling trickling filters performance requires to characterize the hydraulic regime within the filter bed since it influences the transport processes (Ebert, 2006). Many different types of transport processes may coexist in the filter. Advection is described as the transport process of a substance due to bulk motion. Diffusion is defined as the transport mechanism which is driven by concentration gradients. Convection is often used as a synonym for advection although in reality it is the sum of transport by diffusion and advection. Moreover each transport mechanism may have local significance and, at the same time, be negligible at a general level. Literature states that flow velocity has an effect on the relative contribution of convective and diffusive mass transport to the overall substrate transport to the biofilm (Picioreanu et al., 2000b).

Bio-trickling filters are assumed to work as laminar contactors (Kraakman et al., 2011). With laminar flow, fluid flows in parallel lines with minimal interferences between lines. Unlike turbulent flow, laminar regimes are characterized by high diffusion in comparison to advection. Moreover, and unfortunately, flow channelization, air stagnant zones or even possible anaerobic areas are more prone to happen with laminar flow than with turbulent flow. Consequently, significant spatial differences may occur. By contrast, eddies and vortices created by water droplets trickling down may contribute to mixing, compensating at least partially such spatial differences.

Whatever the situation is, literature states that the characteristic parameters to describe the hydrodynamic regime are the Sherwood number, the Reynolds number, the Schmidt number and the specific surface area (Picioreanu et al., 2000a).

Transport

The multiphase system has two interfaces of interest: gas-liquid and liquid-solid (gas-solid is ignored). Modelling has required characterizing the mass transfer resistance at each of these interfaces: (1) the mass transfer between the bulk phase and the biofilm surface; and (2) the mass transfer between the gas phase and the bulk phase. Internal mass transport within the biofilm has been neglected since it has been assumed that all the conversion occurs in the upper layers. The transport through the water layer over the biofilm is caused by concentration gradients of the substrates which diffuses through the external mass transfer layer.

Aeration

Oxygen is one of the substances needed by nitrifiers in order to convert ammonia into nitrite. Theoretically, the oxygen transfer rate could be limiting the rate of ammonium oxidation: the minimum range of dissolved oxygen concentrations needed to reliably achieve nitrification is between 0.6 and 3.4 mg/L (Chen et al., 2006), values which refer to concentrations in the bulk, not in the biofilm. Since the oxygen concentrations measured in the effluent of the filters are always close to saturation, this does not seem probable. But aeration needs to be modelled also due to a second reason: it affects the dissolved gasses in water and, therefore, it is required for a correct pH calculation.

Conversion processes

The model considers one single type of microorganisms (ammonia-oxidizing cells, also known as nitrifers). No nitrite is detected in the regular sampling performed in the effluent of the different filters. For this reason, nitrite is assumed to be fully converted into nitrate and the conversion of nitrite into nitrate has not been modelled. Other conversion processes such as iron and manganese biological oxidation have been considered only in terms of how much they contribute to the oxygen demand and/or affect the carbonic equilibrium.

Concerning the issue of competition between simultaneous biological processes, phosphate (or any other basic nutrient) could be one of the potential causes for competition. Nevertheless,
its modelling is difficult. On the one hand, the chemical fractioning of phosphorus may become a more important limiting factor than the bio-uptake itself. On the other hand diverse phosphate dosing experiments have not provided conclusive results

Clogging

Clogging may affect ammonium removal through influencing the transport processes previously mentioned. On one hand, it may reduce the void space left free for water and air. On the other hand, it may cause the progressive obstruction of some parts of the filter, which would result in the appearance of dead zones and would reduce the contact surface area available. Moreover, clogging is

more likely to occur in the upper layers where most of the nitrification and filtration activity is though to occur, what makes this fact even more undesirable. For all these reasons, clogging had to be considered in the model. Unfortunately, there are not site-specific measurements to properly characterize the process of biomass or accumulation of precipitates in the filter bed. For this reasons clogging has been included in the model only through their effects. More about this is discusses in Paragraph 3.4.4.

Simplifications

The number of processes involved together with the complexity of the possible interactions has made necessary to assume several simplifications. Some of the assumptions may not reflect entirely the reality, but they have allowed reducing the number of parameters and equations to be considered in the model. The simplifications can be found in Annex A.4.

3.3 Model parameters

For modelling it has been vital to consider which parameters to include and which can be excluded. In general, the operation of drinking water treatment processes and, by extension, of any treatment step can ideally be characterised by three types of parameters (Rietveld, 2005):

- Disturbance parameters.
- Controlled parameters.
- Manipulated parameters.
- Design parameters.

Each type is described below. Figure 43 summarizes the model parameters.

Disturbance parameters

The disturbance parameters are those ones which affect the behaviour of a treatment step and cannot be modified. They correspond basically to the raw water quality. In this model, disturbance parameters are:

- Ammonium concentration.
- Oxygen.
- Bicarbonate.
- pH
- Iron.
- Phosphate.
- Temperature.
- Conductivity.

The carbon dioxide content and the m-number are required by the model as well but they can be derived based on the previous ones.

Controlled parameters

They represent the guideline values the system is operated in accordance to. In this case, the only controlled parameter considered is the effluent ammonium concentration.

Manipulated parameters

They represent the operational parameters. This means that they may influence the treatment through active control. In theory, the manipulated parameters can (and must) be changed in order to maintain the controlled parameter within the desired range. Manipulated parameters are the run time, the backwash routine and the air-flow ratio of the forced ventilation system. The situation of the flow is special in this case since in the present circumstances there is no way to control the flow that each filter receives. Nevertheless, the flow rate has been included in this category because many of the recommendations for improvement that will be presented in Section 5.3 are based on the possibility of controlling this parameter.

Design parameters

They represent the characteristics of the system and are also known as internal model parameters. They are the dimensions of the filter and the characteristics of the filter material but also other parameters characterizing the diverse processes occurring in the bio-trickling filters. It is implicit then

that the determination of the value for some of these parameters is not an easy task and becomes one of the key steps in the process of modelling. All the design parameters can be found in Section 3.4, where the model equations are presented. The values assigned to these parameters are either shown in Section 3.4, where they are presented, or during model calibration, in Section 4.3.

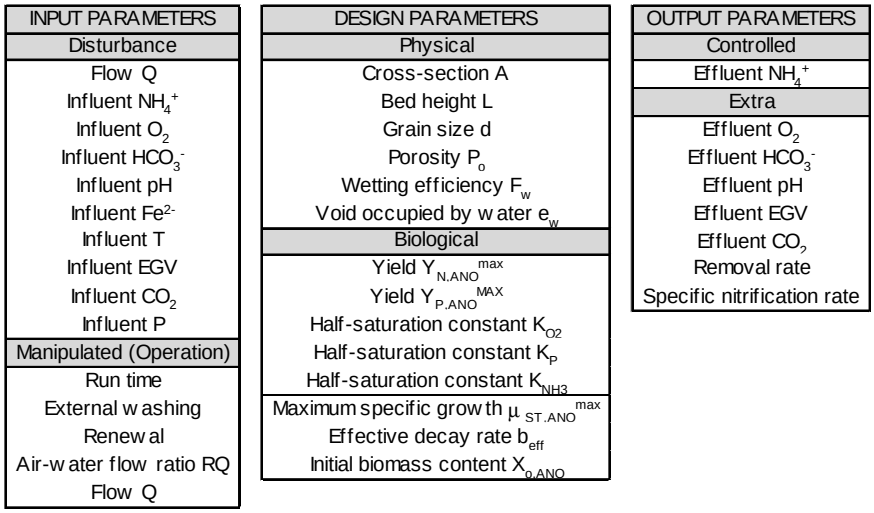

Figure 43 Model parameters

3.4 Model equations

For a greater clarity, the equations are presented grouped according to the different aspects or processes playing a role: (0) model structure; (1) transfer of compounds to and from the air to the water phase (aeration); (2) kinetics of the ammonia-oxidizing organisms; (3) hydraulic regime and fluid conditions; (4) transfer of compounds to and from the water phase to the biofilm; (4) conversion rates in the biofilm; and, (5) biofilm processes, followed by the mass balance equations for all the substances considered are listed.

3.4.1 Structure

The hydraulic regime is approximated by several consecutive completely mixed reactors in series. Hence, at each of these layers, homogeneous characteristics are assumed for all the properties. Figure 44 shows the model structure and illustrate the mentioned aspects. Bulk water flows through the consecutive bed layers. The same happens with the air. The biomass population, the substrate concentrations change from one compartment to the next one. The concentration of each parameter of interest is modelled at the three different phases in each compartment. The sub-index 'g' refers to the concentration in the air. The sub-index 'w' refers to the concentration in the water phase. The sub-index 'b' represents the concentration on the surface of the biofilm. The higher the number of tanks in series is, the closer the flow is to plug flow conditions. Finally, the sub-index 'z' represents the vertical space coordinate.

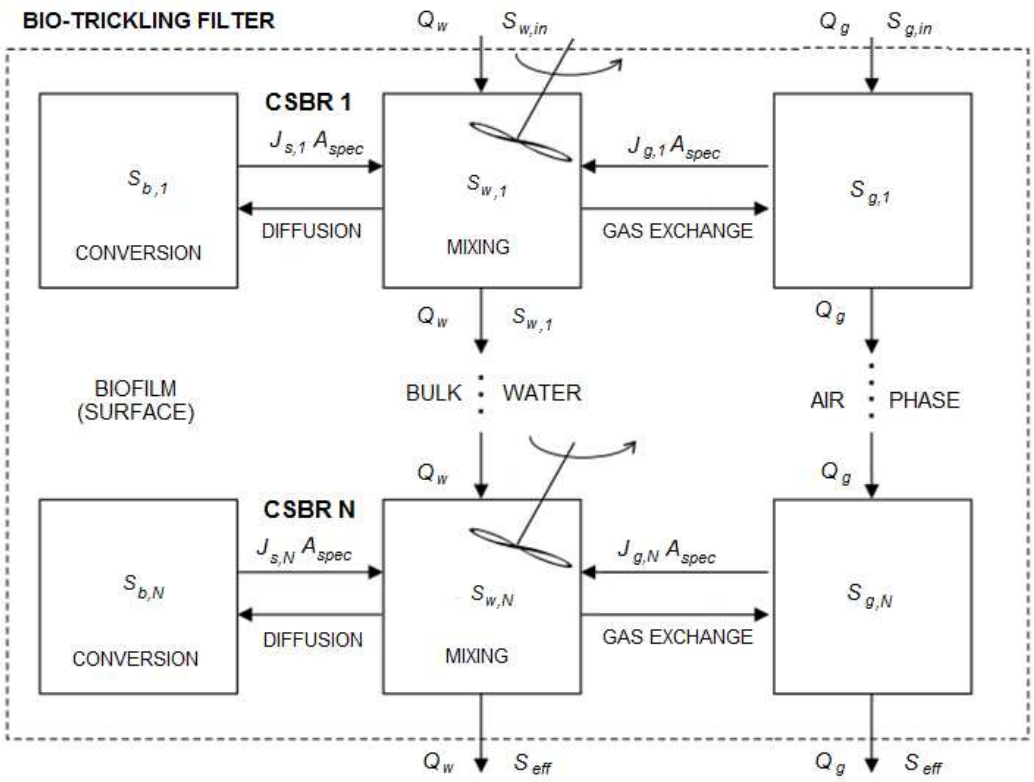

Figure 44 Conceptual diagram of the model structure, phases and transport processes

The residence time is calculated considering the height of the filter and the water velocity:

Equation 6

$$T = \frac{L}{u_z}$$

Where:
T : mean residence time [s].
L : filter bed depth [m].
u_z : mean water velocity [m/s].

The same water velocity is assumed over the entire filter depth. The way it has been estimated it is shown in Paragraph 3.4.4. The residence time together with the number of compartments is used to calculate the height of each compartment and the partial residence time in each compartment:

Equation 7

$$d_z = \frac{L}{N}$$

Equation 8

$$T_z = \frac{T}{N}$$

Where:
N : number of compartments in series [-].
d_z : height of each compartment [m].
T_z : mean residence time of water in each tank [s].

3.4.2 Aeration

There are two consecutive gas transfer systems: spray aerators and tower aeration. Spray aeration occurs before the water enters and therefore has been excluded from the model. Concerning forced aeration, by combining the equilibrium, kinetics and the mass balance equations, the following ordinary differential equation can be developed for the oxygen and carbon dioxide concentrations in the gas phase. The ordinary diferential equations are describing one of the sections that is approximated by a CSTR. The sub-index 'in' refers to the concentration in the influent coming from the previous CSTR.

Equation 9

$$\frac{d[O_2]_g}{dt} = \frac{[O_2]_{g,in} - [O_2]_g}{T_z} - \frac{k_{2,O_2}}{RQ}\left(k_{d,O_2} \cdot [O_2]_g - [O_2]_w\right)$$

Where:
RQ : air-water flow ratio [-].
k_{2,O_2} : oxygen transfer coefficient [s^{-1}].
k_{d,O_2} : Henry's constant for oxygen [-].
$[O_2]_g$: oxygen concentration in the gas phase [g/m^3].
$[O_2]_w$: oxygen concentration in water [g/m^3].

Equation 10

$$\frac{d[CO_2]_g}{dt} = \frac{[CO_2]_{g,in} - [CO_2]_g}{T_z} - \frac{k_{2,CO_2}}{RQ}\left(k_{d,CO_2} \cdot [CO_2]_g - [CO_2]_w\right)$$

Where:
RQ : air-water flow ratio [-].
k_{2,CO_2} : carbon dioxide transfer coefficient [s^{-1}].
k_{d,CO_2} : Henry's constant for carbon dioxide [-].
$[CO_2]_g$: carbon dioxide concentration in the gas phase [g/m^3].
$[CO_2]_w$: carbon dioxide dissolved in water [g/m^3].

The gas transfer coefficients air-water are calculated based on the following expressions:

Equation 11

$$k_{2,O_2} = k_{2,CH4} \cdot \left[\frac{D_{O_2}}{D_{CH_4}}\right]^n$$

Equation 12

$$k_{2,CO_2} = k_{2,CH4} \cdot \left[\frac{D_{CO_2}}{D_{CH_4}}\right]^n$$

Where:
$k_{2,CH4}$: methane transfer coefficient [s^{-1}].
D_{CO_2} : diffusion coefficient for carbon dioxide [m^2/s].
D_{O_2} : diffusion coefficient for oxygen [m^2/s].
D_{CH_4} : diffusion coefficient for methane [m^2/s].
n : coefficient determined experimentally [-] = 1.

The mass-balance equations for the gas compounds in the water phase are presented later, in Paragraph 3.4.8.

3.4.3 Kinetics

When the water reaches the surface of the biofilm it gets in contact with the nitrifiers. If all the consumed substrate is used for growth (maintenance is neglected), the actual growth rate can be modelled with the Michaelis-Menten expression:

Equation 13

$$\mu_S^{spec} = \frac{[S]}{K_S + [S]}\ \mu_S^{max}$$

Where:
μ_S^{spec} : specific growth rate [1/s].
K_S : Half saturation constant or Monod factor [g/m^3].
μ_S^{max} : maximum specific growth rate [1/s].
$[S]$: substrate concentration the microorganism is exposed to (biofilm surface) [g/m^3].

Therefore, the kinetics of growth depends on the substrate concentrations at the surface of the biofilm. Since there are several substrates and in order to determine which one is the limiting, (ammonia, oxygen or microbially available phosphorus) the Monod factor needs to be calculated for each relevant substrate. The maximum growth rate is also corrected to consider the local temperature and pH conditions.

Equation 14

$$\mu_{ANO}^{max} = \alpha_{pH\ AOB} \cdot \alpha_{pH\ AOB} \cdot \mu_{ST\ ANO}^{max} \cdot$$

Where:
μ_{AOB}^{max} : maximum specific growth rate for ANOs at a given temperature and pH [1/s].
α_{pH} : pH adjustment of the maximum specific growth rate for ANOs [-].
α_T : temperature adjustment of the maximum maximum specific growth rate for ANOs [-].
$\mu_{ST\ AOB}^{max}$: maximum specific growth rate for ANOs in standard (reference) conditions [1/s].

Therefore, the maximum specific growth rate yields:

Equation 15

$$\mu_{ANO}^{spec} = min\left(\frac{[NH3]}{K_{NH3} + [NH3]}, \frac{[O_2]}{K_{O_2} + [O_2]}, \frac{[P]}{K_P + [P]}\right) \cdot \mu_{ANO}^{max}$$

3.4.4 Hydrodynamics

The fluid regime is important because it affects the transport of substrates and nutrients from the bulk to the biofilm surface. The most common parameters mentioned in literature to characterize the hydraulic regime are the specific surface area, the Reynolds number and, the Schmidt number (Eberl et al., 2000). The Peclet number, which is often mentioned as well, is not used since it is a combination of the Reynolds number and the Schmidt number.

Specific surface area

The specific surface area of a granular bed is defined as the total surface area of the filter material divided by the bed volume. It is mainly determined by the characteristics of the packing material. For a uniform bed of mono-disperse spheres the specific surface area is given by the expression (Crittenden et al., 2012) :

Equation 16

$$A_{spec} = \frac{6}{\varphi \cdot d} \cdot (1 - P_o)$$

Where:
A_{spec} : packing specific surface area [m^2/m^3].
P_o : filter clean bed porosity [-].
d : average diameter of the filter material grains [m].
φ : sphericity factor (0.95) [-].

The effective surface area may differ from the theoretical surface area due to incomplete wetting. The fraction of the total outer grains surface that is effectively wetted is known as external wetting efficiency. The relation between the total and the wetted surface area is equated to the wetting efficiency. This parameter is important because as the water 'trickles' down, the microorganisms degrade the corresponding compounds so that the higher the contact surface area is, the better. Those parameters which do not have access to the substrates or the basic nutrients do not grow and therefore do not contribute to nitrification.

Equation 17

$$A^*_{spec} = A_{spec} \cdot F_w$$

Where:
A^*_{spec} : effective specific surface area [m^2/m^3].
A_{spec} : packing specific surface area [m^2/m^3].
F_W : wetting efficiency [-].

Surface water velocity

To characterize the fluid regime, it is necessary to determine previously the water velocity. The water velocity in dry filters is independent of the hydraulic load. Theoretically it is determined by the drag forces that result from the water passage and it depends, among many other factors, on the diameter of the capillary channels. They all are hardly measurable and little or not known at all for the filters to be modelled. Therefore, the water velocity needs to be calculated in a simpler way.

In dry filters, pores are not completely filled with water. The air flows through the pores and the layer of water over the filter material grains in thought to be relatively thin. The basic assumption then is that the velocity of the water in the vicinity of the grain surface does not differ significantly from the water velocity at the furthest point of the water layer created around the grain, somewhere in the interstitial space between grains. If that is the case, the water velocity can be calculated with the cross-section area occupied by water. The formula used is presented below:

Equation 18

$$A_w = A \cdot P_o \cdot \varepsilon_w \cdot F_w$$

Where:
A_W : cross-section area occupied by water [m^2].
A : cross-section area of the filter bed [m^2].
P_o : clean bead porosity [-].
ε_W : fraction of void space occupied by water [-].
F_W : wetting efficiency [-]

In the previous expression, the true void space is calculated with the clean bed porosity which is corrected to consider the interstitial space between grains which is filled with water and the wetting efficiency. Then, the superficial velocity yields:

Equation 19

$$u_z = \frac{Q}{A_w}$$

Where:
u_z : average water velocity [m/s].
Q : flow rate [m^3/s].
A_W : average interstitial surface area occupied by water [m^2].

Reynolds

With the velocity the Reynolds number can be calculated. The Reynolds is used to describe whether flow conditions correspond to laminar or turbulent flow. The flow regime does not only influence the substrate transport from the bulk into the biofilm. It also has implications for the heterogeneity of the processes occurring in the filter. Trickling filters are usually associated to laminar flows. For laminar flow gradients spatial differences are expected and mass transfer may differ from place to place. According to classic fluid theory, laminar flow occurs when Reynolds number are lower than 2000. For dry filtration, the Reynolds number can be calculated with the following expression (Kissel, 1986):

Equation 20

$$Re = \frac{u_z}{\upsilon \cdot A_{spec}}$$

Where:
Re : Reynolds number [-].
u_z : average superficial velocity of water [m/s].
υ : kinematic viscosity [m^2/s]
A_{spec} : specific surface area [m^2/m^3].

The values reported range from 0.14 for trickling filters operated at low rates and 5.10 for high flow rates (Kissel, 1986) and 0.013 - 12.6 (Satterfield, 1975).

The temperature dependency of the kinematic viscosity of water is considered with the expression:

Equation 21

$$\upsilon = \frac{497 \cdot 10^{-6}}{(T + 42.5)^{1.5}}$$

Where T is the temperature of water [° C].

Schmidt

The Schmidt numbers is the other parameter used to characterize the hydrodynamic regime. It depends on the fluid properties and is calculated as the ratio of the viscosity and the diffusion coefficient, which are usually available for most compounds in literature (Henze, 2008). The expression looks:

Equation 22

$$S_c = \frac{\nu}{D_w}$$

Where:
S_c : Schmidt number [-].
ν : kinematic viscosity [m^2/s].
D_w : mass diffusivity in water of the compound [m^2/s].

3.4.5 Substrate transport

Substrate transport includes to steps: from the bulk to the biofilm surface first and then within the biofilm. The first step is known as external mass transport. The transfer rate is mainly determined by the concentration gradient between the bulk and the biofilm, the hydraulic regime and the available contact area. The second step, known as internal mass diffusion, is not considered in this model since it has been assumed that all the biological conversion occurs in the outer layer of the biofilm.

Substrate fluxes

The flux between the bulk and the biofilm can be expressed as (Hamdi, 1995):

Equation 23

$$J_s = A^*_{spec} \cdot k_f (S_w - S_b) = k_{2,f} (S_w - S_b)$$

Where:
J_s : flux through the external boundary layer or specific removal rate [g/m^3 s].
A^*_{spec} : effective specific surface area [m^2/m^3].
k_f : external mass transfer coefficient [m/s].
S_w : soluble substrate concentration in the bulk water [g/m^3].
S_b : soluble substrate concentration on the biofilm surface [g/m^3].
$k_{2,f}$: external transfer rate [1/s].

External mass transfer coefficient

The external mass transfer depends on the thickness of the boundary layer (Picioreanu et al., 2000b). In fluid mechanics, the boundary layer is the layer of fluid in the immediate vicinity of a surface where the effects of viscosity are significant. The expression holds:

Equation 24

$$\delta_L = \frac{1}{R_L} = \frac{D_w}{k_f}$$

Where:
D_w : diffusion coefficient in the water phase [m^2/s].
δ_L : thickness of the external mass transfer boundary layer [m].
k_f : external mass transfer coefficient [m/s].
R_L : external mass transfer resistance [s/m].

As intuitively expected, the resistance to external mass transfer diminishes with the thickness of the boundary layer. The Sherwood number is used to determine the external mass transfer (Picioreanu et al., 2000b). Concerning their determination different correlations are available in literature. Such correlations look as:

Equation 25

$$Sh = A + B \cdot Re^m \cdot S_c^n$$

Where:
Sh : Sherwood number [-].
Re : Reynolds number [-].
S_c : Schmidt number [-].

Many of these correlations have been derived for relatively simple chemical engineering applications. The parameters A, B, m and n depend on the system and the geometry of the biofilm support medium and are valid only for a defined range of Reynolds and Schmidt numbers. The drawback is that these correlations should be applied to biofilm systems with caution (Henze, 2008): most of the correlations were derived for rigid particles but it is not known how the heterogeneous and elastic nature of biofilms may influence external mass transfer. In fact, there is no consensus about whether this increases or decreases the external mass transfer resistance. For dual flowing phase packing beds, the correlation looks (Kissel, 1986)[1]:

Equation 26

$$Sh = 1.8 \cdot Re^{0.5} \cdot S_c^{0.33}$$

This expression is only valid for film-like flows. The expression for the external mass transfer rate looks (Kissel, 1986):

Equation 27

$$k_f = D_w \cdot S_{h\cdot} \cdot A^*_{spec}$$

The same author provides some reference values for low and high rate trickling filters. The Sherwood number ranges from 6.4 to 39, respectively, while the liquid-solid mass transfer coefficient k_f yields 11 and 35 cm/day. Some other authors (Satterfield, 1975) have stated that this expression agrees reasonably well with full-scale measurements over the entire liquid flow rate range but at low gas flow rates (e.g.: 0.01 to about 0.1 kg/m2 s), which may bring some uncertainty to the estimation of the external mass transfer rate.

It is implicit behind Equation 27 that the mass transfer properties between the bulk and the biofilm are maintained whenever the fluid conditions do not change. In reality, the different processes may influence each other. The hydrodynamic regime affects the biofilm growth through affecting the substrate concentration at the liquid-solid inter-phase and/or through erosion of the biofilm. But also, the biomass growth may affect the mass transfer from the bulk into the phase by modifying the local hydraulic regime. In this case for simplicity purposes the second case is disregarded.

[1] Krevelen and Krekels (1948).

3.4.6 Conversion rates

Ammonia biological oxidation

The conversion rates are calculated according to the general expression where the maintenance term is neglected:

Equation 28

$$r_S = +/- \left[\mu_{AOB}^{spec} \cdot \frac{[X_{ANO}]_b}{Y_{S,ANO}^{max}} \right]$$

Where:

r_s : volumetric conversion [g/(s·m^3)].
μ_{AOB}^{spec} : specific growth rate [1/s].
$[X_{AOB}]_b$: ammonia-oxidizing organisms concentration [g d.s./m^3].
$Y_{S,AOB}^{max}$: maximum substrate yield [g d.s./g].

The substrates considered in the model are ammonia, oxygen and microbiologically available phosphate (MAP). Concerning the ammonium conversion process, it has been demonstrated that despite ammonium is the main species in water under neutral conditions, the main substrate for ammonia-oxidizing organisms is ammonia (Suzuki et al., 1974) as the name indicates. Ammonia may exist in aqueous solution in two different forms: as unionized ammonia (NH_3) and as ionized ammonia (NH_4^+). The proportion of the first in relation to the second depends on the temperature, the pH and the salinity (Chen et al., 2006). For simplicity purposes, the model ignores the ammonia dissociation process. Nevertheless, more information about this process can be found in Annex A.5.

The specific expressions for each substance are presented below. The wetting factor has been incorporated in order to account for the possibility of not all the microorganisms contributing to the removal process as a result of incomplete wetting. In the expression below the symbol 'Mr' represents the molecular (or atomic) weight of the compound indicated in the sub index.

For ammonia:

Equation 29

$$r_N = -\left[\mu_{AOB}^{spec} \cdot F_w \cdot \frac{[X_{ANO}]_b}{Y_{N,ANO}^{max}} \right] \cdot \frac{Mr_{NH_4^+}}{Mr_N}$$

For oxygen:

Equation 30

$$r_{O2} = -\left[\mu_{AOB}^{spec} \cdot F_w \cdot \frac{[X_{ANO}]_b}{Y_{N,ANO}^{max}} \right] \cdot 1.5 \cdot \frac{Mr_{O_2}}{Mr_N}$$

The factor 1.5 stands for the stoichiometric relationship between ammonium and oxygen according to the reaction given by Equation 1 presented in Paragraph 2.3.1.

For microbiologically available phosphorus:

Equation 31

$$r_P = -\left[\mu_{AOB}^{spec} \cdot F_w \cdot \frac{[X_{AOB}]_b}{Y_{P,AOB}^{max}} \right] \cdot \frac{Mr_{PO_4^{3-}}}{Mr_P}$$

For carbon dioxide and bicarbonate:

Equation 32

$$r_{CO2} = +\left[\mu_{AOB}^{spec} \cdot F_w \cdot \frac{[X_{AOB}]_b}{Y_{N,AOB}^{max}} \right] \cdot 2 \cdot \frac{Mr_{CO_2}}{Mr_N}$$

Equation 33

$$r_{HCO3} = -\left[\mu_{AOB}^{spec} \cdot F_w \cdot \frac{[X_{AOB}]_b}{Y_{N,AOB}^{max}}\right] \cdot 2 \cdot \frac{Mr_{HCO_3}}{Mr_N}$$

The factor 2 comes from Equation 3 and represents the stoichiometric relationship between ammonia, carbon dioxide and bicarbonate.

Other biological processes

Other biological processes occurring in the filter are considered only indirectly: they are not modelled by themselves, only their oxygen demand or their impacts on the carbonic acid equilibrium.

Iron removal:

Equation 34

$$r_{O_2,Fe^{2+}} = -0.25 \cdot \frac{d\left[K_{Fe^{2+}} \cdot [Fe^{2+}]\right]}{dz} \cdot \frac{Mr_{O_2}}{Mr_{Fe}} = -0.25 \cdot \alpha_{Fe^{2+}} \cdot (1 - K_{Fe^{2+}}) \cdot [Fe^{2+}] \cdot \frac{Mr_{O_2}}{Mr_{Fe}}$$

Where:

r_s : volumetric conversion rate for oxygen due to iron oxidation [g/(s·m^3)].
$K_{Fe^{2+}}$: proportion of iron II oxidized during spray aeration [-].
$[Fe^{2+}]$: iron concentration in raw water [g/m^3].
$\alpha_{Fe^{2+}}$: iron oxidation rate [1/s].

For simplicity purposes and in the absence of measurements $K_{Fe^{2+}}$ is assumed to be 0 (therefore it is accepted that the model will overestimate slightly the oxygen requirements). Thus, the model assumes that all the iron is removed in the first compartment of the filter.

Similarly, with the hydrogen carbonate and carbon dioxide balances in the water:

Equation 35

$$r_{HCO3,Fe^{2+}} = -2 \cdot \frac{d\left[K_{Fe^{2+}} \cdot [Fe^{2+}]\right]}{dz} \cdot \frac{Mr_{HCO_3^-}}{Mr_{Fe}}$$

Equation 36

$$r_{CO2,Fe^{2+}} = +2 \cdot \frac{d\left[K_{Fe^{2+}} \cdot [Fe^{2+}]\right]}{dz} \cdot \frac{Mr_{CO_2}}{Mr_{Fe}}$$

Nitrite oxidation: under the assumption that all nitrite is converted into nitrate and according to the reaction expressed by Equation 2, the oxygen demand rate can be calculated as:

Equation 37

$$r_{O2,NOB} = -\left[\mu_{AOB}^{spec} \cdot F_w \cdot \frac{[X_{AOB}]_b}{Y_{N,AOB}^{max}}\right] \cdot \frac{Mr_{O_2}}{Mr_N}$$

3.4.7 Biomass processes

Among all the processes that may intervene on the development of the biofilm, that ones considered by the model are growth, decay and detachment, either during normal operation or backwashing. The equation for growth has been already presented.

Decay

Equation 38

$$b_T = b_{20} \cdot \beta^{(T-20)}$$

Where:

b_T : specific biomass decay rate corrected for temperature [1/s].

b_{20} : specific biomass decay coefficient at 20 °C [1/s].
T : temperature [°C].
β : temperature correction factor for decay [-].

Detachment

It has been widely documented that detachment may significantly influence the overall biofilm performance and structure (Morgenroth and Wilderer, 2000). Biofilm detachment happens in principle when the flow rate rapidly increases since higher shear stress may induce higher detachment rates. But it is also true that that is only a temporary response: it is believed that the biofilm may also becomes acclimated to higher flow rate if they last long enough, reaching a new steady state after some time. It is implicit then that the detachment rate may vary depending on the time period considered and the flow rates during that period.

Therefore, the model is prepared to consider different detachment rates: one for the new biomass and other for the 'old' biomass. This is because the relative position of the biomass influences its level of support and aggregation. For the already attached biomass, the detachment coefficient is considered proportional to the amount of biomass. For the new biomass, a certain proportion is assumed to be lost by diffusion to the bulk. Unfortunately, the mechanics are yet poorly understood. This is one of the reasons because during the calibration phase, decay and detachment will be calibrated as one single parameter.

Net growth

The net growth rate is calculated according to the expression:

Equation 39

$$\mu_{AOB}^{NET} = \left((1 - d_1) \cdot \mu_{AOB}^{spec} - b_T - d_2\right)$$

Where:

μ_{AOB}^{NET} : net growth rate [1/s].
d_1 : new biomass detachment rate [-].
μ_{AOB}^{spec} : specific growth rate [1/s].
b_T : decay rate [1/s].
d_1 : old biomass detachment rate [1/s].

3.4.8 Mass balance equations

The dynamics of the conversion in the trickling filter can be deduced from mass balance considerations for the different components. Transport in the air and water phases and degradation in the solid phase are shown below. During a simulation, the set of differential and algebraic equations contained in the model is solved at each time-step. The equations yield the values of certain state variables, which then are used as data for the calculations at the next time-step. The ordinary differential equations are describing one of the sections that is approximated by a CSTR. The sub-index 'in' refers to the concentration in the influent coming from the previous CSTR.

The mass balances for ammonium are:

Equation 40

$$\frac{d[NH_4^+]_w}{dt} = \frac{[NH_4^+]_{w,in} - [NH_4^+]_w}{T_z} - k_{2,f,NH4} \cdot ([NH_4^+]_w - [NH_4^+]_b)$$

Equation 41

$$\frac{d[NH_4^+]_b}{dt} = k_{2,f,NH4} \cdot ([NH_4^+]_w - [NH_4^+]_b) + r_{NH4+}$$

The mass balances for hydrogen carbonate are:

Equation 42

$$\frac{d[HCO_3^-]_w}{dt} = \frac{[HCO_3^-]_{w,in} - [HCO_3^-]_w}{T_z} - k_{2,f,HCO3} \cdot ([HCO_3^-]_w - [HCO_3^-]_b)$$

Equation 43

$$\frac{d[HCO_3^-]_b}{dt} = k_{2,f,HCO3} \cdot ([HCO_3^-]_w - [HCO_3^-]_b) + r_{HCO3+} + r_{HCO3,Fe^{2+}}$$

The mass balances for oxygen are:

Equation 44

$$\frac{d[O_2]_w}{dt} = \frac{[O_2]_{w,in} - [O_2]_w}{T_z} + k_{2,O_2}\left(k_{d,O_2} \cdot [O_2]_g - [O_2]_w\right) - k_{2,f,O_2} \cdot ([O_2]_w - [O_2]_b)$$

Equation 45

$$\frac{d[O_2]_b}{dt} = k_{2,f,O_2} \cdot ([O_2]_w - [O_2]_b) + r_{O2} + r_{o_2,Fe^{2+}} + r_{O2,NOB}$$

The mass balances for carbon dioxide are:

Equation 46

$$\frac{d[CO_2]_w}{dt} = \frac{[CO_2]_{w,in} - [O_2]_w}{T_z} + k_{2,CO_2}\left(k_{d,CO_2} \cdot [CO_2]_g - [CO_2]_w\right) - k_{2,f,CO_2} \cdot ([CO_2]_w - [CO_2]_b)$$

Equation 47

$$\frac{d[CO_2]_b}{dt} = + k_{2,f,CO_2} \cdot ([CO_2]_w - [CO_2]_b) + r_{CO2} + r_{CO2,Fe^{2+}}$$

The mass balance for phosphate is:

Equation 48

$$\frac{d[PO_4^{3-}]_b}{dt} = [k_2 \cdot ([PO_4^{3-}]_w - [PO_4^{3-}]_b) + r_{PO4}]$$

Equation 49

$$\frac{d[PO_4^{3-}]_w}{dt} = \frac{[PO_4^{3-}]_{w,in} - [PO_4^{3-}]_w}{T_z} - k_2 \cdot ([PO_4^{3-}]_w - [PO_4^{3-}]_b)$$

It is assumed that all substrate taken up by biomass is converted into biomass. Convective transport of bacteria is neglected: e.g. the inoculation of biomass is neglected; the dead biomass is assumed to be washed out and it is considered through the calculation of the net growth. The mass balance for the oxidizing bacteria results:

Equation 50

$$\frac{d[X_{AOB}]}{dt} = \mu_{AOB}^{NET} \cdot [X_{AOB}] \cdot F_w$$

3.4.9 Others

Performance parameters

A few additional expressions has been added to the model to better characterize the nitrifying activity of the filter and not only with the effluent ammonium concentration and the ammonium removal rate. The parameters are:

Sand specific nitrification rate per mass unit:

Equation 51

$$r_{N,Mass} = \frac{([NH_4^+]_{IN} - [NH_4^+]_{EFF})}{M} \cdot Q \cdot \frac{Mr_N}{Mr_{NH_4}}$$

Where:

$r_{N,Mass}$: sand-specific nitrification rate per mass unit of filter material [mg N / h kg].
$[NH_4^+]_{IN}$: ammonium concentration in the influent [mg/L].
$[NH_4^+]_{EFF}$: ammonium concentration in the effluent [mg/L].
Q : flow rate [m^3/h].
M : mass filter material [kg].

Cell specific nitrification rate per unit volume of filter material:

Equation 52

$$r_{N,Volume} = \frac{([NH_4^+]_{IN} - [NH_4^+]_{EFF})}{V \cdot (1 - P_o)} \cdot Q \cdot \frac{Mr_N}{Mr_{NH_4}}$$

Where:

$r_{N,Mass}$: sand-specific nitrification rate per mass unit of filter material [mg N / h kg].
$[NH_4^+]_{IN}$: ammonium concentration in the influent [mg/L].
$[NH_4^+]_{EFF}$: ammonium concentration in the effluent [mg/L].
Q : flow rate [m^3/h].
V : reactor volume [m^3].
P_o : clean bead porosity [-].

Carbonic acid equilibrium

With the oxidation of ammonia, iron and manganese, the carbonic acid equilibrium varies. The pH is mainly determined by the concentration of carbon dioxide and bicarbonate. During biochemical reactions these concentrations change and pH is thus influenced. Furthermore, the pH influences the biological activity of the cells. The model considers the differences in the concentrations of carbon dioxide and carbonate in water and on the biofilm and therefore establish the kinetic activity based on the pH existing in the surface of the biofilm. Stimela includes several modules ready to calculate any of these parameters based on the information that is available. These modules have been used to calculate the m-number and the carbon dioxide content of the influent water and the pH in the filter.

4 Model calibration and validation

4.1 Statistical analysis of full-scale measurements

Controlling the performance of the Tiendweg bio-trickling filters at WTP Lekkerkerk is a regular task for both the treatment plant operators and the water technologist of OASEN. Although they know which the critical events are in these filters, it can be difficult for them to look at them from a different perspective rather than the day-to-day operation. This section is aimed at:

1. Assessing the maximum loading rate for each bio-trickling filter. By definition, the critical loading rate corresponds to the maximum removal capacity of the filter (Tatari et al., 2013). Below the maximum, variation in the influent should have not effect on the effluent. In Section 2.4 it has been shown that loading variations are often experienced in full-scale filters due to fluctuating influent ammonium concentrations and unstable flow rates. Therefore, this parameter is important because it delimits a safe region for operation, where filter performance is expected to be robust to dynamic loading variations.
2. Identifying which operational parameters influence most the filter response and to determine if they change over the filter life cycle.
3. Defining statistically which the usual conditions the filter are operated at.
4. Establishing whether there are differences between filters and how important they are.

All the results shown in this section are based on data sub-sets derived from the original set. The original data set comprises all the available measurement: mainly lab measurements taken on a weekly-monthly basis and hourly flow rate values. The sub-sets have been formed by identifying those measurements in the entire series which coincide in time. This requirement has greatly reduced the size of the series used in the statistical analysis when compared to the size of the original sets. The resulting size (N) of the series considered is indicated in the tables below.

PRIMARY FILTERS

After external washing or filter renewal all primary filters show, qualitatively, the same behaviour which has been previously described and shown in Figures Figure 20, Figure 22 and, Figure 23. Figure 45 is a schematic representation of the typical response. In the figure the range of the usually observed ammonium concentrations in the influent is represented by the upper darker lines while the pattern that follows the ammonium concentration in the effluent is represented by the lighter lines in the lower part of the graph. On the x-axis the filter age, defined as the time elapsed from the moment the filter returned to operation after renewal or external washing. In both cases, the thick lines stand for the average value while the thin lines illustrate in a simplified manner the amplitude of the range of the observed values.

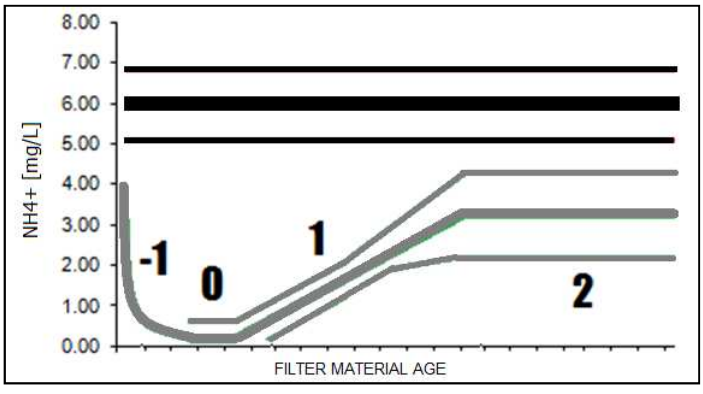

Figure 45 Typical life stages in Tiendweg primary filters

The drawing is a simplification but it clearly illustrates what the typical behaviour is:

- The stage -1 represents the start-up period of the filter. It is short or very short after external washing (sometimes the weekly sampling is not frequent enough to capture this information) and much longer after material renewal (usually ranging between 4-8 months). The loss of the nitrification capacity is probably due to the removal of the microbial population as result of the

cleaning operation. No other limitations to nitrification rather than insufficient bacterial population are thought to exist at this stage of the filter lifecycle.

- During stage +0 there is full or almost full ammonium removal. This does not necessary imply that the filter operates always at its maximum removal capacity. If there is extra capacity it might happen that this is not used. Moreover, the sampling upstream-downstream shows that filters at this stage are able to cope with fluctuations in the influent or, at least, to strongly attenuate such changes.

- During stage +1 the decline in nitrification starts and develops. The removal capacity decreases gradually. Despite this, the filters are still able to cope moderately with fluctuations in the influent. Usually, the relapse develops faster after external washing than after renewal.

- After some time the ageing process (understood as the gradual loss of capacity for removing ammonium) seems to reduce their pace of development. At this stage, stage +2**,** the nitrification capacity is very poor and the filter is unable to cope with fluctuation in the influent. This means that the fluctuations that are present in the influent are seen also in the effluent.

The similar patterns observed after renewal or cleaning suggest that the key processes behind the described behaviour at each stage may be the same. Despite the fact no systematic research has been carried out in order to optimize the cleaning procedures, the observed behaviour after external washing has been statistically analyzed.

Effect of maturity

Three types of graphs have been generated for each primary filter in order to get a better understanding on how the nitrification capacity evolves with time. In Figure 46, Figure 47 and, Figure 48 there is a scatter of points which represent the performance of one primary filter (output) under different operating conditions (input). The figures correspond to one of the primary filters (FF-08) but their aspects are very similar to the figures obtained for the rest of the primary filters. All the figures can be found in Annex A.9.

The performance is represented by either the ammonium removal rate or its relative value with regard to the maximum achieved at each cycle. The working conditions are represented by either the influent load or the filter age. By looking at how the dots are distributed over the plotting space, it is possible to see how diverse the operating conditions and the filter responses were. Moreover, a wider scatter of points on the graph implies that there may be other important factors influencing the outcome rather than the input, which is shown along the x-axis. By contrast, a narrow scattering of points implies that there is a very close relationship between the input and the output.

The first two graphs (Figure 46 and Figure 47) illustrate the relationship between the maturity of the filter (age, expressed in days) and the nitrification capacity of the filter. The dots plotted come from different cycles. The fact that they follow the same trend and even superpose to each other proves that the same or a very similar patter of behavior is observed often in these filters.

In Figure 46, the removal capacity is show on the vertical axis on the left side of the graph while the age is along the x-axis. It is seen that the nitrification capacity gradually decreases. From 229 g NH_4^+/h to values in the final life stage within the range 125 ± 38 g NH_4^+/h. If the removal rates are converted into specific values per cubic meter of filter bed, the nitrification capacity evolves from 3.99 to 2.07 ($\pm$ 1.01) g of ammonium per hour and m^3 of filter bed. In Figure 47, the nitrification capacity in the y-axis is substituted by the removal ratio, defined as the removal rate divided by the loading rate.

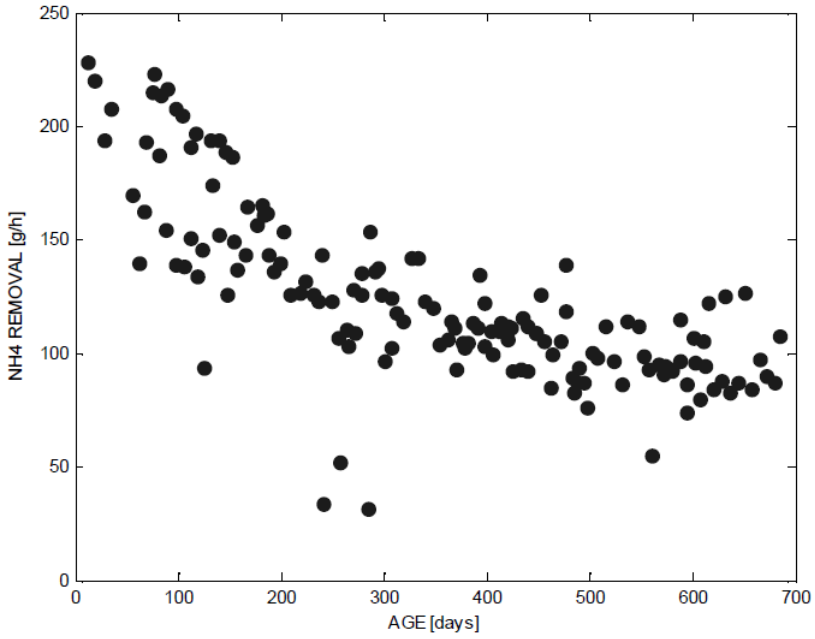

Figure 46 Ageing process of the ammonium removal rate of filter FF-08 after external washing

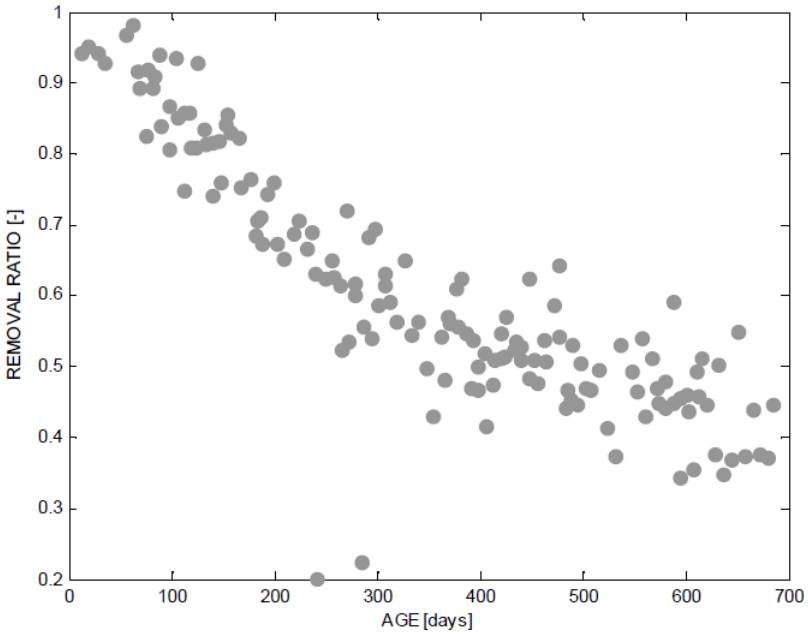

Figure 47 Variation with age of the ratio of removal of filter FF-08 after external washing

By looking at the above shown graphs it is concluded that:

- The age seems to be an excellent predictor of the behavior of the filter. Dots which are to the right of the plotting space represent the performance of the filter at the end of its life. They are significant lower than dots towards the left which correspond to a filter where external washing is still recent.
- The relapse in nitrification develops steadily until a certain age value (around 350 days, in this case). Then the removal ratio starts leveling of.
- The scattering of the dots also varies. Figure 47 proves that the scattering significantly increases in the final life stage of the filter (from day 350 in advance in the figure). This does not mean that the age is not a powerful influence anymore but that there may be other factors that matter as well. The reasons or the factors behind this bigger scattering are not fully understood.
- The scattering of the dots represents the fluctuation of the nitrification capacity of the filters at their final life stage.

Figure 48 combines at once the influent load, the age and the removal. In the figure there are different families of dots grouped by colours. Each colour represents a specific age range expressed in days. The ranges have been chosen so that the entire filter life cycle is covered. The load is represented in the horizontal axis while the removal is in the vertical axis. If all these three parameters are plotted together, the graph looks like:

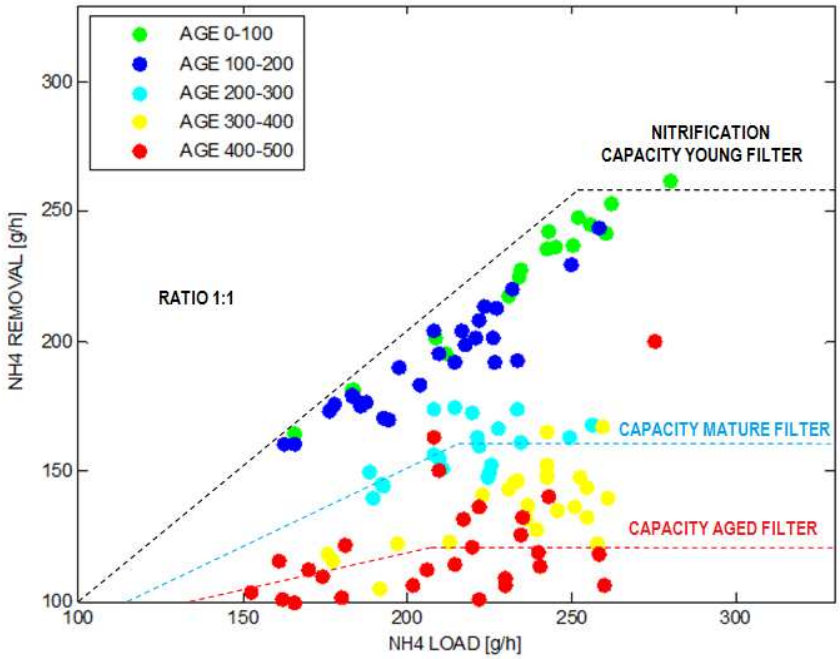

Figure 48 Nitrification rates at different filter ages for different ammonium loading rates in filter FF-08

It can be seen that the dots move down in the graph with the age. According to the life stages presented in Figure 45, green dots correspond to stage 0, when there is complete ammonium removal. Red dots correspond to stage 2, when the filter shows a very low ammonium removal. Dark and light blue and yellow dots correspond to the transition period (stage 1). It is interesting to notice that the higher the load is (the dots more to the right), the greater the vertical displacement results.

Nitrification capacity

Table 9 provides an overview of the typical working conditions and response of the primary filters at Tiendweg in the last years. The given values represent all filters. After disregarding some cycles whose values do not reproduce the usual behavior described before due to unknown causes, the size of the sample resulted in N = 851.

Table 9 Average operational conditions and performance of all primary filters at Tiendweg

OPERATIONAL CONDITIONS	Minimum	Maximum	Mean	St. Dev.	
NH_4^+ Influent [mg/L]	4.02	7.04	5.42	0.67	12%
Q [m^3/h]	15	55	39	5	12%
Loading NH_4^+ [g/h]	96	304	211	34	16%
Filter Age [days]	0	680	361	185	51%
PERFORMANCE	Minimum	Maximum	Mean	St. Dev.	
NH_4^+ Effluent [mg/L]	0.04	4.13	2.07	0.96	46%
Removal NH_4^+ [g/h]	43	243	130	38	29%
Specific capacity [g NH_4^+/h m^3 bed]	1.20	6.74	3.62	1.07	29%

The results indicate that primary filters were externally washed on average after 680 days of operation. The usual ammonium loading rate was 211 ± 34 g NH_4^+/h with peak values of up to 304 g NH_4^+/h. These peak values can have been caused either by flow increases, influent concentration peaks or a combination of both. The influent ammonium concentration was mostly in the range 5.42 ± 0.67 while the flow yielded 39 ± 5 m^3/h with some very high sporadic values (55 m^3/h).

The average maximum nitrification capacity after external washing was 243 g NH_4^+/h, which corresponds to a sand-specific nitrification rate of 6.47 g NH_4^+/h m^3. This value is lower than the maximum nitrification rates reported by some authors (van den Akker et al., 2008) in drinking water trickling filters: up to 12 g N h^{-1} m^{-3} of filter bed with influent NH_4-N concentrations between 4 and 5 mg/L. If the nitrification capacity is expressed per cubic meter of filter bed, the results indicate that on average the nitrification capacity descends to 3.62 (± 1.07) g of ammonium per hour and m^3 of filter bed on average.

The given average maximum capacity does not reflect properly the differences existing between filters. Figure 49 shows the average maximum capacity for each filter.

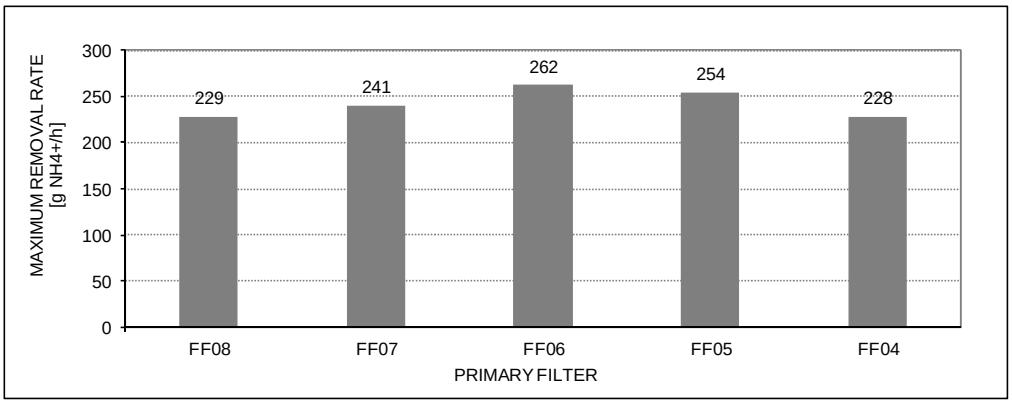

Figure 49 Maximum ammonium removal rates observed in Tiendweg primary filters after external washing

According to Figure 49, the primary filters with better working after external washing are filters FF-06 and FF-05 with maximum removal rates of 262 and 254 g NH_4^+/h (7.29 and 7.06 g NH_4^+/h m^3 respectively). Filters FF-08 and FF-04 show the lowest values: 229 and 228 g NH_4^+/h (6.33 and 6.35 g NH_4^+/h m^3 respectively). Filter FF-05 is at an intermediate situation (254 g NH_4^+/h and 6.69 g NH_4^+/h m^3). The reasons for such discrepancies could not be determined. Among the possible causes there are differences in the effectiveness of external washing or the measurement times.

Statistical relationships

Effect of age

The results previously shown indicate that there is a strong relation between the filter performance and its maturity. The statistical analysis of the data set of each filter confirms this idea. Table 10 summarizes the importance of each factor and the strength of the correlation between the ammonium concentration in the effluent, the filter age and the average load.

Table 10 Operational parameters with highest impact on the effluent ammonium concentration of primary filters at Tiendweg

	R^2 NH4+ Effluent ~		
Primary Filter	Age	Age & NH_4^+ Load	N
FF-08	0.75	0.79	150
FF-07	0.47	0.67	64
FF-06	0.62	0.74	197
FF-05	0.60	0.71	205
FF-04	0.32	0.45	225

According to Table 10, both the age and the ammonium load are statistically significant in order to predict the response (ammonium concentration in the effluent). The correlation is in almost all cases around 0.7. The filters with the most easily predictable response are filters FF-08, FF-05 and, FF-06. The results confirm that the age of the filter is by far the strongest factor as well.

The search for the same type of relationship considering only values corresponding to the last stage of life of the filters has not yielded positive results. This confirms the unpredictable nature of the observed fluctuations (bigger scattering of dots in Figure 46 and Figure 47).

Finally, other parameters apart from the load and the age have been also analyzed in order to find other factors contributing to a better characterization of the relapse of nitrification after external washing. None of them improves the shown R^2 values. For instance, the contribution of the iron load is negligible. Additionally, it has not been possible to identify patterns or factors that allow predicting the moment at which the filter changes from one stage to another.

Effect of backwashing

The data shown in Figure 17 in Paragraph 2.3.2 has been analyzed in the search of correlations between the flow, the pH and the effluent ammonium concentration. The two parameters analyzed are the effluent ammonium concentration and pH. According to the values shown in the figure, it is seen that in each cycle the effluent pH increases simultaneously to the observed decrease in the ammonium concentration in the effluent. This pattern is against what it was intuitively expected (the acidification of the media due to the higher biological activity) and the reasons for that behaviour are unknown. One hypothesis is that it could be indicative of some improvement in the transport-diffusion of oxygen and carbon dioxide between the gas and the solid phase over time. The resulting increase in the pH would result in a higher biological activity that would result in the higher ammonium removal. Although this issue will be further discussed when the model equations are presented (Section 3.4) none of these hypothesis has been demonstrated. The statistical analysis indicates that such patter is statistically significant. In fact, there exists a statistical correlation between the flow, the pH and the effluent ammonium concentration in such case: $R^2 = 0.42$.

Special cases

There are two specific cases that would have been of interest in the search for statistically relationships. Those cases were presented in Figure 24 and Figure 26. As discussed in Paragraph 2.3.1, nitrification in filter FF-04 has being occurring in the absence of iron for a long time period. With regard filter FF-05, which has its nitrification capacity reduced, it has been half-loaded for a long time-period. Unfortunately in both cases no significant relationships have been for diverse reasons (e.g.: shortness of the data series; there are other factors influencing performance which have not been taken into account such as phosphate dosage and changing backwash frequency). A more complex and sophisticated analysis of this raw information is needed and recommended.

SECONDARY FILTERS

Full scale measurements suggest that when primary filter removes at least half of the ammonium present in the influent, there is no breakthrough after backwashing in the secondary filter. This means that the way secondary filters react to backwash depends on their influent load: the higher the influent load is, the higher the ammonium breakthrough results. The results of the statistical analysis are summarized in Table 11.

Table 11 Operational parameters with highest impact on the effluent ammonium concentration of secondary filters at Tiendweg

	R2 NH_4^+ Effluent ~		
Secondary Filter	Op. Time	Op. Time & NH_4^+ Load	N
FK-08	0.40	0.49	41
FK-07	0.62	0.69	40
FK-06	0.30	0.41	39
FK-05	0.31	0.41	40
FK-04	-	-	41

According to these results it is proved statistically that the response of the filter is mainly dependent on the same two factors in all cases: the operating time and the load. The results also indicate that the influence of the operating time is higher than the impact of the load. Results are not available for filter FK04 since no ammonium breakthrough is observed there. The analysis has also allowed the identification of some threshold values for the load (see Table 12). This means that breakthrough after backwashing only occurs if the load is above the threshold. Some figures in Annex A.9 illustrate the existence of the threshold values determined statistically.

Table 12 Critical load of secondary filters (Tiendweg)

Secondary Filter	Critical Load [g NH4+/H]
FK-08	97
FK-07	76
FK-06	88
FK-05	87
FK-04	Unknown

Values given in Table 12 suggest that the nitrification capacity after backwashing may change from filter to filter. The found values range from 76 g NH_4^+/h in filter FK-07 to 97 g NH_4^+/h in filter FK-08. The reasons for such differences are not clear. Since the backwash programme is the same for all the secondary filters, it is hypothesized that the threshold value at each case can be linked to the specific loading conditions at each case, which depend on the performance of the filter upstream. Table 13 summarizes the average loads and removal rates for each case.

Table 13 Average ammonium loads and removal rates of secondary filters (Tiendweg)

Secondary Filter	Average Load [g NH4+/h]	Average Removal [g NH4+/h]
FK-08	104.98	100.23
FK-07	80.59	70.16
FK-06	88.77	83.89
FK-05	80.76	78.58
FK-04	38.11	37.62

By comparing the values given in Table 12 and Table 13 it can be seen then that the filters with the highest loads are those ones with highest threshold values (filter FK-08).

To conclude, ammonium breakthrough in secondary filters is an issue only after backwashing. Moreover, breakthrough only occurs when the load is above a certain threshold value. Although the threshold value varies from filter to filter, the values for all cases are within the range 79-97 g NH_4^+/h. Consequently, any action aimed at reducing the number of ammonium breakthrough episodes is linked to: (1) either assuring that the effluent of the primary filter is such that the threshold value for the secondary filter is not exceeded; or (2) reducing the frequency of backwashing in secondary filters if possible.

4.2 Site-specific measurements

In modelling the values for many model parameters are generally assumed from either literature or, preferably, full-scale specific measurements. But in some other cases, information may not be available. Authors state that the calibration and validation of mathematical models in drinking water treatment applications often asks for specific information that needs to be gathered through special monitoring programs in full-scale installations, laboratory experiments and/or pilot installations (Van Schagen, 2009).

Fortunately OASEN has a long history of experiments being performed on their own facilities. The construction of the model has required the analysis of the data gathered during the realization of three types of experiments: (1) tracer experiments to characterize the fluid regime within dry filters; (2) measurements in sprayers to estimate their efficiencies; and, (3) internal measurements to assess the nitrification activity and the abundance of ammonia-oxidizing microorganisms in dry filters. These experiments have covered most of the model requirements. Their results have been used either for a better estimation of some internal model parameters as well as for better supporting of some modelling decisions.

Conservative tracer experiments

The analyzed results from tracer experiments refer to different moments of the run cycle. Special attention has been paid to the results of the experiments performed before and after backwashing. None of the filters analyzed were one of the bio-trickling filters at WTP Lekkerkerk showing typically nitrification problems. Although there are differences between these filters and the filters where the experiments where took place, it is assumed that the results can be used to have a better idea on the characteristics of the fluid regime in the bio-trickling filters and, if possible, to evaluate how certain the hypothesis of high wetting efficiency is in the dry filters studied. The results can be found in Annex A.10.

When looking at the differential residence time distribution curves before and after backwashing it is seen that before backwashing the curve is less normally distributed. This change of shape indicates greater heterogeneity concerning the residence time. This increasing heterogeneity could be partially explained by flow channelling (Wik, 2003) which might be enhanced by clogging.

Both the curves and the parameters used to characterize the flow regime (the Morill-dispersion index and the Peclet number) indicate that the degree of mixing evolves and suggest the apparition of preferential flows and/or dead spaces as soon as clogging is thought to develop. Nevertheless, this

does not automatically prove that clogging has significant effects on the nitrification capacity of the filter. By contrast, the time at which the peak concentration value is detected in the effluent of the filter hardly changes.

Supposedly the flow conditions can be assimilated to a certain number of ideal mixers in series. The results confirm that the flow conditions in trickling filters are closer to ideal mixing (N=1) than to plug flow (N=∞). This seems to confirm the idea that despite the flow regime is likely laminar in trickling filters, eddies and vortices created by water droplets trickling down contribute to enhance mixing in this type of filters. In all cases this number is within the range N = 1-5.

Although the observed residence times must be used with caution since they correspond to filters with different dimensions than the filters that are going to be modelled, they have been used to acquire a certain order of magnitude of the velocity of water within the filters. The heterogeneity in the residence times shown by the residence time distribution curves might be indicative of the existence of some heterogeneity also in the water velocities within the filter. The water velocity has been estimated based on the height of the filter bed and the residence times. Measurements suggested that fluctuations in the flow rate influence the average residence time and the distribution and therefore these results need to be taken with caution. The estimated values oscillate within the range 7-17 m/h. The mean average water velocity of all the experiments was 10 m/h.

Internal measurements

A deeper understanding of the dynamics of the population of ammonia-oxidizing microorganisms requires assessing the quantity and the activity of the nitrifying microorganisms present in the filters. A summary of all the results can be found in Annex A.11. The main conclusions are:

- Measurements have shown that filters with poor nitrification show very low cell and sand specific nitrification rates while filters while filters with robust nitrification have very active cells. Sand-specific nitrification rates are around 1.2-3.1 N h^{-1} kg^{-1} in the first case (De Vet et al., 2011b) while are up to 9 g N h^{-1} kg^{-1} in the second case (De Vet et al., 2009a).

- Moreover, in filters that perform well the nitrification activity is highly stratified and mainly concentrates in the upper layers. Contrarily, measurements in filters with poor ammonium removal show low nitrification rates over the entire filter bed. The same is thought to occur with the distribution of ammonia-oxidizing microorganisms over the filter depth (De Vet et al., 2011b).

- Measurements prove that the loss of cells is much higher during backwashing than during filtration (De Vet et al., 2011b). Results suggest that the importance of detachment during normal operation evolves and increases with the filter lifetime. The comparison of the numbers of ammonia-oxidizing microorganisms in the bed, effluent, filtrate and backwash water suggest that biomass detachment is unlikely the cause of incomplete nitrification.

All this suggest that poor ammonium removal part of the ammonia-oxidizing microorganisms are either dead or their activity is severely affected (De Vet et al., 2009a) either due to inhibition or substrate (and/or nutrient) limitation.

Aeration measurements

In order to determine the best way of modelling aeration in the low-pressure sprayers placed above of the filters and the actual quality of the water entering into the filters, data from other sites with the same aeration system has been analyzed. The results are summarized in Annex A.12. The results are conditioned by the fraction of iron that is oxidized during spray aeration. If it is assumed that most of the iron is oxidized during spray aeration, then the bottom efficiencies can be estimated. For oxygenation, they are within the range 36% and 70% depending on the raw water quality. For carbon dioxide stripping the efficiencies are within the range 25%-44%.

Considering the raw water quality at Lekkerkerk, these results suggest that low pressure-sprayers used in the primary filters FF-04 to FF-08 might achieve efficiencies around 25-35 % concerning carbon dioxide stripping and around 57-70 % concerning oxygenation. The results also suggest that the sprayers do not succeed on achieving complete methane removal. The reported removal efficiencies range between 64-77%. The remaining methane is thought to be removed by forced ventilation in the first layers of the primary filters.

With respect to the secondary filters, regular sampling indicates that the effluent of the primary filters are close to oxygen saturation. Moreover, methane has been completely removed in the first filtration step. Therefore, the use of these sprayers is more linked to ensuring a uniform distribution of flow than to the supply of oxygen for nitrification.

4.3 Model calibration

Broadly speaking there are two main approaches for model calibration: (1) to perform systems analysis that aim to ground the calibration by following some parameter estimation techniques such as sensitivity analysis; and, (2) to rely more on a tailored calibration approach which takes as reference previous model fitting experiences, parameter subset selection and manual fine-tuning. The second option fits better with the specific needs of this model and, hence, has been chosen. The followed steps taken have been:

1. Literature review and site-specific measurements (data gathering).
2. Parameter sub-set selection based on uncertainty.
3. Parameter sub-set selection based on sensitivity.
4. Parameter sub-set definition.
5. Initialization.
6. Stepped calibration (several scenarios).

First, the internal model parameters have been listed and classified into three major categories. Subsequently, several sources of information, including site-specific measurements, full-scale experiments and related literature, have been consulted in order to have a first idea of the available information. The categories have been:

- Microbial parameters:
  - Maximum specific growth rate of ammonia-oxidizing organisms (ANOs).
  - Specific endogenous respiration for nitrifiers (decay rate).
  - Half saturation constant for N, O_2 and P.
  - Yield coefficients for N and P.
  - Detachment rates for old and new biomass.
  - Initial ammonia-oxidizing organisms content (ANOs).
  - Temperature and pH sensitivity for nitrification and endogenous respiration for ANOs.
- Mass-transfer related parameters independent of the system design or operation:
  - Diffusion in water.
- Mass-transfer related parameters dependent of the system.
  - External mass transfer resistance.
  - Air-water flow ratio.
  - Wetting efficiency.
  - Filter material characteristics (size, density, porosity, packing specific surface area).
  - Fraction of void volume occupied by water.
  - Number of unit elements.

Table 14, Table 15 and Table 16 summarize the reference values.

Table 14 Reference values for kinetic and biofilm parameters

Parameter	Units	Value	References	Comments
Maximum specific growth rate	[1/s]	3.36E-06 5.43E-06 1.10E-05 (0.382-2.37-2.95)E-05 (0.33-2.44)E-05	(Gujer and Boller, 1986) (Gujer and Boller, 1986) (Wanner and Reichert, 1996) (Brockmann et al., 2008) (Keen and Prosser, 1987)	10oC 15oC 20oC 30oC 30oC
Growth rate correction factor for T	[-]	$1.123^{(T-20)}$	(Henze, 2008)	
Yield N	[g ds/g NH4-N]	2.86E-03 7.14E-04 0.17	(De Vet, 2011) (De Vet, 2011) (Keen and Prosser, 1987)	Tiendweg filters Schuwacht filters
Yield P	[g ds/g PO43-P]	39.10	(Van der Aa, 1999)	
Decay rate	[1/s]	5.78E-07 (0.347-1.5-5.79)E-06	(Wanner and Reichert, 1996) (Brockmann et al., 2008)	20oC Several temperatures
Affinity constant N	[g/m3 NH4-N]	0.15 0.23 0.40 1.00 10.00 0.73-1.00 0.03 0.20-2.40-7.50	(Van der Aa, 1999) (Gujer and Boller, 1986) (Gujer and Boller, 1986) (Wanner and Reichert, 1996) (Suzuki, 1974) (Zhu and Chen, 2001) (Picioreanu, 1997) (Brockmann et al., 2008)	 10oC 15oC 20oC 20oC Several temperatures
Affinity constant P	[g/m3 PO43-P]	0.45 0.11	(De Vet, 2011) (Van der Aa, 1999)	
Affinity constant O2	[g/m3 O2]	0.30-2.00 0.10 0.40-0.60-2.00 0.30	(Henze, 2008) (Wanner and Reichert, 1996) (Brockmann et al., 2008) (Picioreanu, 1997)	 20oC Several temperatures
Growth rate correction for pH	[-]	$(1+0.041\ (10^{\text{abs}(8.4-\text{pH})}))^{-1}$	(Van der Aa, 1999)	
Detachment rates	[g/m2 s]	Several detachment rate expressions depending on the mechanism of detachment: excessive biofilm thickness, shear forces, backwashing, etc.	(Henze, 2008)	The process is site-specific: e.g. based on reactor type or operation.

Table 15 Reference values for mass transfer related parameters independent of the system

Parameter	Units	Value	References	Comments
Diffusion Oxygen Diffusion Ammonium Diffusion Bicarbonate	[m2/s]	2.40E-09 1.86E-09 1.00E-09	(Crank, 1975) (Wilke et al, 1955)	30oC

Table 16 Reference values for mass transfer related parameters dependent on the system.

Parameter	Units	Value	References	Comments
Air-water flow ratio	[-]	FF: 16 FK:13	Site specific values	Forced ventilation at its maximum
Wetting efficiency	[-]	Site-specific parameter	No measurements	
Fraction void volume occupied by water	[-]	Site-specific parameter	No measurements	
Number of CSTR compartments	[-]	Site-specific parameter		See Section 4.2
Packing material characteristics		Site-specific parameter		See Section 2.3.1
Reynolds	[-]	0.14 5.10	(Kissel, 1986)	Low rates High rates
Sherwood	[-]	6.40 39.00	(Kissel, 1986)	Low rates High rates
External mass transfer coefficient	[m/s]	1.27E-06 4.05E-06	(Kissel, 1986)	Low rates High rates
		Empirical equations. Diverse packing materials.	(Dorado et al., 2009) (Van Krevelen, 1948) (Kim et al., 2008) (Onda et al., 1968)	For clay pellets (the most similar placking material among those reported): 4.33E-04 to 7.08E-7

Subsequently, the internal model parameters were divided into two groups. The first group is formed by those model parameters whose uncertainty is considered low or very low. For some of them there are site-specific measurements (e.g.: filter bed dimensions, filter material characteristics, air-water flow ratio and, number of complete stirred tanks that better approximate the hydraulic regime in the filter). For others, the values are site-independent, well known and documented (e.g.: diffusivities for aqueous solutions; correction factors for growth and decay; yield factor for phosphorus).

Concerning the number of completely mixed reactors has got a calibration value of 5, since tracer experiment results indicate that that is the number that better characterizes the fluid regime. With regard the diffusion coefficients and for the sake of simplicity, the model will assume one unique value (the value for oxygen) since they all have share the same order of magnitude. As for the characteristics of the filter media, they have been assimilated to the sand media characteristics.

The second group is formed by the parameters which are considered to have medium-high uncertainty. In general, the kinetic parameters are considered relatively uncertain due to the dispersion of the values reported. For instance, the maximum growth is considered rather uncertain due to the discrepancy between literature-based and site-specific values. For the detachment rates there are not site-specific values that make possible to select and use one of the expressions given in literature (Morgenroth and Wilderer, 2000). The affinity constants have been considered high-moderately uncertain although this depends on the compound. Regarding the amount of ammonia-oxidizing organisms, although there are some site-specific values they are insufficient to characterize how the biomass content evolves through the filter life cycle. The thickness of the mass transfer boundary layer is considered to be highly uncertain as well. This is not only because the fact that the true value is difficult to be measured but also due to the supposed changing hydrodynamic conditions within the filters(Boltz et al., 2011). The same occurs with the wetting factor: although it is intuitively assumed that the wetted specific surface area is high, there are no full-scale experiments that prove this idea. The residence time is considered only as moderately uncertain since there are values that come from tracer experiments although those measurements took place in other dry filters. The uncertainty also comes from the variability of the measured values and how that might be linked to some operation parameters such as the filter age and the filter run time.

Therefore, the parameters which are considered moderately-highly uncertain are:

- Microbial parameters:
  - Maximum specific growth rate of ammonia-oxidizing organisms (ANOs).
  - Specific endogenous respiration for nitrifiers (decay rate).
  - Half saturation constant for N, O2 and P.
  - Yield coefficients for N and P.
  - Detachment rates for old and new biomass.
  - Initial ammonia-oxidizing organisms content (ANOs).
- Mass-transfer related parameters dependent of the system:
  - External mass transfer resistance.
  - Wetting fraction.
  - Fraction of void volume occupied by water.

In order to make simpler the calibration, this second group of parameters were divided into two sub-groups according to the impact of each parameter on the model results (ammonium concentration in

the effluent), which were roughly assessed with a sensitivity analysis. The aim of this subdivision is to reduce the number of parameters to be included in the iterative process of calibration. This sensitivity analysis is not included here, only its conclusions. Ideally, the results of this analysis will be confirmed by a second sensitivity analysis to be performed once the model has been calibrated and validated (see Section 4.5).

The results have indicated that the most influential internal parameters are the maximum growth rate and the yield together with the size of the population of ammonia-oxidizing microorganisms. The detachment and the decay rates also have great influence. With regard to the affinity constants, they have only a relative influence. The wetting efficiency has a great impact since it controls the amount of biomass that is exposed to the substrate. Finally, the fraction of the void volume occupied by water has a relative influence. Moreover, it can be roughly estimated based in order to make that the residence time matches with the tracer experiment results, idea that is also applicable to the water velocity.

Therefore, the parameters which are considered moderately-highly uncertain and that strongly influence the model response are:

- Microbial parameters:
  - Maximum growth rate of ammonia-oxidizing organisms (ANOs).
  - Decay rate of ammonia-oxidizing organisms (ANOs).
  - Yield coefficient for N.
  - Detachment rates.
  - Initial ammonia-oxidizing organisms content (ANOs).
- Mass-transfer related parameters dependent of the system.
  - Wetting fraction.

These parameters are candidates to be the first ones to be calibrated ("calibration sub-set"). The other parameters, those ones with significant uncertainty but lower impact are excluded from the first calibration efforts. They will be more easily adjusted when the values of the parameters of the calibration sub-set are known. For the moment they take the most common value reported in literature.

The number of parameters included in the calibration sub-set (6) is still too high to successfully calibrate the model manually. For this reason, it is necessary to further reduce their number:

Decay rate

Considering that (1) the shear rates causing detachment are often difficult to predict under trickling flow conditions and that there are no references about what are the physical characteristics of the biofilm that allow to roughly estimate how important each of these processes might be, it has been decided to merge detachment and decay rates in one single parameter. The effective decay rate is defined as the net contribution of all the physical or biological processes counteracting biomass growth. Therefore, it mainly comprises the following processes:

- Natural decay rate.
- Biomass washout (due to backwashing).
- Biomass detachment (due to flow rates during operation).
- Biomass inactivation (due to inhibition and/or low substrate concentrations).

Equation 53

$$b_{EFFECTIVE} = b_{NATURAL} + d_{WASHOUT} + d_{DETACHMENT} + b_{INACTIVATION}$$

Wetting efficiency

Concerning the wetting efficiency, in principle is thought to be high due to several reasons. First, the water to be treated is distributed as evenly as possible with sprayers. Moreover, the fluid regime in trickling filters (the existence of water droplets and swirls) is though to contribute to good mixing and distribution. Finally, forced aeration is used in the filters which may increase the turbulence of the flow and enhance mixing. Consequently, if incomplete wetting occurs, the causes must be internal and only present temporally (e.g. during clogging). Therefore, the wetting efficiency will receive the value of 1 by default in the model.

Yield coefficient

For the maximum biomass yield of ANO cells on ammonium (N), the site-specific value has been taken despite the fact that value may be only partially representative and differs significantly from literature values. This lower growth yield may be related to multiple causes (De Vet et al., 2011b): competition for nutrients with other microorganisms, inhibition by deposited compounds, decrease in the growth

rate and/or influence of the pH and temperature. If the first calibration efforts do not provide satisfactory results, then the value will be readjusted.

Biomass content

Regarding the biomass content and its distribution is highly unknown. Consequently, the initialization of this parameter will depended of each calibration scenario.

Water velocity

The water velocity on the vicinity of the surface of the filter grains is completely unknown. Nevertheless, the model assumes that it might be approximated by ensuring that the mean residence time is within the range of the reported values in past tracer experiments (see Section 4.2).

Parameter sub-set for calibration

Finally, the parameter sub-set for calibration is conformed by: (1) the maximum growth rate of ammonia-oxidizing organisms; (2) the effective decay rate of ammonia-oxidizing organisms; and, (3) the initial content of ammonia-oxidizing organisms. The values of these three parameters will depend on the situation to be modeled ("calibration case"). Therefore one calibration sub-set will be produced for each calibration period. These periods and the results of calibration are presented below. The value for the other model parameters are fixed and can be found in Annex A.14

Calibration cases

Different time periods have been selected (see Figure 45). Each time period is aimed at facilitating the calibration of at least one of the three parameters of the calibration sub-set. For the model of nitrification in the first filtration step, six different calibration periods have been defined. The periods cover different times and all the possible life stages of these filters. The data used for each case correspond to the filter whose name is given between brackets below. Since all the primary filters go through the same life stages and are similarly loaded, the calibration results derived from one filter are assumed to be valid for other filters showing similar behaviours. For the model of nitrification in the second filtration step, several consecutive run cycles are considered.

The periods are:

I. For primary filters with high ammonium removal:

- **Calibration case 1.1:** short-term operation (FF-07) between backwash events.
- **Calibration case 1.2:** start-up period (FF-07) after filter material replacement.
- **Calibration case 1.3:** start-up period (FF-08) after filter material replacement.

II. For primary filters with poor ammonium removal:

- **Calibration case 1.4**: long-term operation (FF-05) of fully loaded filter with reduced capacity.
- **Calibration case 1.5**: long-term operation (FF-05) of half-loaded filter with reduced capacity.

III. For primary filters with both high and poor ammonium removal:

- **Calibration case 1.6**: long-term operation (FF-05) through all four life stages (stages -1, 0, 1 and, 2).

IV. For the second filtration step filters:

- **Calibration case 2.1:** long-term operation (FK-05).

The characteristics of each calibration period are summarized in Table 17.

Table 17 Calibration cases

CALIBRATION CASE	1.1	1.2	1.3	1.4	1.5	1.6		2.1
Filtration step	First							Second
Origin of data-set	FF-07	FF-07	FF-08	FF-05	FF-05	FF-05		FK-05
Filter performance	High ammonium removal	Start-up after renew al	Start-up after renew al	Poor ammonium removal	Poor ammonium removal	Start-up after external w ashing	Relapse of nitrification	High ammonium removal
Duration	Short-term	Long-term	Long-term	Long-term	Long-term	Long-term		Long-term
Comments	Single run cycle betw een backw ash events				Half-loaded	Life cycle betw een external w ashing events		Several consecutive run cycles

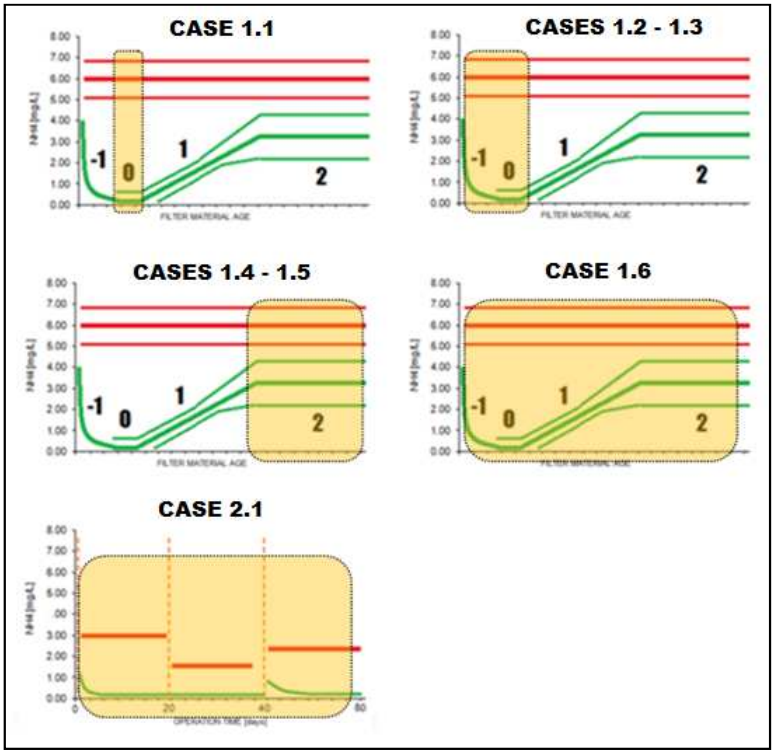

Figure 50 Calibration cases

Calibration approach

Although the calibration periods are presented here consecutively, the calibration process has been in reality iterative: after each new calibration, the calibration values for the other periods have been either reviewed or adjusted with the objective of identifying those values that are equally valid for as many periods as possible. Although it will be shown later, this approach has resulted on assuming that the growth rate is independent on the calibration period while the biomass content and the effective decay rate vary. This assumption is, in principle, as valid as the complementary option: keeping fixed the decay and varying the growth rate. Actually both options respond to the same idea: the need to build a model in which the net growth rate of microorganisms varies accordingly to both the observed full-scale and internal measurements.

Model variables initialization

To start the iterative calibration process, initial values are needed for all the derived state variables.
In general, the initial conditions of the model are the water quality and the biomass content within the filter. All the scenarios defined above start after any cleaning activity. For those scenarios starting after backwashing, the initial values will correspond to clean water. For those scenarios starting after external washing or filter renewal, standard raw water values have been chosen as initial values. Table 18 summarizes the standard values for both cases. The initial biomass content has been

excluded from this table since it depends on each scenario and due to dual nature of this factor: it is at the same time a state variable and an internal model parameter.

Table 18 Initial values for model state variables

Parameter	Units	Backw ash w ater	Raw w ater	Air
Oxygen	[mg O2/L]	10.00	0.00	280.00
Carbon dioxide	[mg CO2/L]	4.00	23.00	0.40
Bicarbonate	[mg HCO3-/L]	90.00	230.00	-
Ammonium	[mg NH4+/L]	0.01	5.00	-
Ortho-phosphate	[mg P/L]	0.05	2.00	-

Assessment of the goodness of calibration

Simulation results are calculated and compared to the measured ammonium concentrations in the effluent in the same time period. The accuracy of the model has been assessed according to the fitting between the measured and the calculated effluent ammonium concentration. The parameter used has been the coefficient of determination. The most general definition of the coefficient of determination is:

Equation 54

$$R^2 = 1 - \frac{\sum_i (f_i - y_i)^2}{\sum_i (y_i - \bar{y})^2}$$

In the above shown expression:
y_i : measured effluent ammonium concentrations.
$\bar{y}$: mean of the measured effluent ammonium concentrations.
f_i : modelled effluent ammonium concentrations.

The variability of the data set is assessed through the sums of squares. The numerator stands for the sum of the squares of residuals and expresses the accuracy of the model fits. The lower this value is, the better the prediction results. It penalizes the big discrepancies by giving them a heavier weight in the sum. The denominator is a scaling factor which is proportional to the sample variance.

Calibration case 1.1

This case represents the typical behavior of a dual media bio-trickling filter with high ammonium removal along one run cycle (3 days in the figures below). Figure 51 and Figure 52 correspond to one of these filters and clearly illustrate the typically behavior: at first there is observed a kind of ripening period (hours 0-30); following, the performance slightly improves (hours 30-36) and complete ammonium removal is achieved (hours 36-72). Simultaneously to the decrease in the ammonium concentration of the effluent the pH slightly increases.

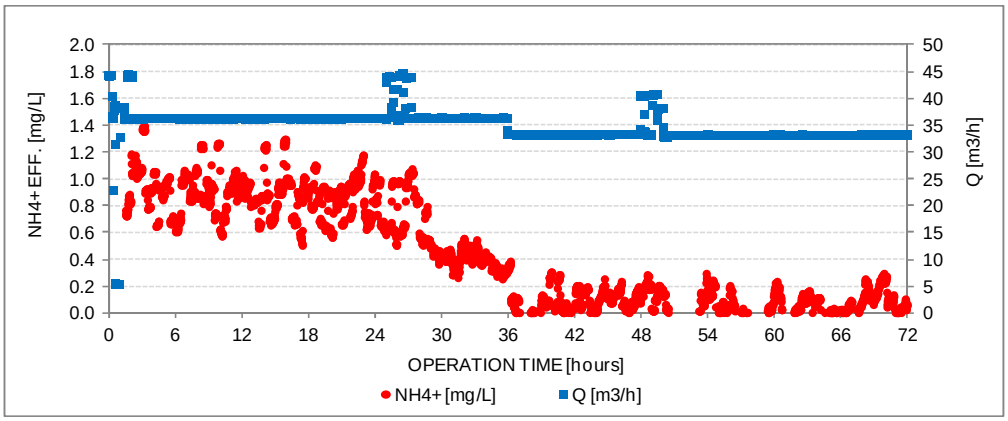

Figure 51 Calibration case 1.1: continuous effluent ammonium concentration and flow in primary filter with high nitrification

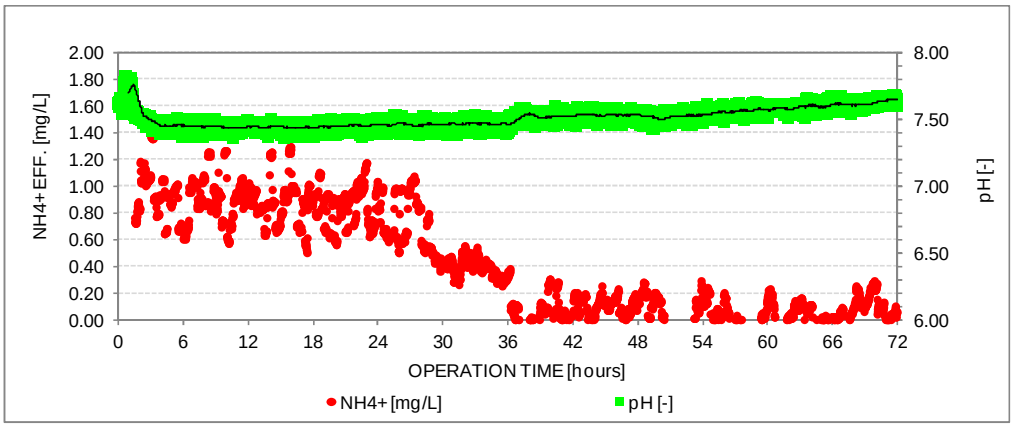

Figure 52 Calibration case 1.1: continuous effluent ammonium concentration and pH in primary filter with high nitrification

With the exception of the flow rates, which have been taken from available continuous measurements, the raw water quality has been estimated based on the available weekly samples taken about the same dates. All the values the model has been charged with can be found in Annex A.13.

The parameter set has been calibrated by trial and error in order to achieve the best possible fit. The results are shown in Figure 53, where both the measured and the simulated ammonium concentration in the effluent are plotted, and in Table 19, where the resulting model parameter values are given.

Table 19 Calibration values for case 1.1

Parameter	Units	Value
Max. grow th rate	[1/s]	2.40E-06
Decay rate	[1/s]	4.63E-08
Initial biomass content	[g DM/m3]	31.50

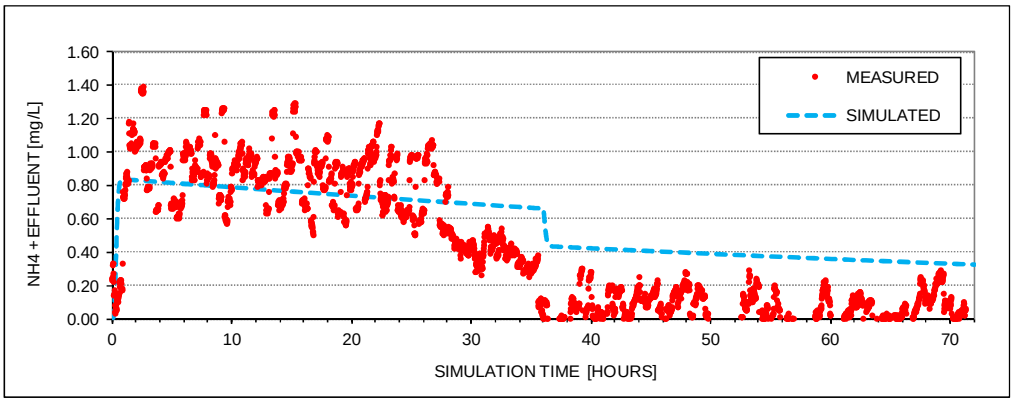

Figure 53 Simulation results for calibration case 1.1.

The goodness of the fitting is poor, $R^2 = 0.44$, due to two aspects that the model does not reproduce properly: (1) the fluctuations in the measured ammonium effluent concentration; and, (2) the significant decrease in the ammonium concentrations occurring between hours 28 and 36. Both events may have been caused either by internal or external causes (changes within the filter or changes in the influent conditions, respectively). Since only the flow but not the influent ammonium concentration was continuously monitored, it has not been possible to elucidate where the origin for such features might be. This issue is of interest because if the first option is the reason for those changes, then the model would need further improvement while if the second option is the cause, then that would indicate that there is nothing wrong with the model rather than it has not been properly loaded.

Calibration cases 1.2 and 1.3

These two scenarios represent the start-up period observed in the filters after replacement of the bed material as described in Section 2.3.2. During the start-up period with new-filter material, microorganisms multiply until they form a sufficiently large population able to remove all ammonium. Consequently, it is reasonable to assume that the content of ammonia-oxidizing organisms is low or very low in the early days of operation. This lower uncertainty around the initial biomass content has

not necessarily resulted in an easier calibration if compared to the previous scenario. In fact, the difficulty has been similar since this time there is greater uncertainty concerning the effective decay rate value as the simulation period is much longer than in the previous calibration case. Full-scale measurements (see Figure 54 and Figure 55) indicate that the start-up process took approximately 4-6 months. Since these scenarios represent the filter long-term response after filter material renewal, they can be used to investigate the process of stratification of the nitrification activity as well. For simplicity purposes and due to the extension of the study period, the raw water characteristics the model has been charged with have been averaged. The taken values are shown in Annex A.13.

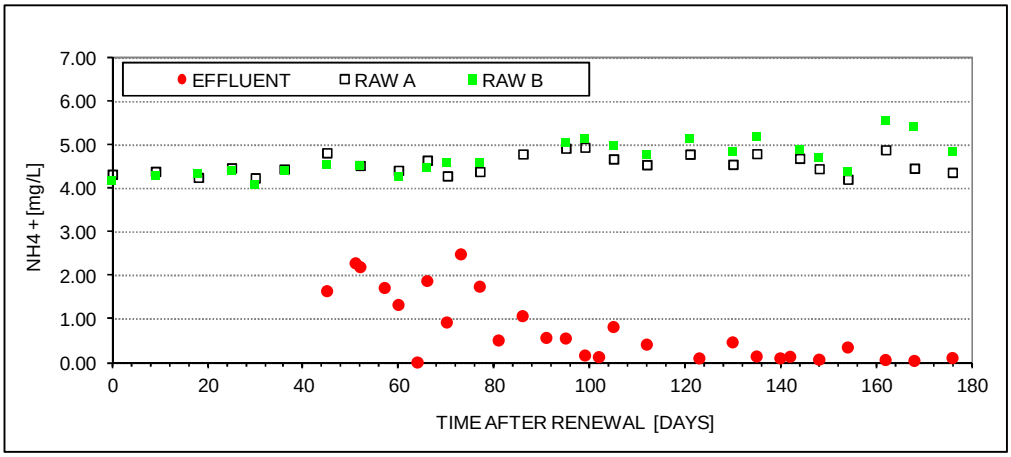

Figure 54 Calibration case 1.2: influent and effluent ammonium concentrations in primary filter (FF-07) after material renewal

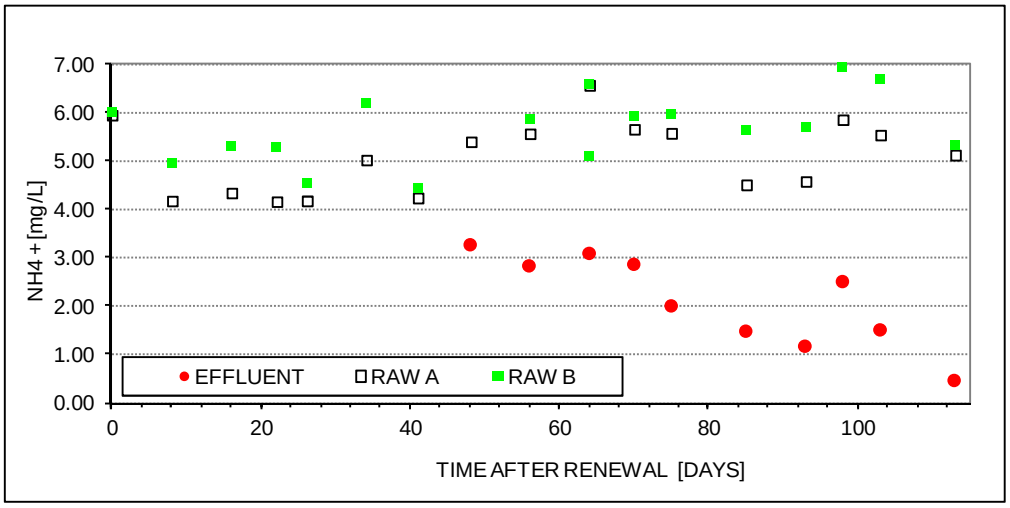

Figure 55 Calibration case 1.3: influent and effluent ammonium concentrations in primary filter (FF-08) after material renewal

During model calibration, it turned out that the model can be calibrated for both cases by using very similar values, whose average values are given in Table 20.

Table 20 Calibration values for cases 1.2 and 1.3

Parameter	Units	Value
Max. grow th rate	[1/s]	2.40E-06
Decay rate	[1/s]	5.63E-07
Initial biomass content	[g DM/m3]	5.00

The calibration results are plotted in Figure 56 and Figure 57. The fitting is considered as acceptable, taken into account the fluctuation of the influent ammonium concentration. The resulting fitting is $R^2 = 0.66$ and $R^2 = 0.43$ for cases 1.2 and 1.3, respectively.

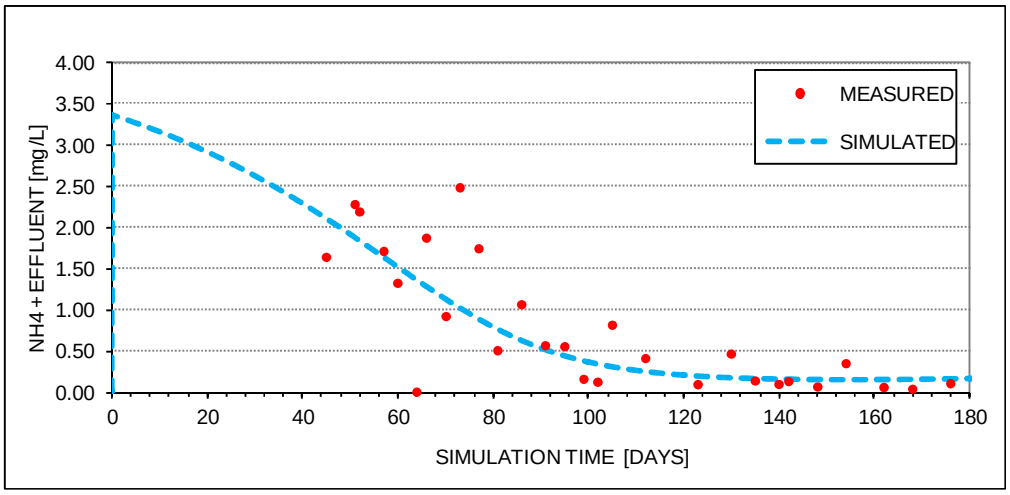

Figure 56 Simulation results for calibration case 1.2

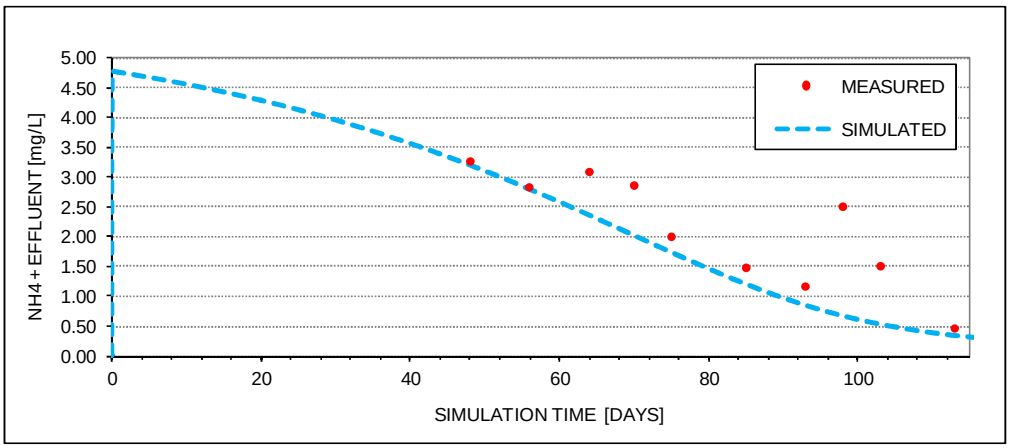

Figure 57 Simulation results for calibration case 1.3

It is seen that the decay rate takes a higher value than in the previous scenario. This is because this time the decay does not only represent natural biomass loss processes such as decay and desorption due to shear forces during normal operation (as in Scenario 1.1) but also biomass wash-out during backwashing.

The results also suggest that the start-up period is strongly conditioned by the natural growth dynamics of nitrifiers and the processes counteracting that growth (decay, desorption, washout) but what makes the difference from one case to another must be either the initial biomass content, the loading over the time or both of them. Figure 58, which shows the evolution of the biomass content for scenarios 1.2 and 1.3, illustrates this idea.

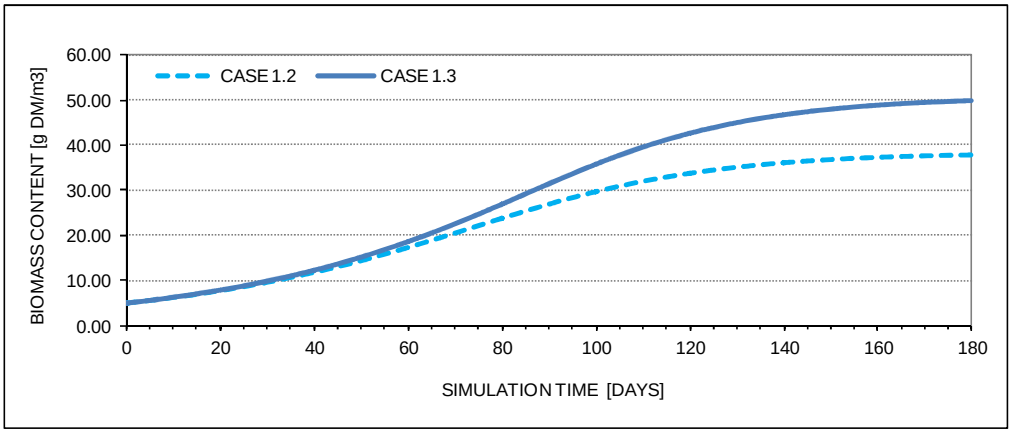

Figure 58 Simulated content of nitrifying biomass for calibration cases 1.2 and 1.3

If the model is run long enough it can be checked when the system achieves steady-state. For the case 1.3 the system achieves complete ammonium removal after 4.6 months and the average biomass content reaches a maximum of around 51 g/m^3. For the case 1.2, the system achieves complete ammonium removal also after 4.6 months of operation but the average biomass content stabilizes at a lower value: 37 g/m^3. Assuming that the initial biomass content and the factors counteracting growth are similar between filters, the differences in the final (steady state) ammonia-oxidizing population are though to be mainly caused by differences in the supply of ammonium (load): in average, 210 g NH_4^+/h and 161 g NH_4^+/h, respectively.

In reality, the initial biomass content chosen is just an approximation. The value represents the amount of nitrifiers present in the filter when it returns to operation. The size of the ammonia-oxidizing organisms community at that moment may have two different origins: (1) microorganisms that are naturally present in the new filter material; and, (2) nitrifiers naturally present in the aquifer that are inoculated into the system when it returns to operation.

There is evidence (De Vet, 2011) that in filters with high nitrification activity the activity is mainly concentrated in the upper and upper-intermediate layers. The model shows the same (see Figure 59): the ANO population, which was assumed to be originally uniformly distributed over the different CSTRs, stratifies with time.

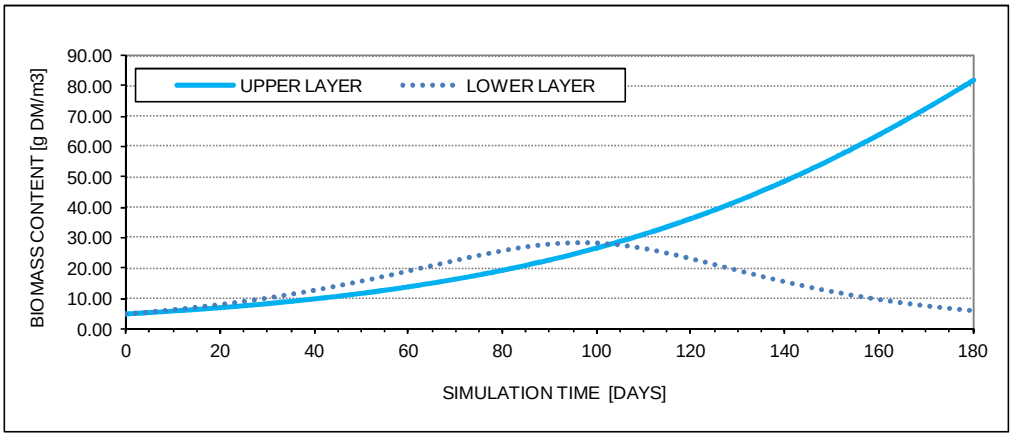

Figure 59 Simulated content of nitrifying biomass at the top and bottom layers of the filter for calibration case 1.2

Ideally, the goodness of the calibration should be supported not only by external but also by internal measurements. Apart from the ammonium concentration in the effluent, there are other parameters that can be used to have a better impression of the goodness of calibration. Those parameters give direct information on the specific biological activity within the filter. These parameters are presented in Annex A.11. Unfortunately, the existing measurements just provide a certain order of magnitude for Tiendweg filters with poor ammonium removal and, consequently, are not applicable to these calibration cases.

Calibration cases 1.4 and 1.5

These cases corresponds to the last stage observed in the lifecycle of primary filters, when the filter filters has lost a significant part of its removal capacity (30-60% according to the values reported in Section 4.1). Figure 60 shows the measured values for these cases. There are two sub-periods (case 1.4 and 1.5, respectively), for which the loading conditions differ significantly. In the first period-case (days 0-165), the filter was fully loaded. In the second period-case (days 165-420, with interruptions) the raw water was mixed (ratio 1:1) with clean water so that although the hydraulic load was still the same, the ammonium load was halved. Consequently, the effluent ammonium concentrations improved. The specific values the model is charged with are shown in Annex A.13.

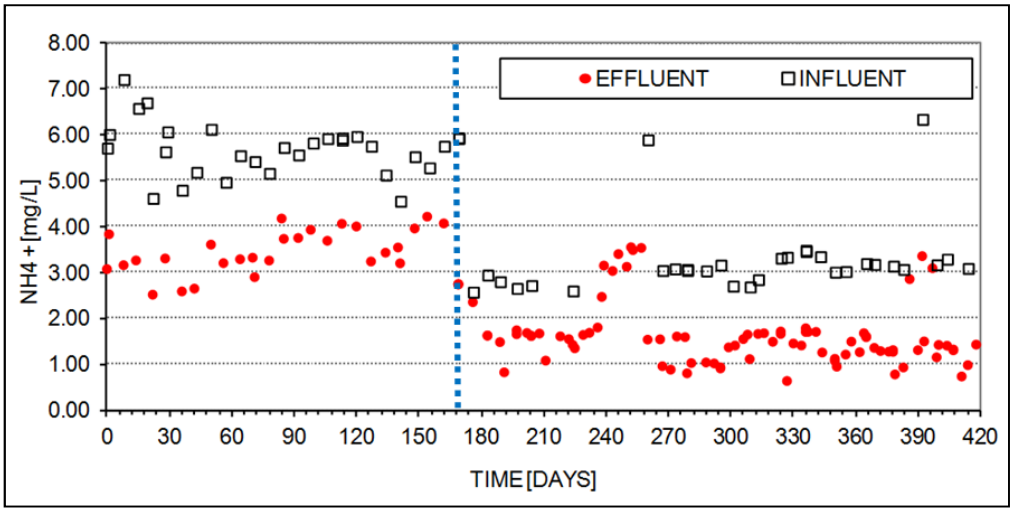

Figure 60 Calibration cases 1.4 and 1.5: influent and effluent ammonium concentrations in primary filter with poor nitrification full (case 1.4) and half-loaded (case 1.5)

The two cases are calibrated together since they correspond to the same filter and there is interesting on seeing whether the same or very similar calibration set is valid for cases. The simulation results are shown in Figure 61 while the resulting values for the model parameters are given in Table 21. The goodness of the fitting for both periods is moderate-high: $R^2 = 0.75$.

Table 21 Calibration values for cases 1.4 and 1.5

Parameter	Units	Case 1.4	Case 1.5
Max. growth rate	[1/s]	2.40E-06	2.40E-06
Decay rate	[1/s]	9.00E-07	6.75E-07
Initial biomass content	[g DM/m3]	13.00	-

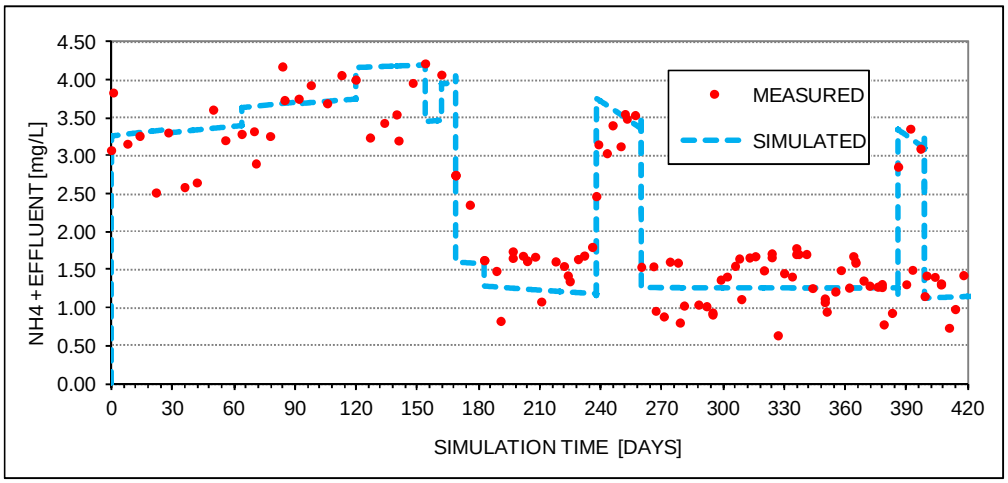

Figure 61 Simulation results for calibration cases 1.4 and 1.5

It is important to highlight that the effective decay rate needed to be adjusted for the second sub-period (case 1.5). This suggests that filters which are loaded differently during long time periods may need different calibration values than those ones determined according for the current loads.

The model results suggest that the change in the calibration value for the effective decay rate has consequences on the biomass content of the filter over the time. Figure 62 shows the evolution in time of the biomass content according to the model.

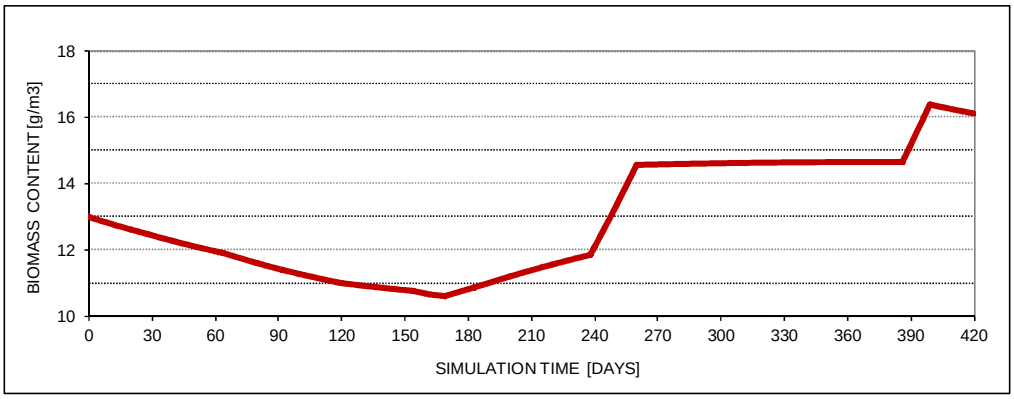

Figure 62 Simulated nitrifying biomass content for calibration cases 1.4 and 1.5

Although the best fitting is achieved with 13 g/m^3 as initial biomass content, the model results indicate that the active biomass content varies between 11 and 16 g/m^3 over the entire simulation period, suggesting that the system operates within a kind of pseudo-steady state despite its reduced nitrification activity**.**

It is necessary to notice that in this case the biomass content is much lower than the cases representing full ammonium removal (cases 1.1 and end of cases 1.2 and 1.3): 11-16 g/m^3 versus 31.50 g/m^3, 51 g/m^3 and 37 g/m^3, respectively. This means that the lower nitrification activity is mimicked in the model through a reduction of the active biomass content, rather than by using an entirely different set of biological kinetic parameters.

Accordingly, when considering only the first sub-period (case 1.4, days 0-160) it can be seen that the biomass content decreases which indicates that the process of relapse in nitrification continues (although at a lower rate than originally) as some internal measurements of sand-specific nitrification rates show (see Annex A.11).

The results also suggest that the decrease in the active biomass content (and therefore in the nitrification capacity of the filter) is counteracted by operating the filter at lower loads. Furthermore, the results also insinuate that the trend may even be reversed provided that the filter is operated in such a way that long periods of low loads are alternated with short periods of high loads. If these hypotheses are confirmed in the reality either through full-scale or column experiments this would imply the existence of a relationship between load and the rate of relapse in nitrification.

Calibration case 1.6

This scenario represents the typical response of primary filters after being externally washed. The filter goes through four life stages (stages -1, 0, 1 and, 2) as defined in Section 4.1 and combines periods of high and low nitrification activity. The full scale measurements are shown in Figure 63.

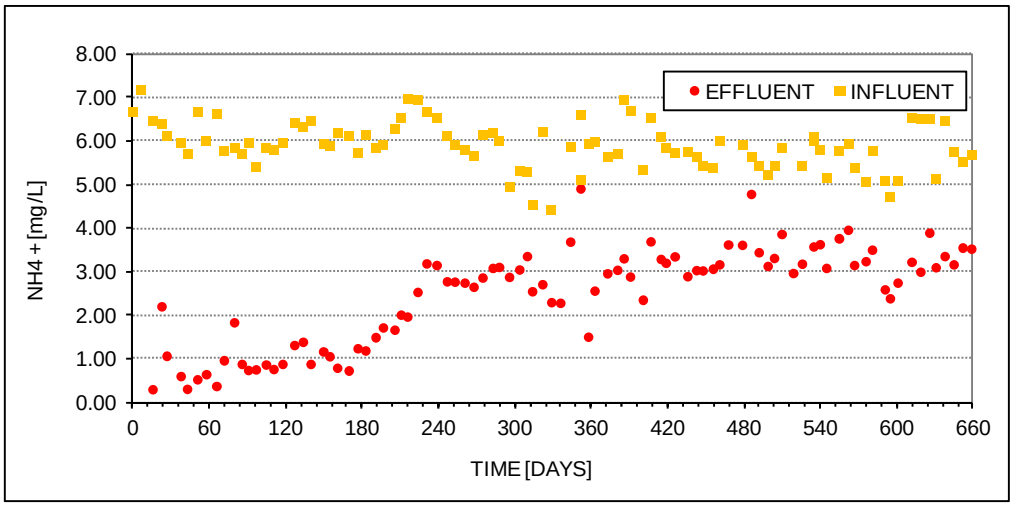

Figure 63 Calibration case 1.6: influent and effluent ammonium concentrations in primary filter over its entire life cycle

The calibration results are shown in Figure 64. The goodness of the fitting is moderate: $R^2 = 0.61$.

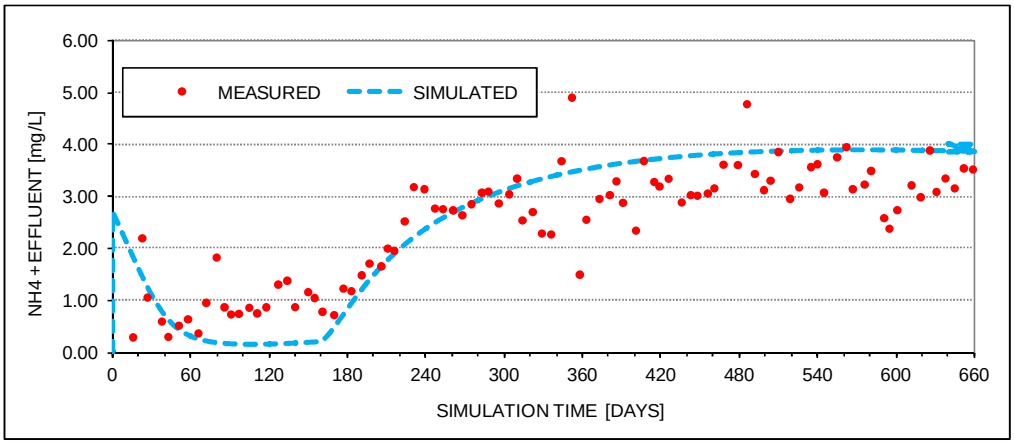

Figure 64 Simulation results for calibration case 1.6

Since this scenario is a combination of some situations for which the model has been previously calibrated, the same calibration values should theoretically provide satisfactory results as it happens. The only difference between this and the previous scenarios is the initial biomass content which takes an intermediate value (20 g/m^3), between the values for filters representing full (above 30 g/m^3) and incomplete nitrification (13 g/m^3). The resulting values from calibration are shown in Table 22.

Table 22 Calibration values for case 1.6

Parameter	Units	Stages -1 and 0	Stages 1 and 2
Max. grow th rate	[1/s]	2.40E-06	2.40E-06
Decay rate	[1/s]	5.60E-07	8.60E-07
Initial biomass content	[g DM/m3]	20.00	-

It is important to highlight that in the transition from stage 0 to stage 1 (day 160), the value for the effective decay rate needed to be adjusted. It has not been possible to find a correlation that allows predicting when the turning point occurs. Figure 65 shows the evolution of the active biomass content according to the model. It can be clearly shown how adjustment of the decay rate strongly modifies the trend.

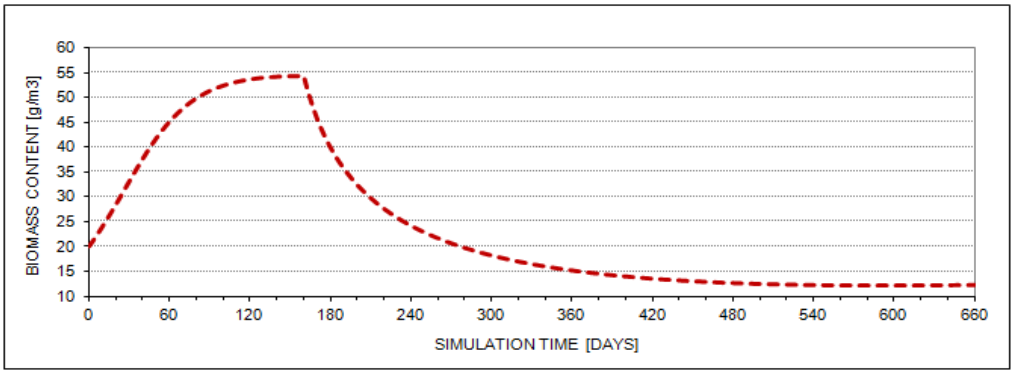

Figure 65 Simulated nitrifying biomass content for calibration case 1.6

Calibration case 2.1

Figure 66 illustrates several consecutive cycles in one filter in the second filtration step. The influent conditions are given by the ammonium concentration in the effluent of the corresponding primary filter. The specific influent conditions the model has been charged with are given in Annex A.13.

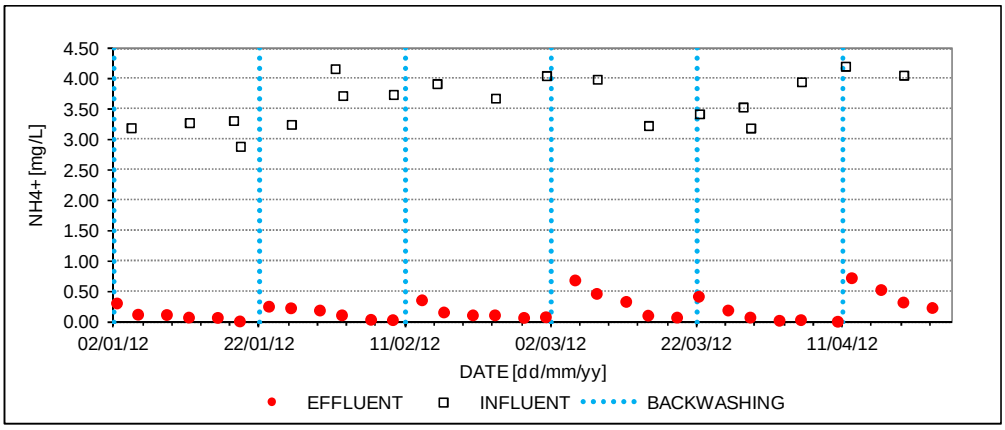

Figure 66 Calibration case 2.1: influent and effluent ammonium concentrations in secondary filter

There is one significant difference between the model developed for secondary filters and the model developed for primary filters. In the first case, backwashing is modelled independently with an independent module. That means that in this model the parameter representing the decay rate does not include the loss of biomass due to washout during backwashing. Alternatively it has been assumed that after each backwashing event, the biomass content returns to the initial value at the beginning of the cycle. That assumption has provided the calibration results shown in Figure 67. The fitting is good, $R^2 = 0.82$, and consequently it is concluded that the model is able to simulate reasonably well ammonium breakthrough for the different loading conditions in secondary filters.

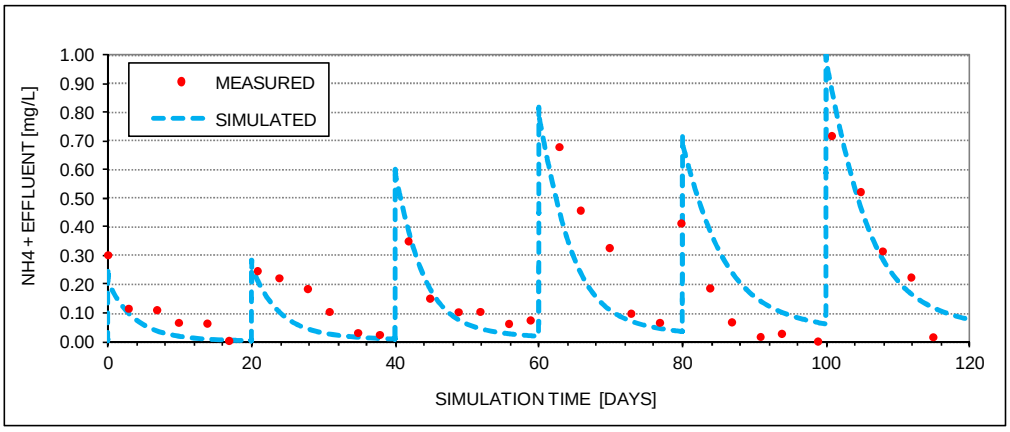

Figure 67 Simulation results for calibration case 2.1

The calibration values are shown in Table 23:

Table 23 Calibration values for case 2.1

Parameter	Units	Value
Max. grow th rate	[1/s]	3.40E-06
Decay rate	[1/s]	4.63E-08
Initial biomass content	[g DM/m3]	15.00

The value for the effective decay rate is the same than in the first calibration case (case 1.1). For the initial biomass content, the chosen value is such that the final value equals the initial value: 15 g/m^3. The growth rate is higher than in all the cases for the model of primary filters. This is explained as linked to the fact that nitrification does not relapse in these filters and, therefore, no processes wither inhibiting or reducing the specific growth rate are likely to occur in these filters. The air-water flow ratio value has been adapted to this specific case accordingly to the site-specific values reported at Table 16. The other model parameters have received the same values than in the previous calibration cases.

4.4 Model validation

During the validation phase the models previously calibrated are tested. The test is done with an independent data set. Filters FF-05 and FK-05 at WTP Lekkerkerk have been chosen to generate that data set. This is because of two reasons. On the one hand, these filters are the only filtration units where the loading conditions can be widely varied independently from the well scheme. This is due to the fact that the feed water in this set is mixed with permeate water from a nearby reverse osmosis installation, as explained before (see Paragraph 2.3.2). By controlling the mixing ratio it is possible to operate this set under different loads. This is a very attractive possibility for validation since the model is aimed at predicting the response of the system when being operated at different loads. A general scheme of the set is shown in Figure 68. On the other hand, filter FF-05 shows a reduced nitrification capacity. Consequently, the validation experiments will contribute to assess the reliability of the model used to simulate the response of filters that work badly which are, by the way, those ones whose response is more unpredictable according to Section 4.1.

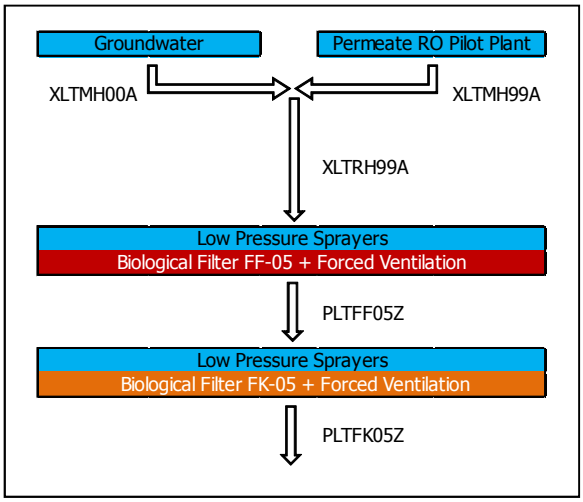

Figure 68 Setup of the filtration set selected for model validation experiments and sampling points

Experiments

The data acquisition experiment has lasted for 21 days and has comprised three different sub-periods of experiments each of which has been characterized by different loading conditions. Experiment 1 goes from day 0 to day 6; experiment 2, from day 7 to day 16; and, experiment 3 comprised the days 17 to 21. The planned values for each period are summarized in Table 24.

Table 24 Planned load conditions for validation experiments

Period	Days	Flow [m3/h]	NH4+ Inf. [mg/L]	Load NH4+ [g/h]
1	0-6	50.00	2.50	125.00
2	7-16	25.00	5.00	125.00
3	17-20	50.00	3.50	175.00

Figure 69 shows the actual conditions according to the regular samples taken which have slightly differed from the original plan.

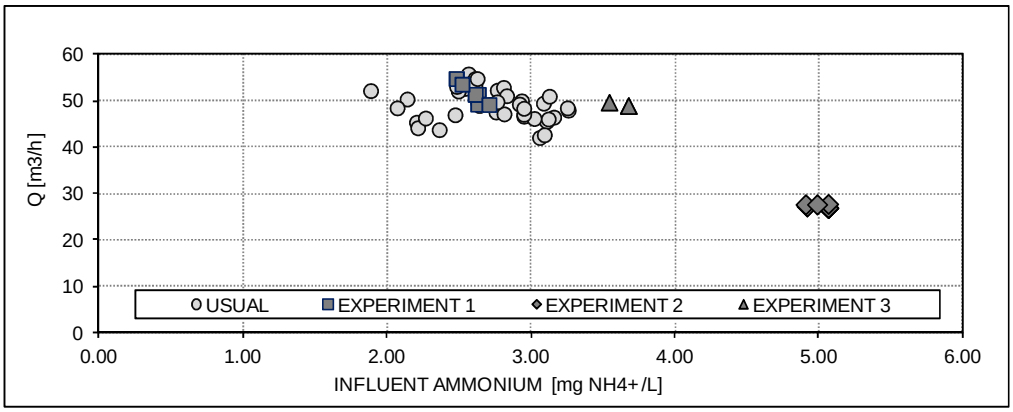

Figure 69 Load conditions in filter FF-05 during normal operation and validation experiments

According to Figure 69, the loading conditions of the second and third experiments have differed from the usual conditions the set is operated at on purpose while the loading conditions during period 1 resembled the usual conditions. More specifically, during the second period, the influent ammonium concentrations were higher than usual while the flow was lower. During the third period the flow rates were similar to the standard values while the influent concentrations were slightly higher.

Besides applying different loads, the experiments also included the performance of backwashing in order to acquire a deeper understanding of its impact. Backwashing was performed two times in the primary filter (in the first period at day 2.57 and, in the second period at day 15.57) and once in the secondary filter (in the second period, at day 16.57).

Results of the validation experiments in the primary filter

Figure 70 shows the results of the experiment for the primary filter. The measured ammonium concentrations in the effluent are the dots in the plotting space, whose range of values is represented in the vertical axis on the left. The x-axis shows the time. Five measurements correspond to the first experiment, eight for the second and two for the third. The extent of each period-experiment is indicated on the horizontal axis to enhance a better understanding of the results. The average loading conditions, removal and effluent concentration during each experiment are given in Table 25. The complete data series can be found in Annex A.15.

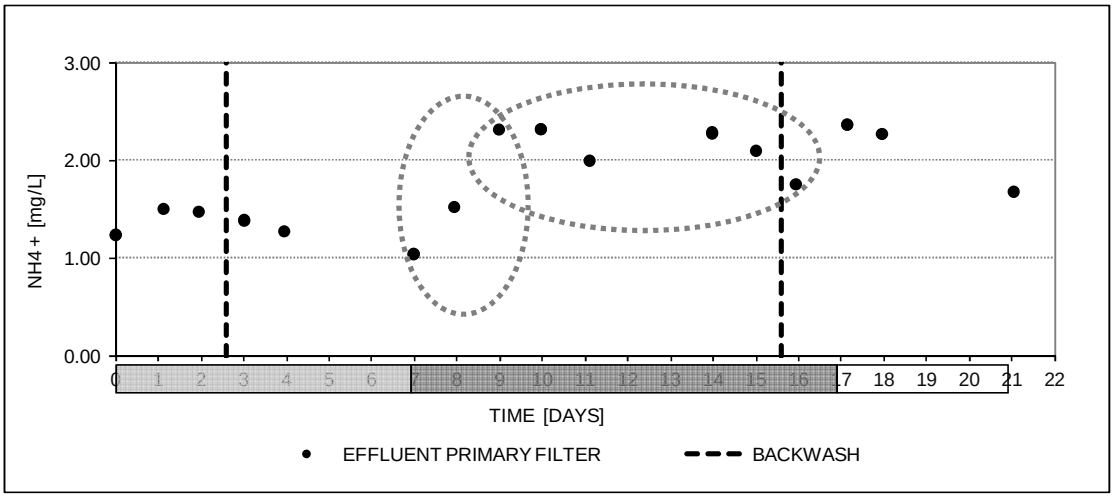

Figure 70 Effluent ammonium concentrations in primary filter during validation experiments

Table 25 Average load conditions, removal rate and effluent ammonium concentration in the primary filter during validation experiments

Experiment	Time [day]	Flow [m3/h]	NH4+ Inf. [mg/L]	Load NH4+ [g/h]	Removal NH4+ [g/h]	NH4+ Eff. [mg/L]
1	0-6	51.92	2.59	136.71	62.18	1.36
2	7-16	27.35	5.00	136.82	84.70	1.91
2, transitory excluded	9-16	27.49	4.98	136.86	77.37	2.17
3	17-20	49.35	3.61	178.11	63.95	2.33

Based on these results, there are several aspects to be highlighted:

1. Surprisingly the response did not worsen after backwashing (days 2.7 and 15.7). There was not ammonium breakthrough as originally expected. By contrast, the effluent concentration followed the same trend than it had before backwashing which suggests that the nitrification capacity was not substantially altered.
2. In spite of applying the same ammonium load (on average, 136.80 g NH_4^+/h) in periods 1 (days 0 to 6) and 2 (days 7 to 16), the filter response was very different. At first, there were lower effluent concentrations and ammonium removal rates (on average, 1.36 mg/L and 62.18 g NH_4^+/h respectively) while later the higher removal rates achieved (84.70 g/h on average) did not were enough to compensate the increase in the load. This resulted in higher effluent concentrations (1.91 mg NH_4^+/L, on average). This points the possibility that filters respond differently to the same ammonium load depending on the influent ammonium concentration and flow.
3. What seemed to be a kind of transitory period occurred at the beginning of experiment 2 (days 7 to 9) followed by what seems to be a new steady state (days 7 to 16) with the concentrations fluctuating around 2.17 mg NH_4^+/L. This is a different steady-state than during experiment 1, when the concentrations fluctuated around 1.3 mg NH_4^+/L.
4. In period 3 (days 17 to 20), the load was increased significantly (from 136.80 to 178.11 g NH_4^+/h) but the effluent concentration did not accordingly. Indeed, the measured effluent concentrations (2.33 mg NH_4^+/L, on average) were within the same range than the values registered during the second experiment after the transient. Furthermore, there seemed not to be a transition period in this occasion.

Before showing the results corresponding to the secondary filter, some further analysis is done around the observed behaviour in the primary filter:

- The results of the first experiment suggest that primary filters with low nitrification activity would provide better results (lower ammonium concentrations in the effluent) when operated at higher flows but lower influent concentrations.
- During the second experiment the nitrification capacity improved despite the fact the ammonium load was the same. Since the velocity in dry filters is thought to be flow-independent, the higher removal rate observed must have other causes rather than longer residence times. The hypotheses are: (1) the wetting improves with lower flows; and, (2) higher concentrations enhance the biological activity.
- Moreover, the increase in the capacity of the filter during the second experiment suggest that the critical loading in dry filters might be insufficiently characterized by the ammonium loading rate as the filter performed differently despite the same load was applied. Other parameters such as the ammonium load per unit of (effective) external surface area should be investigated.
- Primary filters are less exposed to the negative effects of backwashing (ammonium breakthrough) when having low nitrification. This behaviour opposes to the behaviour observed in some primary filters with high ammonium removal (see Figure 17). This discrepancy could be related to the different stratification of the nitrification activity in both types of filters (see Section 4.2). Concerning this, the general model assumption is that backwashing is not influencing the stratification of the biomass content of the filter at any case which could not be true in filters with high nitrification activity.
- The typical fluctuations observed in the effluent of primary filters with poor nitrification may not be caused exclusively by changes in the influent as the influent conditions in this case were controlled and relatively stable. Thus it is necessary to think on internal reasons. In that respect, there is neither a clear explanation around the existence/inexistence of transitory periods in the different experiments. This suggests the existence of other processes which are neither known nor modelled.

All these results advocate for new future experiments. A more complete data conformed by continuous measurements both in the influent and effluent could be used to characterize better the transient behaviour and the critical loading of primary filters at different loading conditions. Moreover, the new data-set would help to establish whether nitrification is mass transfer or kinetically limited. The measurements could be grouped in two families in order to study at which situation ammonium breakthrough happens: either with the same flow rates but changing ammonium concentrations or with a fixed influent concentration but different flows.

Moreover it is recommended that future studies incorporate a greater focus on the different time scales of the processes occurring in bio-trickling filters since the existence of processes with different time-scales may be behind the occurrence of transitory periods: biomass growth occurs at time scales in the order of hours-days while substrate diffusion and hydrodynamic processes are in the order of seconds to minutes (Henze, 2008).

Results of the validation experiments in the secondary filter

Concerning the second filtration step, Figure 71 summarizes the observed influent and effluent conditions. The axis on the left is for the effluent ammonium concentration. The vertical axis on the right corresponds to the ammonium load (ranging from 25 to 120 g NH_4^+/h). The measurements cover more than one operation cycle (20 days), existing 5 measurements before backwashing and 2 after. The complete data series can be found in Annex A.15.

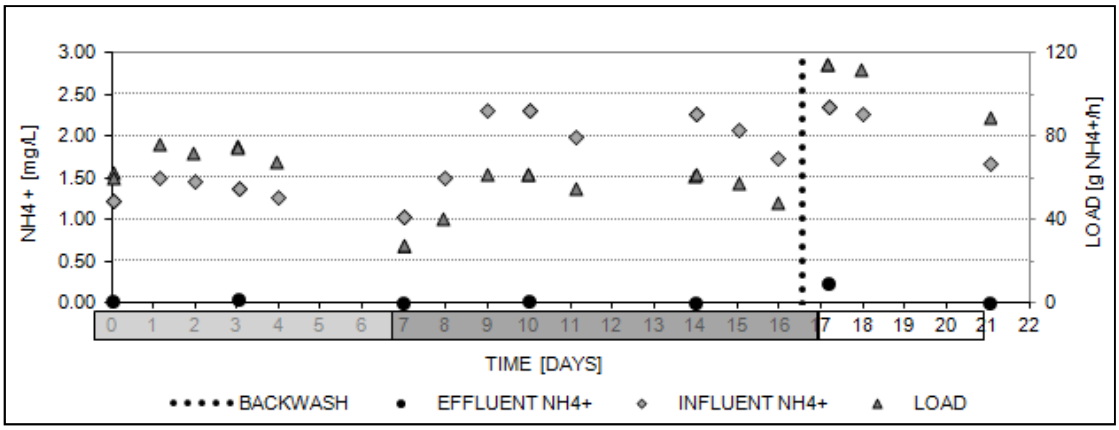

Figure 71 Influent load and influent and effluent ammonium concentrations in secondary filter during validation experiments

The observed results reproduce the typical behaviour described for secondary filters in Section 2.3.2. Full nitrification is achieved most of the time before backwashing (there is complete ammonium removal between days 0 to 16). Ammonium breakthrough was temporarily registered after backwashing of the filter at day 16.5 (0.23 mg NH_4^+/L were measured the day 17). After some time, complete ammonium removal was achieved again as the last available measurement (day 21) indicates.

Model validation

Since the filters have been operated part of the time at loads different to the usual ones, the validation process can be seen as having a double purpose: first, to elucidate if the calibration resulting from certain loading conditions is able to provide good results when the model is operated at loads for which has not been calibrated; and, second, to assess under which of these different loading conditions, the models perform better and worst.

The model used for validation comprises two sub-models in series representing each filtration step. Each model has received the same model parameter values than in the closest calibration period: 1.5 for the model of the primary filter and 2.1 for the model of the secondary filter. The duration of the validation experiments is 22 days which is significantly shorter than most of the periods considered during model calibration in Section 4.3. Since the validation experiment included two backwashing events in the primary filter, it seems reasonable to think that the value for the effective decay rate will remain being valid. The values are shown in Table 26.

Table 26 Calibration values used during model validation

Parameter	Units	FF	FK
Max. growth rate	[1/s]	2.40E-06	3.40E-06
Effective decay rate	[1/s]	6.75E-07	4.63E-08
Initial biomass content	[g DM/m3]	13.00	15.00 (*)
(*): after backwashing			

For the model of the secondary filter, the calibration value for the biomass content refers to the value after backwashing. Since the validation experiment started a few days after backwash was performed in the second filtration step, the biomass content is adjusted accordingly.

The simulation results are shown in Figure 72 (model of the primary filter) and Figure 73 (model of the secondary filter). In these figures, the ammonium concentration in the effluent is show on the vertical axis on the left side. The dots represent the measured ammonium concentration in the effluent while the line corresponds to the simulated concentrations. The dotted vertical lines indicate the times when backwashing was performed.

Based on the results shown in Figure 72 it can be concluded that the model for the first filtration step provides good results for the first (days 0 to 6) and the third (days 17 to 20) experiments, which are the periods when the loading conditions where closer to the usual ones. By contrast, it provides worst results for the second experiment, when the filter was operated at significantly different conditions. More specifically, the model fails in predicting the transitory state observed between days 7 and 9 and the fluctuations occurring between days 9 and 16 despite the fact that the model result resembles the average value during the second period, excluding the transient. The goodness of the fitting has been calculated for the entire data set but also for each sub-period. Accordingly to this description, the best results correspond to the first and the third experiment with $R_{1st}^2 = 0.86$ and $R_{3rd}^2 = 0.72$, respectively. The lower coefficient of determination is for the second experiment: $R_{2nd}^2 = 0.30$. The overall result including all the three periods is moderate: $R^2 = 0.57$.

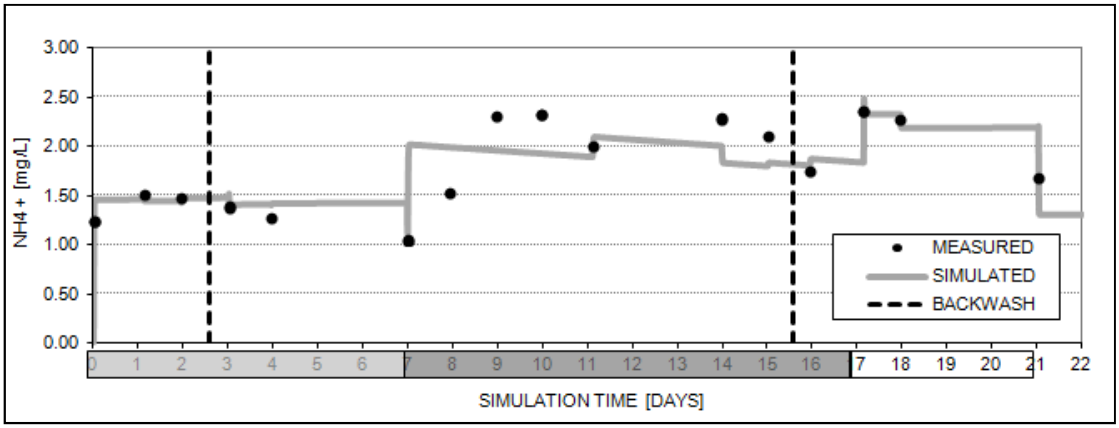

Figure 72 Simulation results during validation of model for primary filters with poor nitrification

Therefore, the model of primary filters with poor nitrification is more reliable at high flows (around 40-50 m^3/h) and lower ammonium concentrations than usual (around 2-4 mg/L) and less reliable when loaded with low hydraulic loads (around 30 m^3/h).

Concerning the second filtration step, the results are shown in Figure 73:

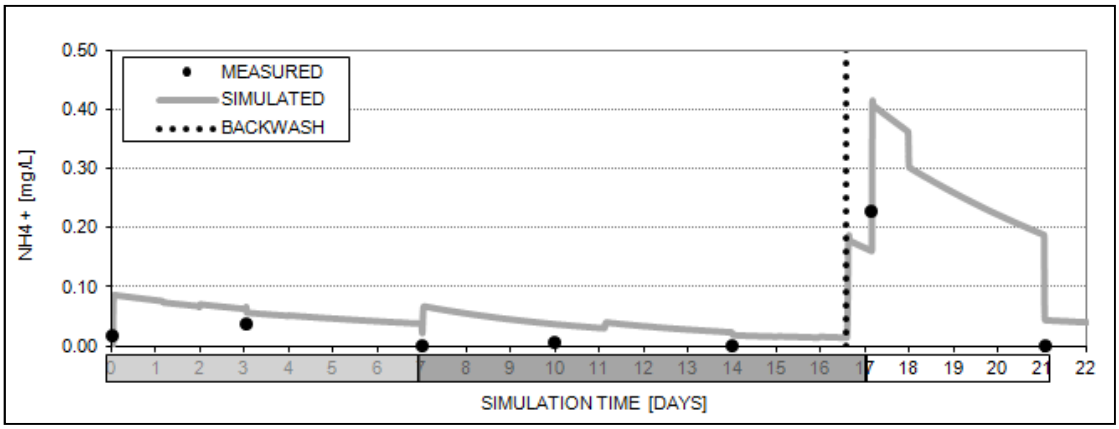

Figure 73 Simulation results during validation of model for secondary filters

Figure 73 indicates that the model is less accurate in predicting the response at high loads than at low loads. Whenever the load is below 90 g NH_4^+/h, the measured and the simulated effluent concentrations are mostly within the same narrow range (below 0.05 mg/L). Contrarily, the simulated value after backwashing is higher (0.40 mg/L is the peak value) than the measured concentration (0.23 mg/L). Therefore, the model provides slightly worse values than the observed. The goodness of the fitting is good $R^2 = 0.71$ but this value is not considered at all representative due to the fact that there is only one single value after backwashing available for validation.

Finally, the models can be used to illustrate how the population of nitrifiers evolves with time in each filter. The main two differences refer to the growth rate and the effect of backwashing. The simulated biomass content at each filter are shown in Figure 74:

- While the number of nitrifiers grows significantly in the secondary filter, the growth is very poor in the primary filter, despite the fact it receives a much higher load. This is consistent with the low nitrification activities reported in filters with poor ammonium removal, as discussed in Section 4.2.
- Backwashing have very different effects on both filtration steps: while it clearly affects the capacity of the secondary filter through biomass washout it does not modify significantly the number of active nitrifiers in the primary filter.

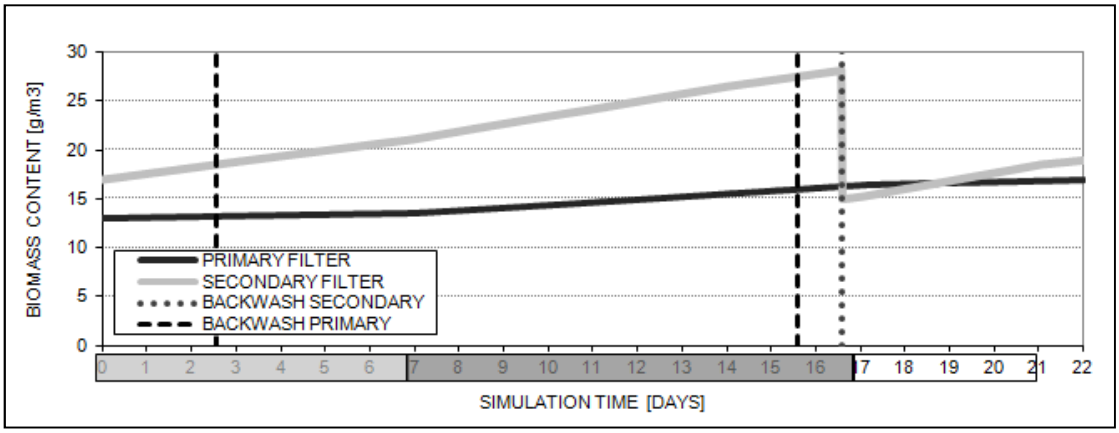

Figure 74 Simulated nitrifying biomass content in primary and secondary filters during model validation experiments

4.5 Sensitivity analysis

Once the model has been calibrated and validated, a sensitivity analysis has been performed. The parameters considered have been both internal and external. The overall goal is to evaluate and compare the impact of the different model parameters so that the parameters with the highest influence are identified. Concerning the internal parameters, the analysis has included those parameters that were excluded from the calibration sub-set defined in Section 4.3, paying special attention to those parameters whose calibration value was uncertain. With regard the external parameters, both some disturbance and manipulated parameters have been included as defined in Section 3.3. The parameters analyzed are:

- Internal model parameters:
  - Wetting efficiency.
  - Number of completely mixed reactors.
  - External mass transfer resistance (water velocity).
  - Mean residence time.
  - Effective decay rate.
  - Maximum growth rate.
  - Biomass content.
  - Yield factor for N.
- External model parameters:
  - Influent ammonium concentration.
  - Water flow rate.
  - Air-water flow ratio.
  - Backwashing program.

Since the sensitivity of the model predictions may depend on the operating conditions (Boltz et al., 2011) all the simulations have considered average operating conditions which are summarized in Table 6 and Figure 9: in short, 39 m^3/h and 5.10 mg NH_4^+/L. Unless the opposite is stated the analysis has been performed with the model of primary filters with low nitrification activity (calibration period 1.4 in Section 4.3). The reasons for that are that that is considered the most unfavourable situation and that one that asks for a deeper knowledge and understanding.

The impact of each parameter has been assessed individually: this means that the other parameter values have been kept fixed. The quantification of the impact has been based solely on the simulated effluent concentration. The results are expressed as percentages of variation of the effluent concentration. This means that a result of -40% means that the effluent ammonium concentration is 0.4 times lower than the effluent ammonium concentration given by the reference model.

Internal model parameters

Understanding of the processes controlling nitrification requires to 'translate' the changes observed in the macro-scale into changes in the micro-scale (Wik, 2003). The internal parameters can be grouped into two sub-groups: biological and mass-transfer related parameters. This means that, ideally, this analysis may provide new insights regarding the causes for poor nitrification since it is unknown if the decline in nitrification has a kinetic or transfer related origin. Strictly speaking these parameters are not directly changeable (as the operational parameters are) but this does not exclude the possibility that their relative importance might depend on the operation regime. Such aspect goes beyond of the performed analysis and it is recommended to be further developed in the future. The results for the internal parameters are given in Table 27.

Table 27 Sensitivity analysis for internal model parameters

INTERNAL PARAMETERS	0%	-40%	-20%	+20%	+40%
Wetting efficiency [%]	100.00	42%	21%	-	-
Number of completely mixed reactors [-]	5.00	0%	0%	0%	0%
External mass tranfer [m/s]	8.13E-05	0%	0%	0%	0%
Mean residence time [s] (*)	518.4	26%	11%	-13%	-26%
Effective decay rate [s^{-1}]	9.00E-07	0%	0%	0%	0%
Maximum grow th rate [s^{-1}]	2.40E-06	23%	11%	-15%	-26%
Initial biomass content [g DW/m^3]	13.00	23%	11%	-15%	-26%
Yield factor N [g DW/g NH_4^+-N]	2.90E-03	-39%	-16%	10%	16%

According to the results presented in Table 27 the following is concluded:

- **Wetting efficiency**: the results clearly confirm that incomplete wetting of the media would strongly limit the system performance as many authors have claimed (Logan, 1993). Once it has been demonstrated that clogging may have tremendous effects on the nitrification capacity of the filter, then two questions arise: (1) if clogging truly contributes to reduce the

nitrification capacity of the studied primary filters; and, (2) if clogging is significant even before becoming externally visible.

- **Number of completely mixed reactors:** the results indicate that this parameter does not impact significantly the response of the filters with low nitrification activity. Although intuitively it is expected that this may not be the case for the model of filters with high nitrification activity, this aspect has not been tested. In principle, the more stratified the biomass content is, the more accurate the calibration of N should be. These results also suggest that the nitrification capacity of the filters may be the result not only of the number of cells and their specific nitrification activity but also of the level of stratification of these cells. Indeed, model simulations have demonstrated that any assumption regarding how much stratified is the biomass has implications in the removal capacity predicted by the model.

- **External mass transfer**: despite the fact that the external mass transfer resistance has been determined in the model according to some literature based expressions, it is also true that mass transfer coefficients are often difficult to predict under trickling flow (Rasmussen and Lewandowski, 1998). Indirectly, assessing the importance of this parameter is equivalent to assess the importance of the water velocity since the used expressions assume that the external mass transfer rate strongly depends on the water velocity. The results show that the impact of the external mass transfer resistance on the model response is negligible. Additional simulations whose results are not shown have indicated that this parameter would start being predominant when taking values around 10^{-7} m/s or lower which are well below the range of values resulting from calibration: around 8.0 10^{-5} m/s. Hence, only if the filter is operated under very different conditions may occur that the transport from the bulk to the grains becomes limiting. Below 2.5 10^{-06} m/s, as the mass transfer coefficient decreases (the external mass transfer resistance increases) the effluent concentration increases. These results match with the idea that concentrations on the biofilm surface might be very similar to concentrations in the bulk as the model suggest. Accordingly, the transport from the bulk to the biofilm surface does not seem to be limiting nitrification in the studied filters. Whether there is depletion of substrates and/or nutrients within the biofilm or not is something that cannot be studied with this model.

- **Average residence time:** the results of the sensitivity analysis indicate that the concentrations in the effluent are highly affected by residence time variations. As intuitively expected, the shorter the residence time is the higher the effluent concentration results. The uncertainty in the travel time used by the model is relatively large according to tracer experiment results (see Section 4.2). Additionally, clogging increases the heterogeneity of the residence times either through the apparition of short-circuiting, dead-zones and flow channelling.

- **Effective decay rate and maximum specific growth rate**: these two parameters are commented together since they both define the effective net growth rate, which is ultimately the parameter that decides the evolution of the population of the nitrifying organisms in the filter. The results confirm the importance of the specific growth rate and minimize the contribution of the decay rate. Since the decay was crucial during model calibration, there is an apparent contradiction between these results and the calibration process. This is thought to be due to the different time scales considered in each analysis. During model calibration, the majority of the cases consisted on time periods of long-duration (weeks to months). By contrast, the sensitivity analysis has consisted on simulations of a few days (3 to 4 days, which is equivalent equal to the duration of the run cycle in primary filters). It is expected then that the importance of the decay rate would have been much higher if longer time scales would had been considered for the sensitivity analysis.

- **Yield factor for N**: the results confirm that the biological degradation of ammonium is strongly characterized by the biomass yield. This confirms the importance of this parameter and suggests its inclusion in the group of parameters that define mostly the model response.. The observed yield in some bio-trickling filters was taken as reference value for the model and excluded from the calibration sub-set used to simulate each calibration case. This means that this parameter has taken the same value always, regardless of whether the model corresponds to a filter with high or poor nitrification. This simplification was necessary in order to reduce the number of parameters to be adjusted during manual calibration. When the observed yield is compared to other published studies it is seen that there are important difference. Some possible causes for the observed low yield were listed in Section 4.3. To conclude, it is hypothesized that the observed decrease in the nitrification capacity in primary filters may be linked not only to a reduced growth rate but also to a changeable yield factor.

External model parameters (operational parameters)

The objective of this part of the sensitivity analysis is to investigate how the filters may react to changes in the way they are operated. Ideally, this analysis must provide better insight into what are the operational parameters with the greatest impact on the effluent water quality. The results are presented in Table 28.

Table 28 Sensitivity analysis for external model parameters

EXTERNAL PARAMETERS	0%	-40%	-20%	+20%	+40%
Influent ammonium concentration [mg NH_4^+/L]	5.10	-60%	-31%	31%	63%
Flow [m^3/h] (*)	39.00	-3%	-2%	2%	3%
Air-water flow ratio RQ [-]	16	3%	2%	-	-

The results are:

- **Loading:** between the influent ammonium concentration and the flow, the modelling results indicate that the response of the filter is much more conditioned by the influent ammonium concentration than for the flow rate. The results also indicate that the response fluctuates more than the input. These result advocates for a better knowledge of the ammonium concentrations in the raw water but also for having a more stable raw water quality.

- **Air flow:** the forced ventilation system currently works at its maximum. The model suggests that very similar results could be achieved if working at lower air flow rates. In this respect it is important to remember some of the model limitations around aeration. First, the model is not able to asses how much the forced ventilation system contributes to enhance mixing and whether that contribution is crucial for nitrification. Moreover, the model does not consider other biological processes apart from ammonia oxidation. Consequently, the consequences of any change in the aeration system over the growing conditions (e.g.: pH) for the iron oxidizing microorganisms (e.g.: Gallionella spp.) are not known. The same occurs with the removal of methane. Site specific measurements have suggested that low pressure sprayers do not succeed in achieving complete methane removal and, consequently, is the forced ventilation system which completes that work. Finally, the model is not prepared either to study what the effect of having counter-current air flow would be.

The special case of backwashing

It has been previously said that if the control of the flow rate is excluded from the set of actions that define the operation regime of the filters, the backwash programme is one of the key factors defining the operation regime nowadays. Ideally, the model could be used to simulate the response of the primary filters to different backwash programmes. Unfortunately there are not measurements with which to compare the results of the simulations and, therefore, this issued could not be included in the calibration phase. Consequently, the analysis of the effects of changing the backwash programme must rely on pure hypotheses.

It is hypothesized that the rate of relapse in nitrification observed in the Tiendweg primary filters at WTP Lekkerkerk can be influenced through backwashing. The slow down in the relapse could be achieved with:

1) a higher filter bed expansion that would be possible by substitution of the sand fraction by anthracite.
2) a complementary backwash programme capable of removing the inactive biomass which is thought to be the cause of low specific activity. The characteristics of this programme should be defined experimentally.

More about these two issues is commented in Chapter 6, when some research recommendations are presented. Assuming that any of these hypotheses is true, the model would allow simulating the response of the primary filters to this change. The results are plotted in Figure 75**,** which illustrates how the model could be used for this purpose. The upper line corresponds to the current situation for which primary filters lose about half of their capacities after around 12 months of operation. The yellow line stands for the improved situation, for which a slower rate of relapse is achieved.

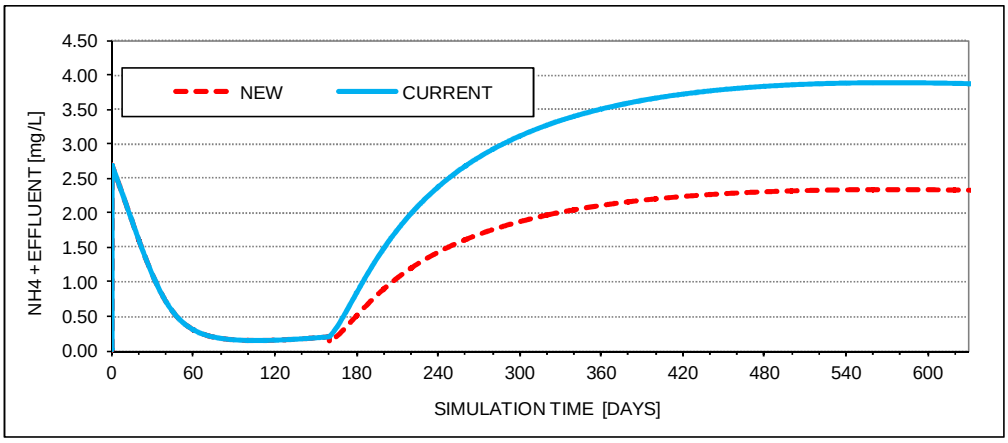

Figure 75 Simulated change in the rate of relapse in nitrification with new backwash programme

Moreover, the model has also suggested that secondary filters have high biomass growth rates (see Figure 74). Intuitively, this suggests that is possible to bring their biomass content to a new (and higher) steady state by slightly reducing the frequency of backwashing in these filters. By doing so the risk of ammonium breakthrough in these filters would decrease due to two reasons: first, the critical loading is increased (threshold values defined in Section 4.1); and, second, the number of backwash events is reduced. Unfortunately, there are not site-specific values to model the effect of backwash on the biomass content as a function of the operation conditions.

Conclusion of sensitivity analysis

The parameters that influence most the ammonium concentration in the effluent of bio-trickling filters are the influent ammonium concentration, the wetting efficiency, the biomass content, the net growth rate, the yield factor and, the residence time. Besides, backwashing seems to be also an important factor but the lack of data to quantify their impact under different operating conditions prevented a better modelling. Consequently, future efforts for improving the operation of these filters and/or a better characterization of nitrification in these filters should focus on these parameters.

4.6 Conclusions

A dynamic model that describes the process of ammonium removal in bio-trickling filters has been developed to mimic the three general cases that can be found in the filters fed by the Tiendweg well field at WTP Lekkerkerk: primary filter with high nitrification, primary filter with low nitrification and secondary filter.

A key model simplification has consisted on assuming that only nitrifiers in the outer layers of the biofilm, which have better access to substrates in the bulk phase, contribute significantly to the overall substrate removal. By doing this it has been automatically excluded from the modelling efforts the processes occurring within the biofilm. This assumption is equivalent to consider that there is full penetration of substrates and nutrients into the biofilm. Full penetration seems more plausible in thin biofilms. Since filters are operated at high flow rates (if compared to what literature states for trickling filters in tertiary water treatment), that seems to be the case. The model also assumes that the velocity of water in the vicinity of the grain surface does not differ significantly from the velocity of water at the furthest point of the water layer created around the grain, somewhere in the interstitial space between grains.

After revision of the values reported by literature and site-specific measurements, the calibration set has been reduced to three system specific parameters: growth rate, effective decay rate and initial biomass content. Such approach has been caused by the necessity the number of parameters to be calibrated. This means that the values of these parameters are what decide what kind of filter behaviour the model reproduces. The remaining model parameters either have fixed values or take values which are internally calculated based on influent conditions.

Concerning the effective decay rate, it represents several biological and physical processes counteracting growth: cell decay, detachment and inactivation. The model for secondary filters includes a separate module representing backwashing since this was the only way of reproducing the ammonium breakthrough events observed in the effluent of these filters. Consequently, biomass

washout in these filters must not be considered when calibrating this parameter in secondary filters. In primary filters the meaning of the effective decay term also varies with the duration of the simulation period. While for long term simulations (longer than one run cycle) this model parameter includes the washout of biomass due to backwashing, for short term simulations (shorter or equal to one run cycle) it is excluded.

About the (initial) biomass content, it refers to the ammonia-oxidizing microorganisms attached to the filter grains. The term excludes other types of biomass and it only accounts for active cells excluding both inhibited and dead cells. There is significant uncertainty around how the number of ANO cells evolves over the course of the time in the filters despite the great impact that it strongly influences the response of the system. This means that the lower nitrification activity observed in full-scale filters is mimicked in the model through reducing the biomass content, rather than by using an entirely different set of biological kinetic parameters to represent cells with different activity levels.

A stepped-calibration approach has been followed and has required considering several calibration periods. Efforts have been put into determining whether the same model parameters are capable of mimicking the behaviours observed at different filter life stages and filtration units or not. With the purpose of having a time and cost effective approach to calibration, the calibration has relied on bulk-phase measurements (effluent ammonium concentration) rather than on internal measurements such as the characteristics of the nitrification activity on the grains. Nevertheless, once the model has been calibrated it has been seen that the model results are consistent with full-scale internal measurements that have shown that filters with poor nitrification have very low cell and sand specific nitrification rates while filters with robust nitrification have very active cells. Table 29 summarizes the parameter values and the goodness of fitting for each calibration period considered.

Table 29 Summary of calibration cases, parameter values and simulation results

CALIBRATION CASE	1.1	1.2	1.3	1.4	1.5	1.6		2.1
Filtration step	First							Second
Filter performance	High ammonium removal	Start-up after renewal	Start-up after renewal	Poor ammonium removal	Poor ammonium removal	Start-up after external washing	Relapse of nitrification	High ammonium removal
Duration	Short-term 3 days	Long-term 180 days	Long-term 115 days	Long-term 160 days	Long-term 260 days	Long-term 660 days		Long-term 120 days
Comments	Single run cycle between backwash events				Half-loaded	Life cycle between external washing events		Several consecutive run cycles
CALIBRATION VALUES								
Maximum specific growth rate [1/s]	2.4E-06							3.4E-06
Effective decay rate [1/s]	4.6E-08	5.6E-07	5.6E-07	9.0E-07	6.8E-07	5.6E-07	8.60E-07	4.6E-08
Initial ANOs content [g DW/m3]	31.5	5.0	5.0	13.0	(11.0)	20.0	(55.0)	15.0
GOODNESS-OF-FIT	0.44	0.66	0.43	0.75		0.61		0.82
NET GROWTH [1/day]	0.20	0.16	0.16	0.13	0.15	0.16	0.13	0.29

The need to build a model in which the net growth rate of microorganisms varies accordingly to both the observed full-scale and internal measurements has resulted on assuming that the specific maximum growth rate is independent on the calibration period but it depends on the filtration step while the effective decay rate varies only with the life stage the filter is at. When reviewing the values obtained for the various parameters it is seen that secondary filters (filters without simultaneous iron and manganese removal) have higher growth values than primary filters (filters with simultaneous iron and manganese removal). Moreover, the differences in the decay rates in primary filters at the different life stages suggest the possibility that the factor behind the relapse of nitrification is related to the accumulation of either biomass (e.g. iron-oxidizing or manganese-oxidizing organisms) or other clogging material (e.g. inorganic deposits).

In general the model is able to predict the system behaviour under different conditions. In those cases the goodness of fitting varies between 0.66 and 0.82. By contrast, the model fails in predicting the typically observed fluctuations of the effluent ammonium concentration. This might be partially due to the unknown origin of these fluctuations.

It is also important to notice that in general the values given to growth and decay are several orders of magnitude lower than the values reported by literature.

Only once the model has been calibrated the model has been tested through validation in order to assess its reliability and its ability to predict the behaviour of the system under different operation conditions (e.g. raw water quality and flow). The calibrated models have been validated with an independent data set gathered during 20 days from the filtration set FF-FK-05. The set has been operated at different ammonium and hydraulic loading rates: during experiment 1 the load conditions

were the same than usual; during experiments 2 and 3 they varied. Table 30 summarizes the parameter values and the goodness of fitting for each validation experiment and filtration step.

Table 30 Summary of validation experiments, loading conditions and simulation results

VALIDATON EXPERIMENT	1	2	3	1	2	3
Filtration step	First			Second		
Situation	Poor ammonium removal			High ammonium removal		
Duration	7 days	10 days	4 days	7 days	10 days	4 days
Comments	Backw ash; Same loading conditions	Backw ash; Different loading conditions	Simlar loading conditions		Backw ash	
CALIBRATION VALUES						
Maximum specific grow th rate [1/s]	2.4E-06			3.4E-06		
Effective decay rate [1/s]	6.8E-07			4.6E-08		
Initial ANOs content [g DW/m3]	13.0			15.0		
GOODNESS-OF-FIT	0.86	0.30	0.72	0.71		
NET GROWTH [1/day]	0.15			0.29		

Based on the validation results in Table 30 it can be concluded that the model provides in general good results although it fails in capturing some parts of the response of the filters. More specifically, the model does not reproduce the transitory response of the primary filter when its load shifted to completely different values than usual (R^2 = 0.30). According to the model the operation of a filter during a long time at very different loading conditions would bring the system to a different steady state, which has implications in terms of the nitrification capacity of the system. This suggests that the model may require re-calibration if filters are operated at very different loading rates during long time periods.

The process of constructing the model has also provided information about the best factors to optimize the performance of the trickling filters. The parameters that influence most the ammonium concentration in the effluent are: the influent ammonium concentration, the wetting efficiency, the biomass content, the net growth rate, the yield factor and the residence time. The same results also suggest that there is no transport limitation from the bulk to the surface of the biofilm. Overall these model parameters represent the four main conditions to achieve complete biological ammonium removal: (1) having sufficient biomass content; (2) having adequate specific surface area (high or complete wetting); (3) having enough long contact time; and, (4) having active enough cells. Two of them are directly related to the characteristics of the filter bed while the other two deal exclusively with the microbial community and its activity.

Finally, both calibration and validation have provided interesting insights into nitrification. These insights suggest ways through which nitrification could be influenced. They are presented in Section 6.1 where the model-based conclusions regarding operation are summarized.

5 Model supported operational improvements

5.1 Introduction

Ammonium removal from anaerobic groundwater is a process that requires both ammonia-oxidizing organisms (ANOs) and nitrite oxidizing organisms (NNOs) to grow adequately. It has been shown (see Paragraph 2.3.2) that there are not significant problems with converting nitrite (NO_2^-) to nitrate (NO_3) in the Tiendweg bio-trickling filters at WTP Lekkerkerk. The problem lies in the conversion of ammonia into nitrite. The evaluation of the performance of the filters has shown (see Section 4.1) that the ammonium removal capacity of these filters is significantly affected by regular operations such as external washing, backwashing or renewal of the filter material have a great impact on nitrification. Ammonium breakthrough events may be caused by sudden change sin the influent conditions as well. All this results in the occasional no compliance of the company guideline value for ammonium in the mixed filtrate (see Section 2.5), which is applicable to the mixed stream resulting from mixing the effluent of all filter sets (Schuwacht and Tiendweg).

In order to optimize the operation of the filters, the process of constructing and calibrating the mathematical model has been indispensable. The modelling has been done using a conceptual-dynamic model approach based on kinetics and mass balance equations. The fitting of the model was based on the data from full-scale measurements. The overall aim was to construct a model able to reproduce the observed behaviour and to anticipate the filter's response to different loading conditions. In this chapter, different strategies in order to improve the operation are presented and discussed.

Section 5.2 deals with the operation of the filters for the current control regime. Section 5.3 does the same but considers a new operation strategy, based on distributing the load according to the life stage each primary filter is at. Section 5.4 deals specifically with the operation of the filters during maintenance events for both the current and the new control strategy. Finally, Section 5.5 focuses on some recommendations based on the pipe through which the supply to the Tiendweg filters should be given.

5.2 Current operation regime

The current operation of the Tiendweg bio-trickling filters at WTP Lekkerkerk is rather fixed. There is no intervention on the way the total abstracted flow is divided between the filters. The operation of primary filters is currently restricted to backwashing, external cleaning or renewal of the filter material. For secondary filters, only backwashing is performed. These operations, which impact the quality of the filter effluent, are not applied simultaneously so that their negative effects on the water quality of the effluent do not overlap ideally. Therefore, the final water quality (ammonium content) is the result of the respective ammonium concentrations and flow rates.

Furthermore, despite the fact that the operation of the well fields Schuwacht and Tiendweg follows some pre-defined schemes aimed at ensuring a relatively stable raw water abstraction and quality, there occur sudden variations.

Consequently, the so called 'nitrification problem' at WTP Lekkerkerk refers to two different events: (1) instantaneous peaks in the effluent ammonium concentration downstream each filter; and, (2) a gradual loss of efficiency observed in primary filters. These events may have different causes and, hence, solutions. While the first class likely has internal and external causes, the second group is thought to be mainly motivated by internal factors.

Integrated Model

The integrated model comprises of 10 sub-models representing the Tiendweg filters: 5 filters in the first filtration step and other 5 in the second filtration step. Each sub-model has received the calibration values that correspond to the situation the filter is at. Concerning the biomass content, the initial condition for each filter corresponds to the steady-state previously determined during the calibration process. Figure 76 shows how the integrated model looks.

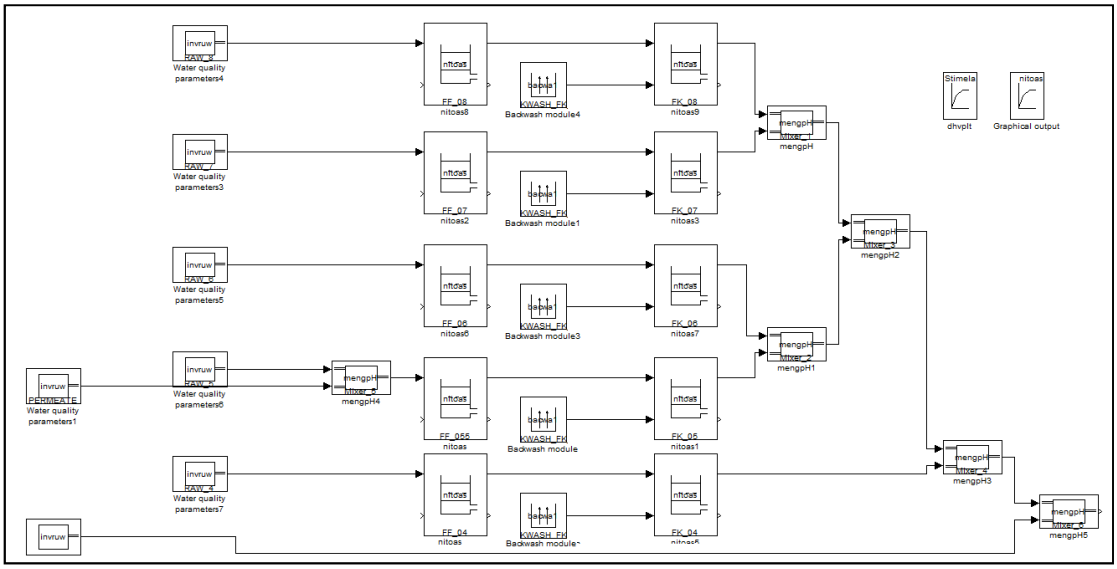

Figure 76 Aspect of the integrated model for ammonium removal at WTP Lekkerkerk

Having an integrated model has several advantages. One of the most important benefits is that the overall nitrification capacity of the entire system can be estimated. The overall capacity does not equals the sum of the individual nitrification capacities of each filtration set. This is because there are several factors in the system disturbing linearity. One factor is the existence of threshold values that define different behaviours in the filters. Another aspect is the dilution effect achieved by the mixing of streams with different water qualities. Another advantage of the integrated model is that since all the filters are represented, each ammonium breakthrough episode can be analyzed in detail based on the various contributing factors, their relative weights and the root causes. Ideally, by combining the previous analyses, different solutions can be tested and evaluated.

Consequently, this part of the research has focused on: (1) understanding better the current operation regime with the help of the model; and (2) assessing the treatment capacity of the whole set of filters for different scenarios. Based on these, some recommendations for the current operation will be presented.

Load

The ammonium loading rate depends on the ammonium content of the abstracted water and the flow to be treated. From September 2012 the supply is done permanently through the header A, which shows lower ammonium concentrations than the header B, according to the values reported in Table 7. The simulations have been performed considering the highest ammonium concentration reported in the last 2.5 years: **6.10 mg NH_4^+/L**.

For the flow, three aspects have been considered in order to determine the individual hydraulic load each filtration set is loaded with:

- The flow rates through Tiendweg are mostly within the range 130 - 240 m^3/h (see Figure 33).
- For the current control strategy, it is assumed that the flow distribution between filtration sets is relatively homogeneous. The specific case of the filter set FF-FK-05 is taken into account since this set receives approximately half of the raw water than the rest of the sets.
- The number of filters in operation: all the results shown in this section assume that all filters are in operation. Special cases when one or two of the filters are out of service temporally are analyzed separately (see Section 5.4).

The first simulations have quickly shown that in the low part of the possible range of flows (flow rates below 150 m^3/h) the water quality is guaranteed. The same simulation have also shown that for the given raw water quality and with flows above 240 m^3/h, complete nitrification is hardly achievable. For this reason the analysis has considered some extreme cases such as the hours and days of maximum as well. The combination of these flows with the mentioned ammonium concentration in the influent has resulted in the load range 900-1680 g NH_4^+/h.

Based on the recent history of the filters (see Table 8), up to 6 different situations have been defined and studied. These situations are summarized in Table 31. They cover the entire range of possible combinations of filters with different ages and at different life stage. Scenarios that include some filters in state of transition from complete to incomplete nitrification have been excluded from this selection since it is assumed that they all are intermediate situations between any of the situations

shown above and therefore, their results are theoretically within the range defined by the results of the delimiting scenarios.

The most favourable situation is on the left of the table and corresponds to the five filters having complete nitrification. The specific case of the filter FF-05 has been considered in five of the six scenarios. As it was explained at the end of Paragraph 2.3.2, the effluent quality of this filter is good despite the fact its nitrification capacity is low. This is because the raw water at that set is mixed with permeate from a nearby RO installation which makes that that set is half-loaded. The most unfavourable scenario is on the right side and represents one hypothetical situation for which all the five filters have reduced nitrification capacities. In between these two extreme scenarios, there are a few intermediate possibilities ranging from 1 to 3 primary filters having poor effluent quality.

So far, the real situation of the family of filters can always be approximated to one of these scenarios: the combination of some filters having complete nitrification working simultaneously with some filters with poor ammonium removal.

Table 31 Scenarios for system analysis

Primary Filter	Filter state					
FF-04						
FF-05		RO	RO	RO	RO	RO
FF-06						
FF-07						
FF-08						
Number FF's with low nitrification	0	1	2	3	4	5
Number FF's with poor effluent	0	0	1	2	3	4

Model output

The integrated model provides the water quality in the effluent of each filter. By considering the water quality and the flow of each of these filtrates, the model calculates the water quality of the mixed filtrate of the Schuwacht and Tiendweg filters and the mixed final effluent quality resulting from combining these two streams. By doing so, it is possible to evaluate separately how much each of these aspects (the overall nitrification capacity of the filters and the mixing with the Schuwacht filtrate) contributes to the ammonium concentration in the final effluent. This also means that, unless the opposite is stated, the ammonium concentrations shown in this section correspond to the simulated quality of the mixed filtrate of all Tiendweg filters.

With the help of the integrated model, how much the response of each filter impacts on the overall quality can be nicely illustrated. For a randomly chosen scenario Figure 77 shows the simulated ammonium concentration in the effluent of each filter set over a period of 100 days. There are different lines. Each line represents the effluent of each filtration set. The boldest line represents the ammonium concentration that results from mixing all the five streams. In the horizontal axis it is represented the time. In the vertical axis on the left, there is the ammonium concentration.

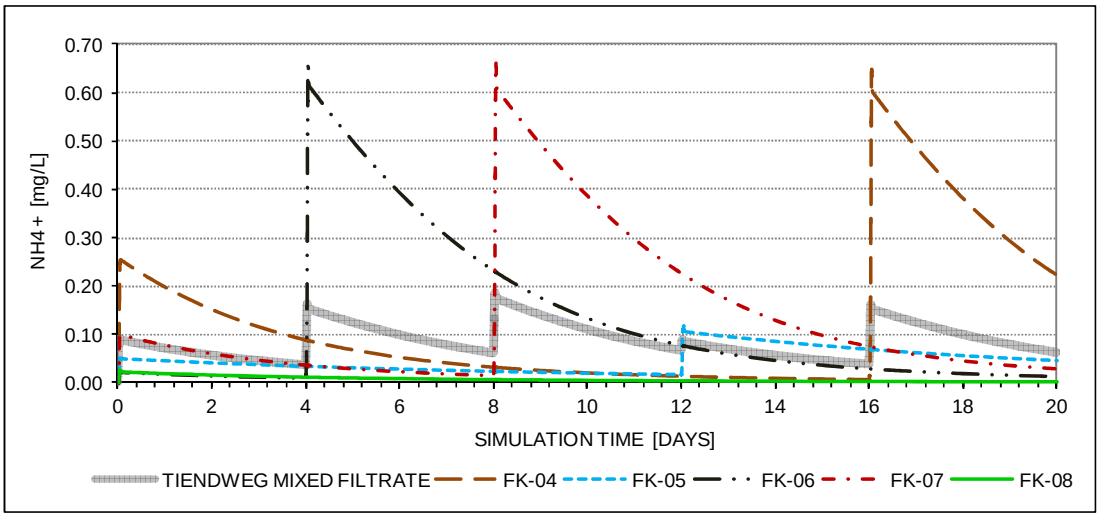

Figure 77 Ammonium concentrations in the effluent of each Tiendweg secondary filter and in the mixed filtrate for Q Tiendweg = 170 m3/h and three primary filters with poor ammonium removal with current operation regime

The abrupt change in each of the finest lines corresponds to the moment at which each secondary filter has been backwashed (every 20 days). One of the first things to be noticed in Figure 77 is that there are differences between the different effluents. These differences are caused by the differences in the state of the primary filters. The second important thing is that in the mixed filtrate there are up to a maximum of 5 peak values that correspond to the times backwash is performed in the secondary filters. As the peak value in the effluent of each secondary filter always occur after backwashing, the same occurs in the mixed filtrate: the highest value correspond to one of the moments when one of the secondary filters is backwashed. Therefore, the frequency of backwashing in filters in the second filtration step strongly influences the number of peaks in the mixed filtrate. Moreover, the peaks in the mixed filtrate are smaller than in the single effluents due to the mixing effect. In addition, it is interesting to notice how the tail of each individual curve in Figure 77 may contribute significantly to worsen the water quality of the mixed filtrate. This is known as the 'tail effect' and will have implications regarding how the backwashing sequence should be.

The typical effect of mixing the stream from the Tiendweg filters with the stream derived from the Schuwacht filters is illustrated by Figure 77. In the figure there are two curves: the curve with higher values represents the simulated ammonium concentrations in the mixed filtrate of the Tiendweg filters. The curve with lower values corresponds to the quality in the final mixed filtrate, after mixing with the Schuwacht mixed filtrate which is (almost) ammonium-free: most of the time lower than 0.015 mg NH_4^+/L according to Figure 11. This implies that the model assumes that the Schuwacht filters keep achieving complete ammonium removal.

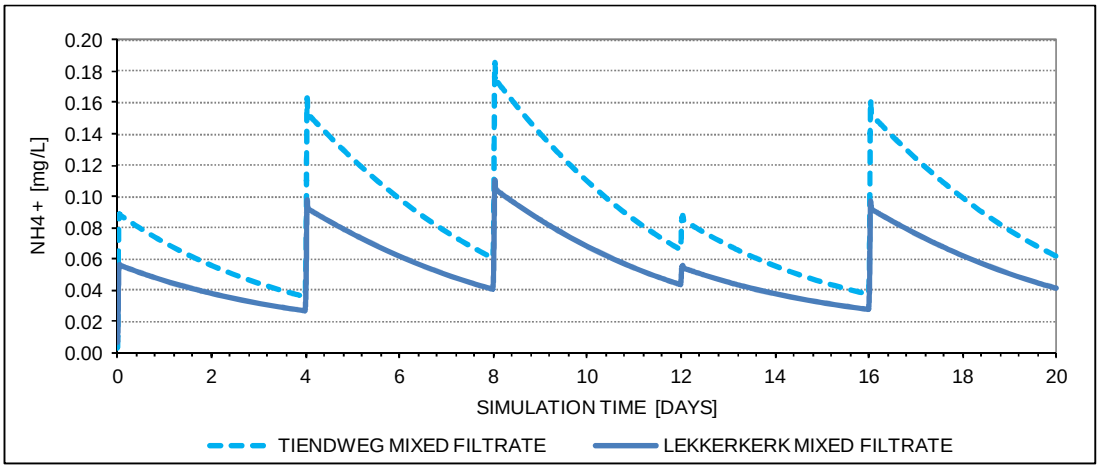

Figure 78 Ammonium concentrations in the mixed filtrate of all Tienweg filters and in the final effluent of Schuwacht and Tiendweg for Q Tiendweg = 170 m3/h with current operation regime and three primary filters with poor ammonium removal

Simulation results

After being loaded with ammonium loads ranging from 900 to 1680 g NH_4^+/h (148 to 275 m^3/h and 6.1 mg NH_4^+/L in the influent water), and considering up to 6 possible combination of filter states for each of these loads, the same kind of figures than shown above have been obtained. All these results are summarized in Figure 79. The overall ammonium load applied is represented along the x-axis. In the vertical axis on the left there is the highest ammonium concentration expected (simulated value) in the mixed filtrate coming from all the Tiendweg filters (Schuwacht excluded). In the plotting space there are different families of dots grouped by dotted trend lines. Each group represents a different scenario, which is basically defined by the number of filters with poor nitrification that are simultaneously in operation. Each dot is one single value taken from the complete series resulting from a 100 days simulation (5 cycles of 20 days) that corresponds to the highest ammonium concentration (worst case) for that scenario and demand (load).

In the same figure there are represented two horizontal dotted lines. The lowest (0.10 mg/L) represents the company's guideline value, applicable to the mixed effluent of Tiendweg and Schuwacht. Dots below this line represent situations for which compliance with the guideline is guaranteed as the final quality will be better due to dilution of the Tiendweg stream with the Schuwacht filtrate, which traditionally is ammonium-free. For dots above the same dotted horizontal line the compliance will depend on having the right flow rate through Schuwacht to reduce the concentration values low enough.

The highest horizontal dotted line (0.20 mg/L) corresponds to twice the guideline value, which is the maximum legally permissible. But this line is also a first rough estimation of the maximum ammonium concentration admissible in the mixed filtrate of all Tiendweg filters considering the abstraction capacity of the Schuwacht well field (about 270 m^3/h). This means that the dots above the 0.20 mg/L

horizontal dotted line represent situations that should be clearly avoided since the highest ammonium concentration is such that it would require a flow through Schuwacht that cannot be provided.

In short, the dots below 0.20 mg NH_4^+/L represent cases for which the compliance of the quality guideline is either guaranteed (dots below 0.10 mg NH_4^+/L) or conditioned (dots between 0.1 and 0.2 mg NH_4^+/L) to a proper mixing with Schuwacht. By contrast, the system should not be operated for all the cases represented by dots above 0.20 mg NH_4^+/L.

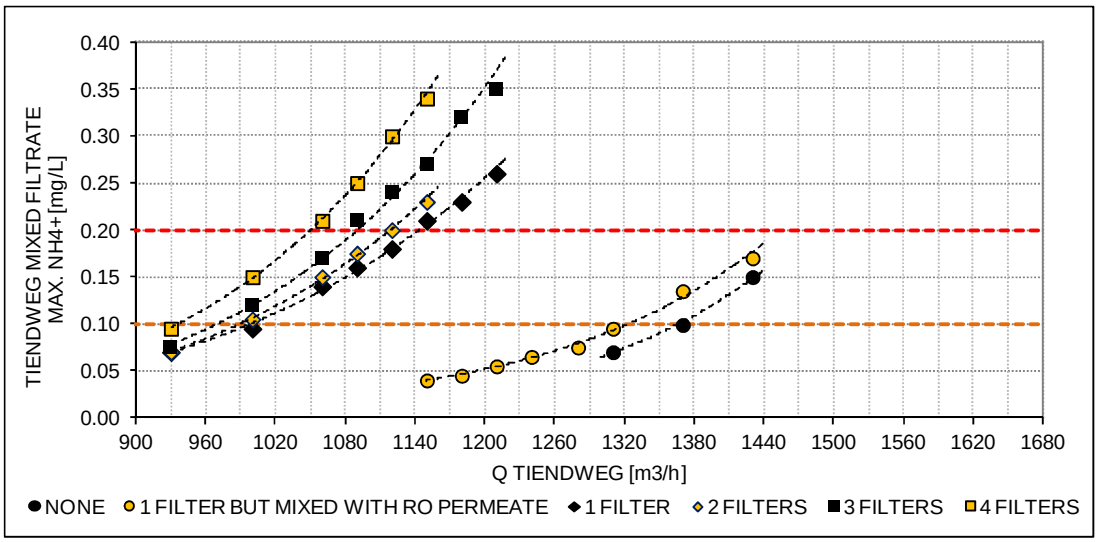

Figure 79 Simulated maximum ammonium concentrations in Tiendweg mixed filtrate for different scenarios, loads and with current operation regime

Based on the results shown in Figure 79, different aspects need to be highlighted:

- As expected, the higher the load is, the higher the peak ammonium concentration results for each scenario (trend line curve).
- The big picture shows that the dots are distributed in two big groups. The group on the right represents the two most favourable cases, without any filter with nitrification problems or, if so, that filter is fed with better raw water (filtration set FF-FK-05 in the current situation).The group on the left of the plotting space represents the most unfavourable cases, with 1 to 4 primary filters with low ammonium removal. For the same load (vertical line in the figure), the expected highest ammonium concentration in the mixed filtrate is significantly higher for the group of dots more to the left side than for the group of dots more to the right.
- The curves in the group on the right side are very close to each other. This demonstrates that the loss of nitrification capacity can be almost totally compensated by adapting the load to the filter actual nitrification capacity, as it is currently done for filter FF-05.
- There are no dots in between the two groups or, in other words, the existence of one single primary filter with poor ammonium removal clearly determines the worst ammonium concentration in the mixed filtrate.
- The maximum recommended load can be determined by identifying the intersection of each trend line with the corresponding dashed horizontal line. The lower the number of filters with poor nitrification, the wider the rage of safe loads is.
- Furthermore, the higher the number of filters with nitrification problems in operation is, the greater the slope of the trend lines results. This indicates that the relative impact of any new filter with nitrification problems varies. This is probably due to the 'tail' effect previously discussed.

In Figure 80, the loading capacity has been converted into the equivalent flow so that the previous results can be translated into maximum flow rate recommendations.

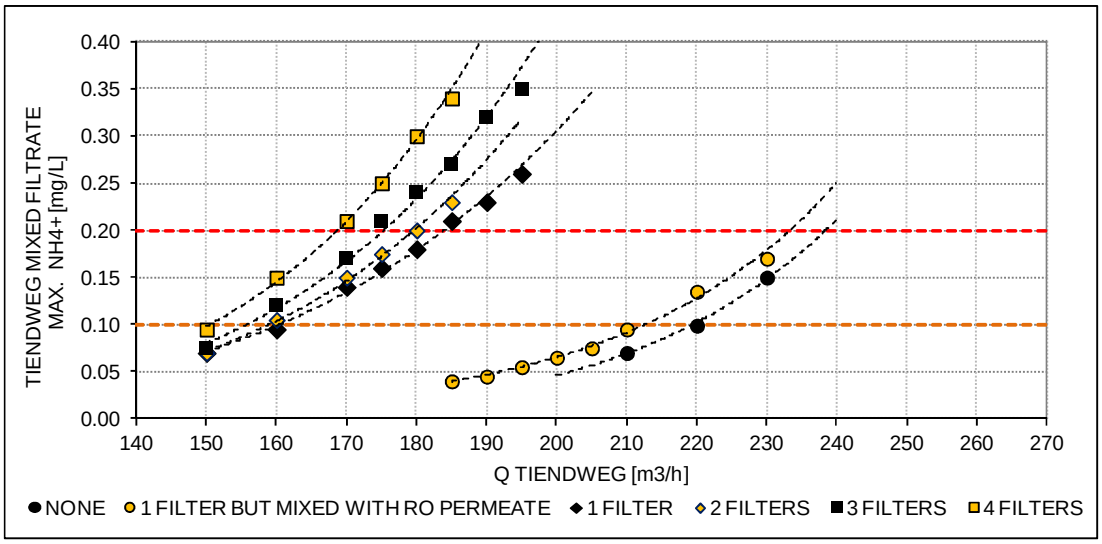

Figure 80 Simulated maximum ammonium concentration in Tiendweg mixed filtrate for different scenarios and loads and with current operation regime

According to this figure, peak ammonium concentrations greater than 0.20 mg NH_4^+/L are hardly avoidable for most of the flow rate values when having 1, 2, 3 or 4 primary filters with poor ammonium removal. By contrast, the compliance is guaranteed for most of the flows when all filters perform well or when there is one that does not but whose influent water quality is improved through mixing with ammonium-free water. Analogously, the range of "safe" flows (those ones for which the compliance of the guideline is guaranteed) decreases with the increasing number of primary filters having poor nitrification. If the results are confronted with the actual production scenario (Figure 33, values from 2012), it becomes clear that the system it will always be operated above its nitrification capacity for a certain number of days per year as far as the same production regime and operational regime are followed. The number of days will depend on the state of the primary filters.

Since the hourly flows are known, the results can be expressed in terms of probability. Figure 81 is the result of combining the data shown in Figure 33 and Figure 80. In the vertical axis there is the probability of having a concentration equal or greater than the value in the x-axis. The dots in the plotting space are grouped by trend-lines that represent the different scenarios (number of filters with reduced nitrification capacity in operation). These probabilities correspond to the highest expected value in the Tiendweg mixed filtrate under the considered conditions: 6.1 mg/L of ammonium in the raw water and all the sets in operation. The occurrence of maintenance events out of the normal operation of the filters has been excluded from this analysis. Having higher or lower raw water concentrations or a different probability distribution function for the flow rates would modify these results.

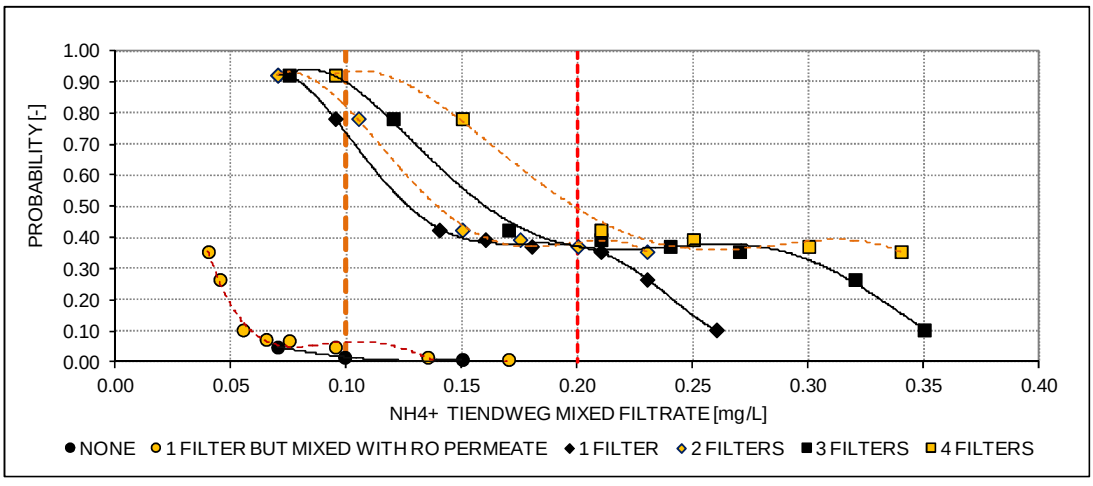

Figure 81 Probability of exceeding the ammonium concentration given in the x-axis in Tiendweg mixed filtrate for different scenarios and with current operation regime (maintenance events excluded)

The results shown in Figure 81 confirm that with the current control strategy (no control of the flow distribution between the different filtration sets) there are no major differences between having one or more than one aged filters in operation. For instance, the probability of having concentrations greater

than 0.10 mg NH_4^+/L is very high in all 4 cases (0.73 or higher). The probability of having values greater than 0.20 mg NH_4^+/L is much lower but still important (it drops to 0.38-0.50, depending on the situation).

Nitrification capacity versus treatment capacity

In order to provide OASEN with more practical recommendations, the removal capacity of Tiendweg due to both internal (nitrification capacities of the filters) and external (mixing with the Schuwacht filtrate) factors has been quantified with the help of the model. On the following pages, the removal capacity attributable to the filters will be referred as "nitrification capacity". The "treatment capacity" is defined as the nitrification capacity plus the extra load the filters can be loaded with due to the beneficial effect of mixing the Tiendweg filtrate with the ammonium-free filtrate derived from Schuwacht filters. This aspect has been illustrated in Figure 78.

In the two figures below both the nitrification and treatment capacity of Tiendweg are represented. The dark bars correspond to the nitrification capacity while the light bars show the treatment capacity. The different scenarios concerning the age of the filters are represented in the horizontal axis. The capacities are either expressed in load (see Figure 82) or flow rate units (see Figure 83).

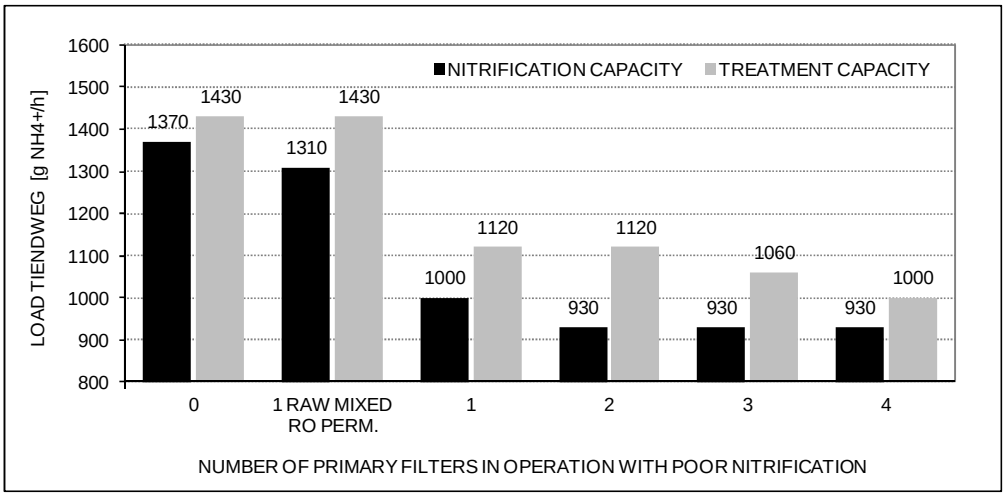

Figure 82 Tiendweg maximum load to not exceed 0.1 mg NH_4^+/L (dark bars) or 0.2 mg NH4+/L (light bars) in Tiendweg mixed filtrate

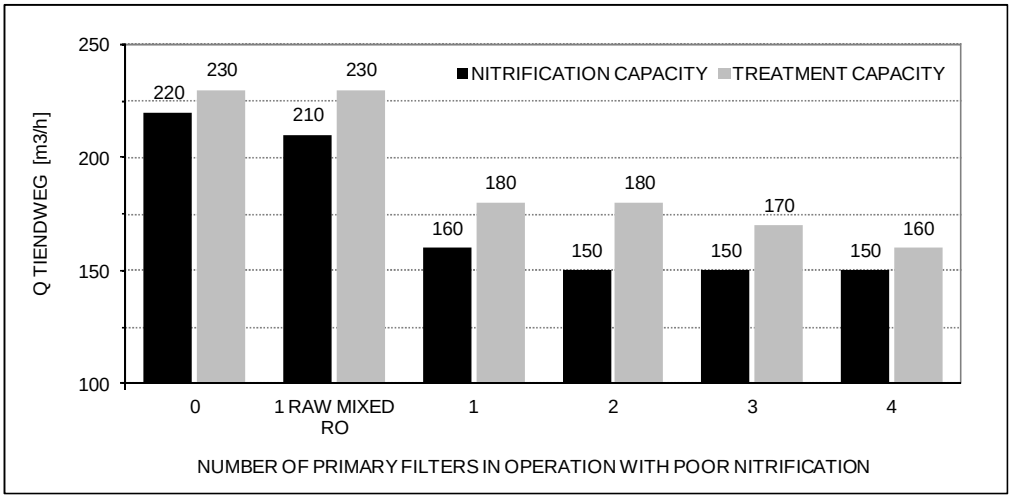

Figure 83 Tiendweg maximum flow to not exceed 0.1 mg NH_4^+/L (dark bars) or 0.2 mg NH4+/L (light bars) in Tiendweg mixed filtrate for different scenarios for different scenarios

Figure 83 clearly illustrates how much the capacity of the system varies with the state of the filters. Above the values represented by the light bars, the compliance of the company guideline is not guaranteed. Consequently flows greater than the blue ones should not be assigned to Tiendweg. The better the state of the filters is (lower number of primary filters with poor ammonium removal), the higher the capacity of the system results. It is seen that the biggest shift occurs between having 0-1 filters in operation with incomplete nitrification and having 1 or more than 1. The figure also shows

how the system capacity clearly increases due to the mixing with the Schuwacht: the increase in the capacity ranges from 7 to 20%, depending on the scenario. The highest increases correspond to the two intermediate situations (scenarios with 1 or 2 primary filters with poor ammonium effluent concentrations).

Recommended production shares

Without having the possibility of changing the flow distribution between filters, the only possible strategy is to adapt the share Tiendweg-Schuwacht to the actual scenario. According to this, specific recommendations can be given in order to guarantee full nitrification under special demand days which have been considered of interest:

- High demand season: the maximum production week and day.
- Low demand season: the minimum production day.

High demand season

A couple of examples with real values are presented in Figure 84 and Figure 85. These figures show the recommended flow division between Schuwacht and Tiendweg to assure the quality of the mixed filtrate for the week and the day, respectively, of maximum production. In both figures, the bar located leftmost in the plotting area represents the actual flow division in 2012 so the actual situation can be compared to the recommendations for the different scenarios.

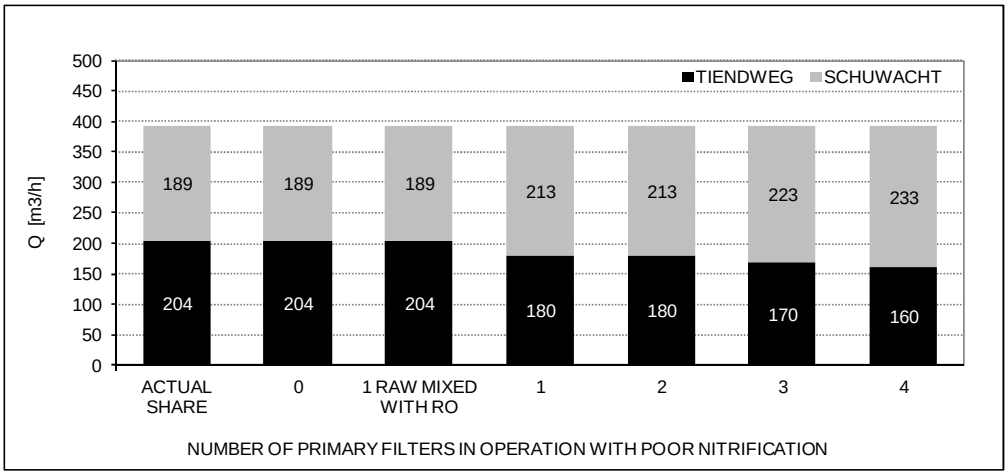

Figure 84 Actual and recommended production shares during the week of maximum demand for different scenarios and with current operation regime

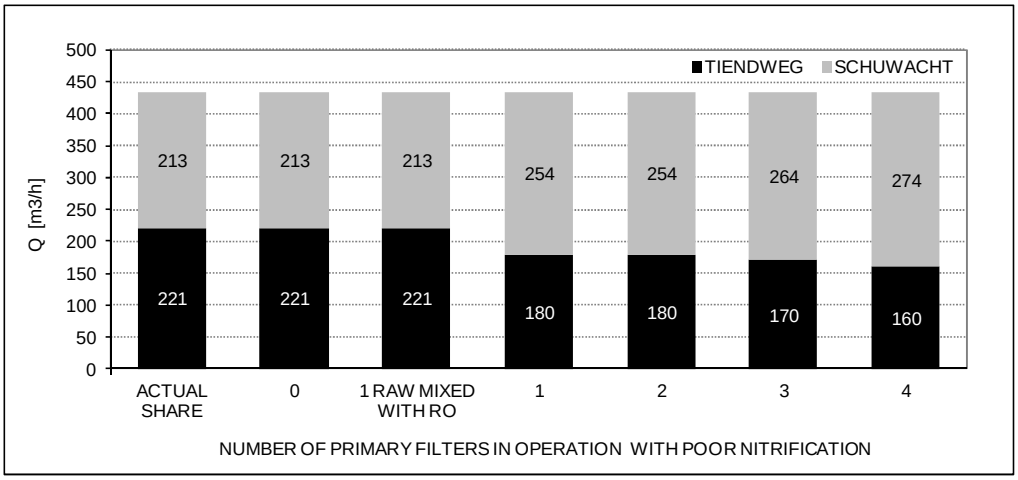

Figure 85 Actual and recommended production shares during the day of maximum demand for different scenarios and with current operation regime

In general, the shares of Schuwacht and Tiendweg should be adjusted during high demand periods (total production equal or greater than 390 m^3/h) whenever there is one or more primary filters with poor nitrification. The flow assigned to Tiendweg should be reduced in order to not exceeding the

maximum capacities defined in Figure 83. Additionally, the production assigned to Schuwacht should be temporally increased to compensate the reduction of flow through Tiendweg.

The recommended flows through Schuwacht are always below the installed abstraction capacity but they might be incompatible with the legal concession regarding the maximum amount of abstracted water from this aquifer which is about 1.7 million m^3 per year (on average, 194 m^3/h). This aspect goes beyond the boundaries of this study and should be further studied.

Low demand day

Model simulations indicate that during periods of low demand the water quality may be compromised only if the flow rate through Schuwacht is too low. For example, the case corresponding to the day of minimum demand in 2012 is taken. The average production of the plant that day was 230 m^3/h. Figure 86 shows that for such demand situation the flow rate through Schuwacht should not be lower than 70-80 m^3/h whenever there are one or more filters with reduced nitrification capacity. Otherwise, the compliance of the guideline may be compromised.

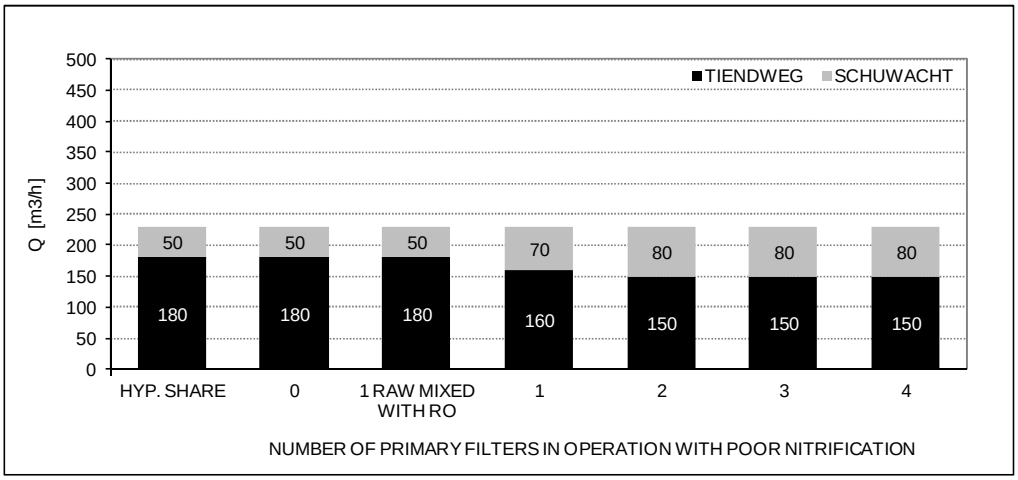

Figure 86 Recommended production shares during the week of maximum demand for different scenarios and with current operation regime

Conclusion

All the results suggest that the total flow through Tiendweg should be adapted to the actual treatment capacity of the system whenever there is 1 or more primary filters with poor ammonium removal in order to guarantee the mixed effluent quality continuously. The most unfavourable scenarios correspond to having 3 or 4 primary filters with poor ammonium removal, situations that should be strongly avoided, since they clearly compromises the compliance of the guideline whatever the demand is.

Since the production that Schuwacht can assume is limited and the impact of having one single primary filter with poor ammonium removal clearly compromises the overall nitrification capacity of the system, a different strategy rather than relying exclusively on modifying the share Schuwacht-Tiendweg is presented in the next section.

5.3 New operation regime

In Section 5.2 it has been shown how the existence of one single primary filter with poor nitrification strongly reduces the treatment capacity of the system. This happens mostly because all filtration sets are treated equally, without making any distinction based on their ages (primary filters) or runtimes (secondary filters) despite the fact different ages and nitrification capacities coexist. They all receive the same load (flow) even though it is known that they do not have the same nitrification capacity.

At the moment, flow control is not possible as there are no flow controlled valves that can help fulfil that purpose. Nevertheless, the model has proved that the effluent water quality can significantly be improved by adapting the flow (and, hence, the ammonium load) through each filtration set to the operational age of the primary filter. The integrated model has been used to investigate what the

effects of this new strategy are and how it should be implemented, assessing how much the optimal loads for each set is.

Figure 87 is representative of the modelling results obtained for most of the scenarios. It corresponds to the scenario representing one out of five of the primary filters showing poor ammonium removal. The flow is along the horizontal line at the bottom. The scale for the different outcomes is shown on the vertical line on the left side of the graph and it represents the highest ammonium concentration (simulated value) in the mixed filtrate of all the Tiendweg filters. Dots representing high flows are to the right while dots with low flows are towards the left of the graph. There are two groups of dots representing the current situation (equal flow distribution, light colored dots) and the new operational strategy (unequal flow distribution, dark colored dots).

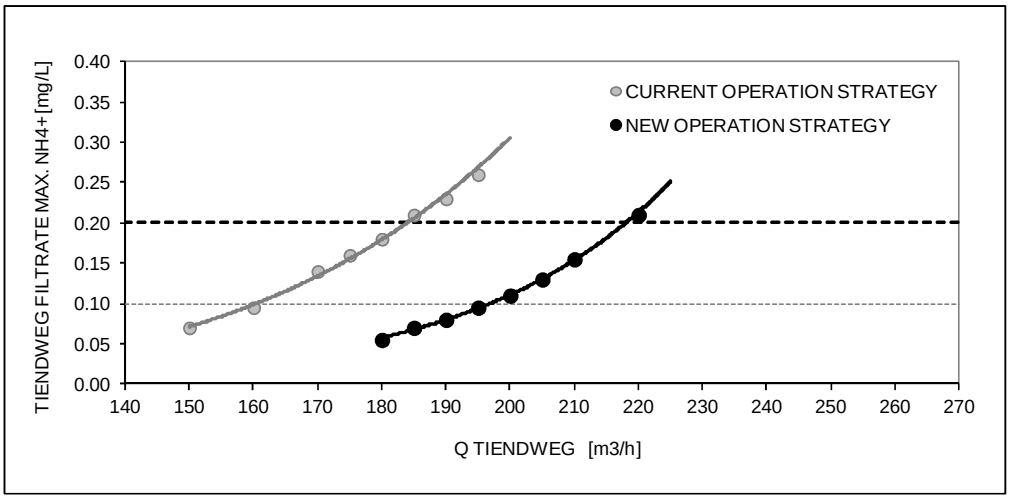

Figure 87 Simulated maximum ammonium concentration in Tiendweg mixed filtrate with current and new operation regimes if having three primary filters with poor ammonium removal

From Figure 87 it can be concluded that the improvement achieved by controlling the flow is significant: the range of "safe" flows (those ones not necessarily resulting in ammonium peak levels above the threshold values) is much wider with the new operation strategy (up to 200-220 m^3/h) than with the current control strategy (up to 160-185 m^3/h).

Before showing the results for all the scenarios, the basis of this new operational strategy is illustrated with one random example. Analogously to what has been described in the previous section, the model provides the ammonium concentration in the effluent of each filter set over a period of 100 days and the ammonium concentration in the resulting mixed filtrate. Figure 88 illustrates the positive effect of redistributing the load according to the state of each filter. The line with higher ammonium values correspond to the quality in the mixed filtrate for the current situation (no flow control-distribution between filters) while the curve with lower values represents the water quality for the new strategy. The figure shows that with the new control strategy lower peak values and a more stable water quality are achieved.

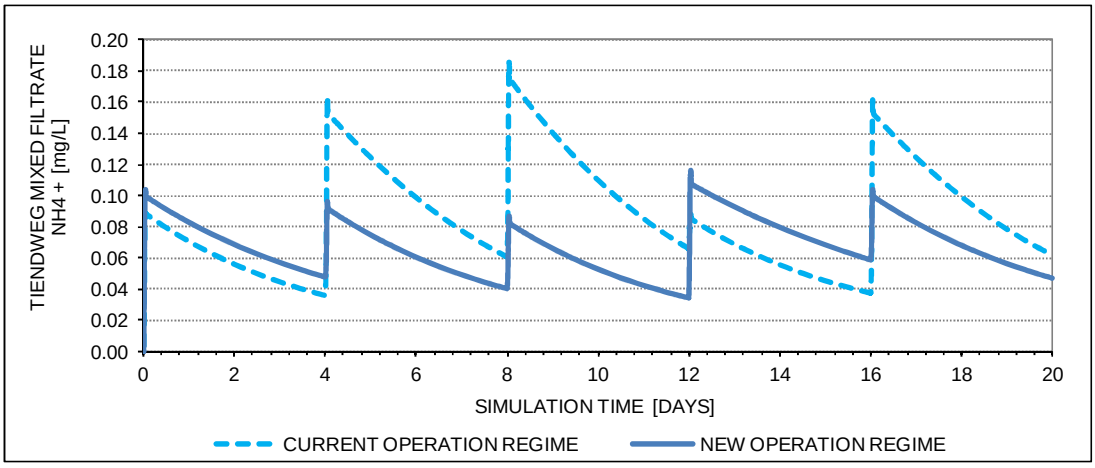

Figure 88 Ammonium concentrations in the mixed filtrate of all Tiendweg filters for Q Tiendweg = 170 m3/h and three primary filters with poor ammonium removal for current and new operation regimes

The effect of the same new operation strategy has been investigated for two more scenarios: two and three out of five of the primary filters having poor ammonium removal. The same range of flow rates than considered in Section 5.2 has been used this time so that the results are comparable. The best load (flow) distribution has been determined manually for each specific scenario. The results for all the possible scenarios are presented in Figure 89. Analogously to Figure 87, each group of dots represents one scenario and each dot represents the highest ammonium concentration expected in the mixed filtrate for a given flow rate.

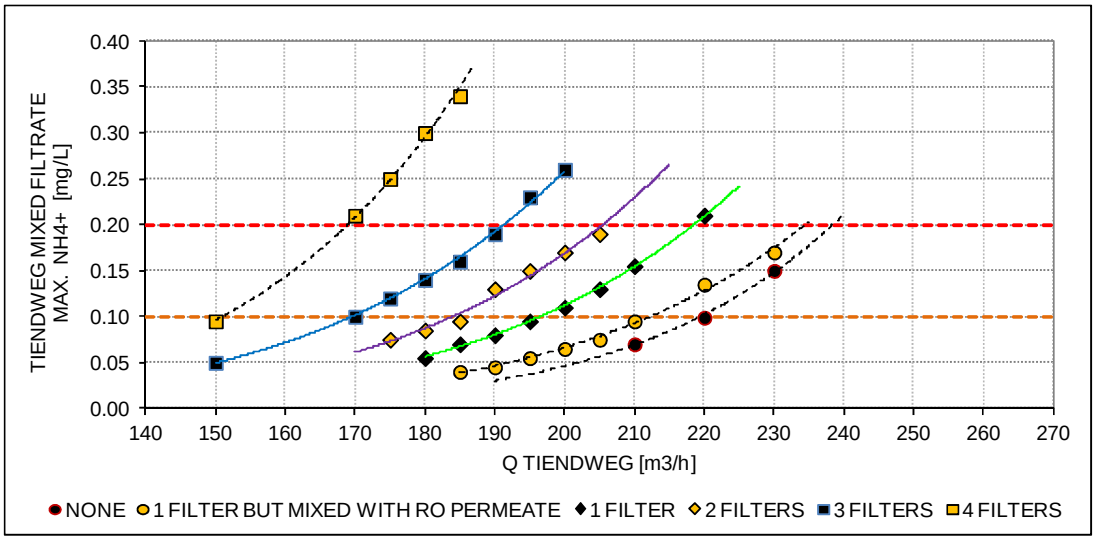

Figure 89 Simulated maximum ammonium concentration in Tiendweg mixed filtrate for different scenarios and flows and with new operation regime

When these results are compared to the results for the current operational strategy (see Figure 80), it is seen that the new control strategy offers great improvements for the intermediate scenarios (1, 2 or 3 primary filters with poor effluent quality, they all having continuous trend lines in the figure): the range of "safe" flows (those ones not necessarily resulting in ammonium peak levels above the threshold values) is much wider than for Figure 79. By contrast, there is no improvement or it is negligible for the extreme scenarios, which are represented with dotted trend lines in the same figure.

Moreover, the positive impact of the new control strategy varies with the number of filters with poor ammonium removal. The greatest impact is achievable when there is only 1 filter with relapsed nitrification, while the smaller improvement corresponds to the case when there are 3 filters with low nitrification efficiency.

Higher capacity

Figure 90 and Figure 91 quantify the increase in the capacity of Tiendweg with the new operation regime. In both figures, the scenario is represented along the x-axis. On the left side there is the best possible scenario, with zero filters with relapsed nitrification. On the right side the worst possible scenario considered, with four filters with relapsed nitrification. The bars with light colour represent the value for the current operation regime while the darker bars correspond to the new regime. The scale for the outcomes is shown on the y-axis on the left side of the graph and represents the maximum recommended flow rate for Tiendweg. Figure 90 stands for the overall nitrification capacity while Figure 91 shows the treatment capacity.

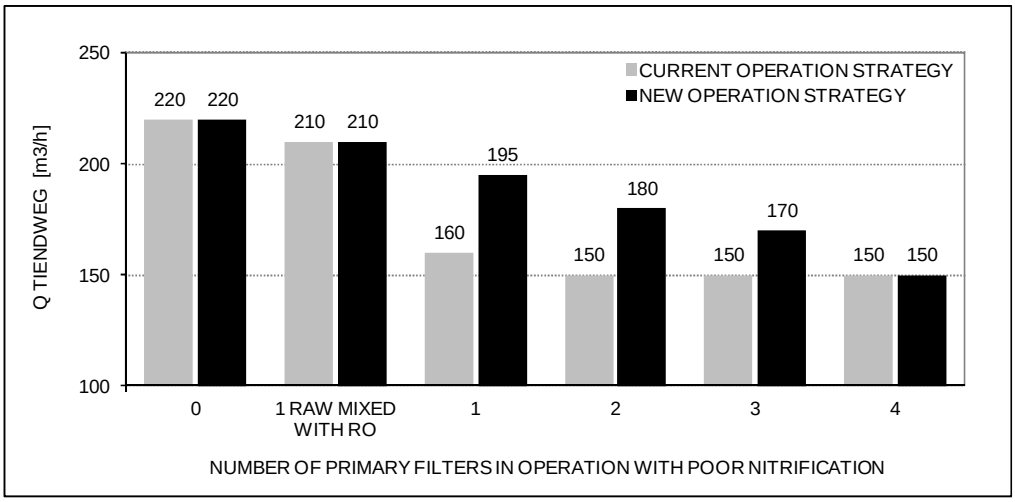

Figure 90 Tiendweg maximum flows to not exceed 0.1 mg NH4+/L in Tiendweg mixed filtrate for different scenarios with current and new operation regime

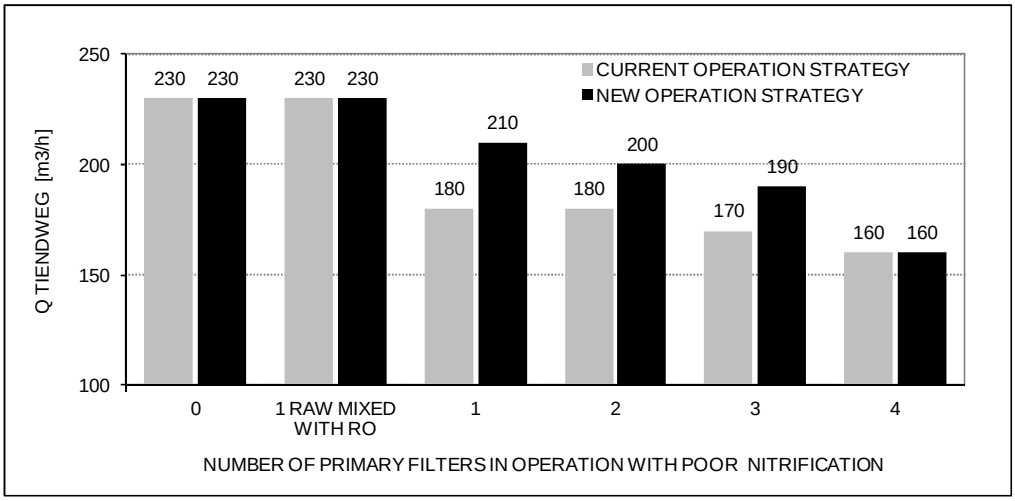

Figure 91 Tiendweg maximum flows to not exceed 0.2 mg NH4+/L in Tiendweg mixed filtrate for different scenarios with current and new operation regimes

In Figure 90, the largest increase in the nitrification capacity corresponds to the scenario with only one primary filter with poor ammonium removal, with a 22% improvement (from 160 to 195 m^3/h). Then the cases with two and three filters with poor nitrification follow, with increases of 20% (from 150 to 180 m^3/h) and 13% (from 150 to 170 m^3/h) respectively. There is no improvement for the other three cases.

Figure 91 shows the maximum flows at which Tiendweg could be operated with the new strategy. The improvement when compared to the current control strategy is: 17% increase if there is one filter with reduced nitrification (from 180 to 210 m^3/h), 11% increase if the number is two (from 180 to 200 m^3/h) and 12% increase if there are three (from 170 to 190 m^3/h). Above these values, the water quality of the mixed filtrate is not guaranteed.

Optimal load distribution

The optimal flow distribution has been established with the help of the model. The model simulations have indicted that it depends on the scenario and the load. As a thumb of rule, the total load (flow) should be distributed over the filters according to the values shown in Table 32.

Table 32 Model-based optimal load distribution

	Optimal load distribution [g NH4+/h]	Scenario: number FF's with poor effluent		
		1	2	3
Primary Filter	With good nitrification	300	300	270
	With poor nitrification	220	220	230
	With poor nitrification but mixed 50-50% with RO permeate	170	170	150

Based on the results shown in the table, it is concluded that the load distribution between filters does not change significantly if there are one or two filters with low ammonium removal. By contrast, having three primary filters with poor nitrification clearly advocates for adjusting the load distribution.

Backwashing sequence

The sequence in which the secondary filters are backwashed should also be adapted considering the scenario at which the system is. In the first scenario there are no constraints since there is only one primary filter with low ammonium removal. In the second and third scenarios the rule of thumb consists on not to backwash consecutively (after 20 days) the two secondary filters downstream the primary filters having nitrification problems. The specific optimal loads (flows) and backwashing sequence can be more carefully determined with tailored model simulations.

Lower risk of ammonium breakthrough

The new control strategy results in a wider range of flow values within which is possible to guarantee full nitrification (mixed filtrate of all sets below the company guideline for ammonium 0.10 mg NH_4^+/L). This is illustrated in Figure 92, which quantifies the probability of exceeding the threshold values for the different scenarios.

Similarly to that shown in Figure 81, the probability has been calculated as the number of hours per year, based on the probability distribution function of the hourly flows through Tiendweg in 2012 (see Figure 33) when the guideline value would be exceeded. Each scenario is represented by the dots grouped by the same trend line. The dotted trend lines in the figure correspond to the extreme scenarios, when none or all the primary filters have nitrification problems. As said previously, under any of these two situations, the new operation strategy is inapplicable and, consequently, the risk of ammonium breakthrough does not change when compared to the current situation (see the equivalent trend lines in Figure 81). In contrast, the situation clearly improves for the other three scenarios, with 1, 2 or 3 filters with poor nitrification in operation. The vertical dotted line on the left (0.10 mg NH_4^+/L) represents the guideline value for the Schuwacht-Tiendweg mixed filtrate. The vertical dotted line on the right (0.20 mg NH_4^+/L) is the maximum admissible value in the mixed effluent of all Tiendweg filters with which it is still possible to meet the guideline value of 0.10 mg NH_4^+/L if having a proper mixing ratio between Tiendweg and Schuwacht.

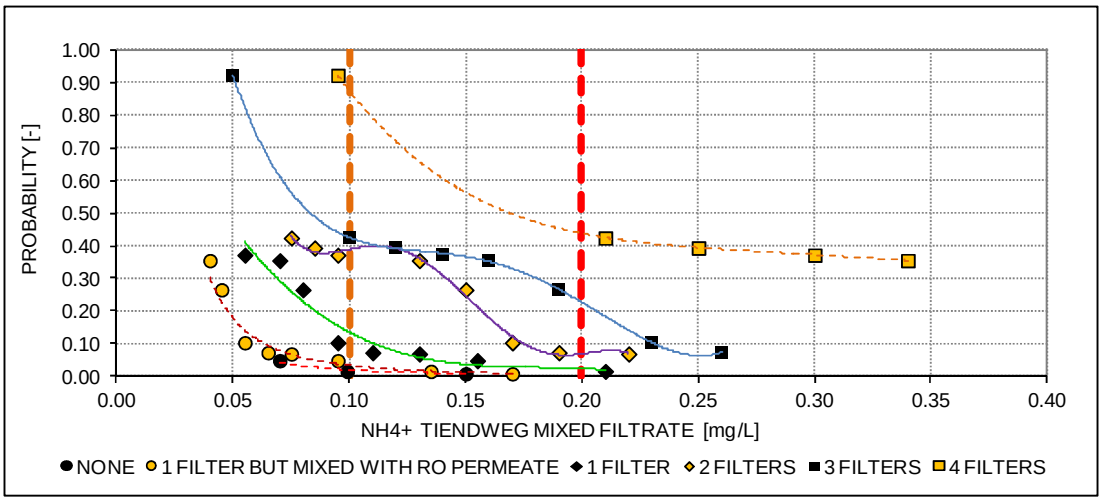

Figure 92 Probability of exceeding the ammonium concentration given in the x-axis in Tiendweg mixed filtrate for different scenarios with new operation regime (maintenance events excluded)

The figure confirms that although it does not disappear completely, in general the probability of having ammonium breakthrough (ammonium concentrations greater than 0.20 mg NH_4^+/L) is much lower than with the current operation strategy. It is 0.03, 0.08 and 0.22 when having one, two or three Tiendweg primary filters in operation with poor ammonium removal, respectively. Two out of

three of these values are significant lower than the values for the current strategy, which were around 0.3 and 0.4 (see Figure 81). It is concluded then that the maximum allowable number of primary filters with poor nitrification is 2.

Tiendweg–Schuwacht shares

The increase in the capacity of Tiendweg shown in Figure 90 and Figure 91 implies that the compliance with the guideline is less dependent on having a proper ratio Schuwacht-Tiendweg than in the previous case. Figure 93, Figure 94 and Figure 95 show how the requirements over the share Tiendweg-Schuwacht are less strict for three special: the week of maximum demand (393 m^3/h), the day of maximum demand (434 m^3/h) and the day of minimum demand (230 m^3/h). All flow values correspond to 2012. The figures compare the actual share, which is the leftmost bar in the graphs, with the recommended share for each scenario.

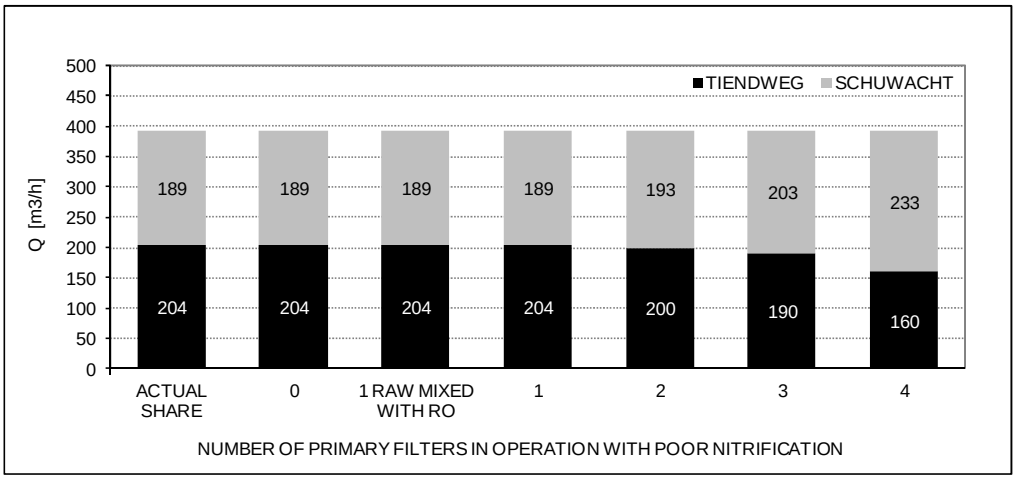

Figure 93 Actual and recommended production shares during the week of maximum demand for different scenarios with new operation regime

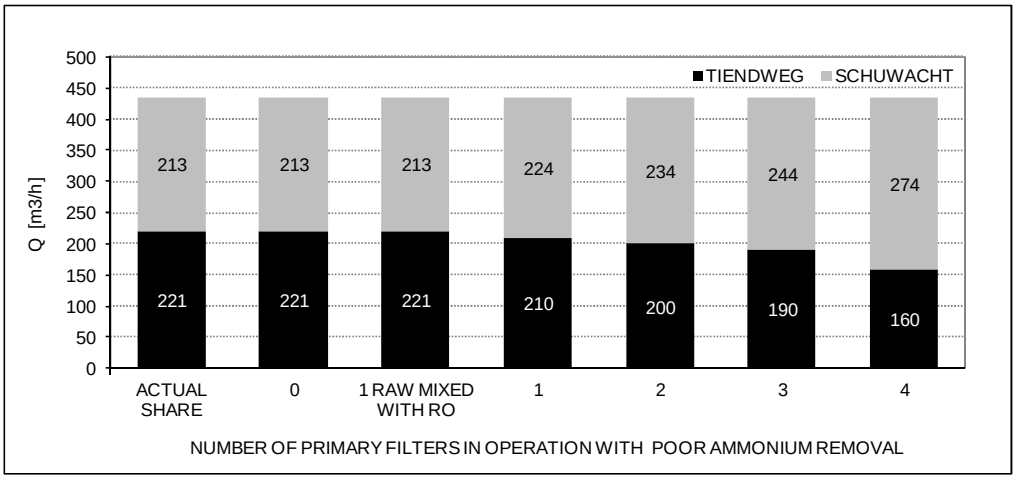

Figure 94 Actual and recommended production shares during the day of maximum demand for different scenarios with new operation regime

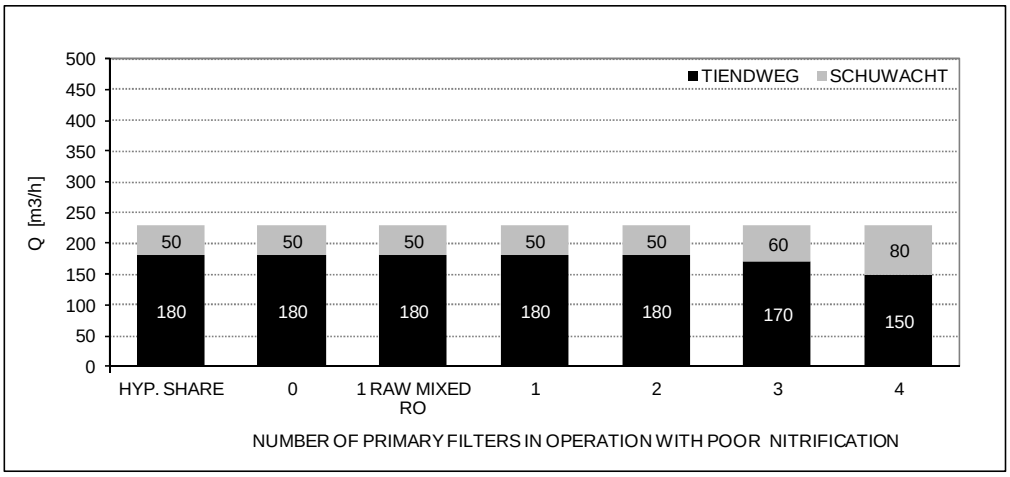

Figure 95 Recommended production shares during the day of minimum demand for different scenarios with new operation regime

In general, the recommended share is equal or very similar to the actual share whenever there are 0, 1 or 2 primary filters with poor ammonium removal. The exception is the day of maximum demand, which keeps being a situation when the risk of ammonium breakthrough significantly increases. Therefore, for days like this, the flow distribution between Schuwacht and Tiendweg should be adjusted according to the values shown in Figure 94.

The results also show that if having 3 or 4 primary filters in Tiendweg with poor nitrification, the share Tiendweg-Schuwacht should be modified not only during special days (e.g. high demand days) but almost continuously which seems hardly implementable because of legal constraints regarding the maximum volume of water that can be abstracted by the Schuwacht well field.

5.4 Maintenance operations

The previous two sections have dealt with the operation of the filter sets when all the primary filters are in service, both under the current and the new control strategy. This section deals with the operation of the system when the load through the individual filtration sets increases as a result of 1 or 2 filters going out of operation.

The first part of the analysis comprises the study of the consequences and the presentation of some recommendations based on model simulations. By looking at the model results the main two conclusions are:

- The load increase associated to maintenance operations have equal or higher risks that the worst demand scenario (day-week of peak production): in both cases there are filtration sets that are overloaded but while in the second case the high ammonium concentrations in the effluent of the individual set are partially compensated by the highest overall flow which contributes to reduce the highest concentration by dilution, in the first case the dilution effect is much smaller due to the lower overall flow.

- There should not be more than one filter set out of service simultaneously whatever the scenario and the operation regime is. Depending on case, there may be some additional requirements in order to guarantee the quality of the mixed final effluent. In other words, the maintenance activities should take place only during low demand periods and, in some cases, after slightly modifying the ratio Schuwacht-Tiendweg.

Table 33, Table 34 and, Table 35 summarize the specific recommendations for three different scenarios under the current operation regime: when having zero, one or two primary filters with poor ammonium removal. All the recommendations are based on simulation results. The flow limitations vary with the filter that goes out of service. Presumably it is one of the filters with reduced nitrification capacity. But recommendations are given also for the case when one of the filters with high nitrification goes out of service.

Table 33 Recommendations around maintenance operations if none of the primary filters shows poor ammonium removal

Scenario				
Nr. FF filters with good nitrification:		4		
Nr. FF filters with poor nitrification:		0		
Nr. FF filters like FF-05:		1		
FF filters out of service	FF Filter	Plant demand	Flow share recommendations	
1	Any	Q Total > 296 m3/h	Not allowed (guideline exceeded)	
		Q Total < 296 m3/h	170 m3/h > Q Tiendweg > 160 m3/h	Q Schuwacht > 126 m3/h
			Q Tiendweg < 160 m3/h	None
2	Any	Any	Not allowed (guideline exceeded)	

Table 34 Recommendations around maintenance operations if 1 primary filter shows poor ammonium removal

Scenario				
Nr. FF filters with good nitrification:		3		
Nr. FF filters with poor nitrification:		1		
Nr. FF filters like FF-05:		1		
FF filters out of service	FF Filter	Plant demand	Flow share recommendations	
1	Filter with poor activity	Q Total > 296 m3/h	Not allowed (guideline exceeded)	
		Q Total < 296 m3/h	170 m3/h > Q Tiendweg > 160 m3/h	Q Schuwacht > 126 m3/h
			Q Tiendweg < 160 m3/h	None
	Filter with high activity	Q Total > 239 m3/h	Not Allowed	
		Q Total < 239 m3/h	130 m3/h > Q Tiendweg > 120 m3/h	Q Schuwacht > 109 m3/h
			Q Tiendweg < 120 m3/h	None
2	Any	Any	Not allowed (guideline exceeded)	

Table 35 Recommendations around maintenance operations if 2 primary filters show with poor ammonium removal

Scenario				
Nr. FF filters with good nitrification:		2		
Nr. FF filters with poor nitrification:		2		
Nr. FF filters like FF-05:		1		
FF filters out of service	FF Filter	Plant demand	Flow share recommendations	
1	Filter with poor activity	Q Total > 239 m3/h	Not allowed (guideline exceeded)	
		Q Total < 239 m3/h	130 m3/h > Q Tiendweg > 120 m3/h	Q Schuwacht > 109 m3/h
			Q Tiendweg < 120 m3/h	None
	Filter with high activity	Q Total > 258 m3/h	Not Allowed	
		Q Total < 258 m3/h	130 m3/h > Q Tiendweg > 120 m3/h	Q Schuwacht > 128 m3/h
			Q Tiendweg < 120 m3/h	None
2	Any	Any	Not allowed (guideline exceeded)	

Cleaning frequency

The cost of operation of the bio-trickling filters is mainly determined by the application of external washing and renewal of the filter material, the frequency of backwashing and the energy consumed by the pumps. In practice, external washing takes place either when the bed height reaches a maximum or when the performance is too bad. Renewal of the filter material is usually applied after two external washings. The costs of external washing (around 10,000 €) and replacement (around 26,000 €) prevails over the costs associated to backwashing. Consequently, any reduction in the frequency of any of these two operations would result on reducing the operational cost and environmental impact of the filters.

For the current operation regime: the model simulations have confirmed that there should be not more than 0-1 primary filters having poor ammonium removal simultaneously in operation. This would require performing the external washing at a certain frequency. If considering a life cycle in primary filters of around 13-14 months, the need of external washings per year results in up to 4 external washings per year. Any reduction of the number of external washing events in the current situation would depend on improving the current maintenance regime either through incorporating one of the techniques currently under research or through optimization of the backwash programme.

With flow distribution between the filters according to its capacity: the maximum number of primary filters with poor nitrification that is compatible with the compliance of the guideline increases to 2 according to the results shown in Figure 89. This would allow the extension of the service life of the filters which would result in the reduction of the number of external cleanings required in 1-2 per year, which corresponds to yearly saving of around 10,000-20,000 €.

5.5 Others

Supply to Tiendweg through pipe B

With the model, the effects of supplying the Tiendweg filters through the header B has been assessed (from September 2012 the supply takes place continuously through the header A, as indicated in Section 2.4). The results presented in Figure 96 and Figure 97 show the maximum flows compatible with the compliance of the company guideline of 0.1 mg NH_4^+/L under the current operation regime. Figure 96 stands for the nitrification capacity while Figure 97 compares the treatment capacities.

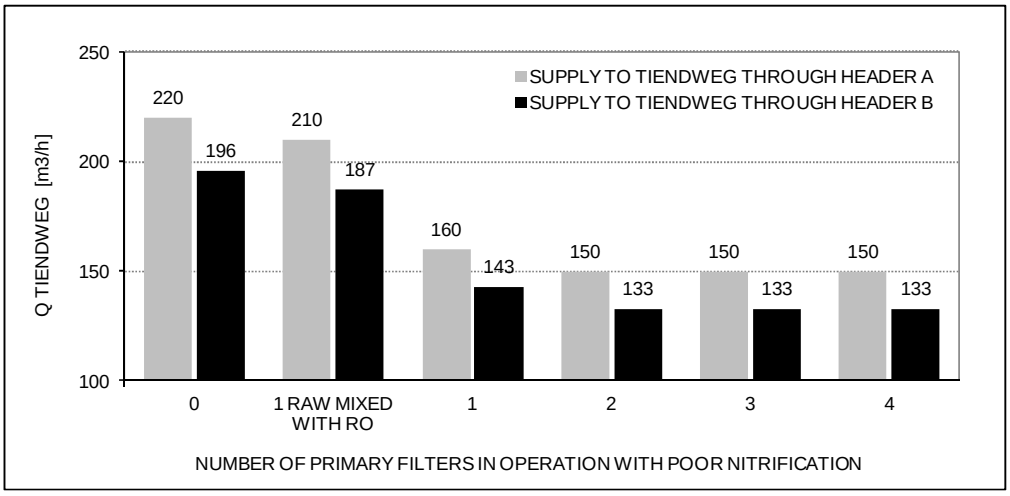

Figure 96 Tiendweg maximum flows to not exceed 0.1 mg NH4+/L in Tiendweg mixed filtrate for different scenarios if the supply is given through header A or B

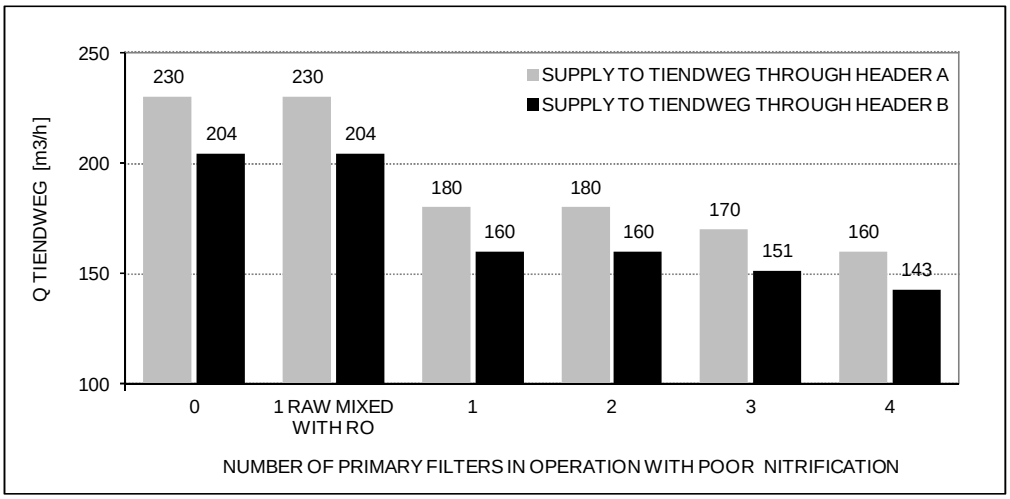

Figure 97 Tiendweg maximum flows to not exceed 0.2 mg NH4+/L in Tiendweg mixed filtrate for different scenarios if the supply is given through header A or B

In general, the shift in the pipe used to feed the Tiendweg filters results in a reduction of the maximum admissible flow. This is due to the higher ammonium concentrations detected in the influent water when the supply is given through the header B (see Table 7). On average, the reduction is around 11%.

For this reason it is recommended not to supply through the pipe B. If that was necessary (i.e. due to planned maintenance operations) then that should be done only during periods of low or very low demand (e.g. week of minimum production demand of the year). Or, alternatively, the flow assigned to the Tiendweg well field should be reduced to the values indicated above.

Concerning what would be the situation if the supply is done through the pipe B with the new operation regime this requires the realization of a new series of simulations as well as the manual determination of a new optimal flow distribution for each scenario. Such analysis has been excluded from this study due to its extension. Nevertheless, everything suggests that the beneficial effects of

distributing the flow according to the specific condition (nitrification capacity) of each filter would be smaller than shown in Figure 89 (curves located higher up and more to the left).

Flow reduction during ripening period in secondary filter

Finally, one more control strategy has been evaluated. This option consists on reducing the flow during the ripening period of the secondary filter (first hours after backwashing) in order to reduce either the risk or the magnitude of ammonium breakthrough in the effluent of secondary filters. The simulation results, which are not included in this document, clearly show that either there are not positive effects or they are not significant enough.

6 Conclusions and recommendations

6.1 Conclusions

Problem description

The so-called nitrification problem in the bio-trickling filters fed by the Tiendweg well field at the treatment plant of Lekkekerk is perceived as two different problems that superpose to each other:

- Problem 1: On one hand, loading variations are often experienced due to fluctuating influent ammonium concentrations and unstable flow rates.

- Problem 2: On the other hand, the nitrification capacity of primary filters relapses. This is repeatedly observed in each cycle after external washing. Typically after 4-6 months of (almost) complete ammonium removal, the cell specific nitrification activity of the primary filter starts decreasing from around 6.74 g NH_4^+ h^{-1} m^{-3} to around 3.72 g NH_4^+ h^{-1} m^{-3} (average values). Consequently the ammonium removal rate drops to 30-60% of the original capacity. It is a gradual process whose causes are unknown and therefore difficult to prevent. Different actions are under research and have provided different results.

Each of these problems results in ammonium breakthrough in the mixed final filtrate during time periods of different extension. While the first issue is prone to produce sporadic ammonium peak values, the second issue can be linked to the non-compliance with the guideline for longer time periods. Despite this difference in the duration, the sequence of events that explain the failure to meet the quality standards is the same: at least one (or several) primary filter works above its critical loading capacity either because a sudden increase in the loading occurs or because the capacity of the filter drops and the load keeps being the same. Any of these events lead to the increase in the ammonium concentration in the effluent of the first filtration step. This enhances the risk of having ammonium breakthrough in the effluent of the secondary filter, especially after being backwashed. The quality of the mixed filtrate of all the Tiendweg filters is mixed with the ammonium-free mixed filtrate derived from the Schuwacht filters, which results in slightly better (lower) ammonium concentration in the final mixed filtrate than in the Tiendweg mixed filtrate.

The first problem, which should be solved by having a more stable production, goes beyond the scope of this thesis. The second problem can be counteracted by adapting the operation to the real situation of the filters. In order to establish if it is possible to guarantee full nitrification a mathematical model has been developed. With the help of the model different ways of improving the operation have been investigated. The research questions have been:

- How can mathematical models be used to guarantee full nitrification (mixed filtrate of all sets always below the company guideline value of 0.10 mg NH_4^+/L)?
- What is an optimal operation and maintenance regime for all filters?
- How should filters be optimally operated during periods of low and high demand?
- How should the filter sets be operated in case of instant loading increase due to maintenance?

SINGLE MODEL

Ammonium removal is mainly due to the size of the colony of nitrifies attached to the filter media grains (biofilms) and their specific nitrification activity. Since biofilms are adaptive systems the model has been used to investigate how environmental conditions influence the removal capacity of the filter. In this respect the process of constructing the model has resulted especially useful for integrating the available knowledge in one single place (the model) and for filling the gaps between processes occurring in the micro-scale (e.g.: internal filter measurements) and the macro-scale (e.g.: operation).

Three of the main aspirations around modelling ammonium removal in a bio-trickling filter have been: first, to acquire better insight into the processes influencing nitrification; second, to prove that the model is able to reasonably predict the response when the filter is operated at different load condition; and, third, to investigate if the relapse in nitrification observed in primary filters is related to physical (e.g.: mass-transfer) or biological (e.g.: inhibition, competition) processes.

Insights on nitrification:

A. Processes:

- It is the balance between opposing factors what ultimately governs the biofilm formation (biomass content) and decides the nitrification capacity of the filter. These factors can be either physical or biological.
- The model shows how the history and operation of the filter (e.g.: load and cleaning actions) influences the biomass content.
- Long-term changes in the load may impact the nitrification capacity by bringing the size of the population of nitrifiers to a new steady state.
- The parameters with the biggest influence are the influent ammonium concentration, the wetting efficiency, the biomass content, the net growth rate, the yield factor and, the residence time.
- The model suggests that the nitrification capacity is also determined by how the biomass is distributed over the depth.

B. Relapse:

- Concerning the identification of bottlenecks in the process the model suggests that there is no transport limitation from the bulk to the surface of the biofilm. The model is not able to provide any insight about what the situation is regarding the transport of substrates and nutrients within the biofilm. Moreover, full-scale measurements indicate that biomass desorption is negligible when compared to the cell number in the filter. Therefore this points to a greater weight on biological factors (e.g. net growth rate) to explain the relapse on nitrification.
- The model suggests that the loading may influence the nitrification capacity of the filter and the rate of relapse in nitrification. This idea is supported by validation experiment results.

Reliability:

- Individual model results provide a general good impression of the reliability of the model.
- Model results are consistent with full-scale internal measurements that have shown that primary filters with poor nitrification have very low cell and sand specific nitrification rates. The results regarding filters with high ammonium removal are not conclusive since there are no site-specific measurements they can be confronted with.
- Nevertheless the model fails on reproducing the fluctuations typically observed in the effluent in primary filters with both high and low ammonium removal. Moreover, the model is not able to reproduce transient behaviours when load conditions shifts. Nevertheless, the model predicts properly the new steady state.
- Additionally, if full-scale filters are operated at very different loads during long periods, the model may require re-calibration.

Consequences on operation:

- Model simulations have indicated that the range of loads within each filter should be operated is relatively narrow. It is believed that this is due to the different characteristic times of biological and hydrodynamic processes occurring in the filters. This is applicable both for filters with low nitrification activity and filters that perform well. This advocates for having a less unstable loading.
- Critical loading might be insufficiently characterized by the ammonium loading rate. This idea is also supported by validation experiment results. In addition to this the model also indicates that the influent ammonium concentration influences more nitrification than the flow.
- The model insinuates that the rate of relapse in nitrification can be reduced by reducing the load. Furthermore, the model also suggest that the negative trend might even be compensated provided that the filter is operated alternating low load long periods and high load short periods.

INTEGRATED MODEL

The integrated model has provided a valuable insight on the interactions between the different filtration sets, steps and streams. The model have been used to: (1) assess the individual nitrification capacity of each filter; (2) assess the overall capacity of the system; (3) predict the mixed effluent quality. With this information, the maximum number of primary filters with poor ammonium removal permissible in order to guarantee full nitrification even the day of maximum demand has been assessed. The above mentioned information has been generated for different 'scenarios' (number of primary filters with poor effluent ammonium concentrations) and demands. The model also distinguishes between 'nitrification capacity' and 'treatment capacity'. The first refers to the maximum capacity of the system based on the individual capacities of the filters. The second considers overloading slightly the system due to the beneficial effect that mixing the Tiendweg filtrate with the

ammonium-free stream coming from Schuwacht has. Two regimes of operation defined by the way the flow is distribution between the different filters have been compared.

Current operation regime

The integrated model has demonstrated that having one single primary filter with poor ammonium removal compromises the overall treatment capacity of the system with the current flow distribution regime (Figure 82).

With the current flow distribution between Schuwacht and Tiendweg the model indicates that the system will work above its treatment capacity (company guideline exceeded) over a third (35%) of the hours of the year if having just one primary filter with poor nitrification in operation. The percentage increases with the number of primary filters that are allowed to operate when showing poor ammonium removal.

The model have confirmed the highly beneficial effect that mixing raw water and permeate water form the nearby reverse osmosis plant has on the effluent of primary filters with relapsed nitrification (see Figure 79). The model also warns about the inconvenience of performing maintenance operations during periods of high demand.

These results advocates for not having primary filters with poor ammonium removal during periods of high demand. For the rest of the year the number of primary filters with poor nitrification should not be higher than one. Likewise maintenance operations should not be realized simultaneously over two filters so that there is never less than four filters at Tiendweg in operation.

One of the major drawbacks of the current control regime is that the number of the known operational parameters is limited. Any improvement is limited to modify either the frequency of cleaning operations or the share that each well field assumes. The first option has significant economic costs. Concerning the second alternative, this would require redefining the well schemes. Moreover, this option might be incompatible with the legal concession on the maximum volume of water that can be abstracted from Schuwacht. For these reasons a new operation strategy has been subsequently investigated.

New operation regime

The new regime basically consists on adapting the flow distribution so that each filtration set receives a load according to its individual capacity. This means that the filters with high nitrification rates will work with higher loads compared to the current situation while filters with poor ammonium removal will work at lower loads.

The results indicate that such way of operating the filters has three important consequences. First, the effluent water quality will be improved (lower peak values, Figure 89) whatever the demand is and whenever the number of primary filters with poor effluent is within the range 1-3. Second, it will lead to a more stable mixed effluent water quality (Figure 88). And, third, it will reduce the need (frequency) of external washing with the corresponding economic savings. The results indicate that the maximum number of primary filters with poor ammonium removal would increase to 2 with the new control strategy. Nevertheless, the model is not able of either confirming or neglecting whether higher loads being applied to filters with full nitrification will contribute to accelerate the apparition of relapse in nitrification and its development or not which could compromise this savings.

The optimum load distribution depends on the scenario considered and requires individual simulations for each specific case. However, some rules of thumb are given (Table 32). In addition to this, it has been investigated if there is an operation setting that may allow minimizing the maintenance requirements without compromising the overall effluent water quality.

In conclusion, the model has confirmed that the optimal response of the system (lower mixed effluent ammonium concentration) requires the individual filtration sets being working closer to their individual optimums rather than being operated at the same common load. This new strategy will help to reduce cost and environmental impact and will ensure the company guideline about ammonium in the mixed effluent during longer times. This does not imply that the problem of relapse in nitrification is solved itself but at least it does not compromise the mixed effluent water quality. Recommendations about how to counteract nitrification at a single level and other research recommendations based on the insights provided by the model are presented in the next section.

6.2 Recommendations

The research performed through modelling of nitrification in the Tiendweg bio-trickling filters have provided better insight into the so called 'nitrification problem' and it has contributed to identify some promising future actions. Although there is extensive information concerning the processes occurring inside the filter, a better understanding of these bio-trickling filters require to fill the gaps between the processes occurring in the micro-scale (e.g.: internal filter measurements) and the macro-scale (e.g.: filter operation and full scale measurements) in order to improve the operation. The developed mathematical model has contributed to that purpose but there are still several issues that require further investigation. They are indicated below. These research recommendations are not necessarily aimed towards a further model-development but they will have also that side-effect.

Increase the operation measurements

A stronger attention on operation measurements is considered necessary and one of previous steps before the optimization of the operation of the filters. Some of these actions are currently under development (e.g. the continuous monitoring of the raw water quality through the development of soft sensors). Additionally, the installation of individual flow meters at each filter should be considered as the model has proved that the range of loads within the filter should be operated are relatively narrow.

Tailored measurements for a better knowledge of the dynamics of nitrification

A tailored campaign of continuous measurements to be performed upstream-downstream some selected filters is recommended. It is firmly believed that the occurrence of ammonium breakthrough at the effluent of a single filter is partially the cause of insufficient understanding of the dynamics of nitrification in these filters. The campaign could consist on simultaneous control of the influent and effluent in three filters: two primary filters with high and poor nitrification respectively; and one secondary filter. The campaign should start at the middle of the operation cycle and end at the middle of the next cycle. By doing this, the measurement would provide a valuable insight into the dynamics of growth of the nitrifiers but also on the issue of backwashing and how it may affect nitrification in each type of filter. The same data set could be used to characterize better the transient behaviour and the critical loading since it is likely that the filters are operated at different loading conditions during the experiment. Ideally, this also could provide some information about the different time scales of the processes occurring in bio-trickling filters

Nitrifiers and biofilm characteristics

Nitrification is strongly determined by the presence of the right organisms in the appropriate numbers and with a level of activity high enough. The reliability of the current model is partially limited to the current range of operational conditions. On the contrary, with a stronger insight in nitrification kinetics a wider range of conditions could ideally be modelled. Neither the biofilm characteristics and processes nor the specific biological and kinetic parameters are sufficiently known. For that reason, several of the research recommendations are aimed to perform more internal measurements.

- Size of the population of nitrifiers and effective growth rate: site specific measurements are recommended in order to have better insight into the variability of the population of ammonia-oxidizing organisms over the filter life cycle.

- Stratification of the nitrification activity: it would be also interesting to know how microbial abundance is over the depth of the filter and how it differs between filters with poor nitrification and filters with good nitrification. Although literature states that backwashing does not affect the biomass stratification, there is no complete consensus on that and the effects may depend on the backwash program, the characteristics of the biofilm (composition, density, thickness and strength of attachment) and the existence of inorganic deposits. Therefore site-specific data regarding the stratification of ANO population before and after backwash is of interest.

- High-flow rates and biomass detachment: although in attached growth systems the hydraulic retention time is decoupled from the solid retention time, it should be noted that changing the hydraulic conditions may also affect the growth through detachment. Therefore, the effect of both high and low flow rates on the nitrification efficiency of both primary and secondary filters should be further investigated through operating the filters at different flow rates for short times.

- Long-term response to changes in the load: the proposed new operation regime implies changing the loading applied on the long term. This may have implications on the biomass

population existing in the filter and, consequently on its ammonium removal capacity. Additionally, there is the risk that if a primary filter in good conditions is operated at higher loads than currently, then it might happen that the relapse in nitrification develops faster. These aspects should be studied more carefully so that it is better known how they respond in the long-term to changes in their loads.

- Specific-nitrification rate and yield factor: the activity of nitrifying microorganisms present in Tiendweg filters showing high ammonium removal should be investigated since the available internal measurements are limited to filters with poor nitrification and Schuwacht filters. The last ones may not be entirely representative of the situation at Tiendweg filters with high ammonium removal as they work at very different loading (much lower) and the absence of simultaneous iron biological oxidation.

Counteracting relapse in nitrification

There are different options that should be investigated around ways of counteracting the relapse in nitrification in primary filters. All the presented options are direct or indirectly linked to backwashing.

- Achievement of higher expansion during backwash: the choice of a suitable filter medium seems to have a significant impact on the efficiency of backwashing. Previous research has demonstrated that one way of delaying the relapse of nitrification was by substituting one single media sand filters by dual media anthracite and sand filters. The hypothesis is that the improvement was caused by the achievement of expansion during backwash. In that respect, it should be investigated if the substitution of the sand layer by anthracite in the primary filters would contribute to delay even more the deterioration of nitrification.

- Different backwashing frequency: if the efficiency of backwash (measured through the achieved level of expansions) impacts the rate of relapse in nitrification, it is reasonable to think that the same would happen with the frequency. Consequently, it is recommended to investigate how the rate of relapse may change by modifying the frequency of backwashing.

- Removal of fluffy biomass: backwash could be re-oriented to remove not only inorganic deposits but also inert or inactive biomass. That implies that either the current programme is re-defined or that a targeted backwash programme is defined and alternated with the current programme. A less vigorous backwash could be useful to prevent fluffy biomass structures from interfering bio-uptake by active cells. If backwashing is not an option, then the alternative of applying very high flows during a short time period could also be studied.

Thin biofilm hypothesis

In order to prove the hypothesis of thin biofilm, it is recommended to perform the following experiments (Sin et al., 2008). The average biofilm thickness of sand particles could be measured based on measurements of the Kjeldahl nitrogen in sand. Next, the biofilm content of the sand can be calculated assuming a certain percentage of nitrogen content on the mass based on site-specific measurements. Then, the volume of the biofilm layer could be calculated with the measured biofilm density. Finally the biofilm could be estimated by dividing the biofilm volume to the surface area of the sand using the average sand diameter. Furthermore, the same procedure could be repeated at different times in order to have a first assessment on how the biofilm thickness varies with time. Although these may be seen as an excessive approximation, they would allow to have a first estimation of the Thiele number, which is defined as the biofilm internal resistance to mass transfer: at low Thiele number values implies having a high internal substrate transfer rate (this is one of the hypotheses the model is based on) so that the substrate penetrates deep into the biofilm and the internal resistance to mass transfer can be neglected.

Impact of reduced aeration

Both the simulation results and full scale measurements suggest that aerations performs in general well, achieving complete oxygen saturation of the bulk water and a good carbon dioxide removal, with the consequent increase in pH. In that respect, the concentration in the bulk would be mainly affected by the microbial kinetics and not by mass transfer parameters, as long as the forced ventilation system remains in operation. It is proposed to reduce air flow in secondary filter in order to assess whether the ventilation system is working above what is actually required by the filters.

Mass-transfer rates in triple-media filters

Most of the literature consulted refers to biological wet filters that perform nitrification but so far there are not so may documented examples of trickling filters used for that purpose in the field of water

treatment. Out of that application, the closest case consists on bio-dry-trickling filters used for gas treatment. Different ways of assessing the transfer rates could be investigated so it is possible to have some site-specific measurements of the true transfer-rates. Ideally, they could be measured at different filter ages and run times.

Implementation of the new operation regime

Since there are individual flow meters in two filters, motorized valves could be installed in these two filters in order to check the model and as a previous phase to start implementing the optimization. Any future shift in the manner the filters are operated, from a constant and fixed regime towards an a more flexible operation should take place in a gradual manner. The two mentioned filters could be used to further validate the model results and hypotheses. The actions listed before could be performed in any of these two filters so that the information gathered covers all the manipulated (external) variables affecting nitrification. The new gathered information will contribute to a better understanding of how the operation conditions impact the development of the biofilm. With this new information the model calibration could be re-adjusted if necessary in order to increase the model reliability.

7 References

BOLLER, M., GUJER, W. & TSCHUI, M. 1994. Parameters affecting nitrifying biofilm reactors. Water Science and Technology, 29, 10-11.

BOLTZ, J., MORGENROTH, E., BROCKMANN, D., BOTT, C., GELLNER, W. & VANROLLEGHEM, P. 2011. Systematic evaluation of biofilm models for engineering practice: components and critical assumptions. Water Science and Technology, 64, 930.

BROCKMANN, D., ROSENWINKEL, K. H. & MORGENROTH, E. 2008. Practical identifiability of biokinetic parameters of a model describing two-step nitrification in biofilms. Biotechnology and Bioengineering, 101, 497-514.

CHEN, S., LING, J. & BLANCHETON, J.-P. 2006. Nitrification kinetics of biofilm as affected by water quality factors. Aquacultural Engineering, 34, 179-197.

CLEGG, S. L. & WHITFIELD, M. 1995. A chemical model of seawater including dissolved ammonia and the stoichiometric dissociation constant of ammonia in estuarine water and seawater from −2 to 40°C. Geochimica et Cosmochimica Acta, 59, 2403-2421.

CRANK, J. 1975. The Mathematics of Diffusion: 2d Ed, Clarendon Press.

CRITTENDEN, J. C., TRUSSELL, R. R., HAND, D. W., HOWE, K. J. & TCHOBANOGLOUS, G. 2012. MWH's Water Treatment - Principles and Design (3rd Edition). John Wiley & Sons.

DE MOEL, P. J., VERBERK, J. Q. & VAN DIJK, J. 2006. Drinking water: principles and practices, World Scientific.

DE VET, W. 2011. Biological drinking water treatment of anaerobic groundwater trickling filters. TU Delft.

DE VET, W., DINKLA, I., ABBAS, B., RIETVELD, L. & VAN LOOSDRECHT, M. 2012a. Gallionella spp. in trickling filtration of subsurface aerated and natural groundwater. Biotechnology and Bioengineering, 109, 904-912.

DE VET, W., DINKLA, I., MUYZER, G., RIETVELD, L. & VAN LOOSDRECHT, M. 2009a. Molecular characterization of microbial populations in groundwater sources and sand filters for drinking water production. Water Research, 43, 182-194.

DE VET, W., DINKLA, I., RIETVELD, L. & VAN LOOSDRECHT, M. 2011a. Biological iron oxidation by< i> Gallionella</i> spp. in drinking water production under fully aerated conditions. Water research, 45, 5389-5398.

DE VET, W., KLEEREBEZEM, R., VAN DER WIELEN, P., RIETVELD, L. & VAN LOOSDRECHT, M. 2011b. Assessment of nitrification in groundwater filters for drinking water production by qPCR and activity measurement. Water research, 45, 4008-4018.

DE VET, W., RIETVELD, L. & VAN LOOSDRECHT, M. 2009b. Influence of iron on nitrification in full-scale drinking water trickling filters. Journal of Water Supply: Research and Technology—AQUA, 58, 247-256.

DE VET, W., VAN GENUCHTEN, C., VAN LOOSDRECHT, M. & VAN DIJK, J. 2010. Water quality and treatment of river bank filtrate. Drinking Water Eng. Sci, 3, 79-90.

DE VET, W., VAN LOOSDRECHT, M. & RIETVELD, L. 2012b. Phosphorus limitation in nitrifying groundwater filters. Water research, 46, 1061-1069.

DE VET, W. W. J. M., DINKLA, I. J. T., RIETVELD, L. C. & VAN LOOSDRECHT, M. C. M. 2011c. Biological iron oxidation by Gallionella spp. in drinking water production under fully aerated conditions. Water Research, 45, 5389-5398.

DE VET, W. W. J. M., RIETVELD, L. C. & VAN LOOSDRECHT, M. C. M. 2009c. Influence of iron on nitrification in full-scale drinking water trickling filters. Journal of Water Supply Research and Technology-Aqua, 58, 247-256.

DORADO, A. D., RODRÍGUEZ, G., RIBERA, G., BONSFILLS, A., GABRIEL, D., LAFUENTE, J. & GAMISANS, X. 2009. Evaluation of Mass Transfer Coefficients in Biotrickling Filters: Experimental Determination and Comparison to Correlations. Chemical Engineering & Technology, 32, 1941-1950.

EBERL, H. J., PICIOREANU, C., HEIJNEN, J. J. & VAN LOOSDRECHT, M. C. M. 2000. A three-dimensional numerical study on the correlation of spatial structure, hydrodynamic conditions, and mass transfer and conversion in biofilms. Chemical Engineering Science, 55, 6209-6222.

EBERT, H. 2006. Mathematical modeling of biofilms, IWA publishing.

GUJER, W. & BOLLER, M. 1986. Design of a nitrifying tertiary trickling filter based on theoretical concepts. Water Research, 20, 1353-1362.

HAMDI, M. 1995. Biofilm thickness effect on the diffusion limitation in the bioprocess reaction: Biofloc critical diameter significance. Bioprocess engineering, 12, 193-197.

HENZE, M. 2008. Biological Wastewater Treatment: Principles, Modeling, and Design, International Water Assn.

ILIUTA, I. & LARACHI, F. Ç. 2006. Dynamics of cells attachment, aggregation, growth and detachment in trickle-bed bioreactors. Chemical Engineering Science, 61, 4893-4908.

KATSOYIANNIS, I. A. & ZOUBOULIS, A. I. 2004. Biological treatment of Mn(II) and Fe(II) containing groundwater: kinetic considerations and product characterization. Water Research, 38, 1922-1932.

KEEN, G. & PROSSER, J. 1987. Steady state and transient growth of autotrophic nitrifying bacteria. Archives of microbiology, 147, 73-79.

KIM, S. & DESHUSSES, M. A. 2008. Determination of mass transfer coefficients for packing materials used in biofilters and biotrickling filters for air pollution control. 1. Experimental results. Chemical Engineering Science, 63, 841-855.

KISSEL, J. C. 1986. Modeling mass transfer in biological wastewater treatment processes. Water Science & Technology, 18, 35-45.

KRAAKMAN, N. J., ROCHA-RIOS, J. & VAN LOOSDRECHT, M. C. 2011. Review of mass transfer aspects for biological gas treatment. Applied microbiology and biotechnology, 91, 873-886.

LAWLER, D. & NASON, J. 2006. Granular media filtration: old process, new thoughts. Water Science & Technology, 53, 1-7.

LING, J. & CHEN, S. 2005. Impact of organic carbon on nitrification performance of different biofilters. Aquacultural engineering, 33, 150-162.

LOGAN, B. E. 1993. Oxygen transfer in trickling filters. Journal of Environmental Engineering, 119, 1059-1076.

MANEM, J. & RITTMANN, B. 1990. Scaling procedure for biofilm processes. Water science and technology, 22, 329-346.

MORGENROTH, E. & WILDERER, P. A. 2000. Influence of detachment mechanisms on competition in biofilms. Water Research, 34, 417-426.

ONDA, K., TAKEUCHI, H. & OKUMOTO, Y. 1968. Mass transfer coefficients between gas and liquid phases in packed columns. Journal of Chemical Engineering of Japan, 1, 56-62.

PARKER, D., LUTZ, M., DAHL, R. & BERNKOPF, S. 1989. Enhancing reaction rates in nitrifying trickling filters through biofilm control. Journal (Water Pollution Control Federation), 618-631.

PICIOREANU, C., VAN LOOSDRECHT, M. & HEIJNEN, J. 1997. Modelling the effect of oxygen concentration on nitrite accumulation in a biofilm airlift suspension reactor. Water Science and Technology, 36, 147-156.

PICIOREANU, C., VAN LOOSDRECHT, M. & HEIJNEN, J. 1999. Discrete-differential modelling of biofilm structure. Water Science and Technology, 39, 115-122.

PICIOREANU, C., VAN LOOSDRECHT, M. C. & HEIJNEN, J. J. 2000a. Effect of diffusive and convective substrate transport on biofilm structure formation: a two-dimensional modeling study. Biotechnology and bioengineering, 69, 504-515.

PICIOREANU, C., VAN LOOSDRECHT, M. C. & HEIJNEN, J. J. 2000b. A theoretical study on the effect of surface roughness on mass transport and transformation in biofilms. Biotechnology and Bioengineering, 68, 355-369.

PICIOREANU, C., VAN LOOSDRECHT, M. C. & HEIJNEN, J. J. 2001. Two-dimensional model of biofilm detachment caused by internal stress from liquid flow. Biotechnology & Bioengineering, 72, 205-218.

QUEINNEC, I., OCHOA, J. C., WOUWER, A. V. & PAUL, E. 2006. Development and calibration of a nitrification PDE model based on experimental data issued from biofilter treating drinking water. Biotechnology and Bioengineering, 94, 209-222.

RASMUSSEN, K. & LEWANDOWSKI, Z. 1998. Microelectrode measurements of local mass transport rates in heterogeneous biofilms. Biotechnology and Bioengineering, 59, 302-309.

RIETVELD, L. C. 2005. Improving operation of drinking water treatment through modelling.

SATTERFIELD, C. N. 1975. Trickle-bed reactors. AIChE Journal, 21, 209-228.

SAVENIJE, H. 2009. HESS Opinions" The art of hydrology". Hydrology and Earth System Sciences, 13, 157.

SIEGRIST, H. & GUJER, W. 1987. Demonstration of mass transfer and pH effects in a nitrifying biofilm. Water Research, 21, 1481-1487.

SIN, G., WEIJMA, J., SPANJERS, H. & NOPENS, I. 2008. Dynamic model development and validation for a nitrifying moving bed biofilter: Effect of temperature and influent load on the performance. Process Biochemistry, 43, 384-397.

STEMBAL, T., MARKIC, M., RIBICIC, N., BRISKI, F. & SIPOS, L. 2005. Removal of ammonia, iron and manganese from groundwaters of northern Croatia - pilot plant studies. Process Biochemistry, 40, 327-335.

SUZUKI, I., DULAR, U. & KWOK, S. 1974. Ammonia or Ammonium Ion as Substrate for Oxidation by Nitrosomonas europaea Cells and Extracts. JOURNAL OF BACTERIOLOGY, 556-558.

TATARI, K., SMETS, B. F. & ALBRECHTSEN, H. J. 2013. A novel bench-scale column assay to investigate site-specific nitrification biokinetics in biological rapid sand filters. Water Research, 47, 6380-6387.

TEKERLEKOPOULOU, A. G., PAVLOU, S. & VAYENAS, D. V. 2013. Removal of ammonium, iron and manganese from potable water in biofiltration units: A review. Journal of Chemical Technology & Biotechnology, n/a-n/a.

UPADHYAYA, G., CLANCY, T. M., SNYDER, K. V., BROWN, J., HAYES, K. F. & RASKIN, L. 2012. Effect of air-assisted backwashing on the performance of an anaerobic fixed-bed bioreactor that simultaneously removes nitrate and arsenic from drinking water sources. Water Research, 46, 1309-1317.

UPADHYAYA, G., JACKSON, J., CLANCY, T. M., HYUN, S. P., BROWN, J., HAYES, K. F. & RASKIN, L. 2010. Simultaneous removal of nitrate and arsenic from drinking water sources utilizing a fixed-bed bioreactor system. Water Research, 44, 4958-4969.

USEPA 1984. Methods for the Chemical Analysis of Water and Wastewater, Environmental Protection Agency

VAN DEN AKKER, B., HOLMES, M., CROMAR, N. & FALLOWFIELD, H. 2008. Application of high rate nitrifying trickling filters for potable water treatment. Water research, 42, 4514-4524.

VAN DER AA, L. T. J. 1999. Nitrificatie in snelfilters: Praktijkonderzoek Rivier-Plassenwaterleiding GWA en modellering. MSc, TU Delft, Delft University of Technology

VAN HULLE, S. W. H., VERSTRAETE, J., HOGIE, J., DEJANS, P. & DUMOULIN, A. 2007. Modelling and simulation of a nitrification biofilter for drinking water purification. Water SA, 32, 257-264.

VAN KREVELEN, D. & KREKELS, J. T. C. 1948. Rate of Dissolution of Solid Substances Part I. Rate of mass transfer in granular beds (Physical dissolution). Recueil des Travaux Chimiques des Pays-Bas, 67, 512-520.

VAN LOOSDRECHT, M., HEIJNEN, J., EBERL, H., KREFT, J. & PICIOREANU, C. 2002. Mathematical modelling of biofilm structures. Antonie van Leeuwenhoek, 81, 245-256.

VAN LOOSDRECHT, M., LYKLEMA, J., NORDE, W. & ZEHNDER, A. 1990. Influence of interfaces on microbial activity. Microbiological Reviews, 54, 75-87.

VAN LOOSDRECHT, M. C. M., EIKELBOOM, D., GJALTEMA, A., MULDER, A., TIJHUIS, L. & HEIJNEN, J. J. 1995. Biofilm structures. Water Science and Technology, 32, 35-43.

VAN SCHAGEN, K. 2009. Model-based control of drinking-water treatment plants.

VAYENAS, D. V., PAVLOU, S. & LYBERATOS, G. 1997. Development of a dynamic model describing nitritification and nitratification in trickling filters. Water Research, 31, 1135-1147.

VROM, D. M. O. 2001. Waterleidingbesluit. In: NEDERLANDEN, S. V. H. K. D. (ed.).

WANNER, O. & REICHERT, P. 1996. Mathematical modeling of mixed-culture biofilms. Biotechnology and Bioengineering, 49, 172-184.

WHO, G. 2006. Guidelines for drinking water quality. WHO: World Health Organization.

WIK, T. 2003. Trickling filters and biofilm reactor modelling. Reviews in Environmental Science and Biotechnology, 2, 193-212.

WILKE, C. R. & CHANG, P. 1955. Correlation of diffusion coefficients in dilute solutions. AIChE Journal, 1, 264-270.

ZHANG, T., FU, Y. & BISHOP, P. 1994. Competition in biofilms. Water Science and Technology, 29, 263-270.

ZHANG, T. C. & BISHOP, P. L. 1996. Evaluation of substrate and pH effects in a nitrifying biofilm. Water environment research, 1107-1115.

ZHU, I. X., GETTING, T. & BRUCE, D. 2010. Review of biologically active filters in drinking water applications. Journal of the American Water Works Association, 102.

ZHU, S. & CHEN, S. 2001. Impacts of Reynolds number on nitrification biofilm kinetics. Aquacultural Engineering, 24, 213-229.

Annexes

A.1 Process flow diagram

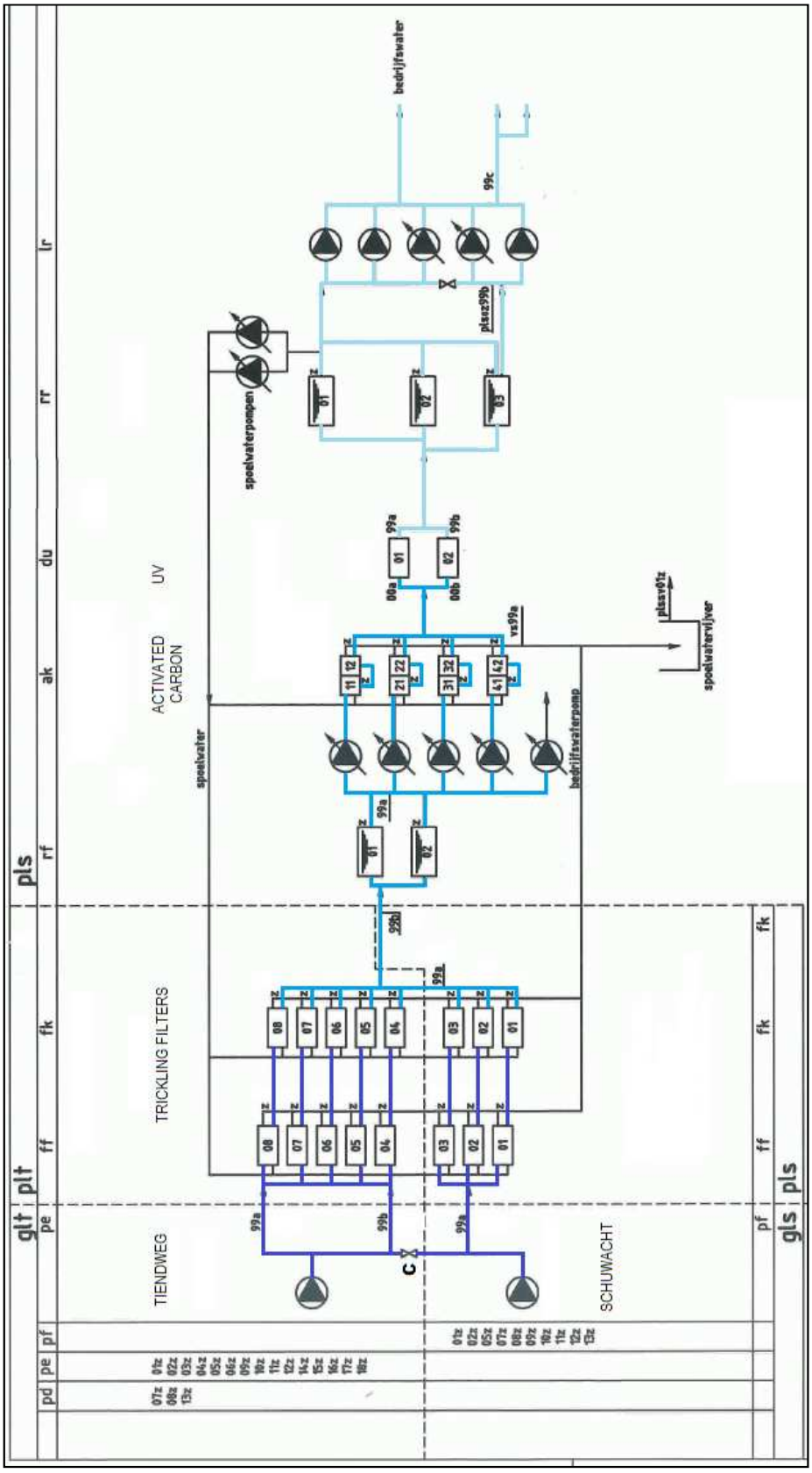

A.2 Full-scale measurements

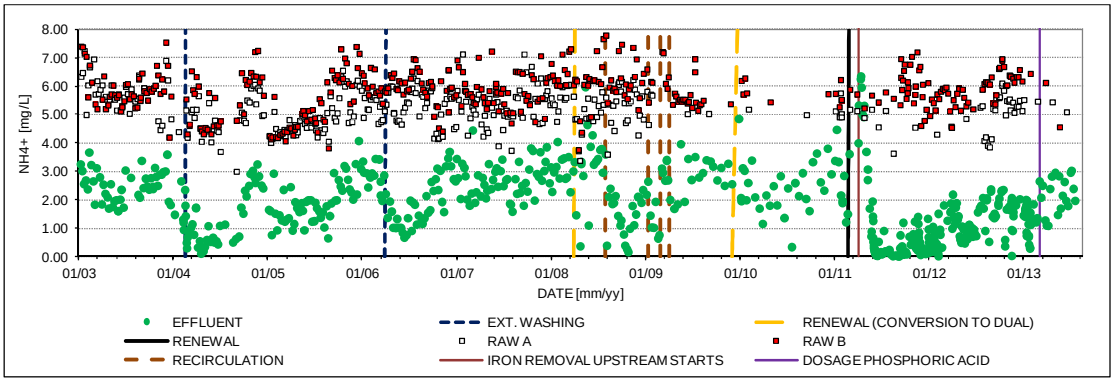

Figure A2.1 Influent and effluent ammonium concentrations and maintenance actions in filter FF-04

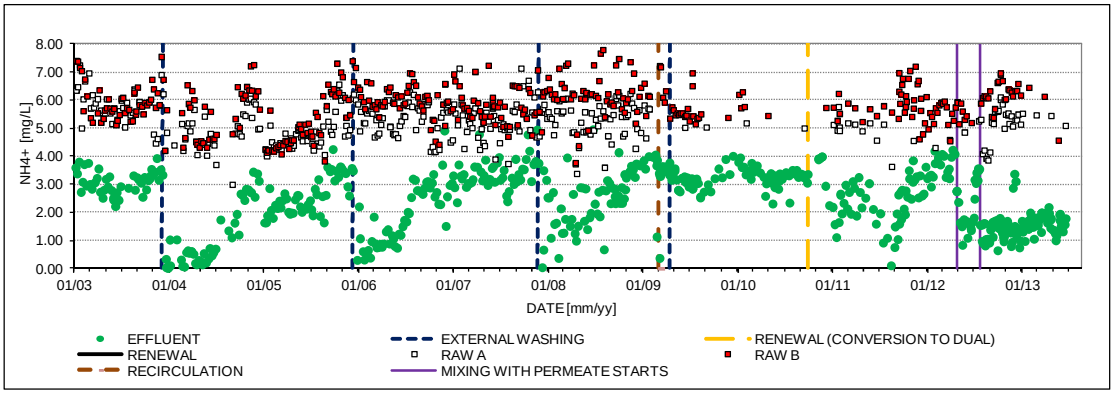

Figure A2.2 Influent and effluent ammonium concentrations and maintenance actions in filter FF-05

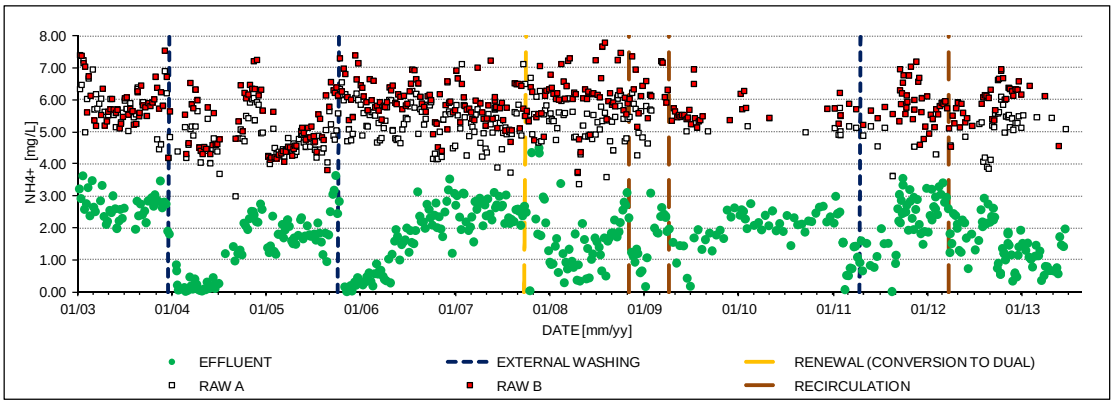

Figure A2.3 Influent and effluent ammonium concentrations and maintenance actions in filter FF-06

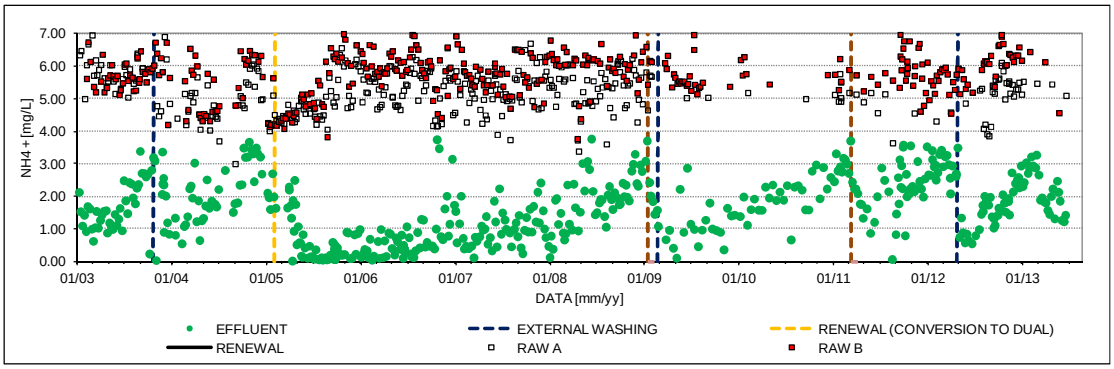

Figure A2.4 Influent and effluent ammonium concentrations and maintenance actions in filter FF-07

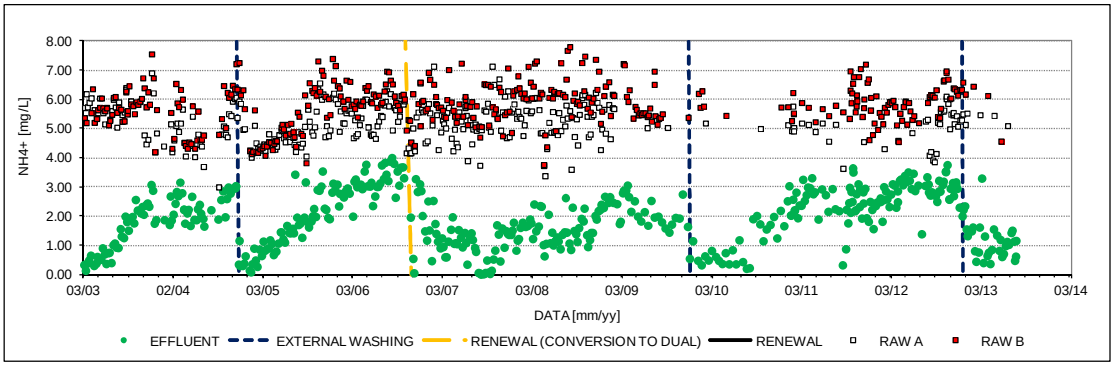

Figure A2.5 Influent and effluent ammonium concentrations and maintenance actions in filter FF-08

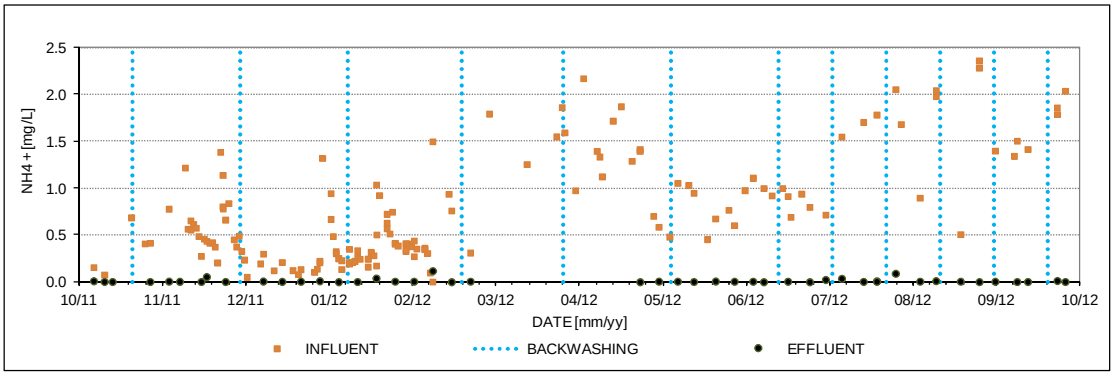

Figure A2.6 Influent and effluent ammonium concentrations and maintenance actions in filter FK-04

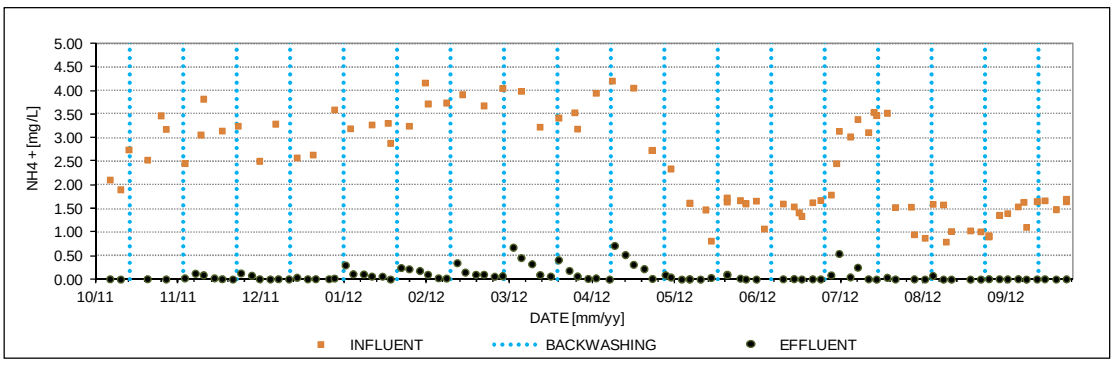

Figure A2.7 Influent and effluent ammonium concentrations and maintenance actions in filter FK-05

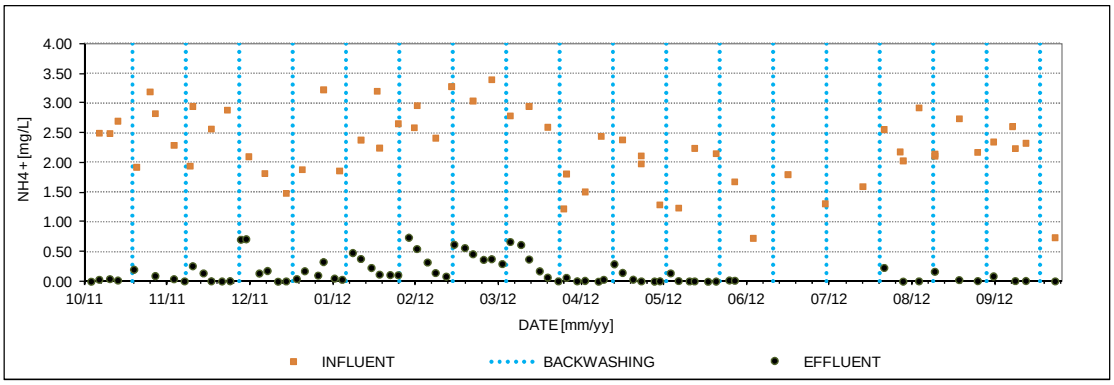

Figure A2.8 Influent and effluent ammonium concentrations and maintenance actions in filter FK-06

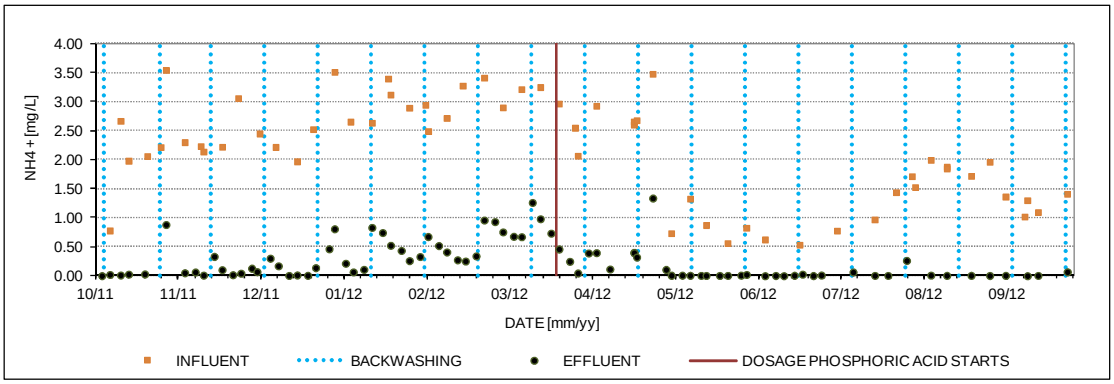

Figure A2.9 Influent and effluent ammonium concentrations and maintenance actions in filter FK-07

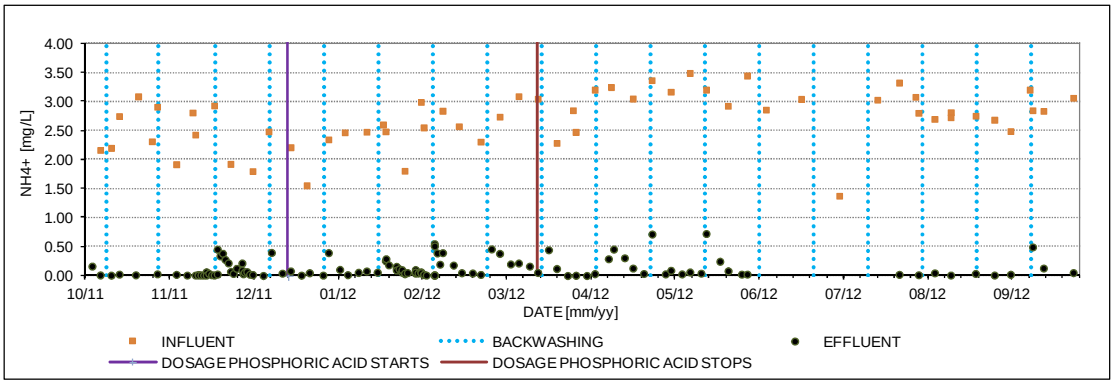

Figure A2.10 Influent and effluent ammonium concentrations and maintenance actions in filter FK-08

A.3 Theoretical background on biofilms

A biofilm is a layer-like aggregation of microorganisms attached to a solid surface. Theoretically, in an aqueous medium, biological conversion processes (as biological nitrification) can equally happen under a suspended growth environment or in an attached growth system (Chen et al., 2006). The first one refers to the case where the microorganisms freely move in the bulk water. In the second case, microorganisms grow in a biofilm that is attached to the surface of a solid support medium. In trickling filters, microorganisms are immobilized which is why nitrification mainly corresponds to the second case (Wik, 2003). These systems are also known as fixed film systems.

Autotrophic versus heterotrophic

The characteristics of biofilms depend on the conditions they are exposed to. In standard trickling filters, the two possible extremes consist on having either purely autotrohophic or purely heterotrophic biofilms. The predominant conditions at each specific place determine which one prevails. The two types of microorganisms may compete for oxygen, basic nutrients and space. In an environment where organic matter is available in high concentrations, heterotrophs are expected to grow faster and out-compete slower growing nitrifiers for oxygen in the biofilm. Trickling filters for waste water treatment purposes are used to remove both organic and inorganic compounds. Therefore, the operation conditions needed are such that both kinds of microorganisms are able to develop. But trickling filters for drinking water production have a different purpose since they are used to remove inorganic compounds naturally present in anaerobic groundwater such as iron, manganese, ammonium and others. In that case, autotrophic organisms prevail.

Governing processes

Since ammonium removal is mainly the cause of the growth of the nitrifiers that are attached to the filter media grains, a better knowledge of the processes influencing the development of biofilm is crucial. Some of the interactions that decide the biofilm characteristics can be intuitively understood but various others can be really complex (Van Loosdrecht et al., 2002). Their characteristics are the result of a series of processes which can be classified as 'positive' and 'negative' processes (Picioreanu et al., 2000b): while the former ones contribute to the development of the biofilm (e.g., cell attachment, cell growth), the latter ones lead to biofilm shrinking (e.g., cell death and cell detachment). It has been experimentally proved that it is the balance between these opposing processes what ultimately governs the biofilm formation and decides its structural properties (van Loosdrecht et al., 1995, Van Loosdrecht et al., 2002).

Some authors have stated that biomass detachment from the biofilm is one of the primary processes balancing the biofilm development in biofilm reactor (van Loosdrecht et al., 1995). It consists on the loss of cells or aggregates of cells from the biofilm attached to the carrier into the bulk liquid and it can be caused by a diversity of mechanisms being erosion, sloughing and abrasion among the most common ones.

Erosion and abrasion are smaller processes in comparison to sloughing. Both are thought to cause small losses of cells. The first one is caused by shear forces of the liquid in contact with the biofilm. The second one is caused by the collision of biofilm support particles with each other during, for instance, backwashing. Sloughing refers to the loss of large portions of the biofilm through detachment. The causes are diverse and usually this kind of event is linked both to external (e.g. shear rate) and internal causes (e.g. biofilm resistance and characteristics). In general, systems with high shear forces, there are higher chances of high detachment occurring in the form of erosion, which results in smoother biofilms. In systems with low detachment forces, detachment occurs mainly by sloughing and biofilms tend to become more porous.

The same processes that explain the steady state reached (or not) by the biofilm, can be used for a better understanding of the process of microbial colonization. After filter material replacement, the cell population attached to the surface of the filter media is thought to be very low. Biomass growth only may happen after microorganisms colonize the carriers. The process is thought to happen according to the following sequence of steps (Van Loosdrecht et al., 1990): first, the microorganism, which are naturally present in the environment, need to reach the carriers. Following this is initial adhesion which can be reversible or irreversible. After the microorganisms have been deposited on the carriers surface, special cell surface structures such as polymers may develop so that attachment of cells to each other and to the solid surface happens. Last in the sequence is surface colonization: biofilm develop if cells start growing and new cells remain attached to each other. Therefore, cells aggregation is a complex process with multiple steps like motility, collision and adhesion.

Fluid dynamics, transport processes and biofilm characteristics

Therefore, biofilms are adaptive systems that result from environmental conditions and respond to them. The issue then becomes if the processes can be affected by operating conditions. Results from different authors are consistent affirming the influence of turbulence on the performance of bio-filters. It can be instinctively understood that kinetics are influenced by mass transport issues (Rasmussen and Lewandowski, 1998): a slow substrate transfer regime is more likely to occur with slow flow (high external mass transfer resistance) or with small substrate diffusivities in the biofilm (high internal resistance to mass transfer); by contrast: a substrate non-limited case is more likely to occur with fast flow and fast internal diffusion.

Literature indicates that a determining factor controlling the biofilm characteristics is the ratio between biofilm surface loading rate and detachment rate (Van Loosdrecht et al., 2002). While the substrate uptake is determined by the amount of nitrifying biomass, the specific growth rate and the yield coefficient, the substrate supply is determined by the transport rates. In addition, the ratio between bacterial growth and the substrate transfer rate to the biofilm influences the biofilm roughness and porosity which in turn affect the mass transfer processes (Picioreanu et al., 1999). When a biofilm is rate-limited it tends to become compact and homogeneous. When the diffusion is the rate-limiting step, the biofilm tends to be porous and heterogeneous. Hence, a rough and open biofilm with high porosity are more prone to occur with slow substrate transfer regimes, which may be generated either by slow flows (low Reynolds numbers and high external mass transfer resistance) or by small substrate diffusivity in the biofilm (high internal resistance to mass transfer). In opposition, with high surface transfer rates (fast flow and fast internal diffusion), no substrate limitation is likely to occur and therefore the biofilm develops as a more compact structure.

It can be intuitively understood that with a lower substrate loading rate a thinner biofilm will be formed. Also, a higher shear rate will lead to a thinner biofilm. In spherical biofilms, any increase in the thickness of the biofilm implies an increase in the surface area which involves both the decrease in the surface loading rate but the increase in the shear rate. Substrate concentration at the biofilm surface and fluid shear are among the most cited factors controlling nitrification in biofilms (Manem and Rittmann, 1990). Both parameters are influenced by the fluid dynamics existing in the areas near to the biofilm surface. Some authors (Zhu and Chen, 2001) have shown how the local Reynolds number, representing the hydraulic conditions at the biofilm surface, has a significant impact on the nitrification rate. Higher nitrification rates have been reported with high turbulence values (Ling and Chen, 2005). Turbulence would affect inversely the thickness of the water film around the biofilm and, consequently, the transfer resistance of substrates from the bulk liquid into the biofilm. For instance, it has been hypothesized that the oxygen transfer rate may limit the rate of ammonium oxidation in nitrifying trickling filters (Parker et al., 1989). According to this idea, having 'thin' nitrifying biofilms is critical for keeping the nitrification rate high.

Fluid dynamics may play a role not only in transport processes but also in biomass detachment and biofilm characteristics. If the biofilm is grown at low sheer rates, the biofilm grows out more rapidly and the main detachment is caused by regular sloughing periods. Contrarily, at high shear rates (or low biofilm growth rates), the biofilm is subjected to continuous erosion processes resulting in a smoother biofilm (Van Loosdrecht et al., 2002). Dry filters are thought to operate at laminar flow (Kraakman et al., 2011). In theory, in trickling filters the shear forces are expected not to be high and, therefore, biofilm growth is not thought to be controlled by them. But unluckily both mass transfer and fluid shear rates are often difficult to predict under trickling flow conditions.

An example of all this is the diffusion of oxygen. For instance, in some places the oxygen could penetrate not completely into the biofilm. In that case, underneath, the environment could be anaerobic. Similarly, if all substrate is consumed in the outer layers, the microorganisms may enter in an endogenous respiration state and lose their ability to cling to the substratum. This issue together with the shear stress makes biofilm especially vulnerable to be washed away, causing sloughing. Sloughing, besides reducing the removal capacity of the filter may cause clogging if the sloughing intensity is very high (Wik, 2003).

Consequently the question of how fluid conditions within the reactor and biofilm characteristics influence nitrification is entirely valid and becomes one of the core issues to be understood for a correct model conceptualization (Eberl et al., 2000).

Transport processes

The substrate and nutrients transport from the bulk to the biofilm in order to feed the microorganisms can be understood as a two-step process (Chen et al., 2006): external mass transfer and internal mass diffusion.

External mass transfer

The first step comprises advection and molecular diffusion occurring in the bulk liquid near to the biofilm. External mass transfer is usually expressed through the Sherwood number, which represents the ratio between the total external mass transport and the diffusive transport (Van Loosdrecht et al., 2002). Diffusive transport is due to Brownian motion, which corresponds to random contacts. By contrast, in convective transport substrate moves due to the flow.

In the pores and channels existing in the biofilm (Van Loosdrecht et al., 2002) there are higher liquid velocities and the mass transfer is thought to be dominated by convection. Diffusive transport is slow compared with transport by convective flow due to its nature. In particular, around the biofilm there is a water film that acts as inter-phase layer between the biofilm and the bulk water. Diffusive transport is in exclusive responsible for crossing any diffusion layer, across which no convection can take place. Hence, the supply of substrates into the bacteria film in the biofilm is a diffusion-controlled process driven by the concentration gradient across the biofilm (Chen et al., 2006). For all these reasons, when the overall mass transfer from the bulk liquid to the biofilm is considered, diffusive transport is likely to control the process.

Internal mass diffusion

Internal mass diffusion refers to the transport processes occurring within the biofilm. Existing information for biofilm systems is usually limited to measurements either in the bulk phase or within the biofilm with micro-electrodes. Experiments also indicate that molecular diffusion decreases with the biofilm thickness, which could be attributable to a higher biofilm density (Siegrist and Gujer, 1987). The same authors have reported diffusion coefficients 40-80% lower than the value in pure water in homogeneous nitrifying biofilms, depending on the biofilm thickness. Even, some studies have shown how thinner biofilms achieve better ammonium removal (Wik, 2003). In any case, these different diffusion coefficients inside the biofilm explain why growth conditions inside the biofilm may diverge appreciably from those in the bulk and even on the biofilm surface (Brockmann et al., 2008).

Since the substrate concentration is a major factor influencing the kinetics of nitrification, the kinetics may change over the position and depth in the biofilm. The Monod kinetics equation indicates that a zero-order reaction can be expected at high substrate concentrations while the conversion rate would become a first-order reaction at low substrate concentrations.

Moreover, there may be differences in the transport rates of the different substances within the biofilm. For instance, it has been reported how in some cases the oxygen concentration may become the limiting factor for nitrification despite the fact that the bulk solution have sufficiently high dissolved oxygen concentration values (Zhang et al., 1994). According to the same authors the oxygen concentration would drop significantly due to a double resistance, in the external boundary layer and in the biofilm itself. Finally, literature also reports that low dissolved oxygen concentrations may inhibit nitrite oxidizers and, therefore, cause nitrite accumulation in the biofilter (Picioreanu et al., 1997). This does not seem to be the case with the OASEN's bio-trickling filters, since no nitrite is detected in the effluent.

The variability of the diffusion coefficients with depth inside the biofilm also explains why the pH may decrease within the biofilm as the mole ratio HCO_3^-/O_2 changes (Zhang and Bishop, 1996): with a mole ratio higher than 5, the maximum pH decrease within the nitrifying biofilm was <0.4–0.6; when this ratio was <3, a pH decrease of 1.4–1.6 could occur within the biofilm. For double layer biofilms (autotrophic and heterotrophic) the difference can be even higher. Theoretically, nitrification rates could be improved by increasing the bulk pH until there is the optimum neutral pH within the biofilm.

In short, the situation inside the biofilm may be far more complex than assuming a pure culture under single limiting-substrate conditions. Also, they concentration gradients may help to determine which step controls the overall process. If the substrate consumption rate exceeds the mass transport rate of substrates by convection or diffusion, then diffusion gradients occur (Van Loosdrecht et al., 2002). Accordingly, the faster the growth process relative to the diffusion process the stronger the substrate gradient will be.

In recent years, it has been often proved that biofilms are less homogeneous that they were thought to be (Van Loosdrecht et al., 2002). Nitrifying biofilms are generally thinner than heterotrophic biofilms due to the relatively slow growth of nitrifiers (Wik, 2003). Despite the low shear forces typical of trickling filters and due to the low growth of nitrifiers and the lower substrate concentrations on the biofilm surface, compared to the bulk, the biofilm structure is considered as a homogeneous structure with uniform composition, thickness and density.

Moreover, dry filters are thought to operate at laminar flow (Kraakman et al., 2011), which is characterized by high momentum diffusion and low momentum convection. In those circumstances, the transport in the bulk liquid phase is dominated by convection while the pore-based convective transport (transport inside the biofilm) decreases and the biofilm-phase transport is dominated by

diffusion. There are also time-scale differences between transfer mechanisms which may influence the mechanisms to be modelled. For instance, momentum transport (by convection) is much faster than diffusion. In the biofilm systems, characteristic parameters are the Sherwood number, the Reynolds number, the Schmidt number and the specific area (Picioreanu et al., 2000).

Conclusion

Therefore, there are many processes and factors affecting the nitrification rate of a biofilm, which reveals the complexity of the system. Changes in the nitrification rate can be due to changes in the biofilm activity but also they may be due to changes in the biofilm characteristics (e.g., thickness, density, etc), changes in the influent water compositions, changes in the wetting, etc. Although these factors can be seen as potential options for improving the performance of the filter, some of them are more easily changeable than others. The factors can be grouped into three major categories. The first group refers to those that affect the biochemical process such as pH, temperature and the presence of inhibitors. The second category includes those influencing the supply to the biofilm such as the fluid regime, the substrate concentrations and the dissolved oxygen. The last and third category represents those that affect both the supply and the growth, such as the competition for space or essential nutrients.

A.4 Model simplifications

Justification for each assumption can be either here or in Section 3.4, where the model equations are presented. The simplifications are presented by groups around the different topics involved:

Filter characteristics and hydraulics:

1. All three phases, e.g. liquid (water), gas (air) and solid (biofilm) behaves as a continuum.
2. Both the inter-phase surface areas air-water and water-biofilm are assumed to be equal every moment.
3. The existence of both dual and single media layers is approached by considering one single media with uniform initial porosity and single-sized grains.
4. The filter is divided into a number of consecutive compartments with the same dimensions. In each compartment, conditions are assumed to be homogeneous. Biofilm growing on different grains in the same compartment is exposed to the same substrate loading and other environmental conditions. The hydraulic regime is assimilated to plug flow behaviour within each compartment. The number of compartments represents the hydraulic regime in the filter.
5. The filter bed can be partially or totally wetted. For the part wetted, there is uniform distribution of gas and liquid phases through the filter column in each layer.

Biofilm characteristics and ammonia conversion:

6. Within each compartment the filter is divided in, the biofilm is assumed to be homogeneous and uniformly distributed at each filter layer.
7. This also means that bacteria will be assumed to be evenly distributed throughout the biofilm and have direct access to both substrates and macronutrients diffusing from the bulk liquid into the biofilm.
8. Microorganisms are mainly present in the solid phase. Suspended microorganisms do not contribute significantly to nitrification.
9. Only bacteria in the outer layers of the biofilm contribute to the overall substrate removal since bacteria in the outer layers have better access to substrates in the bulk phase and the thickness of the biofilm is assumed to be very thin even in the upper layers, where the bigger bacteria populations are expected .
10. The biofilm itself is not modelled, meaning that all the biofilm activity (biological conversion) is assumed to occur in the surface.
11. The specific growth rate is described assuming Monod kinetic for the electron donor (NH_3), oxygen and generic nutrients.
12. Decay, detachment and aggregation are modelled as a single parameter (overall decay rate).
13. Maintenance requirements in the microorganisms are disregarded.
14. Furthermore, the possibility of having the nitrifying biofilm covered by heterotrophic biofilms is disregarded due to the absence of organic matter in the raw water. Only autotrophs are considered.
15. Growth of biofilms on spherical carriers will be assimilated to growth on planar surface in order to reduce the complexity of the model (Picioreanu et al., 1999).
16. It could happen that a heterotrophic layer exists below the autotrophic one in reality. Since this possibility needs first to be proved, for simplicity purposes it is ignored for the moment.

Transport-diffusion:

17. A stagnant liquid layer is considered over the biofilm. The thickness of that layer defines the diffusion limitation of the dissolved compounds in water.
18. Diffusion through the interphase water biofilm play a major role than diffusion through the biofilm.
19. Same diffusion coefficient for oxygen is applicable to other substances: ammonium, phosphate, carbon dioxide, carbonate.
20. Gradients and diffusion are one-dimensional.
21. Soluble compounds resulting from the biological conversion processes occurring in the biofilm diffuse out to the bulk water where mix immediately. An instantaneous steady-state substrate profile is assumed.

Aeration:

22. Gasses (oxygen, carbon dioxide) diffuse from the gas phase to the bulk liquid and from the bulk liquid to the biofilm.
23. Air flow behaves as plug flow and no existence of stagnant air zones while no clogging exists.

Operation conditions:

24. Backwashing is not influencing the stratification of the biomass content of the filter.

A.5 Ammonia dissociation

It has been demonstrated that despite ammonium is the main species in water under neutral conditions, the main substrate for ammonia-oxidizing organisms is ammonia (Suzuki et al., 1974). Ammonia, usually expressed as nitrogen, is extremely soluble in water depending on the temperature. The term ammonia often refers to the non-ionized (NH_3) and ionized (NH_4^+) species. The equilibrium between ammonia and the ammonium ion in aqueous solution is described by the following equation:

Equation A5.1

$$NH_{4\,(aq)}^{+} = H_{(aq)}^{+} + NH_{3\,(aq)}$$

According to this reaction, the speciation of ammonia nitrogen will depend on the pH value, the equilibrium being displaced to the left in alkaline water. The ammonium ion is largely predominant at neutral or slightly basic pH. Note that aqueous ammonia formed is removed from the solution by water/gas exchange.

The stoichiometric (or apparent) dissociation constant of ammonium includes the value for the various activity coefficients and is defined according to the following equation:

Equation A5.2

$$K_a^* = \frac{[NH_{3\,(aq)}]\,[H_{(aq)}^{+}]}{[NH_{4\,(aq)}^{+}]}$$

In this expression, the terms between brackets are in mole/kg of solution, also known as molality. Conversion of molarity into molality (mole/kg) can be done by taking into account the density of water as a function of temperature and salinity.

The formulation used for the calculation of the apparent dissociation constant is an empirical expression (Clegg and Whitfield, 1995) for computing the value of the dissociation constant for a temperature range and salinity (–2 to 40°C and from 0 to 40) that clearly comprises the groundwater characteristics.

Equation A5.3

$$pK_a^*(T) = pK_a(T) + \left(a_1 + \frac{a_1}{T} + a_3T^2\right)S^{0.5} + \left(a_4 + a_5T + \frac{a_6}{T}\right)S + \left(a_7 + \frac{a_8}{T}\right)S^2 + (a_9 + \frac{a_{10}}{T})\,S^3$$

Where:
T is the water absolute temperature [K].
S is the salinity.

The general expression, which is based on using molality is in terms of a free H^+ concentration, can be enormously simplified when the salinity is zero, since only remains the first term on the right side:

Equation A5.4

$$pK_a^*(T) = pK_a(T) = 9.244605 - 2729.33\,(\frac{1}{298.15} - \frac{1}{T + 273.15})$$

Where:
T is the relative water temperature [° C].

Therefore, to convert ammonia into ammonium:

Equation A5.5

$$[NH_4^+] = \frac{[H^+][NH_3\,]}{K_a^*}$$

According to these expressions, the order of magnitude of ammonia present in water would be several orders of magnitude lower than ammonium:

Table A5.1 Ammonia and ammonium concentrations for pH = 7.5 and NH_4^+ = 6.00 mg/L

NH4+ [g/m3]	6.00
pH	7.25
pKa	9.24E+00
NH3 [mol/m3]	3.40E-03
NH4 [mol/m3]	3.33E-01
H [mol/m3]	5.62E-08
Ka	5.75E-10
NH3 [g/m3]	0.06

In the model for simplicity purposes, it is assumed that ammonium would dissociate into ammonia at the same time that is converted by nitrifiers.

A.6 Internal filtration rate

For the determination of the internal filtration rate and the residence time of the water in the filter, the model could consider the existence of a bundle of capillaries that work as channels where the water flows through. This channels may not be completely straight, neither vertical so that the length of the capillary tube is longer than the filter bed.

Under this situation, two hypothesis are presented: (1) the speed of the water in a dry filter is in the first instance not dependent on the water flow rate that is placed on the filter; and (2) the speed of the water is dependent on the hydraulic diameter of the capillary and therefore both on the grain diameter and the degree of filling.

The expression for the velocity of water in the capillary can be derived based on the forces involved. The force of gravity over the water is given by:

Equation A6.1

$$F_Z = \rho \cdot g \cdot V_{w,c}$$

Where:
ρ is density of the water g/m^3].
g is the gravitational acceleration [m/s^2].
$V_{w,c}$ is the volume of fluid in the capillary [m^3]

Theoretically, there may be a frictional resistance that opposes to the movement of water. The frictional force varies depending on whether the capillary is straight or curved.

For a straight capillary, the resistance force is given by:

Equation A6.2

$$F_{R,S} = \frac{C_D \cdot A_C \cdot \rho \cdot u_C^2}{2}$$

For a curved capillary, the resistance force is given by:

Equation A6.3

$$F_{R,C} = 4\, F_{R,S}$$

Where:
C_D is the drag coefficient [-].
A_C is the contact surface between the water volume and the capillary [m2]
u_C is the water falling velocity in the capillary [m/2].

The drag coefficient CD is a function of the Reynolds number. In order to determine the theoretical CD, there may be various methods may be used.

The resistance is therefore a greater in curved capillary. In case of curved capillary, the distance the distance to be travelled by each drop of water is greater than the total height of the filter. This may have implications with regard the determination of the hydraulic retention time.

By combining the expressions for the gravity force and the resistance force in curved capillary, an equation for the speed of the water in the capillary can be derived:

Equation A6.4

$$u_C = \sqrt{\frac{V_{w,c}}{A_c} \frac{g}{2 \cdot C_D}}$$

The hydraulic diameter can be calculated as:

Equation A6.5

$$d_h = 4 \cdot \frac{A_{cs}}{P_c}$$

Where:

A_{cs} is the cross-sectional area [m2].
P_c is the wetted perimeter of the cross-section [m].

Which is true both for totally or partially filled flow conditions. Assuming that there is the same degree of filling along the capillary:

Equation A6.6

$$d_h = 4 \cdot \frac{A_{cs}}{P_c} = 4 \cdot \frac{A_{cs} \cdot L_c}{P_c \cdot L_c} = 4 \cdot \frac{V_{w,c}}{A_c}$$

Where:
L_c is the length of the capillary [m].

can be determined from the diameter of the capillaries and the filling degree. The hydraulic diameter can be defined as four times the mentioned ratio, which is true both for totally or partially filled flow conditions:

Equation A6.7

$$d_h = 4 \cdot \frac{V_{w,c}}{A_c}$$

The expression for the water velocity can be re-written as:

Equation A6.8

$$u_c = \sqrt{d_h \cdot \frac{g}{8 \cdot C_D}}$$

At a complete filling of the capillary tubes, the water surface is equal to the area of a circle and the wetted perimeter is equal to the circumference of the capillary. In other words:

Equation A6.9

$$d_h = 4 \cdot \frac{V_{w,c}}{A_c} = 4 \cdot \frac{\frac{1}{4}\pi d_C^2}{\pi d_C} = d_C$$

However, partial filling may be the situation as well and, in that case, this equality is not true anymore. In the figure three different cases are represented.

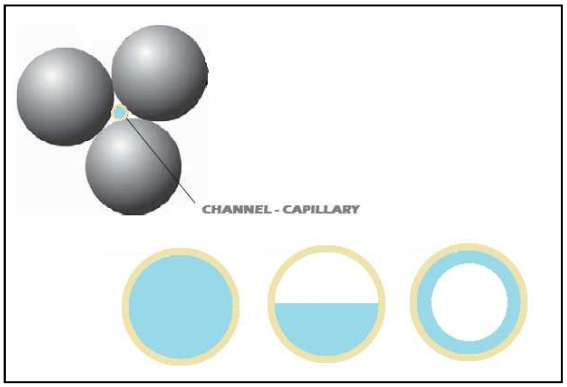

Figure A6.1

Huisman provides a relation between the grain diameter and the diameter of the capillary tubes:

Equation A6.10

$$d_C = \frac{4 \cdot P_o}{A_{spec}}$$

Where:
d_C is the diameter of the capillary [m].
P_o is the filter bed clean porosity [-].
A_{spec} is the specific surface area [m2/m3].

If substituting the expression for the specific surface area, the formula for the diameter of the capillary tubes becomes:

Equation A6.11

$$d_C = \frac{2}{3} \cdot \frac{P_o}{1 - P_o} \cdot d$$

Where:
d is the average size of the filter grains [m].

A.7 Aeration complementary equations

For characterizing gas transfer systems four equations are of interest: (1) the equilibrium equation, (2) the kinetic equation, (3) the mass balance equation and (4) the efficiency of the gas transfer system. First, the concentration of a volatile component in the gas phase will be in equilibrium with the concentration in the water phase, according to Henry's law. The equilibrium concentration can be calculated as:

Equation A7.1

$$c_s = k_d \cdot c_g$$

Where:
c_s is the equilibrium concentration of the gas in the water phase [g/ m^3]
k_d represents the distribution coefficient [-].
c_g corresponds to the concentration of the gas in air [g/ m^3].

Table A7.1 Distribution coefficient values

Gas	Distribution coefficient		
	0 °C	10 °C	20 °C
Methane	0.0556	0.0433	0.0335
Ammonia	1.3	0.943	0.763
Nitrogen	0.023	0.0192	0.0166
Oxygen	0.0493	0.0398	0.0337
Carbon dioxide	1.71	1.23	0.942

If the temperature of water rises, the solubility of gases in water decreases. The distribution coefficient is temperature dependent, therefore. The usual temperature of the raw water is in the range 11-13 ° C. The distribution coefficient values for these temperatures can be interpolated according to the expression:

Equation A7.1

$$k_{d,T_2} = k_{d,T_1} \cdot exp\left[\frac{\Delta H}{R \cdot T_1 \cdot T_2} \cdot (T_1 - T_2)\right]$$

Where the term $\frac{\Delta H}{R \cdot T_1 \cdot T_2}$ is constant and can be determined based on the values in the Table A7.1.

As soon as water and air become in contact, gas molecules are exchanged continuously. The changes in concentration are determined by the magnitude of the gas transfer coefficient and the driving force represented by the difference between the saturation and the actual concentration of the gas in water. The velocity of gas transfer is determined by the kinetic equation:

Equation A7.1

$$\frac{dc_w}{dt} = k_2 \cdot (c_s - c_w)$$

Where:
c_w is the concentration of a gas in water [g/ m^3].
$k_{2,g}$ represents the gas transfer coefficient [1/s].
c_s corresponds to the saturation concentration of the gas in water [g/ m^3].

The gas transfer coefficient is a device-dependent parameter. The larger the contact surface area between the air and water and the renewal of this surface area, the better the gas transfer and the higher the gas transfer coefficient. Since the variation in the gas concentration in the air cannot be neglected, the mass balance is needed:

Equation A7.1

$$Q_w \cdot c_{w,o} + Q_a \cdot c_{a,o} = Q_w \cdot c_{w,e} + Q_a \cdot c_{a,e}$$

Where:
Q_w is the water flow [m^3/h].
Q_g is the gas flow [m^3/h].

$c_{w,o}$ is the gas concentrations in water before aeration [g/ m^3].
$c_{w,e}$ is the gas concentrations in the water after aeration [g/ m^3].
$c_{g,o}$ is the gas concentration in the air phase before aeration [g/ m^3].
$c_{g,e}$ is the gas concentration in the air phase after aeration [g/ m^3].

The RQ is the ratio between the air flow and the water flow which, by considering the mass balance in a closed system, can be defined as:

Equation A7.1

$$RQ = \frac{Q_g}{Q_w} = \frac{c_{w,e} - c_{wo}}{c_{g,o} - c_{g,e}}$$

Finally, the efficiency K of the gas transfer system can be calculated by dividing the realized gas transfer by the maximum achievable gas transfer.

Equation A7.1

$$K = \frac{c_{w,e} - c_{w,o}}{c_s - c_{w,o}}$$

Where:
K is the efficiency of the gas transfer system [-].
$c_{w,o}$ is the gas concentrations in water before aeration [g/ m^3]
$c_{w,e}$ is the gas concentrations in the water after aeration [g/ m^3].
c_s corresponds to the saturation concentration of the gas in water [g/ m^3].

For such situation, the gas transfer within the dry filter is assimilated to plug flow and the efficiency can be calculated as:

Equation A7.1

$$K_2 = \frac{1 - e^{\left[-k_2 \cdot T \cdot \left(1 + \frac{k_d}{RQ_2}\right)\right]}}{1 + \frac{k_d}{RQ_2}} = \frac{c_{w,e} - c_{w,o}}{c_s - c_{w,o}}$$

Where:
k_2 represents the gas transfer coefficient [s^{-1}].
T is the residence time of water in each step [s].
k_d is the Henry's constant or distribution coefficient [-].
K_2 is the efficiency of the forced aeration system [-].
$c_{w,o}$ is the gas concentrations in water before aeration [g/ m^3]
$c_{w,e}$ is the gas concentrations in the water after aeration [g/ m^3].
c_s is the saturation concentration of the gas in water [g/ m^3].

A.8 Matlab model code

Nitoas.s

```
function [sys,x0,str,ts] = nitoas_s(t,x,u,flag,B,x0,U,P),
%  [sys,x0,str,ts] = nitoas_s(t,x,u,flag,B,x0,U,P),
%    Stimela S-Function
%
% t = time
% x = state vector, filled with continuous states (flag 1) or
%                       discrete states (flag 2)
% u = input vector
%
% P =  proces parameters, filled with nitoas_p.m and defined in nitoas_d.m
% B =  Model size, filled with nitoas_i.m,
% x0 = initial state, filled with nitoas_i.m,
% U = Translationstructure for inout vector, filled in uit Blok00_i.m.
%     Fields are determined by 'st_Varia'
%
% Stimela, 2004

% © Kim van Schagen,

% General purpose calculations
if any(abs(flag)==[1 2 3])

  %%%% MODEL-SPECIFIC => %%%%%%%%%%%%%%%%%%%%%%%%%%%%%%%%%%%%%%%%%%%%%%%%%%%%%%%%
  % optional: convert input vector to user names
  % eg. Temp = u(U.Temperature);
  % in the code it is also possible to use u(U.Temparature) directly.



  %%% Model Parameters (from _d.m) %%%

  NumCel = P.NumCel;
  MuMax_AOB = P.MuMax_AOB;
  AlfaT_AOB = P.AlfaT_AOB;
  KsPO4_AOB = P.KsPO4_AOB;
  KsNH4_AOB = P.KsNH4_AOB;
  KsO2_AOB = P.KsO2_AOB;
  Y_NH4_AOB = P.Y_NH4_AOB;
  Y_O2_AOB = P.Y_O2_AOB;
  Y_PO4_AOB = P.Y_PO4_AOB;
  B_AOB = P.B_AOB;
  D1_AOB =P.D1_AOB;
  D2_AOB =P.D2_AOB;
  A = P.Surf;
  Lbed = P.Lbed;
  Diam = P.Diam;
  FilPor = P.FilPor;
  F_Vw = P.F_Vw;
  F_Aspec = P.F_Aspec;
  k2CH4 = P.k2CH4;
  RQeff = P.RQeff;
  Xo_AOB=P.Xo_AOB;
  Step = P.Step; % 1 = FF; 2 = FK


  q = 0.0000001;
  ds = 0.0001;



  %%% Model Influent Values %%%

  Temp = u(U.Temperature); % [oC]
  Flow = u(U.Flow); % [m3/h]
  CO2 = u(U.Carbon_dioxide); % [g/m3]
  HCO3 = u(U.Bicarbonate); % [g/m3]
  NH4 = u(U.Ammonia); % [g/m3]
  O2 = u(U.Oxygen); % [g/m3]
  PO4 = u(U.Phosphate); % [g/m3]
```

```
  pHo = u(U.pH); % [-]
  EGVo = u(U.Conductivity);  % [mS/m]
  coMn = u(U.Mnumber); % [mmol/l]
  Fe = u(U.Iron2); % [g/m3]


  %%% Air-water flow ratios %%%

  if Step == 1
      RQeff = 620/Flow;
  end
  if Step == 2
      RQeff = 356/Flow;
  end


  %%% Unit conversions and first calcualtions %%%

  Load = Flow*NH4;
  Q = Flow/3600; % [m3/s]
  vel = Q/A; % Surface filtration velocity [m/s]
  Vf = Lbed*A; % Filter volume (m3)
  Vs = Vf*(1-FilPor); % Filter material volume [m3]
  Ms = Vs*1600; % Filter material mass [kg] assuming sand dry density: 1600 kg/m3
  VelReal = 1.0*vel/(FilPor*F_Vw*F_Aspec);  % Pore velocity trickling filter



  Section = A*FilPor*F_Vw*F_Aspec;
  if Step == 1
      ug = 620/Section; % [m/h]
  end
  if Step == 2
      ug = 356/Section; % [m/h]
  end


  Tg = Temp;  % Air temperature = Water temperature [oC]
  dy = Lbed/NumCel; % Used by MatQ, MatQ1, height each layer
  ContactTime = 1*Lbed/VelReal; % Aeration
  TijdStap = ContactTime/NumCel; % Used by MatQ1. Contact time per layer [s]


  %%% Relative molecular and atomic masses [mg/mol] %%%

  MrCO2 = 1000*44.01;
  MrCO3 = 1000*60.01;
  MrHCO3 = 1000*61.02;
  MrH2S = 1000*34.08;
  MrO2 = 1000*31.9988;
  MrCH4 = 1000*16.04303;
  MrN2 = 1000*28.0134;
  MrN = 1000*14.01;
  MrNH4 = 1000*18.03846;
  MrPO4 = 1000*94.9714;
  MrP = 1000*30.9737;
  MrFe = 1000*55.847;


  %%% Constants required for calculation gas constants in air %%%

  Po = 101325; % Standard pressure at sea level
  R = 8.3143;  % Universal gas constant [J/(K*mol)]
  pw = 1070*exp(0.04986*Tg)-525.1; % Partial pressure in water


  %%% Gasses concentrations in air: universal gas law %%%

  cgoO2 = (0.20948*(Po-pw)*(MrO2 /1000))/(R*(Tg+273));
  cgoCO2 = (0.00032*(Po-pw)*(MrCO2/1000))/(R*(Tg+273)); % Used in the co2 balance for
the gas phase: co2g


  %%% Henry's constants or distribution coefficients [-]: equilibrium air-water phases
%%%

  kDO2 = 0.02727*exp(-0.0426*Temp)+0.02202; % kDO2 (10oC) = 0.041
```

```
  kDCH4 = 0.03227*exp(-0.05315*Temp)+0.02352; % kDCH4 (10oC) = 0.043
  kDCO2 = 1.307*exp(-0.04489*Temp)+0.4015; % kDCO2 (10oC) = 1.23 kDCO2 (12oC) = 1.16


  %%% Equations for diffusion coefficients, best fit for 10, 20 and 30 degrees
Celsius, can be used between 0-40 Celsius

  DifO2 = 1/(9.048299e-1 - 1.961736e-2*Temp + 1.076824e-4*Temp^2)*1e-9; % m2/s
  DifCH4 = 1/(1.081256    - 2.310800e-2*Temp + 1.189257e-4*Temp^2)*1e-9; % m2/s
  DifCO2 = 1/(9.644559e-1 - 2.058414e-2*Temp + 1.061623e-4*Temp^2)*1e-9; % m2/s
  DifNH4 = 1860*(10^-6)^2; % m2/s

  %%%  Gas transfer coefficients air-water [1/s]: kinetics air-transfer %%%

  n = 1;
  k2O2 = k2CH4*(DifO2 /DifCH4)^n;
  k2CO2 = k2CH4*(DifCO2/DifCH4)^n;


  %%% External mass transfer water - biofilm  %%%

  Df = 1/(9.048299e-1 - 1.961736e-2*Temp + 1.076824e-4*Temp^2)*1e-9; % DifO2
  nu = ((497e-6)/((Temp+42.5)^1.5));
  Sc = nu/Df;
  Aspec = 6*(1-FilPor)/Diam;
  Reh = VelReal/(nu*Aspec*F_Aspec);
  Sh = 1.8*(Reh^0.5)*(Sc^0.33);
  % Same Df for all substances


  %%% Matrixes exchange phases %%%


  MatQ = d_filmat1(dy,VelReal,NumCel,factor); % Exchange water and biofilm
  MatQ1 = Matrix1(TijdStap,NumCel,factor2); % Exchange gas and water


  %%%  Substrate transport %%%

  kf = Sh*Df*Aspec*F_Aspec; %

  k2 = Aspec*kf*F_Aspec; %
  Delta = Df/kf; % External mass transfer layer thickness [m]

  %%% Carbonic acid equilibrium %%%

  TempK = Temp + 273.15; % [K]
  IonStrength = 0.183*EGVo;
  f = CE_Activity(IonStrength);
  [K1,K2,Kw,Ks] = KValues(TempK);

  %%% M number influent water %%%
  HCO3mmol = (HCO3/MrHCO3)*1000;
  coMn = CE_pHHCO3_M(pHo,HCO3mmol,K1,K2,Kw,f);

  %%%  Carbon dioxide influent water %%%
  coCO2 = CE_pHM_CO2(pHo,coMn,K1,K2,Kw,f); % [mmol/l]
  coCO2 = coCO2*MrCO2/1000; % [g/m3]




  %%%% <= MODEL-SPECIFIC  %%%%%%%%%%%%%%%%%%%%%%%%%%%%%%%%%%%%%%%%%%%%%%%%%%%%

end; % of any(abs(flag)==[1 2 3])

if flag == 1, % Continuous states derivative calculation

  % default derivative =0;
  sys = zeros(B.CStates,1);

  %%%% MODEL-SPECIFIC => %%%%%%%%%%%%%%%%%%%%%%%%%%%%%%%%%%%%%%%%%%%%%%%%%%%%
  %fill sys with the derivatives of the continuous states
  %eg. sys(1) = (u(U.Temperature)-x(1))/P.Volume;
```

```
%%%  Model state variables %%%

o2w=x(1:NumCel);
o2g=x(NumCel+1:2*NumCel);
co2w=x(2*NumCel+1:3*NumCel);
co2g=x(3*NumCel+1:4*NumCel);
nh4w=x(4*NumCel+1:5*NumCel)+q;
nh4b=x(5*NumCel+1:6*NumCel)+q;
x_AOB=x(6*NumCel+1:7*NumCel)+q;
o2b=x(7*NumCel+1:8*NumCel);
co2b=x(8*NumCel+1:9*NumCel);
hco3w=x(9*NumCel+1:10*NumCel);
hco3b=x(10*NumCel+1:11*NumCel);
po4w=x(11*NumCel+1:12*NumCel);
po4b=x(12*NumCel+1:13*NumCel);



%%% Kinetics %%%

co2wmmol = (co2w./MrCO2)*1000;
hco3wmmol = (hco3w./MrHCO3)*1000;
pHw1 = CE_CO2HCO3_pH(co2wmmol,hco3wmmol,K1,K2,Kw,f); %pHw

AlfaT=(AlfaT_AOB)^(Temp-20);
Monod_NH4_AOB= (MrN/MrNH4)*nh4b./(nh4b*(MrN/MrNH4)+(KsNH4_AOB*AlfaT));
Monod_O2_AOB=o2b./(o2b+KsO2_AOB);
Monod_PO4_AOB=po4b./(po4b+KsPO4_AOB);
Monod=min(min(Monod_NH4_AOB,Monod_O2_AOB),Monod_PO4_AOB);
AlfapH_AOB=1./(1+0.041*10.^abs(8.4-pHw1));
MuMax_AOB;
muNAOB=AlfaT.*AlfapH_AOB*MuMax_AOB.*Monod;

B_AOB=B_AOB*ones(NumCel,1);
BetaT=(1.029)^(Temp-20);

b_AOB=B_AOB*BetaT;


%%%  Conversion rates %%%

z = F_X*ones(NumCel,1);
r_NH4 = - (muNAOB.*x_AOB.*z.*F_Aspec/Y_NH4_AOB)*(MrNH4/MrN);
r_O2 = - (muNAOB.*x_AOB.*z.*F_Aspec/Y_NH4_AOB)*1.5*(MrO2/MrN); % Only AOB
r_PO4 = - (muNAOB.*x_AOB.*z.*F_Aspec/Y_PO4_AOB)*(MrPO4/MrP);
r_CO2 =   (muNAOB.*x_AOB.*z.*F_Aspec/Y_NH4_AOB)*2*(MrCO2/MrN);
r_HCO3 = - (muNAOB.*x_AOB.*z.*1*F_Aspec/Y_NH4_AOB)*2*(MrHCO3/MrN);


%%% Contribution simultaneous iron biological oxidation %%%

coFe = Fe;
ReactionFeHCO3 = -1*(coFe*(1/(MrFe/1000))*2*(MrHCO3/1000));
ReactionFeCO2 = 1*(coFe*(1/(MrFe/1000))*2*(MrCO2/1000));
ReactionFeO2 = -1*(coFe*(1/(MrFe/1000))*0.25*(MrO2/1000));
a = zeros(NumCel,1);
a(1,1) = ReactionFeHCO3/TijdStap;
b = zeros(NumCel,1);
b(1,1) = ReactionFeCO2/TijdStap;
c = zeros(NumCel,1);
c(1,1) = ReactionFeO2/TijdStap;


%%% Contribution simultaneous NOB %%%

ReactionNOBO2 = - (muNAOB.*x_AOB*F_Aspec/Y_NH4_AOB)*1.0*(MrO2/MrN);



%%% Balance equations %%%



%o2w:
sys(1:NumCel)=MatQ1*[O2;o2w]+k2O2*kDO2.*o2g-k2O2.*o2w + MatQ*[O2;o2w]-k2*(o2w-o2b);

%o2g:
```

```
  sys(1*NumCel+1:2*NumCel)=MatQ1*[cgoO2;o2g]-
((k2O2*kDO2)/RQeff).*o2g+(k2O2/RQeff).*o2w;

  %co2w:
  sys(2*NumCel+1:3*NumCel)=MatQ1*[coCO2;co2w]+k2CO2*kDCO2.*co2g-k2CO2*co2w +
MatQ*[coCO2;co2w] - k2.*(co2w-co2b);

  %co2g:
  sys(3*NumCel+1:4*NumCel)=MatQ1*[cgoCO2;co2g]-
((k2CO2*kDCO2)/RQeff).*co2g+(k2CO2/RQeff).*co2w;

  %nh4w:
  sys(4*NumCel+1:5*NumCel) = MatQ*[NH4;nh4w]-k2*(nh4w-nh4b);

  %nh4b:
  sys(5*NumCel+1:6*NumCel) = (k2.*(nh4w-nh4b)+ r_NH4);

  %x_aob:
  sys(6*NumCel+1:7*NumCel) = z.*((1-D1_AOB)*muNAOB-b_AOB-D2_AOB).*x_AOB*F_Aspec;   %

  %o2b:
  sys(7*NumCel+1:8*NumCel)= k2.*(o2w-o2b)+ r_O2 + ReactionNOBO2 + c;

  %co2b:
  sys(8*NumCel+1:9*NumCel)= k2.*(co2w-co2b)+ r_CO2 + b;

  %hco3w:
  sys(9*NumCel+1:10*NumCel)= MatQ*[HCO3;hco3w] - k2*(hco3w-hco3b);

  %hco3b:
  sys(10*NumCel+1:11*NumCel)= k2.*(hco3w-hco3b)+ r_HCO3 + a;

  %po4w:
  sys(11*NumCel+1:12*NumCel)= MatQ*[PO4;po4w] - k2*(po4w-po4b); %

  %po4b:
  sys(12*NumCel+1:13*NumCel) = k2.*(po4w-po4b)+r_PO4; % Iron contribution is neglected



   %%% Backwash %%%

   if Step == 2

   spoelen = u(U.Number+1);
   if spoelen == 1
       sys(1:4*NumCel)= -(1/9000)*x(1:4*NumCel);
       if mean(x(6*NumCel+1:7*NumCel)) > 2*15;
           sys(6*NumCel+1:7*NumCel) = -(1/2500)*x(6*NumCel+1:7*NumCel);
       end
       if mean(x(6*NumCel+1:7*NumCel)) < 2*15 & mean(x(6*NumCel+1:7*NumCel)) > 15
           sys(6*NumCel+1:7*NumCel) = -(1/3500)*x(6*NumCel+1:7*NumCel);
       end
       if mean(x(6*NumCel+1:7*NumCel)) < 15
           sys(6*NumCel+1:7*NumCel) = 0;
       end
       sys(7*NumCel+1:13*NumCel)= -(1/9000)*x(7*NumCel+1:13*NumCel);
   end
   end




  %%%% <= MODEL-SPECIFIC %%%%%%%%%%%%%%%%%%%%%%%%%%%%%%%%%%%%%%%%%%%%%%%%%%%%%%%%


elseif flag ==2, %discrete state determination

  % default next sample same states (length is B.DStates)
  sys = x(B.CStates+1:B.CStates+B.DStates);

  %%%% MODEL-SPECIFIC => %%%%%%%%%%%%%%%%%%%%%%%%%%%%%%%%%%%%%%%%%%%%%%%%%%%%%%%%
  % fill sys with the state value on the next sample moment (determined by
  %B.SampleTime)
  %eg. sys(1) = (x(1)+u(U.Temperature))/P.Volume;
```

```
elseif flag ==3, % output data determination

  % default equal to the input with zeros for extra measurements
  sys = [u(1:U.Number); zeros(B.Measurements,1)];

  %%%% MODEL-SPECIFIC => %%%%%%%%%%%%%%%%%%%%%%%%%%%%%%%%%%%%%%%%%%%%%%%%%%


  %%% General output for calculated values %%%

  sys(U.Carbon_dioxide) = x(3*NumCel); %co2w
  sys(U.Bicarbonate) = x(10*NumCel); %hco3w
  sys(U.Ammonia) = x(5*NumCel); %nh4w
  sys(U.Oxygen) = x(1*NumCel); %o2w
  sys(U.Phosphate) = x(12*NumCel); %po4w
  sys(U.Ozone)= x(2*NumCel); %o2g
  sys(U.Nitrite)= x(6*NumCel); %nh4b
  if Step == 1
      sys(U.Conductivity)= 0.96*EGVo;
  end
  if Step == 2
      sys(U.Conductivity)= 0.99*EGVo;
  end

  %%% pH Effluent Calculation %%%
  if Step == 1
      IonStrength = 0.183*0.96*EGVo;
  end
  if Step == 2
      IonStrength = 0.183*0.99*EGVo;
  end
  f = CE_Activity(IonStrength);
  [K1,K2,Kw,Ks] = KValues(TempK);
  pH = CE_CO2HCO3_pH((x(3*NumCel)/MrCO2)*1000,(x(10*NumCel)/MrHCO3)*1000,K1,K2,Kw,f);
  sys(U.pH)= pH;
  HCO3mmol = (x(10*NumCel)/MrHCO3)*1000;
  sys(U.Mnumber) = CE_pHHCO3_M(pH,HCO3mmol,K1,K2,Kw,f);
  sys(U.Iron2) = Fe*0;


  %%% Extra measurementes %%%


  % AOB upper and lower layers
  sys(U.Number+1) = x(6*NumCel+1);
  sys(U.Number+2) = x(7*NumCel);
  % Biomass (g d.w./m3)
  sys(U.Number+3) = mean(x(6*NumCel+1:7*NumCel));
    % Cells
  Biomass = mean(x(6*NumCel+1:7*NumCel)); % Biomass AOB (g d.w./m3)
  Cells = Biomass/(7.2E-14); % Cells AOB (cells/m3) assuming 7.2e-4 g d.w./cell
  Cells_Sand = Cells*Vf/(Ms*1000); % Cells AOB (cells/g sand m-3)
  sys(U.Number+4) = Cells_Sand;


  % Loading rate [g/h]
  sys(U.Number+10) = NH4*Flow;
  % Removal rate [g/h]
  sys(U.Number+11) = (NH4-x(5*NumCel))*Flow;
  % Removal ratio
  sys(U.Number+12) = 100*((NH4-x(5*NumCel))*Flow)/(NH4*Flow);
  % Loading rate [g/h]/10
  sys(U.Number+13) = NH4*Flow/10;
  % Removal rate [g/h]/10
  sys(U.Number+14) = (NH4-x(5*NumCel))*Flow/10;


  % Loading rate [g/h m3 filter]
  sys(U.Number+15) = NH4;
  % Loading rate [g/h m3 filter]
  sys(U.Number+16) = Flow;


  % Loading rate [g/h m3 filter]
  sys(U.Number+17) = NH4*Flow/Vf;
```

```
  % Removal rate [g/h m3 Filter]
  sys(U.Number+18) = (NH4-x(5*NumCel))*Flow/Vf;
  % Loading rate [g/h m3 sand]
  sys(U.Number+19) = NH4*Flow/Vs;
  % Removal rate [g/h m3 Sand]
  sys(U.Number+20) = (NH4-x(5*NumCel))*Flow/Vs;
  % Loading rate [g/h m2]
  sys(U.Number+21) = NH4*Flow/(Aspec*F_Aspec*Vf);
  % Removal rate [g/h m2]
  sys(U.Number+22) = (NH4-x(5*NumCel))*Flow/(Aspec*F_Aspec*Vf);



  %Sand-specific nitrifiation rate (mg N h-1 kg sand)
  sys(U.Number+23) = sys(U.Number+11)*(MrN/MrNH4)*1000/Ms;
  mus = sys(U.Number+11)*(MrN/MrNH4)*1000/Ms;
  % Cell-specific nitrification rate (femto grams N h-1 cell-1)
  sys(U.Number+24) = (mus*(1e+12))/(Cells_Sand*1000);
  %Sand-specific nitrifiation rate (g NH4+ h-1 m3 sand)
  sys(U.Number+25) = sys(U.Number+11)/Vs;
  % Ammonium profile
  sys(U.Number+40) = x(4*NumCel+1);
  sys(U.Number+41) = x(4*NumCel+2);
  sys(U.Number+42) = x(4*NumCel+3);
  sys(U.Number+43) = x(4*NumCel+4);
  sys(U.Number+44) = x(4*NumCel+5);
  sys(U.Number+45) = x(5*NumCel);

  % X profile
  sys(U.Number+31) = x(6*NumCel+1);
  sys(U.Number+32) = x(6*NumCel+2);
  sys(U.Number+33) = x(6*NumCel+3);
  sys(U.Number+34) = x(6*NumCel+4);
  sys(U.Number+35) = x(6*NumCel+5);
  sys(U.Number+36) = x(7*NumCel);



  %%%% <= MODEL-SPECIFIC %%%%%%%%%%%%%%%%%%%%%%%%%%%%%%%%%%%%%%%%%%%%%%%%%%%%


elseif flag == 0
  % initialize Model
  %[cs,ds,out,in,,direct]
  sys = [B.CStates,B.DStates,U.Number+B.Measurements,U.Number+B.Setpoints, 0,
B.Direct,1];
  ts = [B.SampleTime,0];
  str = 'nitoas';
  x0=x0;
else
   % If flag is anything else, no need to return anything
   % since this is a continuous system
    sys = [];
end



function [lambda0F,I0F] = d_filcof(T,v,d,P0)

%%%%%%%%%%%%%%%%%%%%%%%%%%%%%%%%%%%%%%%%%%%%%%%%%%%%
% This function returns the factor coefficient
% for the filtration coefficient
%%%%%%%%%%%%%%%%%%%%%%%%%%%%%%%%%%%%%%%%%%%%%%%%%%%%

% Kinematic viscosity
nu=(497e-6)/((T+42.5)^1.5);

% Factor coefficient for head loss
I0F=(180*nu*(1-P0)^2*v)/(9.81*P0^3*d^2);

lambda0F=(9e-18)/(nu*v*d^3);%Lerk


function val = d_filmat(dy,vp,v,N)

% This function returns the main matrix Q for filtration
%b     = -vp/(2*dy);
```

```
%c     = vp/(2*dy);
%e     = v/(2*dy);
%alpha = -vp/dy;
%beta  = vp/dy;
%v1=[[c*ones(N-1,1);beta], [zeros(N-1,1);alpha], [b*ones(N-1,1);0]];
%q1=spdiags(v1,[0,1,2],N,N+1);
%
%v2=[[e*ones(N-1,1);2*e], [zeros(N-1,1);-2*e], [-e*ones(N-1,1);0]];
%q2=spdiags(v2,[0,1,2],N,N+1);
%
%
%val = [q1;q2];


b     = -vp/(2*dy);
c     = vp/(2*dy);
e     = v/(2*dy);
alpha = -vp/dy;
beta  = vp/dy;
v1=[[c*ones(N,1);beta], [b*ones(N,1);0]];
q1=spdiags(v1,[0,1],N,N+1);

v2=[[e*ones(N,1);2*e], [-e*ones(N,1);0]];
q2=spdiags(v2,[0,1],N,N+1);


val = [q1;q2];

% MatQ1
function val = Matrix1(T,N,f2)

a     = 1./T;
v1=[[a.*ones(N,1)], [-a.*ones(N,1)]];
q1=spdiags(v1,[0,1],N,N+1);
val = [q1];


% MatQ3
function val = Matrix3(T,N)

a     = 1./T;
v1=[[a.*ones(N,1)], [-a.*ones(N,1)]];
q1=spdiags(v1,[0,1],N,2*N);
val = [q1];

% MatQ
function val = d_filmat1(dy,vp,N,f)
a1     = vp/(dy);
a2    = -vp/(dy);
%b     = v/(dy);
alpha = -vp/dy;
beta  = vp/dy;
v1=[[a1*ones(N-1,1);beta], [a2*ones(N-1,1);alpha]];
q1=spdiags(v1,[0,1],N,N+1);
%v2=[b*ones(N,1), -b*ones(N,1)];
%q2=spdiags(v2,[0,1],N,N+1);
val = [q1];
```

A.9 Characterization of filter behaviour

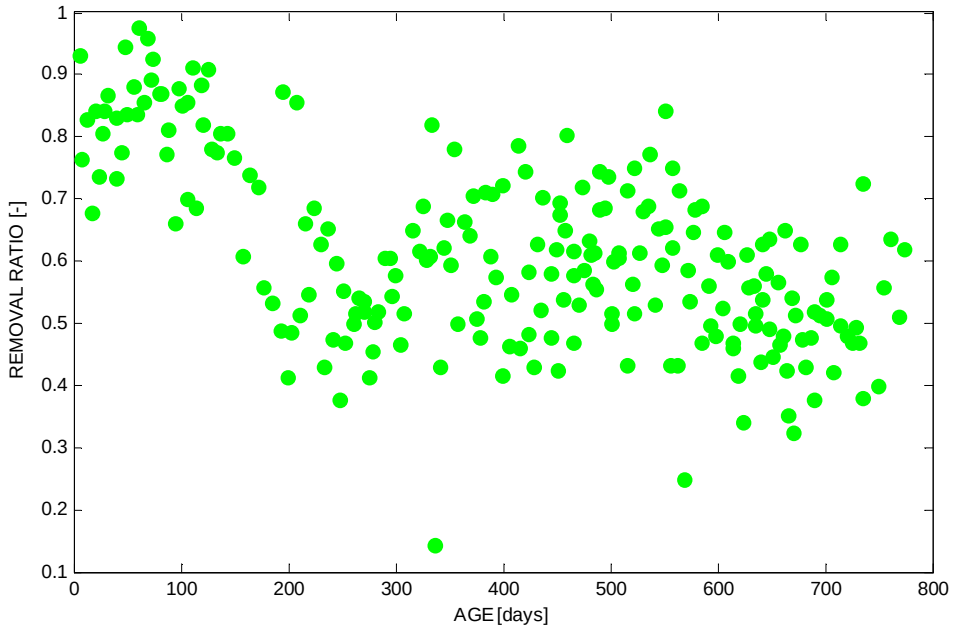

Figure A9.1 Ageing process of the ammonium removal ratio of filter FF-04 after external washing

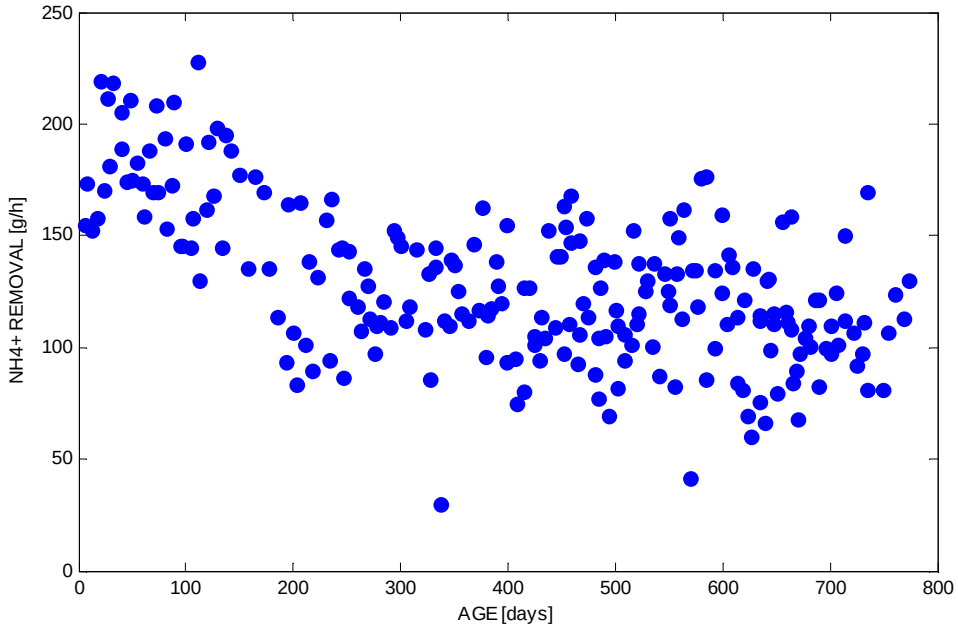

Figure A9.2 Ageing process of the ammonium removal rate of filter FF-04 after external washing

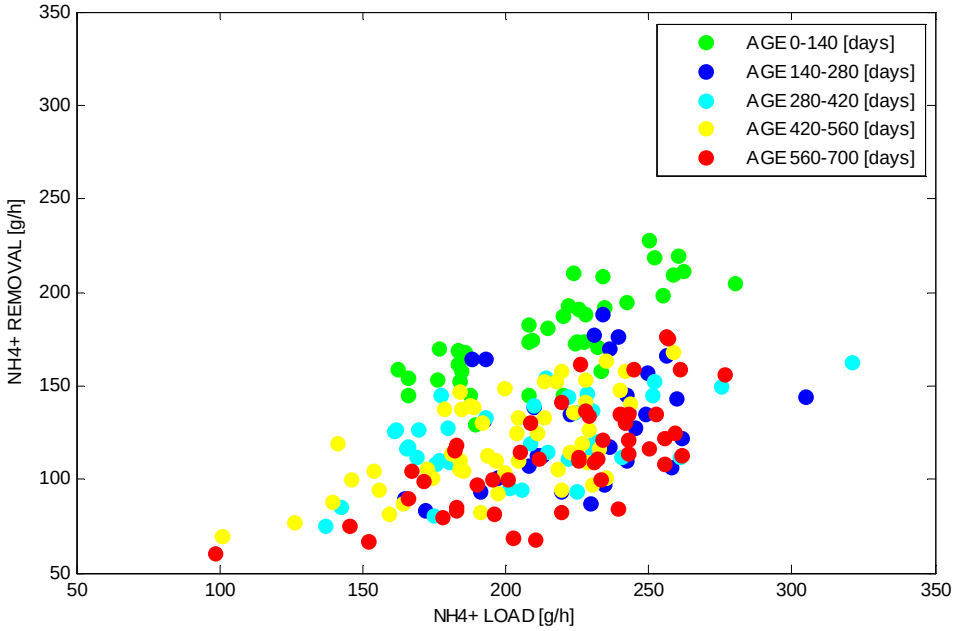

Figure A9.3 Nitrification rates at different filter ages for different ammonium loading rates in filter FF-04 after external washing

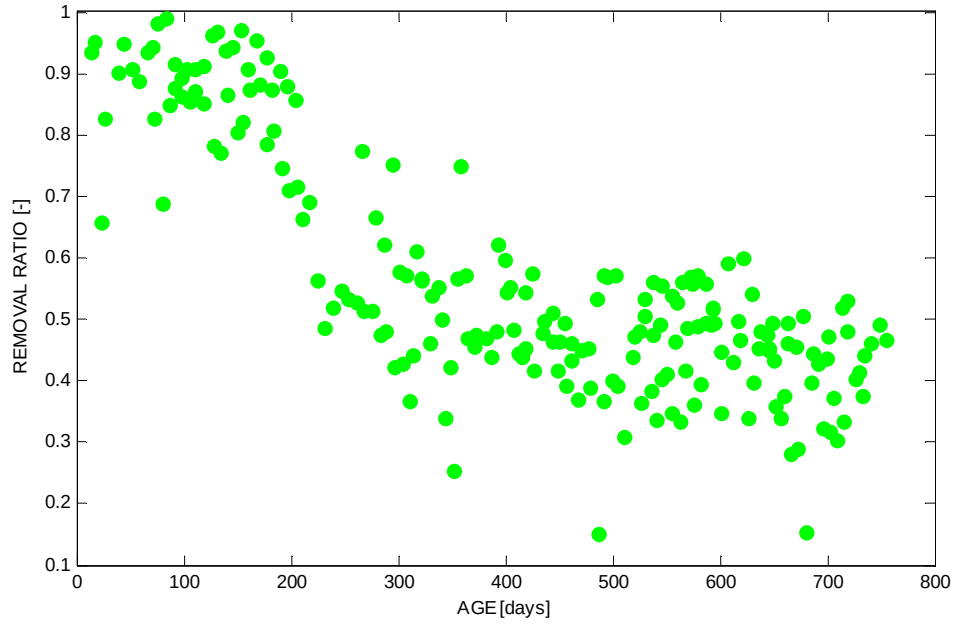

Figure A9.4 Ageing process of the ammonium removal ratio of filter FF-05 after external washing

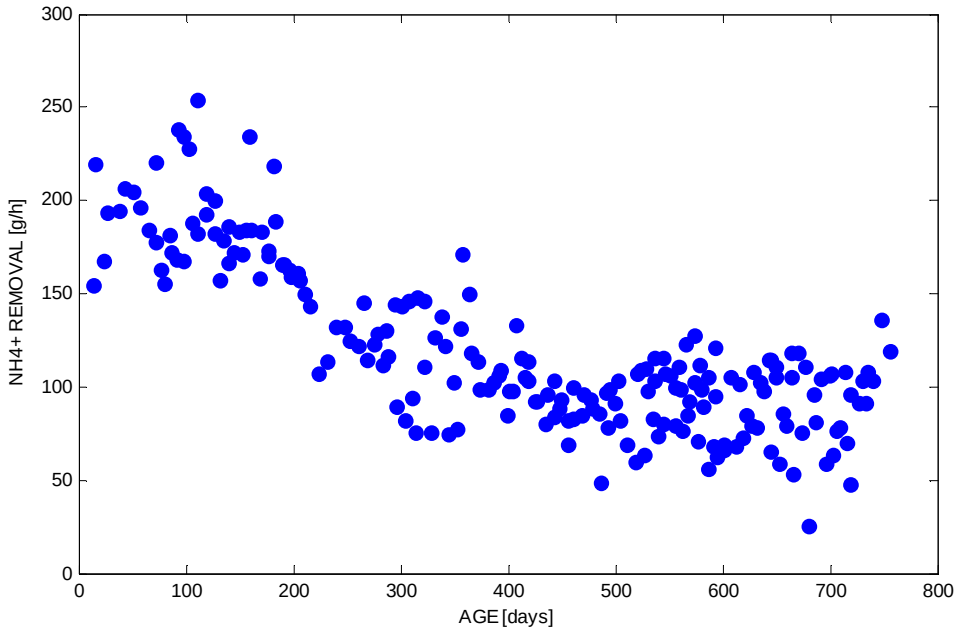

Figure A9.5 Ageing process of the ammonium removal rate of filter FF-05 after external washing

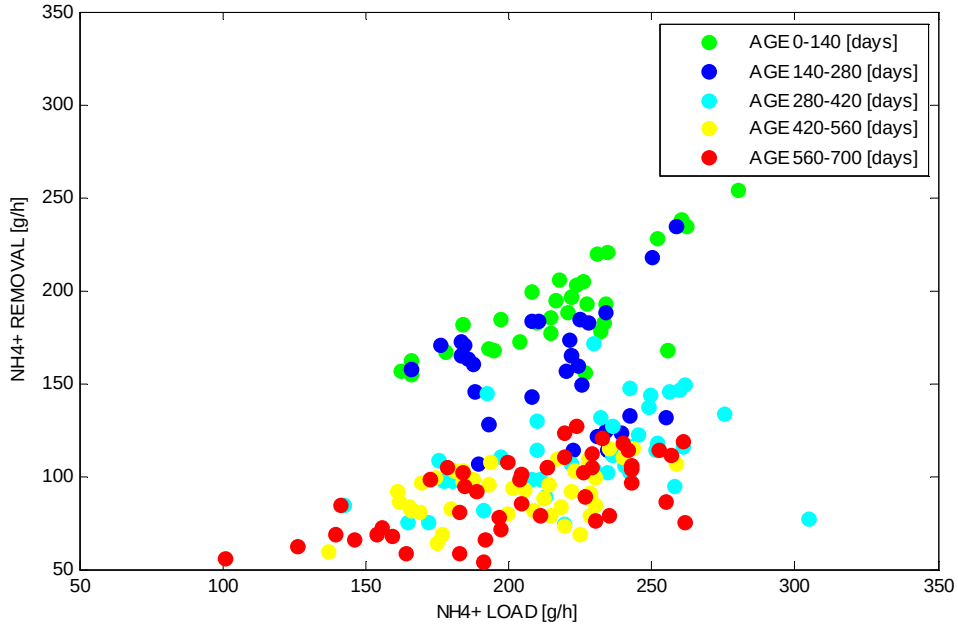

Figure A9.6 Nitrification rates at different filter ages for different ammonium loading rates in filter FF-05 after external washing

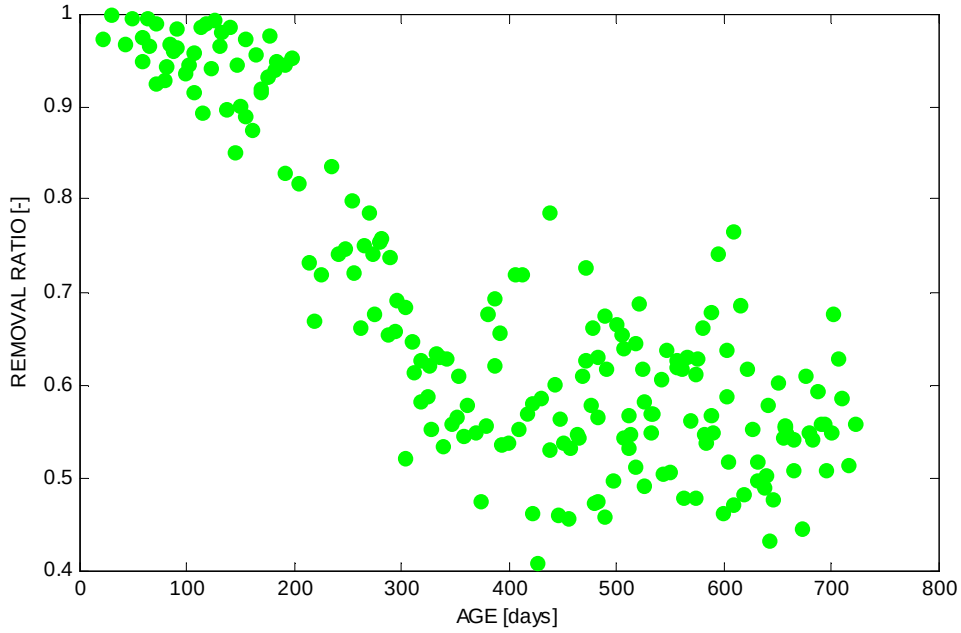

Figure A9.7 Ageing process of the ammonium removal ratio of filter FF-06 after external washing

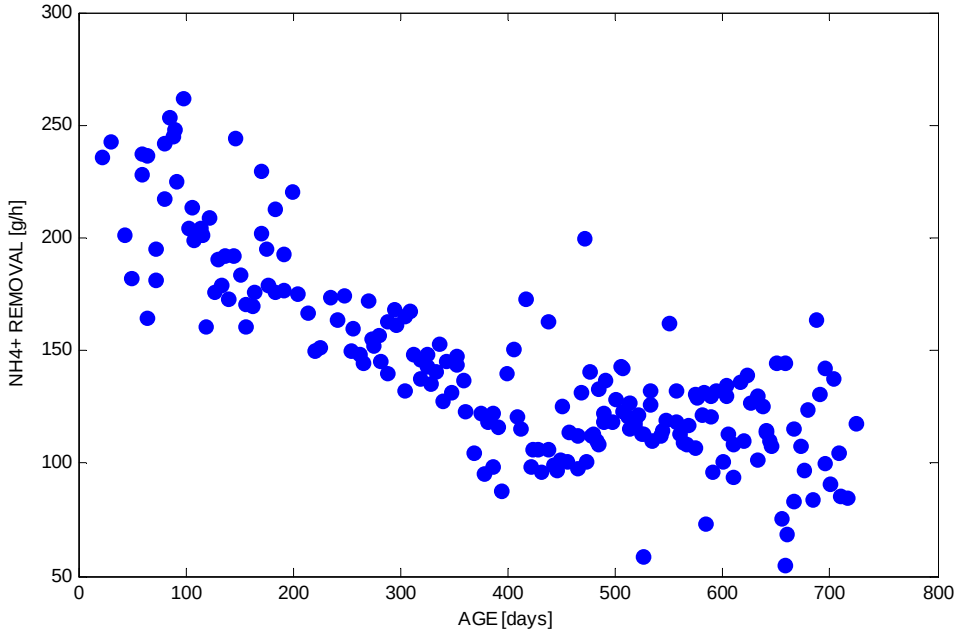

Figure A9.8 Ageing process of the ammonium removal rate of filter FF-06 after external washing

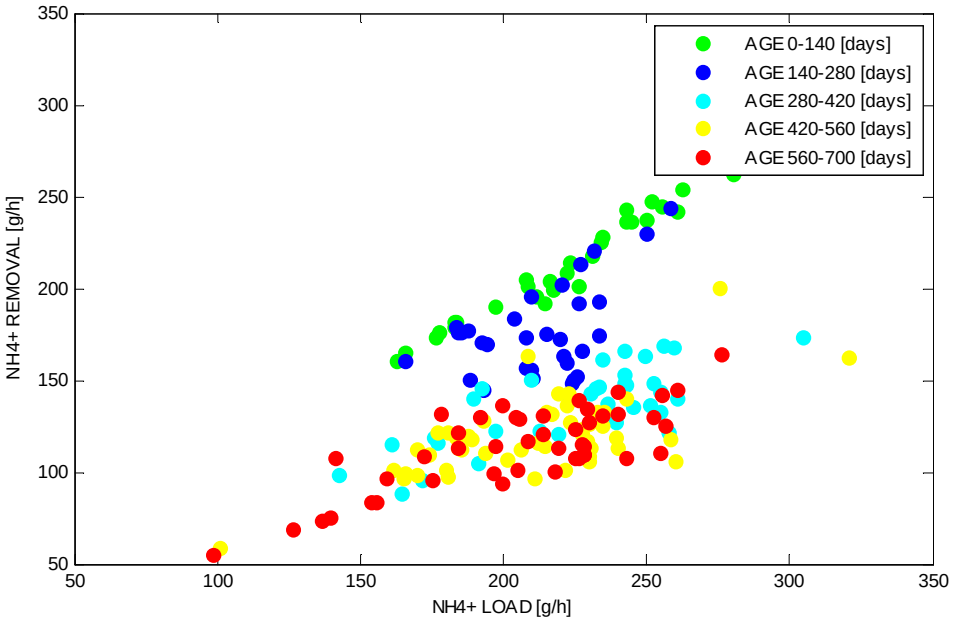

Figure A9.9 Nitrification rates at different filter ages for different ammonium loading rates in filter FF-06 after external washing

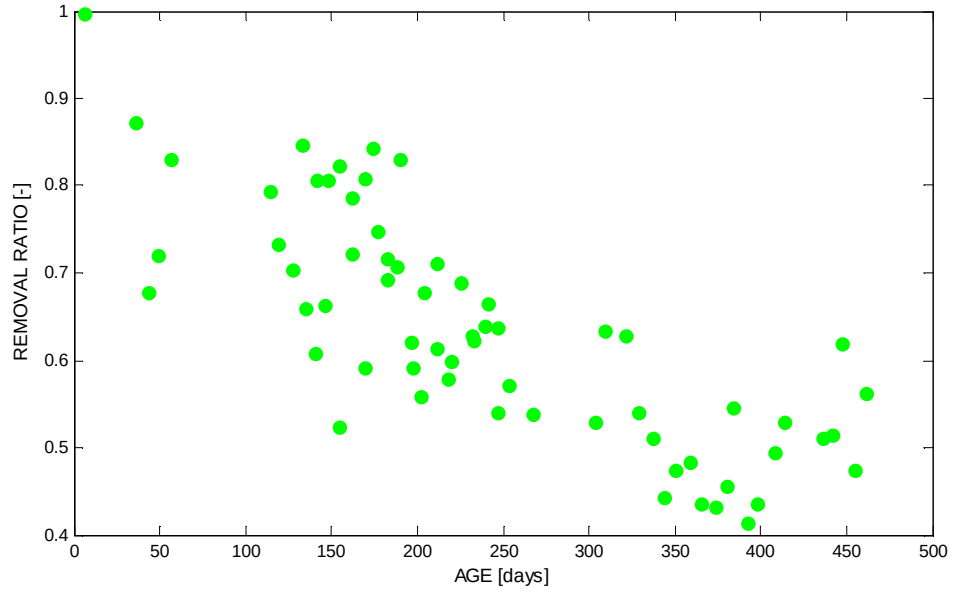

Figure A9.10 Ageing process of the ammonium removal ratio of filter FF-07 after external washing

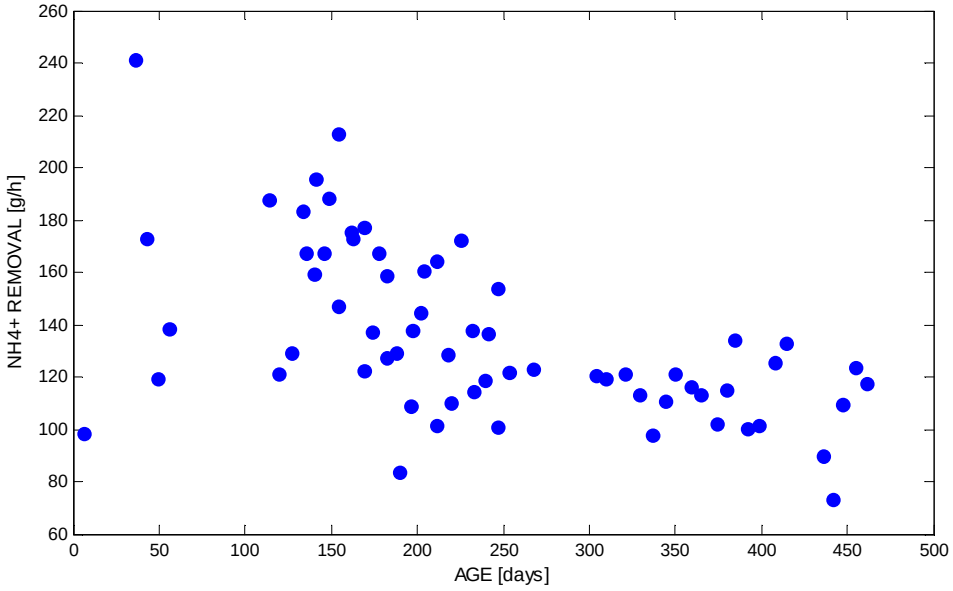

Figure A9.11 Ageing process of the ammonium removal rate of filter FF-07 after external washing

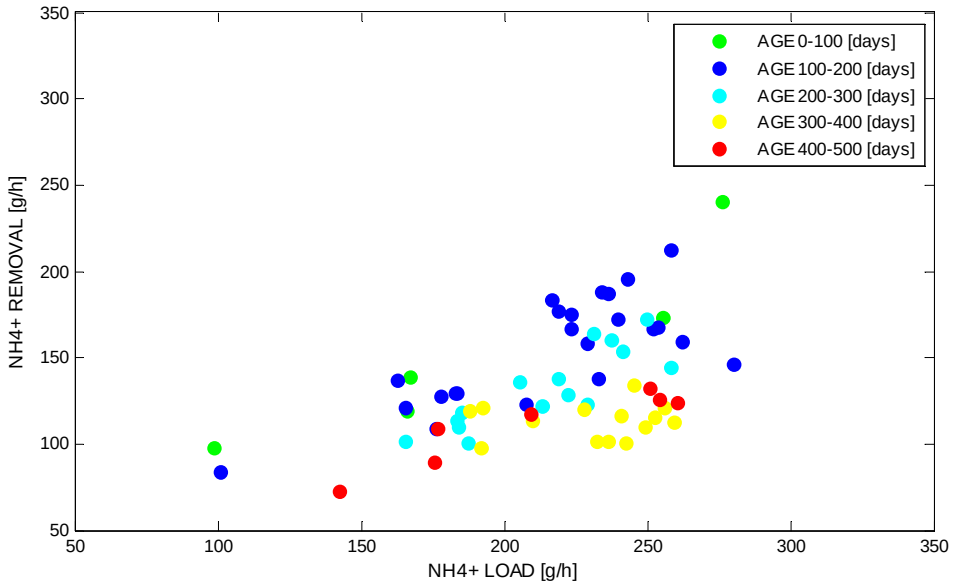

Figure A9.12 Nitrification rates at different filter ages for different ammonium loading rates in filter FF-07 after external washing

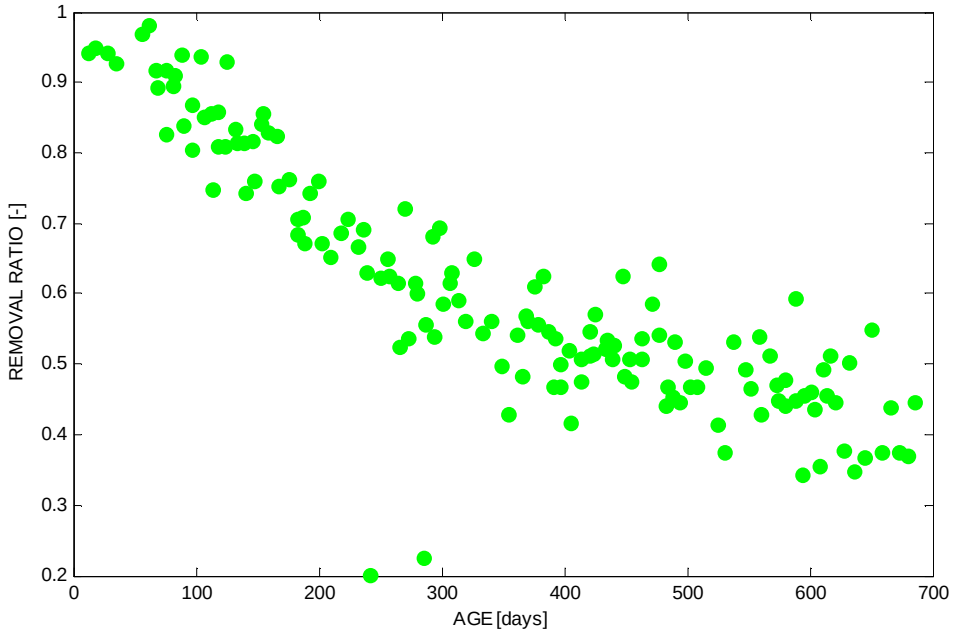

Figure A9.13 Ageing process of the ammonium removal ratio of filter FF-08 after external washing

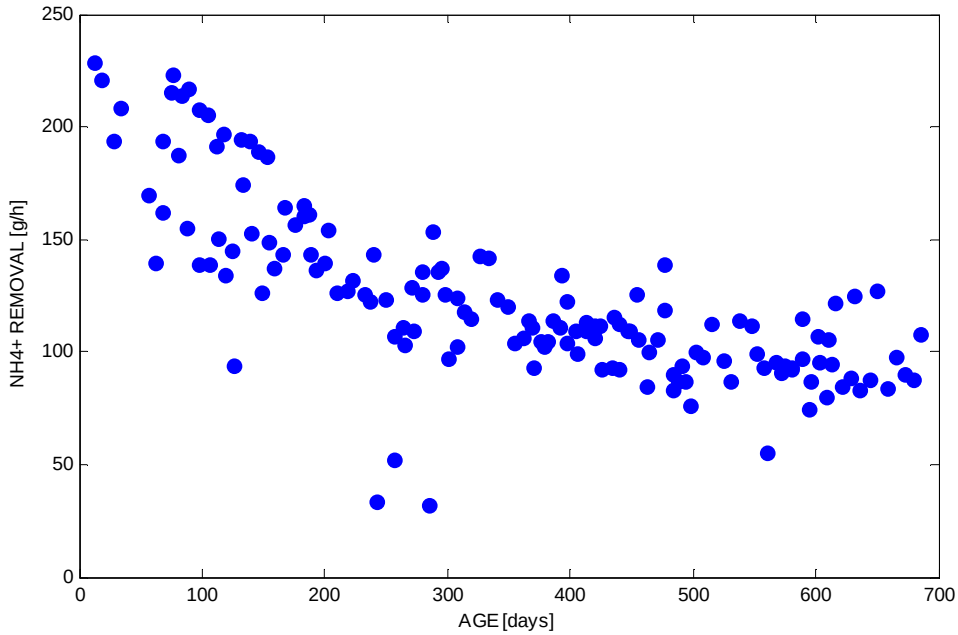

Figure A9.14 Ageing process of the ammonium removal rate of filter FF-08 after external washing

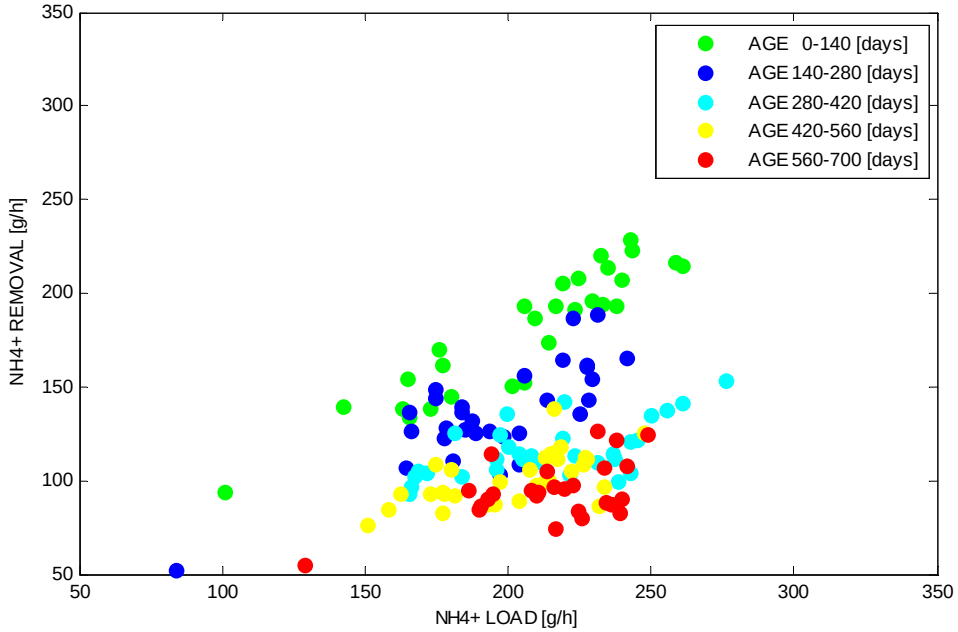

Figure A9.15 Nitrification rates at different filter ages for different ammonium loading rates in filter FF-08 after external washing

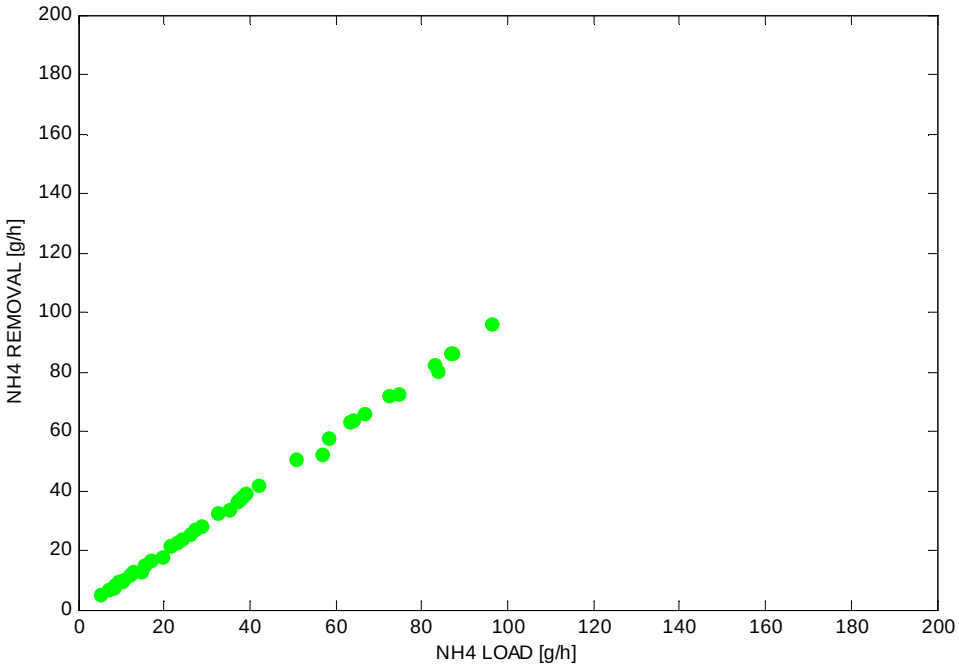

Figure A9.16 Nitrification rates for different ammonium loading rates in filter FK-04

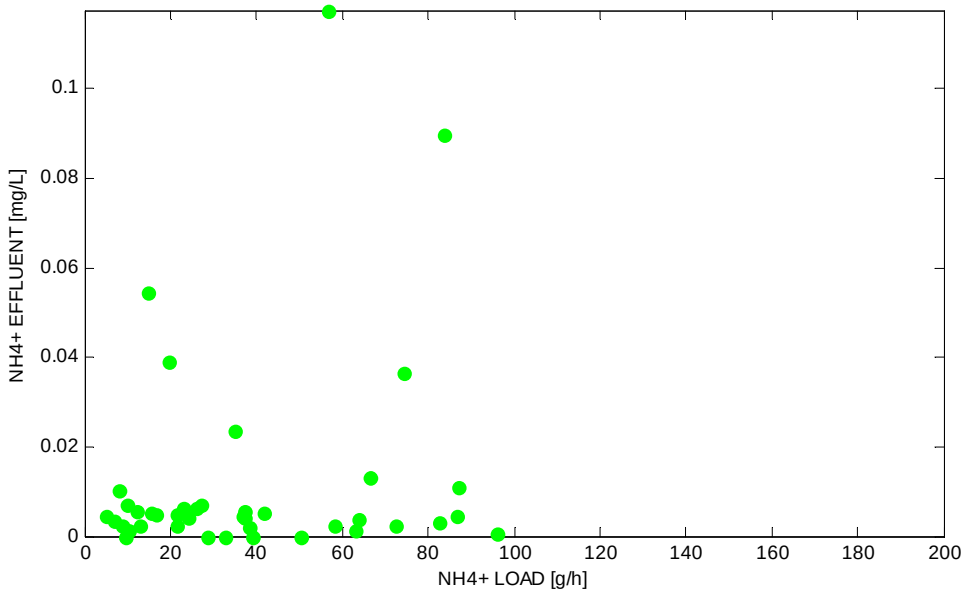

Figure A9.17 Effluent ammonium concentrations for different ammonium loading rates in filter FK-04

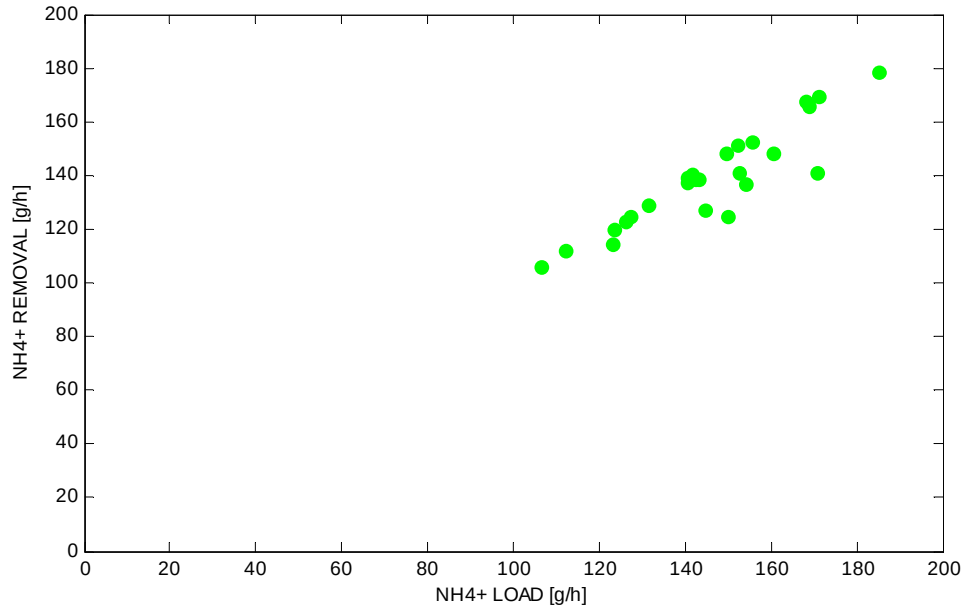

Figure A9.18 Nitrification rates for different ammonium loading rates in filter FK-05

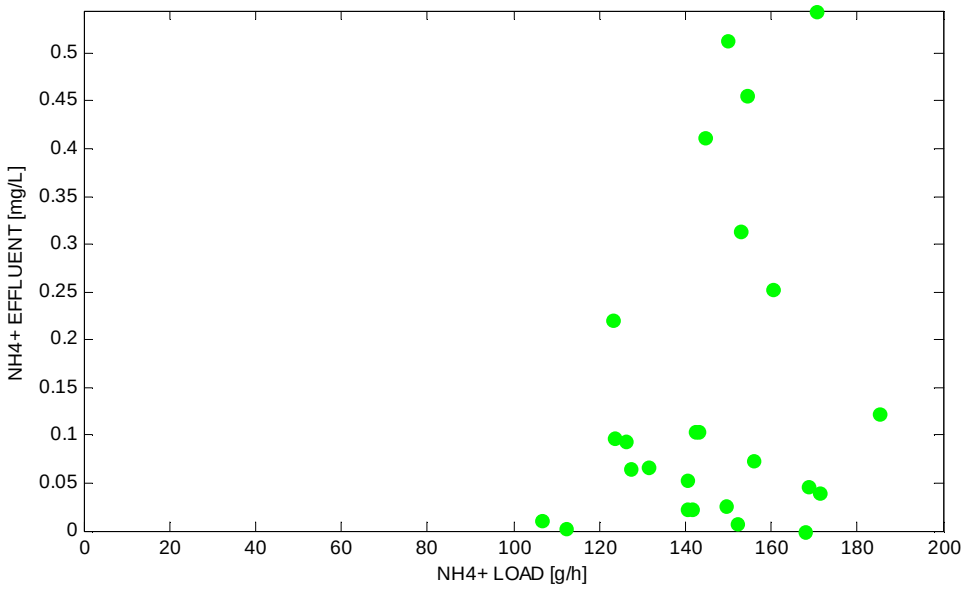

Figure A9.19 Effluent ammonium concentrations for different ammonium loading rates in filter FK-05

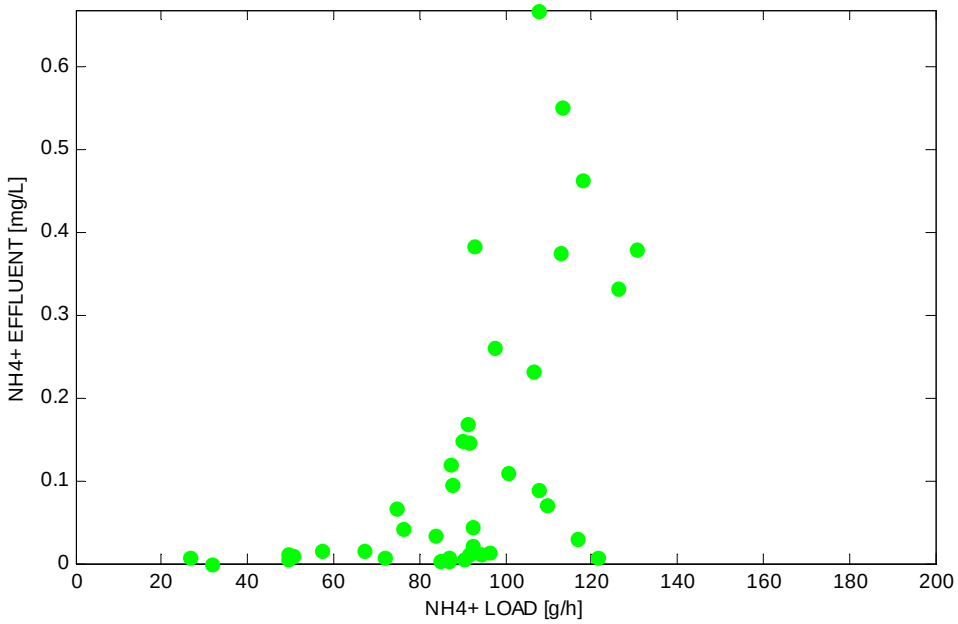

Figure A9.19 Effluent ammonium concentrations for different ammonium loading rates in filter FK-06

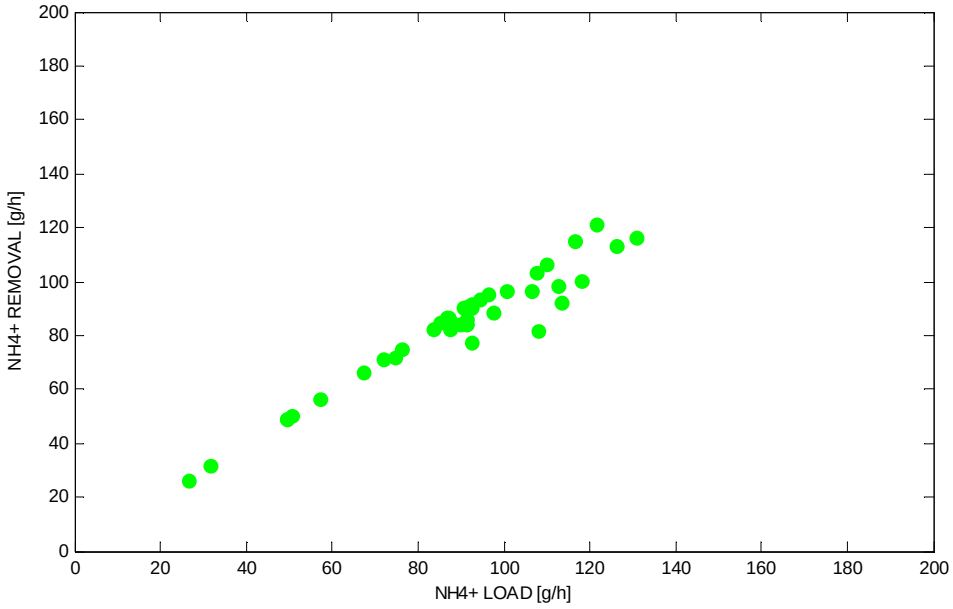

Figure A9.20 Nitrification rates for different ammonium loading rates in filter FK-06

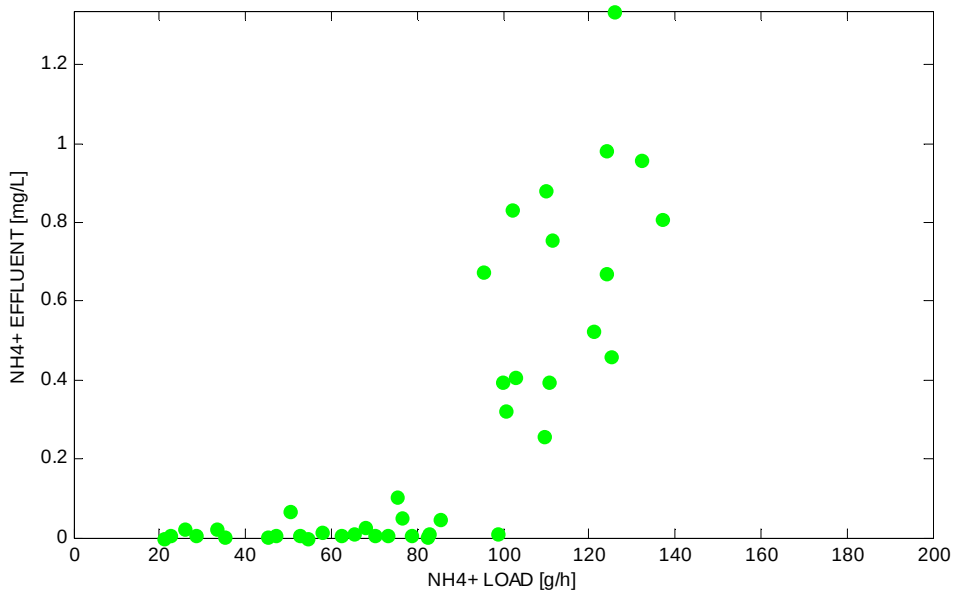

Figure A9.21 Effluent ammonium concentrations for different ammonium loading rates in filter FK-07

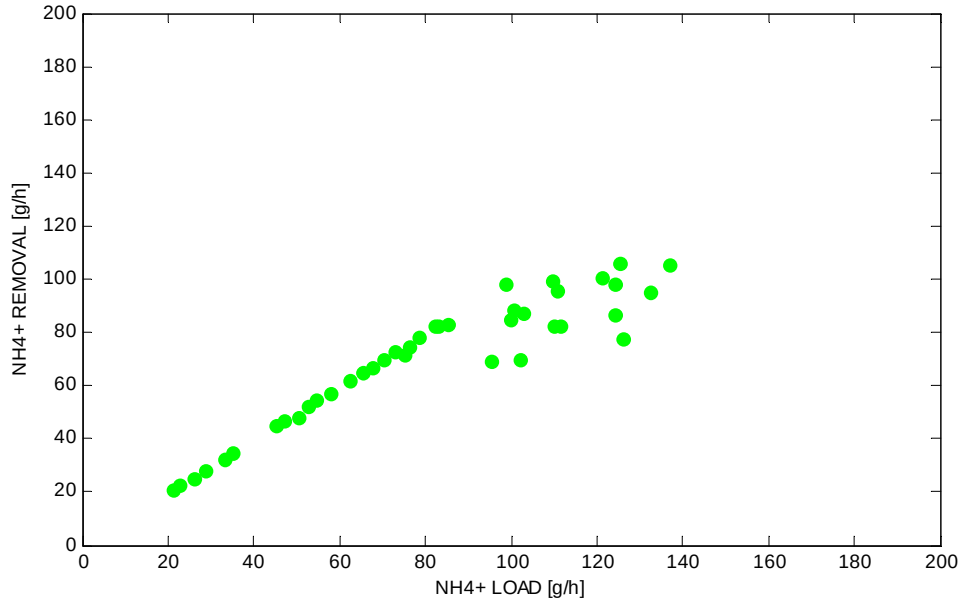

Figure A9.22 Nitrification rates for different ammonium loading rates in filter FK-07

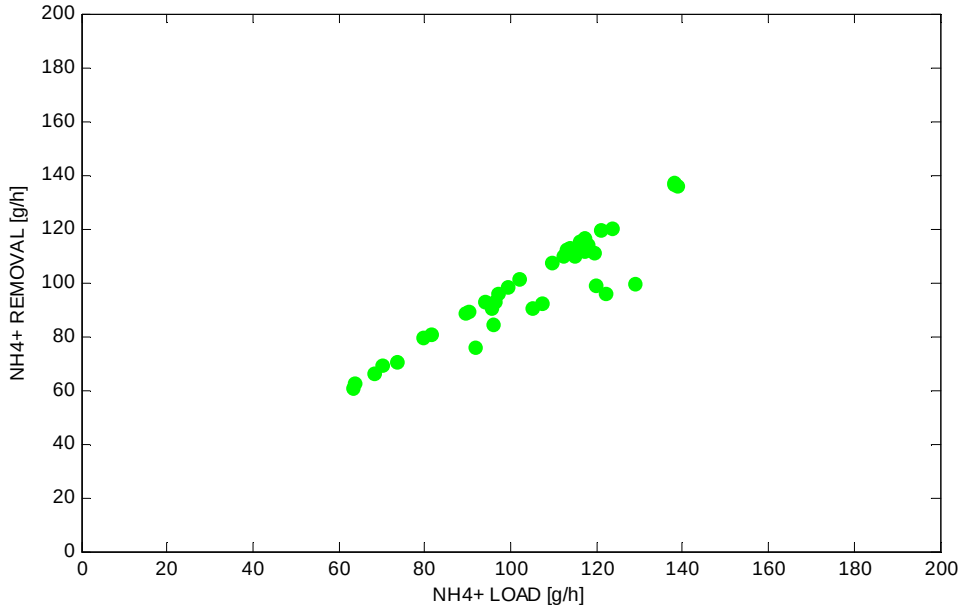

Figure A9.23 Nitrification rates for different ammonium loading rates in filter FK-08

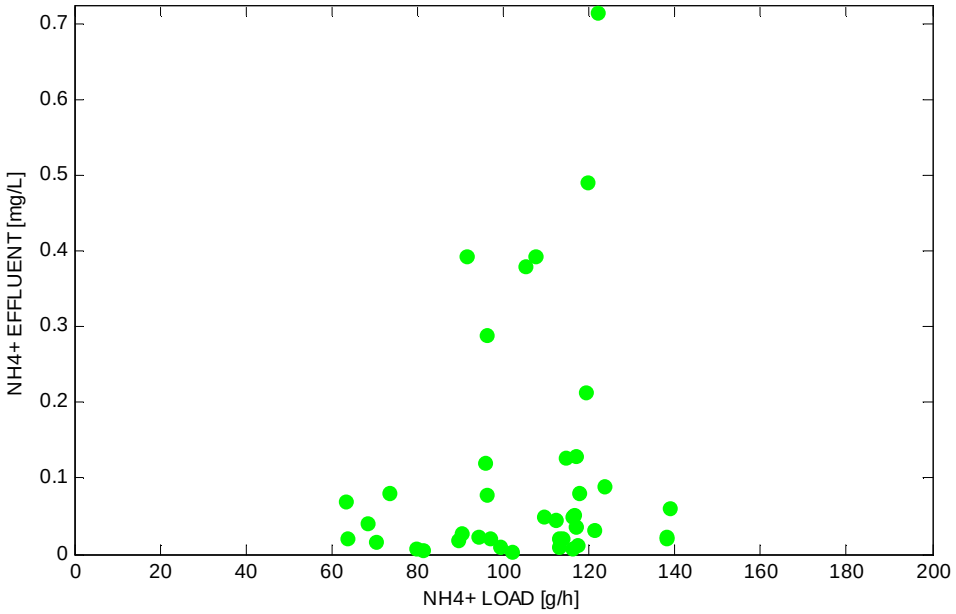

Figure A9.24 Effluent ammonium concentrations for different ammonium loading rates in filter FK-08

A.10 Tracer experiments results

Introduction

Uniform distribution of gas and liquid is desired for efficient operation of bio-trickling filters since its performance may be affected by the gas and liquid flow behaviour. There are several issues that can prevent such circumstance from happening.

- In trickling filters the pores are filled with liquid and air. The liquid flowing downwards may cover only a fraction of the external surface of the filter material grains. This may happen because what is known as rivulet-type flow, which is typical for low liquid flow rates. The fraction of the total outer surface that is effectively wetted is known as the external wetting efficiency. There is an internal wetting efficiency as well, which is defined as the fraction of the internal volume of the grain pores filled with liquid, but in this case it is assumed to be 1 or close to 1 due to capillarity.

- The fraction of the volume of the total filter bed filled with liquid is known as the total liquid holdup. The total liquid holdup can be divided into the static and the dynamic holdup: the former refers to the fraction of liquid that remains after draining the bed while the second one changes with the flow rate. This description is not thought to be used in the model but it is mentioned to show the complexity of hydrodynamics in trickling bed filters.

- In addition to this the prevailing forces explaining the behaviour of the liquid may vary with the flow rate: a gravity-viscosity regime is characteristic of low liquid flow rates while a gravity-inertia regime corresponds to high liquid rates. Multiple flow regimes may occur: the dispersed-bubble flow at high liquid rates, the pulsing flow at increasing gas rates, the spray flow at very high gas rates and the gas-continuous flow at low liquid and gas rates.

- Over the course of the time the accumulation of particles and/or the excess of biomass may cause local clogging resulting on fluid (gas and/or liquid) channelling, the apparition of dead zones and non-uniform distribution of flow(s) across the filter diameter. As a consequence the outer surface of the grains may not be completely covered with liquid.

Whatever the situation is non-uniform liquid distribution is undesirable since it makes the concentration of substrates not to be the same in all places. For systems where the reaction rate is controlled by a non-volatile reactant as in this case, having a reduced wetting efficiency may lead to low removal efficiencies. In literature there are available different correlations to estimate the wetting efficiency. Nevertheless, they have two major drawbacks: first, they require for parameters values which are not easily measurable; and, second, there is no consensus on the accuracy of such relationships. Hence, tracer experiments have been used instead to have a better idea on the characteristics of the fluid regime in the bio-trickling filters and, if possible, to evaluate how certain the hypothesis of high wetting efficiency is in the dry filters studied.

Nomenclature

T: Time.
T: Theoretical residence time.
Θ: Relative residence time.
EGV: Conductivity.
L: Filter bed depth.
S: Filter bed cross-section.
P: Clean bed porosity.
Q: Flow rate.
σ: Standard deviation.
$T_{\%}$: Time in the distribution curve for which % of the tracer has passed through the filter.
N: Number of completely mixed reactors in series.
Mo: Morill-dispersion index.
Pe: Peclet number.

Description

The VTS Model is a spreadsheet that automatically generates a differential and cumulative residence time distribution curves. The cumulative residence time distribution curve represents the % breakdown of salt (tracer) measured as EGV as a function of the (relative) residence time. The EGV value at zero time (start of the experiment) is defined as the background value. Any increase from the background value is assumed to be caused by the dosed salt.

Most of the results rely in a calculated theoretical average distribution time. This theoretical average time is used as reference value, to convert the absolute parameters in relative parameters. This makes possible to compare different filter results and to combine results corresponding to different times of the experiment. By converting the residence time at a relative residence time, it is possible to determine the position and the shape of the curves to compare, independently of the flow rate and the dimensions of the filter bed. The relative residence time is calculated from the quotient of the actual time (t) and the calculated theoretical residence time (T):

Equation A10.1

$$\theta = \frac{t}{T}$$

The absolute values are also converted into relative values by considering a reference time, which correspond to the tracer test 'zero' time: the instant when the salt is dosed into the influent.

Equation A10.2

$$EGV_{relative} = \frac{EGV_{measured}}{EGV_{background}} - 1$$

The available files comprise the results of several tracer experiments carried out in several dry filters located at different treatment plants. Additional information was gathered so that fluid dynamic results can be ideally linked to site specific values such as filter dimensions, lifecycle, experiment duration, filter age, etc. A systematic approach was followed: experiments were conducted twice for each filter, at different moments of the filter lifecycle (usually before and after backwashing).

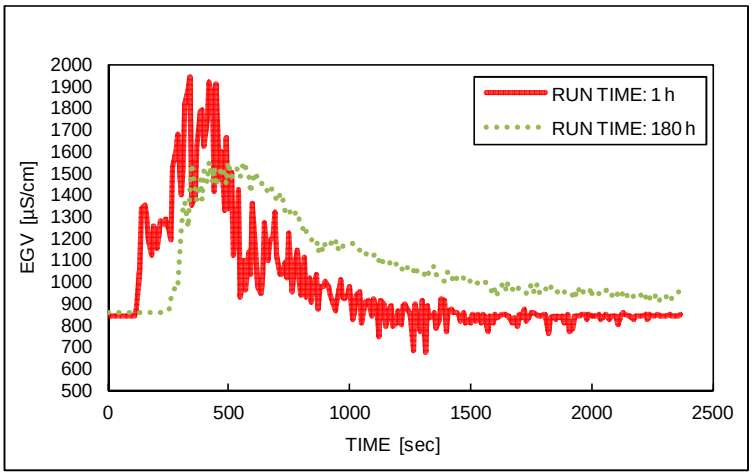

Figure A10.1 Residence time distribution curves for OASEN's dry filter before and after backwash

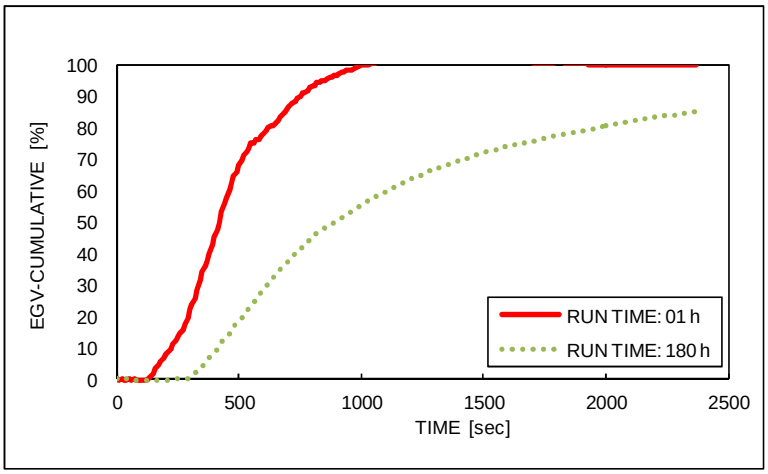

Figure A10.2 Cumulative residence time distribution curves for OASEN's dry filter before and after backwash

Metrics

The metrics that the author(s) use to characterize the flow within the filter are listed below. The way the theoretical residence time corresponds to wet filtration although it is used interchangeably for any case:

Equation A10.3

$$T = \frac{V}{Q} = \frac{L \cdot S \cdot P}{Q}$$

The standard deviation is calculated as:

Equation A10.4

$$\sigma = \frac{\frac{T_{84} - T_{18}}{2}}{T}$$

Three parameters can be used to characterize the hydraulic regime: the number of ideal mixed in cascade (N), the Peclet number (Pe) and the Morill index (Mo).

Supposedly, the flow can be simulated by a cascade of ideal mixers. Where N=1 represents ideal mixing and N=∞ corresponds to full plug flow. On the basis of the average residence time and the standard deviation, the formula to calculate the number of reactors in series reads:

Equation A10.5

$$N = \frac{{T_{50}}^2}{\sigma^2}$$

The Morill dispersion index quantifies the distribution. The closer the Morill index is to 1, the less dispersion is and the closer is the filter to plug flow. The formula reads as:

Equation A10.6

$$Mo = \frac{T_{90}}{T_{10}}$$

The Peclet index is the inverse of the dispersion number and describes the axial mixing in trickle flow. A high Peclet number indicates little diffusion and that the fluid dynamics in the filter approach to plug flow. It is calculated as:

Equation A10.7

$$Pe = \frac{2}{\sigma^2}$$

Theoretically, with a good plug flow there should not be preferential flows and/or dead spaces. Thus, a perfect plug flow shows no dispersion so that the Peclet number and the Morill dispersion index must follow opposite trends: if the Peclet value goes to ∞, the Morill index must approximate to 1.

Results

During the tracer experiments, filters were operated in manual mode so that constant flow is promoted and backwashing is prevented from happening. In many cases the experiment was conducted twice or even three times for the same filter at different moments of the run cycle. These moments are indicated between brackets in the text below. Before showing the results, one remark needs to be done. There results correspond to filters at different plants and positions (filtration step). This may has implications on the importance and characteristics of clogging and the duration of the run cycle for each case. For all these reasons the results should be taken with caution. The results are summarized in Table A10.1.

Table A10.1 Tracer experiments results

Filter															
Plant			Reijerw aard			Hooge	Lekkerkerk								
Name			FC-02	FF-02		FF-05	FF-01	FF-01	FF-02			FF-03			
Height		[m]	2.31	2.00		2.00	1.60		1.60			1.60			
Surface		[m2]	26	18		28	18		18			18			
Operation Cycle		[h]	48	180		36	72		72			72			
Experiment															
Run Time		[h]	47	0	168	35	12	60	13	37	61	14	38	63	
Flow		[m3/h]	58	47	47	70	45	47	43	47	45	47	45	43	
Duration		[h]	1.47	0.82	0.82	0.77	0.17	0.16	0.19	0.17	0.18	0.19	0.19	0.20	
Measurements															
Absolute Residence Time	Tracer Detected 1st Time	[sec]	330	120	240	130	130	120	160	190	350	260	260	240	
	Tracer Peak Value	[sec]	830	450	560	450	470	330	690	760	660	470	460	810	
	10% Tracer Passed	[sec]	610	230	420	280	380	260	450	490	520	400	400	460	
	50% Tracer Passed	[sec]	1400	430	900	570	710	540	730	530	740	610	610	850	
	90% Tracer Passed	[sec]	3430	760	2802	1000	1440	1550	1260	1230	1170	940	1060	1440	
Results															
Relative Residence Time	Tracer Detected 1st Time	[-]	0.22	0.11	0.22	0.11	0.14	0.14	0.17	0.21	0.38	0.29	0.28	0.25	
	Tracer Peak Value	[-]	0.56	0.41	0.51	0.39	0.51	0.37	0.72	0.86	0.72	0.53	0.50	0.84	
	10% Tracer Passed	[-]	0.41	0.21	0.38	0.24	0.41	0.29	0.47	0.55	0.56	0.45	0.43	0.48	
	50% Tracer Passed	[-]	0.94	0.39	0.82	0.49	0.77	0.61	0.76	0.60	0.80	0.69	0.66	0.89	
	90% Tracer Passed	[-]	2.30	0.69	2.54	0.87	1.56	1.75	1.31	1.39	1.27	1.06	1.15	1.50	
Relative Mean Time		[-]	2.30	1.87	2.14	2.04	1.87	2.08	1.62	1.08	1.42	1.53	1.53	1.85	
Morill Dispersion Index		[-]	5.62	3.30	6.67	3.57	3.79	5.96	2.80	2.51	2.25	2.35	2.65	3.13	
Standard Deviation		[-]	0.71	0.18	0.81	0.25	0.62	0.77	0.49	0.55	0.38	0.42	0.53	0.61	
Peclet Number		[-]	3.92	60.83	3.04	31.56	5.20	3.37	8.33	6.61	13.85	11.34	7.12	5.37	
Number Ideal Mixers		[-]	2	5	1	4	2	1	2	1	4	3	2	2	
Velocity	Time Tracer Peak Value	[m/h]	10	16	13	16	12	17	8	8	9	12	13	7	
	Time 50% Tracer Passed	[m/h]	6	17	8	13	8	11	8	11	8	9	9	7	
Void Occupied by Water	Time Tracer Peak Value	[-]	0.56	0.41	0.51	0.39	0.51	0.37	0.72	0.86	0.72	0.53	0.50	0.84	
	Time 50% Tracer Passed	[-]	0.94	0.39	0.82	0.49	0.77	0.61	0.76	0.60	0.80	0.69	0.66	0.89	

The Morill dispersion index quantifies the flow distribution. After backwashing, clean bed situation, the values reported are in general low, ranging from 2.35 (14 hours) to 3.79 (12 hours). Reactors with values below or equal to 2 are considered as effective plug flow reactors according to the Environmental Protection Agency (US-EPA). Therefore, flow conditions in dry filters are close to plug flow regime as intuitively expected. The results of the experiments performed before backwashing indicate that the Morill index increases with the operation time. This happens in all cases but one. The extent of the increase varies. In general, the values reported at the end of the run cycle range from 3.13 (63 hours) to 6.37 (168 hours). Therefore it can be conclude that the general conditions are closer to plug flow. Dispersion increases with the operation and, consequently, preferential flows and/or dead spaces, which are not thought to occur at the beginning, appear as soon as clogging develops.

The results for the Peclet number confirm this idea: high values are reported at the beginning of the cycle, after backwashing although there are important differences between filters. The values range from 8.33 (13 hours) to 60.83 (0 hours). In all cases but one, the values at the end of the cycle are much lower and similar to each other: 3.04 (168 hours) - 5.37 (63 hours).

Accordingly to these results, the highest values for the number of continuous stirred-tank reactors occur for the clean bed situations ranging from 3 (14 hours) to 5 (0 hours). The number decreases with the operation time. N=1 represents ideal mixing and N=∞ corresponds to full plug flow.

The mean residence time is the time for which 50% of the tracer has passed through the filter (with small correction for the duration of dosing). Concerning its evolution with the production time there are not conclusive results. In some cases the mean residence time increases while in the others decreases. The same occurs with the time at which the peak value of the tracer was registered.

Finally, the average velocity is estimated based on the residence time and the bed height. Two residence times are considered: the mean residence time and the time at which the peak concentration value was detected. Although the velocities are higher in the first case than in the second, the values are always within the same range: 7-17 m/h.

A.11 Internal measurements

In order to understand better the nitrification problem occurring at WTP Lekkerkerk, the abundance and the activity of the ammonia-oxidizing populations over a prolonged time period has been extensively investigated in recent years. Samples were taken from two primary filters at WTP Lekkerkerk during a long time period (6-9 months): FF-08 and FF-03. During all that time filter FF-08 showed poor ammonium removal based on regular sampling of the ammonium concentrations in the effluent. By contrast, filter FF-03 showed complete ammonium removal as it is typically observed in the Schuwacht filters. Although the activity measurements corresponding to filter FF-03 could have been considered as representative of the Tiendweg filters showing high ammonium removal, there is no evidence of this. In this respect, it is believed that the lower ammonium influent concentrations in Schuwacht together with the existence of sub-surface aeration prior abstraction may adversely affect the representativeness of these results. Therefore, the activity measurements corresponding to samples collected from the subsurface aerated well are only used for comparison reasons.

Sand-specific nitrification rate over the filter bed depth

In order to quantify the nitrifying activity of the filter samples, the sand-specific nitrification rate was measured. Figure A11.1 illustrates the measured sand-specific nitrification rates over the filter bed height of the two above mentioned filters. The dots on the left correspond to the non subsurface aerated filter while the dots on the right stand for the subsurface aerated filter.

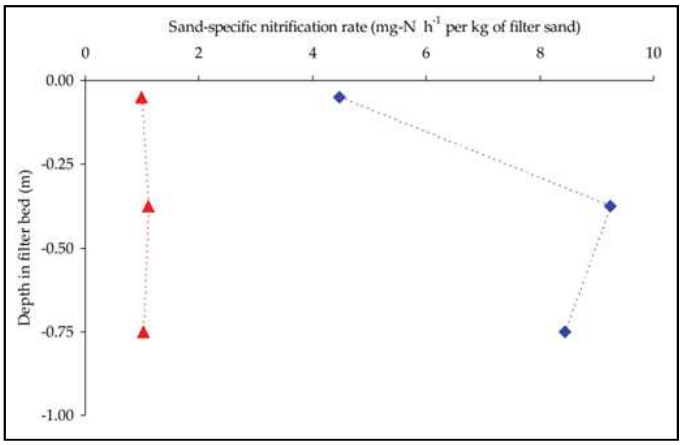

Figure A11.1 Sand-specific nitrification rates over the top half of the filter bed height of two primary bio-trickling filters at WTP Lekkerkerk (De Vet et al., 2009a)

In the figure it can be seen that the nitrification rates are significantly lower in filters with low ammonium removal (around 1 N h^{-1} kg^{-1}) than in filters with high ammonium removal (between 4.2 to 9 g N h^{-1} kg^{-1}). These results suggest that incomplete nitrification coincides with a significantly lower sand-specific nitrification activity. Moreover, the rates are relatively constant over the bed height in filters with relapsed nitrification while in filters with nearly complete ammonium removal the nitrification rate increases below the top layer to decrease afterwards. The lower nitrification rate at the top layer is thought to be due to the absence of ammonia-oxidizing organisms at the top layer after studying the microbial population over the filter bed height for the same two cases.

Sand-specific nitrification rate over the filter life time

Figure A11.2Figure shows the evolution of the sand-specific nitrification rate at different moments of a time-period of 6 months. Each time measurements were performed at different bed heights. The variability of the values is illustrated with the standard deviations plotted.

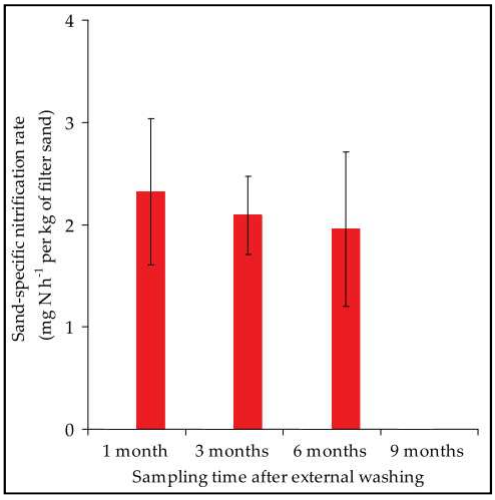

Figure A11.2 Average and standard deviations of sand-specific nitrification rates over the depth of the filter bed for filter sand samples collected from filter FF-08 when showing nitrification problems (adapted based on (De Vet et al., 2011b)

According to the average values show in the figure above it can be concluded that the specific nitrification capacity slightly decreases with time. Despite this the specific nitrification rates measured over the filter bed depth does not change significantly with time. Furthermore, the standard deviations are significant which suggest that there might be important differences in the nitrifying activity among different locations in the filter bed despite the poor ammonium removal observed in the filter for all that time.

In Figure A11.3, the measurements of the specific nitrification rate in the backwash water of the same filter are shown. The measurements indicate that the activity of the ammonia-oxidizing cells existing in the samples of backwash water was very low all the time.

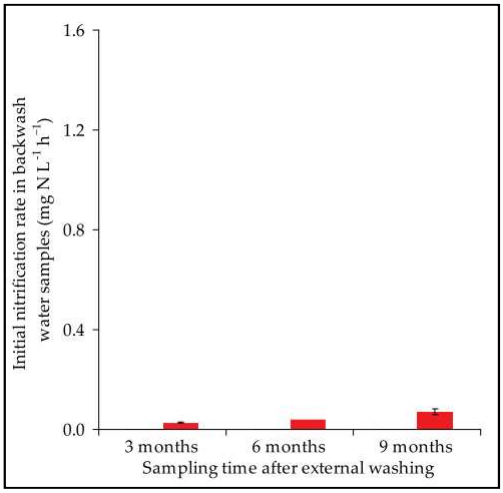

Figure A11.3 Average and standard deviations of sand-specific nitrification rates of the backwash water samples collected from filter FF-08 when showing nitrification problems (adapted based on (De Vet et al., 2011b)

Cell mass balances

Although nitrification has been considered traditionally to be an exclusively Bacterial process (De Vet et al., 2009a), site-specific measurements confirmed that ammonia-oxidizing archae (AOA) are found in significant numbers in these filters. Consequently investigating the abundance of ammonia-oxidizing microorganisms consists on assess the cell numbers for at least two types of microorganisms: the amonia-oxidizing archaea (AOA) and ammonia-oxidizing bacteria (AOB). Figure A11.4 shows the average, minimum and maximum of ammonia-oxidizing micro-organisms cell numbers for all filter sand, influent, effluent and backwash water over a time period of 9 months:

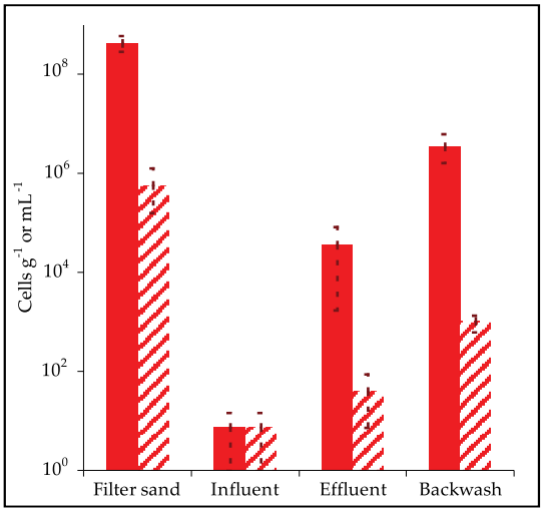

Figure A11.4 Average, minimum and maximum of AOB (solid bars) and AOA (line bars) cell numbers over a period of nine months at filter FF-08 when showing nitrification problems (De Vet et al., 2011b)

Figure A11.4 provides some interesting results.

- The number of inoculated cells from the aquifer is marginal compared with the numbers detected in the filter, filtrate or backwash water.
- The contribution of AOA is marginal: although ammonia-oxidizing archaea grows in the filters, it does it only in low numbers compared to bacteria.
- The cell numbers observed in the samples of the filtrate suggest that regular detachment of the biomass from the grains happens during normal operation. Nevertheless, the numbers are low and consequently this does not seem to be the cause of the loss of nitrifying capacity. The results also suggest that the importance of detachment during normal operation evolves (and increases) with time.
- Detachment is much higher during backwashing than during filtration. Moreover, the low variability of the cell numbers in the backwash water samples over the period of 9 months suggests that the accumulation of inorganic deposits does not change significantly the washout of biomass.

Based on these results, it seems reasonable to conclude that incomplete nitrification is not likely caused by biomass detachment.

Cell abundance over the filter depth

Experiments have also shown (De Vet et al., 2011b) that the distribution of AOB cell numbers over the bed height is comparable to the sand-specific activity described in Figure A11.1. Figure A11.5 shows the average and standard deviations of the AOB cell numbers for filter sand samples at two different depths. The dots on the left correspond to the Schuwacht filter while the dots on the right stand for the Tiendweg filter.

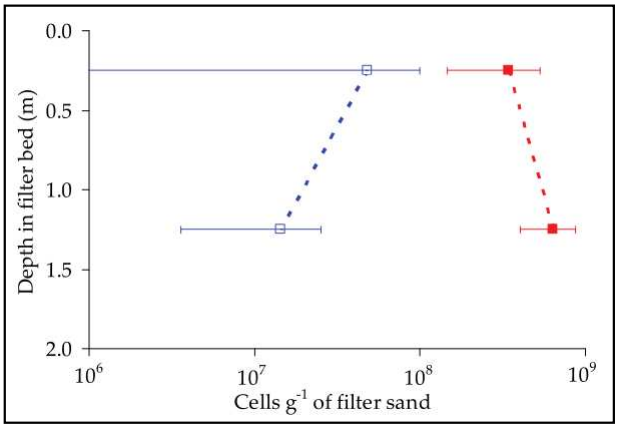

Figure A11.5 Average and standard deviation of AOB cell numbers for filter sand samples over the bed height collected from filter FF-03 (left side results) and filter FF-08 (right side results) over a period of nine month (De Vet et al., 2011b)

In the filter with subsurface aeration and almost complete ammonium removal, the highest cell numbers were found in the layer just below the top. Subsequently, the cell number decreases importantly which is likely the result of substrate limitation. By contrast, in the filter without subsurface aeration and showing poor ammonium removal the cell numbers remain relatively constant throughout the depth. These results are consistent with the previously shown sand-specific nitrification rates.

Cell-specific nitrification rates

Figure shows the cell-specific nitrification rates for filter FF-08, calculated by division of the sand-specific and volumetric rate by the cell number of each sand sample.

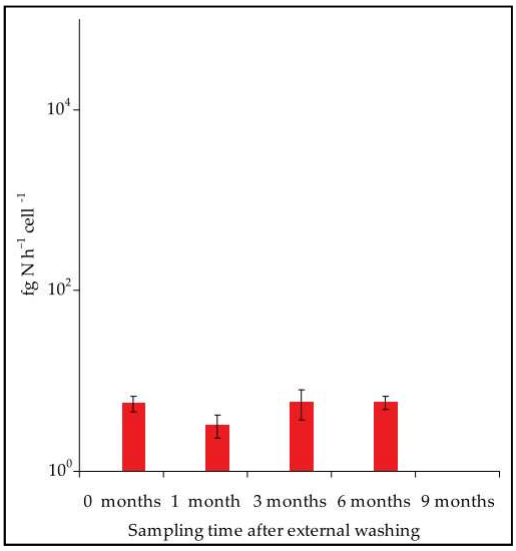

Figure A11.6 *Average and standard deviations of the cell-specific nitrification rate on filter sand*

The cell-specific nitrification rates were constant over time and within the range 0.02 to 0.08 102 fg N h^{-1} $cell^{-1}$. when compared to the values measured in the Schuwacht filter (0.2 to 5.0 fg N h^{-1} $cell^{-1}$) then it results that cells in filters with poor performance show a significantly lower cell-specific nitrification activity compared to the much more active cells in the subsurface aerated filters. This suggest that in trickling filters at WTP Lekkerkerk that show poor ammonium removal, part of the ammonia-oxidizing microorganisms are either dead or their activity is severely affected (De Vet et al., 2009a).

A.12 Sprayers measurements

Table A12.1 summarizes the characteristics of low pressure sprayers at three different treatment plants: Kromme Gat, De Put and Ridderkerk.

Table A12.1 Low pressure sprayers characteristics

Parameter	Unit	Kromme Gat	De Put	Ridderkerk
Number of nozzles per filter	[units]	14	36	18
Nozzle type	[-]	Den Helder	Gouda	Gouda
Drop height	[m]	1.7	1.6	0.40 -0.60
Average flow per nozzle	[m 3 / hour]	4.3	2.5	3.1
Design capacity	[m 3 / hour]	3-9	3-5	3-5
Cleaning frequency	[Weeks]	10-12	12	5

Spray aerators are used not only to promote aeration and methane removal but also a good water distribution over the filter. This measurement campaign was original aimed at obtaining an overall impression of the levels of methane after spray aeration as well as for assessing the approximate efficiency of this type of aeration system. Single and discrete samples were taken at each location in order to evaluate the aeration efficiency. The following parameters were measured: methane, carbon dioxide, oxygen, hydrogen carbonate, iron, manganese and temperature both before and after the sprayers. Since there exist differences in the raw water quality in these locations, such differences need to be taken into account when estimating the respective efficiencies. The average raw water qualities are given in Table A12.2.

Table A12.2 Average raw water qualities at different plants operated by OASEN

Treatment Plant	CH4 [µg/l]	CO2 [mg/L]	O2 [mg/L]	HCO3- [mg/L]	Fe [mg/L]	Mn [mg/L]	Temp. [°C]
De Put	515.00	20.00	0.00	235.00	1.40	0.56	12.50
't Kromme Gat	541.00	21.00	0.00	231.00	2.20	0.80	12.60
Reijerwaard	8253.00	76.00	0.00	396.00	6.80	0.44	11.90

The study of the efficiency of the aeration systems as a function of raw water quality, flow, drop height and RQ factor is beyond the scope of this MSc thesis despite the fact it is recognized that large variations can occur in both the raw water quality and the water flow rate.

Results

The measured pH, carbon dioxide and oxygen content after spray aeration are result of three factors: the raw water quality, the efficiency of the aeration device itself and iron oxidation. From the reaction of oxidation of divalent iron (Fe^{2+}) follows that the conversion of 1 mg Fe^{2+} implies the consumption of 0.143 mg of oxygen and the production of 1.577 mg of carbon dioxide. In order to assess better the contribution of aeration to the measured gas concentrations and pH after spray aeration it is necessary to discount the contribution of iron oxidation.

The following figures summarize the average raw water quality and the estimated maximum efficiencies for spray aeration at the different locations. While recognizing that they have different characteristics that may influence their efficiencies, the values shown below are a first estimate of the efficiency of the sprayers installed in Lekkerkerk. By considering the specific raw water qualities at Lekkerkerk, the efficiency of the filters at that plant can be estimated.

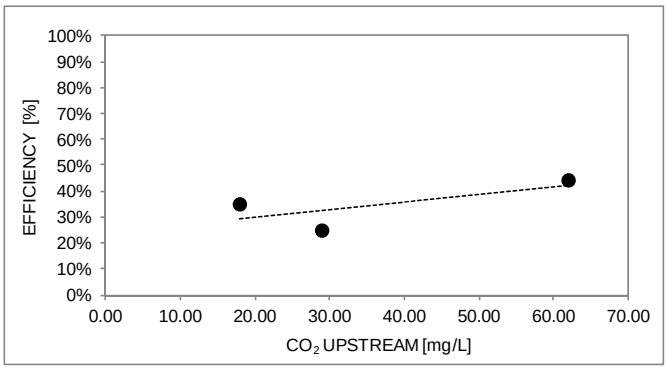

Figure A12.1 Efficiencies of low pressure sprayers for carbon stripping

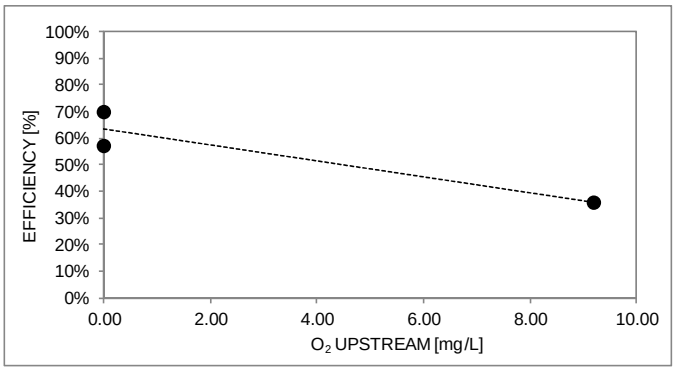

Figure A12.2 Efficiencies of low pressure sprayers for oxygenation

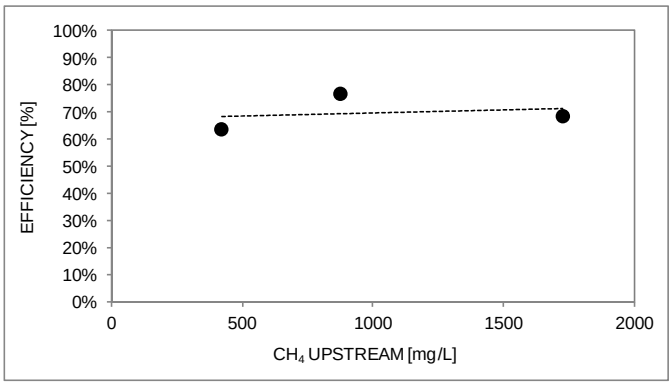

Figure A12.3 Efficiencies of low pressure sprayers for methane removal

A.13 Input conditions for calibration

Table A13.1 Influent conditions for calibration case 1.1

Influent Raw Water Quality Conditions			
Parameter	**Units**	**Range**	**Taken**
Ammonium	[mg/L]	4.5-7.0	5.5
Temperature	[oC]	11.0-13.0	11.5
Bicarbonate	[mg/L]	200-235	210
Oxygen	[mg/L]	0.0	0.0
Ortho-phosphate	[mg/L]	1.0-2.6	2.0
pH	[-]	7.1-7.4	7.2
Conductivity	[mS/m]	69-83	75
Iron II	[mg/L]	5.0-6.0	5.5

Table A13.2 Influent conditions for calibration cases1.2 and 1.3

Influent Raw Water Conditions		Scenario 1.2		Scenario 1.3	
Parameter	Units	Range	Taken	Range	Taken
Ammonium	[mg/L]	4.1-5.2	4.2	4.2-5.7	5.6
Temperature	[oC]	11.0-12.0	11.5	11.0-12.0	11.5
Bicarbonate	[mg/L]	220-236	230	200-235	230
Oxygen	[mg/L]	0.0	0.0	0.0	0.0
Ortho-phosphate	[mg/L]	0.7-1.2	1.0	0.7-1.2	1.0
pH	[-]	7.22-7.29	7.3	7.1-7.4	7.2
Conductivity	[mS/m]	69-76	72	69-83	75
Iron II	[mg/L]	4.8-5.2	5.1	5.3-5.9	5.5
Flow	[m3/h]	36.0-41.0	38.4	35.0-42.0	37.5

Table A13.3 Influent conditions for calibration cases 1.4 and 1.5

Influent Raw Water Conditions		Full Load		50% Load
Parameter	Units	Range	Taken	Taken
Ammonium	[mg/L]	4.5-7.2	5.4	2.6
Temperature	[oC]	11.0-12.0	11.5	11.5
Bicarbonate	[mg/L]	200-236	210	126
Oxygen	[mg/L]	0.0	0.0	5.0
Ortho-phosphate	[mg/L]	1.0-2.6	2.6	0.5
pH	[-]	7.1-7.4	7.3	7.0
Conductivity	[mS/m]	72-82	80	40
Iron II	[mg/L]	4.5-5.5	5.5	2.8
Flow	[m3/h]	33.2-38.6	36.0	51.4

Table A13.4 General water quality parameters for calibration case 2.1

Influent Raw Water Quality Conditions		
Parameter	Units	Value
Temperature	[oC]	11.8
Bicarbonate	[mg/L]	180
Oxygen	[mg/L]	10.6
Ortho-phosphate	[mg/L]	1.0
pH	[-]	7.8
Conductivity	[mS/m]	65
Iron II	[mg/L]	0.0

Table A13.5 Influent flow and ammonium concentrations for calibration case 2.1

Influent Load			
Date	Time [days]	Flow [m3/h]	NH4+ Inf. [mg/L]
02-01-12	0.00	33.40	3.20-3.60
22-01-12	20.00	38.80	2.90-3.25
11-02-12	40.00	38.20	3.70-3.90
02-03-12	60.00	38.00	4.05
22-03-12	80.00	42.00	3.43
11-04-12	100.00	37.80	4.21

A.14 Calibration values

Parameter	Units	Value
Filter cross-section	[m2]	18
Bed height	[m]	2
Grain size	[mm]	2
Porosity	[-]	39
Fraction void volume occupied by w ate	[-]	0.4
Wetting factor	[-]	1
Number complete mixed reactors	[-]	5
RQ forced ventilation	[-]	(*)

(*) FK:16; FK: 13;

Parameter	Units	Value
Maximum grow th rate	[1/s]	Case dependent
Decay rate	[1/s]	Case dependent
Initial biomass content	[g DW/m3]	Case dependent
Grow th rate correction factor for T	[-]	1.123
Affinity constant P	[g/m3 PO43-P]	0.005
Affinity constant N	[g/m3 NH4-N]	1
Affinity constant O2	[g/m3 O2]	0.5
Yield N	[g ds/g NH4-N]	0.00285
Yield P	[g ds/g PO43-P]	39.1

Parameter	Units	Value
Filtration step	[-]	(**)

(**) FF: 1; FK: 2;

(*) FF: 16 FK: 13
(**) FF: 1 FK: 2

A.15 Validation experiment measurements

Table A15.1 Flow values during validation experiments

Time	XLTMH00A	XLTMH99A	XLTRH99A
08-07-2013 10:15	25.00	26.40	51.40
08-07-2013 10:18	25.00	24.30	49.30
09-07-2013 13:08	24.90	26.50	51.40
10-07-2013 08:57	24.80	24.40	49.20
11-07-2013 10:28	24.80	30.00	`
11-07-2013 10:28	24.80	30.00	54.80
12-07-2013 08:58	24.90	28.70	53.60
15-07-2013 09:46	27.00	0.00	27.00
15-07-2013 09:47	27.00	0.00	27.00
16-07-2013 08:37	27.00	0.00	27.00
17-07-2013 09:41	27.00	0.00	27.00
18-07-2013 09:17	27.00	0.00	27.00
18-07-2013 09:17	27.00	0.00	27.00
19-07-2013 12:44	27.80	0.00	27.80
22-07-2013 09:31	27.30	0.00	27.30
22-07-2013 09:33	27.30	0.00	27.30
23-07-2013 10:15	27.70	0.00	27.70
24-07-2013 08:38	27.70	0.00	27.70
25-07-2013 13:28	34.70	14.30	49.00
25-07-2013 13:29	34.70	14.30	49.00
26-07-2013 09:02	34.80	14.90	49.70
29-07-2013 11:07	25.20	28.40	53.60

Table A15.2 Groundwater quality during validation experiments

Time [day]	Sampling Time [dd-mm-yy hh:mm]	NH4+ [mg/L]	pH [-]	EGV [mmol/L]	HCO3- [mg/l]	Fe2+ [mg/L]
0.000	08-07-2013 09:11	5.08	7.30	71.10	231.43	5.11
0.002						
1.120	09-07-2013 13:04	5.05				
1.946	10-07-2013 08:50	5.06				
2.573						
3.009	11-07-2013 10:36	5.09	7.31	72.20	236.62	5.23
3.009						
3.947	12-07-2013 08:55	5.06				
6.980						
6.981						
7.932						
8.976						
9.960						
9.960						
11.103	19-07-2013 12:20	5.06				
13.969	22-07-2013 08:27	4.92	7.28	72.10	236.50	5.21
13.971						
15.000	23-07-2013 10:14	4.91				
15.573						
15.933	24-07-2013 08:47	4.99				4.71
16.573	25-07-2013 00:00					
17.134	25-07-2013 13:22	5.06	7.21	72.30	233.02	5.21
17.135						
17.949	26-07-2013 09:09	4.92				5.42
21.036	29-07-2013 10:07	5.17	7.30	72.30	238.21	5.27

Table A15.3 Water quality of the influent permeate during validation experiments

Time [day]	Sampling Time [dd-mm-yy hh:mm]	NH4+ [mg/L]	pH [-]	EGV [mmol/L]	HCO3 [mg/l]	Fe2+ [mg/L]
0.000	08-07-13 09:18	0.32	5.49	1.81	8.13	0.02
0.002						
1.120		0.32				
1.946		0.32				
2.573						
3.009		0.32	5.49	1.96	8.12	0.03
3.009						
3.947		0.32				
6.980						
6.981						
7.932						
8.976						
9.960						
9.960						
11.103		0.31				
13.969	22-07-13 08:45	0.31	5.75	2.10	8.11	0.03
13.971						
15.000		0.31				
15.573						
15.933		0.31				0.03
16.573						
17.134		0.32	5.62	1.96	8.12	0.03
17.135						
17.949		0.32				
21.036	29-07-13 10:10	0.31	5.58	1.98	8.11	0.03

Table A15.4 Water quality in the effluent of the primary filter during validation experiments

Time [day]	Sampling Time [dd-m-yy hh:mm]	NH4+ [mg/L]	pH [-]	EGV [mmol/L]	HCO3- [mg/l]	Fe2+ [mg/L]
0.000	08-07-13 10:15	1.24	7.47	36.50	105.23	0.03
0.002	08-07-13 10:18	1.24				0.02
1.120	09-07-13 13:08	1.50				
1.946	10-07-13 08:57	1.47				
2.573						
3.009	11-07-13 10:28	1.39	7.34	35.60	105.53	0.03
3.009	11-07-13 10:28	1.38				
3.947	12-07-13 08:58	1.27				
6.980	15-07-13 09:46	1.04	7.55	47.10	121.09	0.03
6.981	15-07-13 09:47	1.04	7.63			0.03
7.932	16-07-13 08:37	1.52				
8.976	17-07-13 09:41	2.31				
9.960	18-07-13 09:17	2.32	7.75	65.80	204.41	
9.960	18-07-13 09:17	2.32				
11.103	19-07-13 12:44	2.00				
13.969	22-07-13 09:31	2.27	7.76	69.50	205.39	0.01
13.971	22-07-13 09:33	2.29				0.01
15.000	23-07-13 10:15	2.10				
15.573						
15.933	24-07-13 08:38	1.75				
16.573						
17.134	25-07-13 13:28	2.37	7.43	50.40	151.28	
17.135	25-07-13 13:29	2.36				
17.949	26-07-13 09:02	2.27				
21.036	29-07-13 11:07	1.68	7.38	38.30	114.26	0.02

Table A15.5 Water quality in the effluent of the secondary filter during validation experiments

Time	Sampling Time	NH4+	pH	EGV	HCO3-	Fe2+
[day]	[dd-mm-yy hh:mm]	[mg/L]	[-]	[mmol/L]	[mg/L]	[mg/L]
0.000	08-07-13 10:27	0.02	7.60	35.70	98.09	0.01
0.002						
1.120						
1.946						
2.573						
3.009	11-07-13 10:25	0.04				0.01
3.009						
3.947						
6.980	15-07-13 10:28	0.00	7.85	40.50	93.51	0.01
6.981						
7.932						
8.976						
9.960	18-07-13 09:28	0.01				0.01
9.960						
11.103						
13.969	22-07-13 09:44	0.00	7.87	67.00	186.66	0.00
13.971						
15.000						
15.573						
15.933						
16.573						
17.134	25-07-13 13:28	0.23				
17.135						
17.949						
21.036	29-07-13 11:28	0.00	7.62	37.60	104.25	0.01

A.16 Discussion on limiting factors

Introduction

Prior to the definition of better operational strategies, the bottlenecks of the process have to be investigated and understood. In the presentation of the modelling problem it was stated that a good model would be that one that is able of: (1) clarifying the causes for the observed incomplete nitrification; and, (2) evaluating how the operating conditions influence nitrification and the limiting factors so that the operation of full-scale filters can be improved. Accordingly, a nice output of this MSc Thesis would consist on making clearer the relations between mass transport parameters, hydrodynamic parameters, the nitrification capacity of the system and the achieved ammonium removal in practice. In short, the greatest challenge is linking the characteristics of the filter (fluid conditions, mass transfer and population dynamics) with the overall system behaviour (filter operation). Subsequently this information could ideally result in new preventive or curative strategies against the decline in nitrification.

Limiting factors

Therefore, one of the main questions to be answered is whether the ammonium removal is mass transfer or kinetically limited.

- Theoretically, in a mass-transfer limited system the overall conversion rate should improve when the biomass gets higher amounts of substrate which occurs if the external mass transfer is increased. If mass transfer is mainly controlled by the hydraulic regime, then more substrate is converted per carrier unit area with high-velocity regimes than with low-velocity regimes, assuming complete or fixed wetting efficiency. If Reynolds number is found to have a significant impact on ammonium removal rate, then it could be concluded that factors determining diffusion rate, like the flow conditions, influence the substrate consumption rate and, consequently, the biofilm growth. But, the point here is the velocity of water in dry filters is not directly dependant on the flow, unlike what happens in wet filters. Therefore, the hypothetical mass transfer limitation should be linked to a different cause rather than mixing or the flow regime.

- Alternatively, in a biologically limited system the overall conversion rate would remain the same if the population size is increased.

It could happen also that different causes for incomplete ammonium removal coexist at the same time. Furthermore, their relative importance may change over the time. In that respect, the determination of the limiting factors needs to be done carefully, since alternatively mass transfer or kinetic limitations could be behind the same issue causing the observed ammonium breakthrough in full-scale filters.

Possible categories

In principle, any limiting factor can be attributed to one of the following general categories:

(1) Diffusion limitation (internal mass transport). It refers to the processes occurring within the biofilm and, therefore, it is related to the characteristics of the biofilm: density, thickness, etc.
(2) Substrate limitation on the biofilm surface (external mass transport).
(3) Dead zones or short-circuiting due to the occurrence of incomplete wetting.
(4) Insufficient size of the ANO population either due to a very low number of cells or specific activity.

In the study of these categories, the issue of scale needs to be considered. The performance of filters is the result of processes occurring at two different scales: the macro scale, which correspond to the size of the reactor and all the transport processes occurring between gas, liquid and solid mediums; and the micro-scale, which corresponds to the transport and biological processes occurring around the filter material grains and in the biofilm.

Model simulations and reasonable hypothesis based on full-scale measurements have been used for acquiring better insight into the possible limiting factors is possible. Special emphasis has been paid to the relations between how the biofilm activity changes and how certain operation conditions may influence the microbiological activity and cell population. Although certainly, the model is not enough to conclude what the cause of the problems of nitrification is but the selection of the strongest ones is presented here. Based on these categories …

Model simulations have indicated that the transport processes in the bulk might not be the cause of the problem since very similar concentrations are observed both in the bulk and in the biofilm surface

for all the substances considered (ammonium-ammonia, oxygen, phosphate). However, the model does not consider the presence of iron deposits accumulating in the filter bed. Besides, literature shows that their diffusion coefficients on aqueous solutions have similar orders of magnitude.

Processes contributing to biofilm development and hypotheses

It is believed that the observed relapse in nitrification is mainly attributable to a combination of factors, all of them controlling the population dynamics. It is hypothesized that ammonium removal is limited mainly by microbial kinetics which could be limited by transport issues. Mass transfer can be almost neglected in the micro-scale, excluding the processes occurring within the biofilm. Mass transfer in a larger scale (reactor) such as wetting efficiency and uniform flows distribution can not be excluded and despite the fact that it may have an huge impact on the filter response according to the model (small reductions in the wetting factor strongly impact the response of the filter).

Reduced growth:

- Limited biological activity affecting all biomass (kinetic limitation) caused by the absence of any basic nutrient (e.g. microbiologically available phosphate, MAP) which cannot reach the ANOs due to the existence of simultaneous iron removal (interference). With this in mind, it has been hypothesized that the precipitation of phosphate with biogenic oxyhydroxides and the competition for phosphate by Gallionella spp. are the causes of phosphate limitation for ammonia-oxidizing bacterial leading to low microbially available phosphate (de Vet et al., 2012b).

- Limited biological activity affecting all biomass (kinetic limitation) caused by the absence of substrate(s) or nutrient(s) which cannot reach the ANOs by transport related problems within the biofilm which results in limited growth and, subsequently, death or inactivation of a significant fraction of the biomass.

Loss of biomass:

- Physical loss of biomass material due to different mechanisms: either by detachment (erosion and/or washout) or removal or iron deposits. Biofilms are exposed to shear due to water, aeration and mixing in the filter vessel. With this is mind, backwashing can be seen as a way of influencing the processes controlling either the loss of biomass or the removal of iron deposits.

Extensive research has been carried out in the last years by OASEN and not conclusive results around the causes for relapsed nitrification have been produced. The hypothesis of phosphate limitation s has been extensively researched in the last years by OASEN. For this reasons, an alternative hypothesis has been developed with the help of the model. This hypothesis corresponds to the second case.

Discussion on some plausible hypotheses

It is hypothesized that the older the filter is, the more important the biological factor becomes. Although there is a great uncertainty in the size of the population of ANOs present in the filter, it seems reasonable to think that the number increases with time, despite the processes causing loss of bacteria, such as washout during backwashing or desorption during normal operation.

However, the reduction in the nitrification efficiency observed after external washing should be linked to the dynamics of the ANO population. Beyond a certain population size, some of the biomass would become inactive or their cell specific nitrification activity would significantly drop, either due to the absence of some basic nutrient(s) or substrate(s) required for growth.

The scarcity of such compounds would depend on the relative position: the outer layers are in a better position in this respect. In addition to this, the deposition of inorganic precipitates between the grains which partially cover the filter material grains, where the biomass grows, would enhance this process. Both factors develop with filter age: the biomass content grows with time; also, the sludge content of the filter grows with time as backwashing does not achieve full efficiency in removing the iron deposits that accumulate in the filter bed.

The impact of backwashing on the abundance of nitrifiers is also of interest. On top of all the possible explanations, it needs to be considered that the effects of backwashing may evolve over the course of time just because the growth of the population due to their characteristics but also to possible changes in the characteristics of the filter bed and the biofilm.

For instance, there are several possibilities: first, the effect that backwashing has on cell population is negligible; second, though the number of cells removed is not negligible, they mainly correspond to inactive biomass; and third, the number is not negligible and corresponds to active biomass, which is

in the outer layers of the biofilm but the cell number after backwashing is still high enough to maintain the same nitrification capacity than before backwashing. Additionally, it is also possible that a significant part of the biomass existing in the filter is removed during backwashing so that its nitrification capacity is negatively affected; or that the biomass removed may mainly correspond to active biomass so that the impact becomes visible.

Furthermore, it has to be noted that the growth of population is also conditioned by the load applied: two filters that start to operate after external washing at the same time but which are fed with different loads may evolve differently since the growth will be different.

All these factors would explain the differences in declining nitrification after external washing: although the same pattern can be observed most of the times, the rate of relapse together with the threshold value for the age above which the relapse in nitrification starts and, later, stabilizes varies.